

**Larisse Faroni-Perez**

**EFEITOS DAS MUDANÇAS CLIMÁTICAS EM  
POLIQUETAS CONSTRUTORES DE RECIFES:  
MODELAGEM DE DISTRIBUIÇÃO DE ESPÉCIES,  
BIOCONSTRUÇÃO, E ECOFISIOLOGIA**

**“EFFECTS OF CLIMATE CHANGE  
ON REEF-BUILDING POLYCHAETES:  
SPECIES DISTRIBUTION MODELLING,  
BIOCONSTRUCTION, AND ECOPHYSIOLOGY”**

Tese submetida ao Programa de Pós-  
Graduação em Ecologia da  
Universidade Federal de Santa  
Catarina para a obtenção do Grau de  
Doutora em Ecologia

Orientador: Prof. Dr. Carlos Frederico  
Deluqui Gurgel.



Florianópolis, SC - Brasil  
2017

Ficha de identificação da obra elaborada pelo autor,  
através do Programa de Geração Automática da Biblioteca Universitária da UFSC.

Faroni-Perez, Larisse

Efeitos das mudanças climáticas em poliquetas construtores de recifes: modelagem de distribuição de espécies, bioconstrução e ecofisiologia : Effects of climate change on reef-building polychaetes: species distribution modelling, bioconstruction, and ecophysiology / Larisse Faroni-Perez ; orientador, Carlos Frederico Deluqui Gurgel, 2017. 266 p.

Tese (doutorado) - Universidade Federal de Santa Catarina, Centro de Ciências Biológicas, Programa de Pós-Graduação em Ecologia, Florianópolis, 2017.

Inclui referências.

1. Ecologia. 2. Acidificação dos Oceanos. 3. Biodiversidade Marinha. 4. Mudanças Globais. 5. Zona Costeira. I. Gurgel, Carlos Frederico Deluqui . II. Universidade Federal de Santa Catarina. Programa de Pós-Graduação em Ecologia. III. Título.

**"Efeitos das mudanças climáticas em poliquetas construtores de recifes:  
modelagem de distribuição de espécies, bioconstrução e a ecofisiologia"**

Por

**Larisse Faroni Perez**

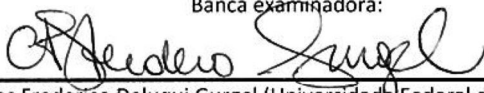
Tese julgada e aprovada em sua forma final pelos membros titulares da Banca Examinadora (20/PPGECO/2017) do Programa de Pós-Graduação em Ecologia - UFSC.



---

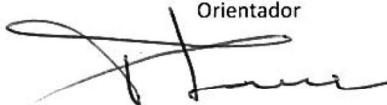
Prof. Dr. Fábio Gonçalves Daura Jorge  
Coordenador do Programa de Pós-Graduação em Ecologia

Banca examinadora:



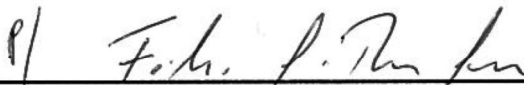
---

Dr. Carlos Frederico Deluqui Gurgel (Universidade Federal de Santa Catarina)  
Orientador



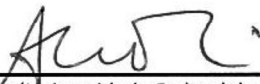
---

Dr. Paulo C. Lana (Centro de Estudos do Mar - Universidade Federal do Paraná)



---

Dr. Ronaldo A. Christofolètti - Por videoconferência (Instituto do Mar - Universidade Federal de São Paulo)



---

Dr. Alberto Lindner (Universidade Federal de Santa Catarina)



---

Dr. Sergio Ricardo Floeter (Universidade Federal de Santa Catarina)

Florianópolis, 01 de dezembro de 2017.



Este trabalho é dedicado aos meus pais: Amabele e Pedro.



## AGRADECIMENTOS

Ao Ministério da Educação (MEC) e Ministério da Ciência, Tecnologia, Inovações e Comunicações (MCTIC) através de suas respectivas agências de financiamento a CAPES e o CNPq pelas bolsas de estudo concedidas no país e no exterior – Ciência sem Fronteiras (CNPq – 201233/2015-0). Estendo este agradecimento aos funcionários que me auxiliaram a superar as muitas questões administrativas referentes às bolsas nesses quatro anos: Jorge Alexandre e Denise de Oliveira (CNPq) e Kelly Queiros (CAPES), e também da UFSC – Pró-Reitoria de Pós-Graduação (PROPG): Vlademir Verzola e Ricardo Covolo Rocha, e na Secretaria Integrada da Pós-Graduação (SIPG): Rodrigo Maschio.

Aos membros do Programa de Pós-Graduação em Ecologia da UFSC. Agradeço ao corpo docente os ensinamentos, desafios e incentivos. Sou agradecida também aos professores que me permitiram estar em sala de aula como ouvinte em disciplinas extra-curriculares somente pelo meu interesse no conteúdo e aprendizado. Agradeço aos colegas discentes a amizade, vivência e colaboração no aprendizado.

Ao Paulo Pagliosa agradeço o convite e incentivo para fazer o doutorado na Ecologia da UFSC. Ao Professor Nivaldo Peroni, agradeço o desafio lançado minutos antes da entrevista no processo de seleção: *“Boa sorte. Você sabe o que é sorte? Sorte é a união da oportunidade e competência. Oportunidade você esta tendo, resta saber se você é competente.”*

Ao professor Carlos Frederico Gurgel agradeço a supervisão e orientação. Sua capacidade de liderança respeitosa e o incentivo nas tomadas de decisões foram fundamentais para o desenvolvimento e a conclusão desta tese.

Ao Jérôme Fournier pelo aceite na supervisão e incentivo no período de 12 meses pelo Ciência sem Fronteiras na França. Aos pesquisadores na França: Flávia Nunes, Fabrice Pernet, Stansilas Dubois, Stéphanie Auzoux-Bordenave, Cédric Hubas e Christophe Goulard; na Austrália: Pat Hutchings e Ingo Burghardt; na Noruega: Maria Capa e Conrad Helm; e na Alemanha: Günter Purschke, Patrick Beckers e Thomas Bartolomaeus, agradeço a credibilidade e o incentivo na pesquisa.

Agradeço a todas as pessoas das instituições UBO, IFREMER (Brest) e MNHN (Concarneau e Paris) que me apoiaram na França:

Aïcha Badou, Alfred Goujon, Alain Van Wormhoudt, Bernard Bourlès, Cédric Hubas, Claudie Guengant, Christophe Goulard, Cyril Gallut, Elisabeth Sellin, Gwénola Burban-Doré, Jean Marie Caraguel, Lionel Feuillassier, Marc Eleaume, Michel Gigan, Nadia Améziane, Pascal Breton, Pierre-Yves Lebon, Samuel Iglésias, Solène Avignon, Stéphanie Auzoux-Bordenave, Sylvain Pont e Tony Robinet pelo apoio ao experimento de acidificação dos oceanos.

Adeline Bidault, Alain Le Mercier, Alain Marhic, Alexandre Garlaschelli, Amelia Curd, Anne Donval, Anne-Sophie Podeur, Bruno Dubief, Charlotte Corporeau, Christine Paillard, Christophe Lambert, Clarisse Lemonnier, Emma Michaud, Eric Dabas, Ewan Harney, Fabrice Pernet, Flávia Nunes, Gaspard Delebecq, Genevieve Cohat, Helene Hegaret, Jean-Philippe Buffet, Jonathan Flye, Luc Chauchat, Nicolas Gayet, Pierrick Le Souchu, Stanislas Dubois, Thibault Le Verge e Valdimere Ferreira pelo apoio ao experimento de ondas de calor.

Alain Van Wormhoudt, Cyndie Dupoux, Flávia Nunes, Jérôme Fournier, Laura Flamme, Marc Eleaume, Nadia Améziane, Nalani Schnell, Noémy Mollaret, Paula Martin-Lefèvre Tarik Meziane pelo apoio aos trabalhos dos órgãos sensoriais e biologia molecular.

Agradeço especialmente a todas as pessoas (de Santa Catarina e de outros estados) que de alguma forma me apoiaram durante estes anos. O apoio de vocês tornou a trajetória menos difícil.

Agradeço a Ana Carolina Grillo, Isabela Zignani e Janaina Geisler agradeço pela amizade e apoio nas horas difíceis e pela alegria infinita nos momentos de vitória e celebração.

Por fim, agradeço à minha família o apoio incondicional, amor pleno e moralidade que são a base de tudo.

A todos que de alguma forma, direta ou indiretamente, contribuíram para a minha formação acadêmica, pessoal e profissional:

**muito obrigada!**



## RESUMO EXPANDIDO

### Introdução

Mudanças climáticas e do ambiente (MCA) representam uma séria ameaça à biodiversidade e aos bens e serviços ecossistêmicos que prestam. Dentre os ambientes marinhos, habitats costeiros do entre-marés podem ser particularmente mais susceptíveis às MCA por estarem expostos a fatores marinhos (e.g. temperatura e pH da água do mar), terrestres (e.g. descarga pluvial e escoamentos de poluentes), e atmosféricos (e.g. temperatura do ar e radiação UV). MCA podem afetar organismos marinhos através de alterações em sua fisiologia, metabolismo e comportamento, incluindo ainda alterações nos padrões de distribuição de populações. Para se testar efeitos das MCA na biodiversidade marinha bentônica, foram usados como modelo biológico anelídeos da família Sabellariidae. Este grupo tem larvas planctônicas, mas os juvenis e adultos são estritamente bentônicos e sedentários. As larvas apresentam órgão sensorial e em algumas espécies com função chave na indução ao assentamento sobre tubos de co-específicos, um comportamento gregário que resulta em formação de recifes no entre-marés e águas rasas (apêndice A). Devido a esta capacidade de formação de habitats estes sabelarídeos são considerados espécies engenheiras de ecossistema. Portanto, entender os possíveis impactos das MCA em sabelarídeos é crucial, devido inclusive aos potenciais efeitos em cascata sobre a biodiversidade associada e dos serviços ecossistêmicos que prestam.

### Objetivos

Para compreender o grau de sensibilidade desse grupo aos impactos das MCA, objetivou-se acessar: i) como é a atual distribuição espacial da adequabilidade de habitat (nicho abiótico) e a predição futura para duas espécies com distribuição nos oceanos Atlântico e Pacífico; *Phragmatopoma caudata* e *P. virgini* respectivamente, (capítulo 1, apêndice B);

ii) Qual a influência da acidificação dos oceanos na construção biogênica do tubo de *Sabellaria alveolata* (capítulo 2); e

ii) como ondas de calor (i.e. hipertermia) determinam a sobrevivência de *S. alveolata* e influenciam sua fisiologia (capítulo 3).

## Metodologia

Para testar as hipóteses (Hs) de mudanças na distribuição de adequabilidade de habitat foram testadas comparações atuais e futuras em cenários alternativos de emissões de CO<sub>2</sub> utilizando modelos de distribuição de espécies de máxima entropia (MDS), climáticos, e estatísticos lineares. Para o caso de acidificação dos oceanos, as Hs foram testadas comparando-se condições atuais de pCO<sub>2</sub> e pH às prováveis futuras, onde analisou-se a bioconstrução pelo volume de bioadesivo secretado e sua composição de aminoácidos. Para testar Hs sobre os efeitos de diferentes intensidades de ondas de calor na sobrevivência e plasticidade fisiológica, analisou-se a mortalidade e a constituição e remodelagem dos lipídios estruturais.

## Resultados e Discussão

Como principais resultados evidencia-se:

i) os MDS previram para a espécie de habitat temperado a expansão de áreas adequadas, e para a espécie tropical expansão ou diminuição sob os cenários de baixas e altas emissões de CO<sub>2</sub> respectivamente;

ii) nas duas condições futuras de pH testadas o volume de bioadesivo aumentou significativamente e as mudanças na composição dos amino ácidos foram dominadas pela regulação positiva do ácido aspártico; e

iii) *S. alveolata* não tem habilidade para neutralizar estresse térmico extremo (34 e 31 °C) resultando em mortalidade, mas, em temperatura sub-letal (28 °C) a espécie sobrevive ao custo de uma complexa e dinâmica remodelagem de seus lipídeos estruturais.

Todos os resultados mostram que MCA causarão mudanças geográficas, comportamentais, e fisiológicas significativas nas populações de espécies de sabelarídeos construtoras de recifes. Estas mudanças podem resultar em dois padrões, não mutuamente excludentes, que são: i) desaparecimentos locais, contrações, e deslocamento latitudinal e/ou batimétrico na distribuição de populações e ii) conservação da área de distribuição atual como resultado de processo de aclimação e adaptação transgeracional.

## **Considerações Finais**

Em conclusão, embora a biodiversidade marinha bêntica possa apresentar plasticidade fisiológica e comportamental potencial para manter populações, as respostas associadas não podem ser generalizadas e dependerão principalmente da frequência, intensidade e período de tempo em que ocorrerão as mudanças do clima e do ambiente.

**Palavras-chave:** Acidificação dos Oceanos, Aquecimento Global, Ecofisiologia, Poliqueta, Zoobentos marinho.

## ABSTRACT

Climate and environment changes (CEC) represent serious hazards to biodiversity and the ecosystem goods and services they provide. Among marine environments, intertidal coastal habitats may be particularly more susceptible to CEC since they are exposed to marine (e.g. sea water temperature and pH), terrestrial (e.g. pollutant drainage and rivers runoff), and atmospheric (e.g. UV radiation and air temperature) conditions. CEC can affect marine organisms through changes in their physiology, metabolism and behaviour, and also in their population distribution patterns. In order to test effects of CEC on benthic marine biodiversity, annelids of Sabellariidae family were used as biological models. Sabellariids have planktonic larvae, but the juveniles and adults are strictly benthic and sedentary organisms. The larvae have sensory organs that, in some species, present a key role in their settlement onto co-specific tubes. Co-specific settlement represents a gregarious behaviour that results in the formation of intertidal and shallow subtidals reefs (Appendix 1). Due to habitat formation sabellariids are considered ecosystem engineers. Therefore, to understand the possible impacts of CEC on sabellariids is crucial due to potential cascade effects on associated biodiversity and ecosystem services. To comprehend the degree of sabellariids sensitivity to the impacts of CEC, the aims of this study were: i) to access current and the future prediction of habitat suitability distribution (abiotic niche) for two species distributed in the Atlantic and Pacific oceans, *Phragmatopoma caudata* and *P. virgini* (Chapter I, Appendix II); ii) test for effects of the ocean acidification on the biogenic construction of *Sabellaria alveolata* (Chapter II); and iii) determine how heat waves (i.e., hyperthermia) influence the survival and the physiology of *S. alveolata* (Chapter III). To test hypotheses (Hs) on changes in habitat suitability distribution, current and futures evaluations were tested for alternative CO<sub>2</sub> emissions scenarios, climatic, linear statistical, species distribution and maximum entropy (MDS) models were used. For oceans acidification, the Hs were tested by comparing current and expected future pCO<sub>2</sub> and pH conditions. Bio-construction analyses were based on volume of bioadhesive secreted and cured, and its amino acid composition. To test Hs on the effects of different intensities of heat waves on survival and physiological plasticity, the mortality and membrane lipids constitution and remodelling were analysed. The main results were: i) the MDS predicted universal expansion of suitable areas for the species of temperate habitat, and for the tropical habitat species expansion and decrease under

the low and high CO<sub>2</sub> emission scenarios respectively; ii) in both future pH conditions tested, the volume of bioadhesive significantly increased as sewerage became more acid. Changes in the amino acids composition were dominated by the up-regulation of aspartic acid; and iii) *S. alveolata* showed no ability to neutralize extreme thermal stress (34 and 31 °C) resulting in mortality. However at sub-lethal temperature (28 °C) the species survived at the cost of complex and dynamic lipids remodelling. All results showed that CEC would trigger significant geographical, behavioural, and physiological changes in populations of reef-building sabellariid species. These changes may result in two non-mutually exclusive patterns: (i) local disappearance, contractions and latitudinal and/or bathymetric shifts in populations distribution, and (ii) upkeep current distributional range as a result of the acclimation and transgenerational adaptation. In conclusion, although benthic marine biodiversity may exhibit potential physiological and behavioral plasticity to maintain populations, the related responses cannot be generalized and will depend primarily on the frequency, intensity, and time period that the changes in climate and in the environment will occur.

**Keywords:** Ecophysiology, Global Warming, Marine Zoobenthos, Ocean Acidification, Polychaeta.



## SUMÁRIO

<b>INTRODUÇÃO.....</b>	<b>17</b>
<b>OBJETIVOS.....</b>	<b>23</b>
Objetivo geral e apresentação da tese:.....	23
Objetivos específicos.....	24
Objetivos complementares.....	26
<b>CHAPTER I.....</b>	<b>31</b>
Abstract.....	33
Introduction.....	35
Materials and Methods.....	37
Results.....	41
Discussion.....	44
References.....	52
SUPPORTING INFORMATION.....	71
<b>CHAPTER II.....</b>	<b>85</b>
Abstract.....	87
Introduction.....	89
Material and Methods.....	92
Results.....	95
Discussion.....	96
References.....	100
SUPPORTING INFORMATION.....	111
<b>CHAPTER III.....</b>	<b>119</b>
Abstract.....	121
Introduction.....	123
Materials and Methods.....	125
Results.....	130
Discussion.....	131
Conclusions.....	139
References.....	140

<b>SUPPORTING INFORMATION</b> .....	<b>152</b>
<b>APPENDIX A</b> .....	<b>161</b>
<b>Abstract</b> .....	163
<b>Introduction</b> .....	165
<b>Methods</b> .....	166
<b>Results</b> .....	172
<b>Discussion</b> .....	178
<b>Conclusions</b> .....	184
<b>References</b> .....	186
<b>SUPPORTING INFORMATION</b> .....	<b>209</b>
<b>APPENDIX B</b> .....	<b>219</b>
<b>Abstract</b> .....	221
<b>Introduction</b> .....	223
<b>Materials and Methods</b> .....	225
<b>Results</b> .....	228
<b>Discussion</b> .....	232
<b>Conclusions</b> .....	236
<b>References</b> .....	237
<b>SUPPORTING INFORMATION</b> .....	<b>255</b>
<b>CONCLUSÃO FINAL DA TESE</b> .....	<b>259</b>
<b>REFERÊNCIAS</b> .....	<b>261</b>



## INTRODUÇÃO

---

Mudanças climáticas e do ambiente (MCA) procedem de uma combinação de alterações abióticas locais, regionais e globais, tais como, atmosféricas (*e.g.* radiação UV, temperatura e circulação do ar), marinhas (*e.g.* salinidade, temperatura, pH e circulação da água do mar) e terrestres (*e.g.* descarga pluvial e escoamentos de poluentes). Entre 1750 e 2010, as emissões para a atmosfera de gases de efeito estufa de origem antropogênica em termos cumulativos globais foram de  $2040 \pm 310$  gigatons de dióxido de carbono (GtCO<sub>2</sub>), sendo ainda que em 2010 a emissão anual total representou quase 45% em relação aos níveis em 1750 (IPCC *et al.*, 2014). Esta crescente e contínua emissão de gases e poluentes para a atmosfera resulta na retenção de parte da energia de calor proveniente do sol e que poderia re-irradiar para o espaço. Este evento foi denominado como ‘efeito estufa’. Sabe-se que esta forçante radiativa acumulada impulsiona o efeito das MCA no planeta como um todo.

Modelos climáticos demonstram que para um cenário de alta emissão destes gases (*i.e.*, RCP 8.5, IPCC-AR5, 2013), no período entre os anos 2071-2100, ocorrerão críticas alterações nos padrões de circulação atmosférica e marinha, precipitação, acidificação dos oceanos, e temperatura do ar e da água, sendo uma média global relativamente bem mais quente do que as registradas e simuladas para os últimos séculos. Ainda, modelos climáticos preditivos preveem ocorrência crescente de eventos climáticos extremos, tais como ciclones, ondas de calor e tempestades de frio. As ondas de calor marinhas (OC), classificadas como evento discreto de anomalia prolongada na temperatura da água em regiões oceânicas (Hobday *et al.*, 2016), têm aumentado em magnitude e frequência em todo o mundo (Lima & Wethey, 2012). OC podem acontecer em qualquer época do ano, tem duração de ao menos 5 dias, e o término é determinado ao fim da anomalia. Entretanto eventos longos com mais de 100 dias já foram registrados (Hobday *et al.*, 2016).

Os oceanos naturalmente absorvem o  $p\text{CO}_2$  resultando na acidificação dos oceanos (AO), que é uma crítica alteração ambiental proveniente da contínua e crescente emissão de CO<sub>2</sub> para atmosfera. De fato, o fluxo de CO<sub>2</sub> entre ar e mar é um processo dinâmico e natural no ciclo global do carbono. Estima-se que entre o período de 1800 a 1994 os oceanos absorveram cerca de 48% do  $p\text{CO}_2$  emitido por queima de combustíveis fósseis (Sabine *et al.*, 2004), e é provável que a proporção

de absorção aumente significativamente durante as próximas décadas (Doney *et al.*, 2009; Orr *et al.*, 2005). Como resultado, o pH médio global da superfície da água do mar diminuiu 0,1 unidade, e espera-se que até o final deste século ocorra um declínio de mais 0,3 a 0,5 unidades (Caldeira & Wickett, 2005). De fato, nos dias atuais o impacto sinérgico das altas emissões destes gases do efeito estufa para a atmosfera já demonstram o desafio da MCA para a conservação da biodiversidade. Portanto, MCA desafia os bens e serviços ecossistêmicos que a biodiversidade presta. Entender como seriam as respostas esperadas dos organismos às MCA é um desafio de grande importância para que se possa compreender a susceptibilidade da biodiversidade costeira em seu conjunto de interações ecológicas. Mais ainda, compreender o balanço local e regional das MCA associado às respostas esperadas da biodiversidade é fundamental para subsidiar ações em favor da gestão de áreas de conservação da biodiversidade costeira e funcionamento do ecossistema.

Estudos recentes têm demonstrado que os organismos marinhos estão mais amplamente distribuídos em seus nichos abióticos do que os correspondentes geográficos terrestres (Pörtner *et al.*, 2017; Sunday *et al.*, 2012). Neste sentido, alterações nos processos abióticos demandam que os animais, principalmente os marinhos, tenham capacidade de neutralizar o estresse para perpetuar a existência. Dentre os ambientes marinhos, a zona do entre-marés na região costeira pode ser particularmente mais vulnerável às MCA uma vez que está exposta aos fatores ambientais atmosféricos, terrestres e marinhos (Doney *et al.* 2007; Doney *et al.* 2009; Hobday *et al.*, 2016). Neste sentido, organismos com ocorrência no entre-marés, principalmente os sésseis e sedentários pouco móveis, podem ser particularmente mais vulneráveis às MCA (Gilman *et al.*, 2006; Helmuth *et al.*, 2006; Somero, 2002; Sunday *et al.*, 2012), já que estão muitas vezes sujeitos a processos abióticos (*e.g.* temperatura) próximos de seus limiares fisiológicos (Somero, 2010) e potencialmente influenciando as funções metabólicas (Braby & Somero, 2006; Pörtner *et al.*, 2017). Portanto, os organismos do entre-marés poderão ser os primeiros a apresentarem alterações comportamentais, fisiológicas e na distribuição de populações em resposta às MCA. Deste modo, espécies do entre-marés representam um modelo biológico ideal para investigar o efeito das mudanças climáticas e ambiental na biodiversidade.

Como resposta aos efeitos das MCA, em termos gerais, a previsão para a distribuição de populações de espécies marinhas e terrestres é uma mudança da área de ocorrência para altas latitudes, onde condições

mais favoráveis poderiam existir, ou, alternativamente, mudanças de distribuição multidirecional poderiam ocorrer (Burrows *et al.*, 2011; García Molinos *et al.*, 2015; Lenoir & Svenning, 2015; VanDerWal *et al.*, 2013). Compreender as respostas das espécies em cenários da MCA é crucial para prever possíveis alterações nos padrões de distribuição de populações e consequentes mudanças seu no conjunto de interações interespecíficas que promovem o funcionamento do ecossistema (Przeslawski *et al.*, 2008). Estudos anteriores de modelagem de distribuição de espécies indicaram que os organismos tropicais são altamente vulneráveis devido à diminuição de habitats adequados intertropicais, e que no geral, a distribuição geográfica dos habitats adequados diminuirá de forma mais rápida e acentuada sob um cenário com altas concentrações de  $p\text{CO}_2$  (García Molinos *et al.*, 2015; Jones & Cheung, 2015). Alternativamente, dentro de grupos de espécies exclusivamente tropicais ou temperadas, nenhum padrão consistente poderia ocorrer devido à respostas variadas na direção das mudanças ou um aumento / diminuição na área adequada (Saupe *et al.*, 2014). Nos últimos anos, uma grande quantidade de estudos de modelagem têm tentado entender a atual distribuição de espécies e de habitats adequados, para então acessar possíveis futuras mudanças de distribuição no contexto de MCA. Contudo, esta abordagem ainda não é comum para avaliar as possíveis respostas em espécies engenheiras de ecossistemas.

Os impactos da acidificação dos oceanos (AO) em vários organismos (*e.g.* algas, corais, moluscos, equinodermos, crustáceos, poliquetas e peixes) foram estudados (Kroeker *et al.*, 2013; Li *et al.*, 2014, Pörtner, 2008; Wittmann & Portner, 2013), e as respostas encontradas são antagonicas. Por exemplo, alteração na bioconstrução resultou em diminuição da espessura do tubo em poliquetas serpulídeos (Li *et al.*, 2014), enquanto que, as taxas de crescimento aumentaram em alguns organismos calcificadores e não calcificadores (Koch *et al.*, 2013; Leung *et al.*, 2017). Portanto, avaliar e prever as respostas dos organismos marinhos aos prováveis futuros níveis de  $p\text{CO}_2$  elevados são cruciais para compreender se uma linhagem, população ou espécie pode ser vulnerável a AO, ou alternativamente, se o desempenho metabólico é resiliente e as espécies têm a capacidade de aclimatar-se. Aclimação é uma resposta de plasticidade fenotípica considerada a medida que os organismos têm habilidade de perceber e converter o estímulo ambiental, através dos processos celulares e metabólicos, que ajustam o seu desempenho fisiológico para neutralizar o estresse ambiental (Pörtner *et al.*, 2017; Pörtner, 2008).

Nos últimos anos, em resposta a eventos de ondas de calor (OC) foram reportadas mudanças na fisiologia e fenologia de espécies e também na estrutura de comunidades (Caputi *et al.*, 2016; Garrabou *et al.*, 2009; Mills *et al.*, 2013; Oliver *et al.*, 2017; Smale *et al.*, 2017, Wernberg *et al.*, 2016; Wernberg *et al.*, 2013). De modo geral, as atividades vitais das células são estruturadas por função da membrana, na qual a composição heterogênea de lipídios desempenha um papel fundamental para o estabelecimento e ativação de proteínas e para a regulação conveniente do transporte e permeabilidade de íons transmembrana (Hazel & Williams, 1990; van Meer *et al.*, 2008). A maioria dos organismos pecilotérmicos pode remodelar os lipídios estruturais para restaurar o equilíbrio e a permeabilidade da membrana, já que os componentes de lipídios da membrana são finamente ajustados às condições ambientais (Hazel & Williams, 1990). Aclimação de espécies pela remodelagem lipídica em função de alterações na temperatura do ambiente tem sido estudada em vários organismos (*e.g.* moluscos, crustáceos, peixes e poliquetas) e no geral, as respostas encontradas são de reestruturação lipídica (Muir *et al.*, 2016; Pernet *et al.*, 2007). Porém, em truta a remodelagem lipídica em condição de elevação térmica ocorre mais tardiamente do que em condição de diminuição de temperatura (Hazel & Landrey, 1988), o que pode sugerir possível ausência de habilidade de aclimação à hipertermia em organismos pecilotérmicos. Portanto, entender as possíveis respostas fisiológicas dos organismos através dos constituintes lipídicos da membrana, e avaliar se em extremos de hipertermia a tolerância é excedida ou ajustada determinando a sobrevivência, é fundamental para prever como os organismos marinhos podem responder a eventos de OC.

Os anelídeos poliquetas da família Sabellariidae são formadores de recifes biogênicos comumente nas zonas costeiras do entre-marés (Faroni-Perez *et al.*, 2016), portanto, são engenheiros de ecossistema (Jones *et al.*, 1994). Por ser um habitat complexo com superfície consolidada, heterogênea e com fendas, estes recifes facilitam a colonização de uma biodiversidade associada que, por vezes, é mais diversificada do que áreas adjacentes (Ataide *et al.*, 2014; Dubois *et al.*, 2002; Gherardi & Cassidy, 1994; Gore *et al.*, 1978; Nelson & Demetriades, 1992). Ressalta-se que animais bentônicos vageis e organismos pelágicos, muitas vezes não são quantificados ainda que estejam associados aos recifes nas marés altas, visto como, por conveniência de amostragem os estudos frequentemente consideram a fauna associada durante o período da maré baixa. Os recifes de sabelarídeos fornecem suprimento alimentar e funcionam como local de

refúgio, abrigo e reprodução a uma diversa comunidade composta principalmente por algas, invertebrados, tartarugas e peixes pelágicos (Gore *et al.*, 1978; Lindeman & Snyder, 1999; Makowski *et al.*, 2006), que interagem de modo permanente ou efêmero. Inclusive, os recifes funcionam ainda como um grande filtro natural, uma vez que os sabelarídeos são animais filtradores (Caline & Kirtley, 1992). Por gerarem uma série de bens e serviços ecossistêmicos, os recifes de sabelarídeos foram designados pela Administração Nacional Oceanográfica e Atmosférica (NOAA, USA) como Habitat Essencial de Peixes, e na Europa é oferecida a proteção aos recifes de sabelarídeos desde a Convenção de Bern 1979. No entanto, evidências baseadas em pesquisas históricas e recentes apontam que a distribuição e abundância de recifes de sabelarídeos já estão mudando em resposta às recentes MCAs (Firth *et al.*, 2015). Portanto, é de fundamental importância compreender a susceptibilidade e os possíveis efeitos das mudanças climáticas e ambientais na sobrevivência e distribuição de sabelarídeos construtores de recifes.

Sabellariidae têm larvas planctônicas e são estritamente tubícolas após a metamorfose e assentamento. A habilidade sensorial inerente das larvas para o assentamento sobre os tubos de seus co-específicos explica a formação e perpetuação dos recifes (Faroni-Perez *et al.*, 2016; Jensen & Morse, 1988; Pawlik & Faulkner, 1988). Para a construção de seus tubos, e portanto, conseqüente formação dos recifes, os sabelarídeos sintetizam e secretam um adesivo que promove a ligação permanente às partículas sedimentares capturadas da coluna de água do mar pelos tentáculos desenvolvidos após a metamorfose (Faroni-Perez *et al.*, 2016; Gruet *et al.*, 1987; Main & Nelson, 1988; Sun *et al.*, 2009). A rápida solidificação do adesivo secretado durante a bioconstrução parece estar vinculada a uma diferença de pH entre as glândulas secretoras do adesivo e da água do mar (Stevens *et al.*, 2007; Stewart *et al.*, 2017; Wang & Stewart, 2012). O processo de solidificação do adesivo confere elevada rigidez, visto como, os recifes biogênicos precisam ser resistentes ao forte impacto hidrodinâmico das áreas onde ocorrem. Portanto, o adesivo do tubo tem fundamental importância ecológica para a sobrevivência e adaptação da espécie. Neste sentido, é importante avaliar se as mudanças ambientais (*i.e.* alteração do pH da água do mar) podem alterar a composição e o funcionamento do adesivo para a bioconstrução. Mais ainda, é igualmente importante entender se em extremos térmicos, tais como eventos de ondas de calor, os organismos restringem funções vitais evocando à mortalidade. Alternativamente, ajustes fisiológicos (*e.g.* remodelagem lipídica) poderiam determinar a

sobrevivência dos organismos, e portanto, resultar em aclimação e adaptação ao longo de gerações.

**Objetivo geral e apresentação da tese:**

Buscou-se avaliar possíveis respostas de distribuição, aclimação e adaptação de organismos do zoobentos marinho às mudanças climáticas e do ambiente (MCA). Então, para entender o efeito das mudanças globais na distribuição e existência de recifes construídos por poliquetas da família Sabellariidae, usou-se abordagens de biogeografia (capítulo I) e experimentação fisiológica (capítulos II–III), os quais são suportados por dois estudos complementares sobre a funcionalidade de órgãos sensoriais nas larvas para o recrutamento gregário e subsequente formação de recifes (apêndice A), e de filogeografia, dispersão larval e conectividade populacional (apêndice B).

Em linhas gerais, o capítulo I aborda a modelagem de distribuição de espécies – MDS em duas linhagens do gênero *Phragmatopoma*, e tem como foco a compreensão do conjunto de condições ambientais que permitem a ocorrência geográfica e persistência das populações em amplas escalas espaciais, e ainda a previsão da distribuição geográfica potencial das espécies considerando a variação climática e ambiental para cenários alternativos: de alta e baixa emissão de gases do efeito estufa. Para isso, o apêndice B esclarece a validade da sinonímia da espécie descrita para a costa brasileira (*P. lapidosa*) com a do Caribe (*P. caudata*) e a conectividade genética das populações. Os capítulos II e III foram desenvolvidos usando-se a espécie *Sabellaria alveolata* de ocorrência majoritária em águas marinhas rasas do Reino Unido, Europa e Norte da África. Estes capítulos levam em consideração a acidificação dos oceanos (capítulo II) e eventos térmicos extremos, isto é, ondas de calor (capítulo III). As variáveis respostas de bioconstrução e sobrevivência e remodelagem dos lipídeos estruturais foram, respectivamente, examinadas. O apêndice A aborda a distribuição global de espécies de poliqueta da família Sabellariidae conforme atributos ecológicos, distribuição batimétrica e comportamento de assentamento larval, e suas possíveis relações com a presença, morfologia, significado filogenético de órgãos sensoriais em diferentes estágios ontogenéticos: larval planctônico e juvenil e adulto bentônicos. Este estudo descreve o desenvolvimento do órgão sensorial na larva de *S. alveolata* o qual tem importante papel no assentamento gregário, que resulta na formação dos

substratos biogênicos, ou recifes. Por fim, o estudo apresentado no apêndice A fornece suporte a todos os outros capítulos.

### **Objetivos específicos**

Predizer possíveis mudanças na distribuição de habitats adequados, avaliar a construção biogênica em condições de acidificação dos oceanos e avaliar respostas fisiológicas e a sobrevivência em condições de hipertermia da água do mar.

#### **Objetivo específico 1:**

Avaliar se a MCA promoverá mudanças na distribuição dos recifes de sabelarídeos (ReSa) tropicais e temperados. Para isso, modelar as distribuições atuais de adequação do habitat e as prováveis futuras, sob as projeções do IPCC-CMIP 5, para dois diferentes intervalos de tempo (metade do século: 2040-2059 e final do século: 2080-2099). Usar como modelos biológicos duas espécies, *Phragmatopoma caudata*, Krøyer in Mörch 1863, e *P. virgini*, Kinberg 1866 que são geneticamente próximas e ocorrem em áreas biogeográficas distintas.

#### **As hipóteses testadas foram:**

- i) sob cenário de baixa concentração de CO<sub>2</sub> e de captação ativa de carbono atmosférico (RCP2.6), os ReSa tropical e temperado manterão suas distribuições atuais, e enfrentarão apenas pequenas alterações biogeográficas multidirecionais ao longo do século; e
- ii) sob um cenário de alta concentração de CO<sub>2</sub> (RCP8.5), ambas as espécies se deslocarão em direção as altas latitudes, com mudanças acentuadas para ReSa tropical e pequenas mudanças para ReSa temperado, especificamente no final do século.

#### **Objetivo específico 2:**

Avaliar se a acidificação dos oceanos (AO) tem efeito na bioconstrução da *Sabellaria alveolata*. Em caso afirmativo, avaliar se as alterações observadas na estrutura e química do bioadesivo correspondem a uma resposta compensatória para manter o desempenho funcional na bioconstrução.



**As hipóteses testadas foram:**

- i) *S. alveolata* poderia manter a síntese e a secreção de bioadesivo para a construção biogênica em futuros cenários de acidificação dos oceanos (pH 7.6 e pH 7.4);
- ii) comparando com o adesivo de organismos expostos a condição dos dias atuais (pH 8.0, controle), os componentes dos aminoácidos e a estrutura do adesivo dos organismos expostos às condições de acidificação dos oceanos (pH 7.6, pH 7.4) poderão apresentar plasticidade;
- iii) as alterações plásticas poderão ser mais acentuadas no adesivo dos tubos construídos pelos organismos submetidos a pH 7.4 do que em pH 7.6.
- iv) os organismos poderiam aclimatar e neutralizar as condições de acidificação dos oceanos, se a plasticidade no processo de bioconstrução permitir um mecanismo compensatório que regule e mantenha o desempenho e a performance do bioadesivo.

**Objetivo específico 3:**

Avaliar se em eventos de simulação de ondas de calor (hipertermia), o perfil de remodelação de lipídios estruturais em *S. alveolata* pode ser usado como índice representativo para o estresse fisiológico e sobrevivência populacional. Em caso afirmativo, avaliar se os dados de remodelação de lipídios estruturais podem ser usados para designar os limites de distribuição de espécies associados à temperatura.

**As hipóteses testadas foram:**

- i) na temperatura mais elevada (34°C), a letalidade seria rapidamente alcançada e os animais não seriam capazes de neutralizar os efeitos térmicos;
- ii) em temperaturas elevadas (28°C e 31°C), as respostas fisiológicas para neutralizar os efeitos térmicos alterariam a composição dos fosfolípidios para sustentar as funções vitais;
- iii) a reestruturação dos lipídios seria mais expressiva em animais expostos a 31°C do que em 28°C, e

- iv) níveis médios mais baixos de índices de insaturação e lipoperoxidação poderiam acontecer em animais expostos ao estresse térmico do que na temperatura de referência, como efeito de diminuição dos níveis de ácidos graxos poliinsaturados (PUFA) em favor de ácidos graxos saturados (SFA) e ácidos graxos monoinsaturados (MUFA).

Assim, testamos se em eventos de hipertermia (HW) a espécie tem capacidade fisiológica de ajustar o estresse metabólico para a sobrevivência. Se assim for, os animais podem aclimatar e provavelmente se adaptarão às futuras condições de mudança climática previsíveis para sua atual área de ocorrência. Alternativamente, se a remodelação lipídica não for ajustada com sucesso, as funções celulares vitais podem falhar, evocando os animais a morte e, portanto, as populações em sua área atual de distribuição estarão, provavelmente, em vulnerabilidade.

### **Objetivos complementares**

Entender a distribuição de recifes construídos por diferentes espécies de sabelarídeos, a interação com processos ecofisiológicos de assentamento e a conectividade de populações.

### **Objetivo complementar 1 (Apêndice A):**

Considerar a distribuição batimétrica e características ecológicas de assentamento larval gregário versus solitário de sabelarídeos, e possíveis relações com a presença, morfologia, plasticidade e significado filogenético de órgãos sensoriais em diferentes estágios ontogenéticos; larval planctônico e juvenil e adulto bentônico.

### **Objetivos específicos foram:**

- i) revisar a informação disponível sobre os órgãos sensoriais anteriores (*i.e.* órgão mediano - MO, *dorsal hump*, palpos) entre os Sabellariidae, considerando atributos ecológicos (*i.e.* habitats, distribuição batimétrica e comportamento de assentamento) e reexaminar espécies descritas para proporcionar dados morfológicos para os palpos e MO;

- ii) reexaminar a variabilidade intra-específica no MO de uma espécie de *Idanthyrus* para testar seu valor como um caracter taxonômico;
- iii) descrever a morfologia dos órgãos sensoriais anteriores, DH e palpos em todo o desenvolvimento ontogenético em uma espécie de sabelariídeo, *Sabellaria alveolata*.

Os órgãos sensoriais em Sabellariidae poderiam evidenciar a habilidade quimiorreceptora altamente desenvolvida para o assentamento gregário, e portanto, a formação de recifes. Ainda, os órgãos sensoriais podem ser úteis para investigações de relações filogenéticas, adaptação morfológica e evolutiva.

#### **Objetivo complementar 2 (Apêndice B):**

Considerar a distribuição do sabelariídeo *Phragmatopoma caudata* (descrito para o Caribe) através da verificação da sinonímia com *Phragmatopoma lapidosa* (descrito para o Brasil) utilizando dados moleculares. Avaliar padrões de diversidade genética e conectividade entre populações da Flórida ao Sul do Brasil.

#### **Objetivos específicos foram:**

- i) examinar se uma única espécie de *Phragmatopoma* ocorre na região do Atlântico Ocidental;
- ii) avaliar se ocorre conectividade genética entre populações de *P. caudata* no Caribe e províncias biogeográficas brasileiras;
- iii) avaliar a eficácia de barreiras biogeográficas putativas na conectividade de *P. caudata*.

O capítulo I e os apêndices A–B estão publicados, e a formatação destes estudos estão padronizadas conforme as regras dos respectivos periódicos.



“Predictive modeling is the art of merge math, statistic and ecology, but it may not be perfect. It is a potential prediction which accuracy will be given by nature.”

(Larisse Faroni-Perez, 2017)



**CLIMATE AND ENVIRONMENTAL CHANGES DRIVING  
IDIOSYNCRATIC SHIFTS IN THE DISTRIBUTION OF  
TROPICAL AND TEMPERATE WORM REEFS**

**Running head:** Biogeographic shifts of worm reefs

Larisse Faroni-Perez

*Published in the*  
Journal of the Marine Biological Association of the United Kingdom

Faroni-Perez, L. (2017). *Journal of the Marine Biological Association of the United Kingdom*, 97, 1023–1035. doi:10.1017/S002531541700087X





## Abstract

An increasing number of studies have forecasted the potential responses of marine life to future climate change. This study predicts how distributional range of temperate and tropical worm reefs (**WRs**) might respond to climate and environmental changes (**CECs**). Compared to current distributions, the tested hypotheses were: *i*) under a low CO<sub>2</sub> concentration and active atmospheric carbon capturing scenario (RCP2.6), both species, tropical and temperate **WRs**, will maintain their current distributions and face only slight multi-directional biogeographical changes along the century; and *ii*) under a high CO<sub>2</sub> concentration scenario (RCP8.5) **WRs** will shift toward higher latitudes, with marked changes for tropical species and slight changes for temperate species, specifically at the end of the 21st century. The hypotheses were tested using species distribution modelling, and exploratory statistical analyses were performed to tune model settings. Under scenario RCP2.6, in the middle of the century, areas of suitable habitat are predicted to slightly increase for the temperate **WRs** and conversely contract for tropical **WRs**. At the end of the century, multi-directional shifts without range retraction were predicted for both species, but tropical **WRs** showed major changes in their distribution. Under scenario RCP8.5 and throughout the century, multi-directional shifts increased the areas of suitable habitat for temperate **WRs**, whereas tropical **WRs** experienced shifts toward high latitudes and significant retraction at low latitudes. Results indicate that biogeographic range shifts are idiosyncratic for temperate and tropical **WRs** depending on the **CECs** scenarios considered.

**Keywords:** Annelida, biodiversity conservation, climate velocity, global changes, IPCC-AR5, local extinction, niche partitioning, ocean acidification, ocean warming, range edge, Sabellariidae.



## Introduction

Climate and environmental changes (CECs) have synergistic impacts on marine ecosystems (e.g. altering temperature, ocean circulation, nutrient concentrations, and sea water pH) and can drive spatio-temporal changes in the distribution and abundance of species, with cascading effects on ecosystem functioning (Harley *et al.*, 2006; Hoegh-Guldberg & Bruno, 2010; Burrows *et al.*, 2011; Gattuso *et al.*, 2015). The expected sign of CECs on marine life reaches from genetic and physiological adaptations to distributional shifts (Harley *et al.*, 2006; Poloczanska *et al.*, 2013; Gotelli & Stanton-Geddes, 2015). Under climate and environmental changes, the general prediction for marine and terrestrial species distribution, based on observations and theories, is a shift towards high latitudes, where more favourable conditions might exist, or alternatively, multi-directional distribution shifts are expected to occur (Burrows *et al.*, 2011; VanDerWal *et al.*, 2013; García Molinos *et al.*, 2015; Lenoir & Svenning, 2015). Marine organisms are valuable to assessing the possible impacts and magnitude of CECs on species distribution (Monaco & Helmuth, 2011; Riebesell & Gattuso, 2015); one such example is ecosystem engineers, organisms that create and provide persistent habitats for the associated biodiversity (Jones *et al.*, 1997; Coleman & Williams, 2002). Understanding the responses of such species under CEC scenarios has become a challenge for marine ecologists. Moreover, it is crucial forecasting possible shifts in the distributional range of ecosystem engineers under CEC (Przeslawski *et al.*, 2008).

A number of approaches (e.g. laboratory and field studies, long-term multigenerational experimental research, and modelling) have been used to assess the impacts of CECs on marine biodiversity (Wernberg *et al.*, 2012; Andersson *et al.*, 2015; Riebesell & Gattuso, 2015). Numerical model simulations of species distribution generate crucial predictive models that can be useful for conservation planning (Andersson *et al.*, 2015). There is strong evidence that recent observations of sea urchin and fish distribution shifts support modelling forecasts (Poloczanska *et al.*, 2016). Although there are some examples of modelling studies using multiple drivers and multiple scenarios showing shifts in marine biodiversity in the global scale (Jones & Cheung, 2015; García Molinos *et al.*, 2015) or considering ecosystem engineer organisms (Couce *et al.*, 2013), there have been few attempts to forecast climate-driven impacts on tropical and temperate species on a large geographical scale (Saupe *et al.*, 2014). Previous modelling

studies have indicated that the expected effects on the distribution of marine organisms are as follows: i) species will exhibit poleward shifts in their distribution, ii) tropical species will be highly vulnerable due to the contraction of suitable habitats, and iii) the geographic distribution of suitable habitats will decrease more quickly and markedly under a scenario with high CO<sub>2</sub> concentrations (García Molinos *et al.*, 2015; Jones & Cheung, 2015). Alternatively, within groups of solely tropical or temperate species, no consistent pattern among species would occur due to varied responses in the direction of shifts or an increase/decrease in the suitable area (Saupe *et al.*, 2014). Although in recent years a large number of modelling studies have shown distributional shifts under CECs, this approach is not yet common to assess the responses in closely related ecosystem engineer species.

In temperate and tropical coastal areas around the world, some species of sabellariids build the so-called worm reefs (**WRs**) (Zamorano *et al.*, 1995; Dubois *et al.*, 2002; Bremec *et al.*, 2014; Faroni-Perez, 2014; Firth *et al.*, 2015; Nishi *et al.*, 2015; Faroni-Perez *et al.*, 2016), which are important biogenic structures, following hermatypic corals and stromatolites (Goldberg, 2013). **WRs** represent habitats of high biodiversity on which hundreds of species of invertebrates and fishes rely for feeding, nursery, refuge and migration (Gherardi & Cassidy, 1994; Dubois *et al.*, 2002; Ataide *et al.*, 2014). There is strong evidence, based on historical and recent surveys that the distribution and abundance of **WRs** are already changing in response to recent CECs (Firth *et al.*, 2015). In the present study, multiple drivers and scenarios were used to target future biogeographic changes in the distribution of two species of polychaetes of the Sabellariidae family that are ecosystem engineers (Coleman & Williams, 2002). Among the sabellariids, the genus *Phragmatopoma* is endemic to the American coastline, contains four valid species and is mainly registered in intertidal and shallow subtidal zones (Capa & Hutchings, 2014; Faroni-Perez *et al.*, 2016). Here, the focus was on two reef-building species, *Phragmatopoma caudata*, Krøyer in Mörch 1863, and *P. virgini*, Kinberg 1866, as they are genetically close related and occur in distinctive areas (Nunes *et al.*, 2016). In terms of marine biogeographic provinces (Briggs & Bowen, 2012), *P. caudata* occurs in the tropical regions of the Western Atlantic, ranging from the Florida coast to the southern coast of Brazil, whereas *P. virgini* occurs in the temperate regions of Southeast Pacific Ocean ranging from Ecuador to Patagonia and toward north up to Uruguay in Southwest Atlantic Ocean.

Therefore, in order to assess if **CECs** will cause distribution shifts in tropical and temperate **WRs**, present-day habitat suitability distributions were modelled, as well as under IPCC-CMIP 5 projections for two different time intervals (mid-century: 2040–2059 and late-century: 2080–2099). The tested hypotheses was as follows: i) under a low CO<sub>2</sub> concentration and active atmospheric carbon capturing scenario (RCP2.6), both tropical and temperate **WR** species will maintain their current distributions and face only slight multi-directional biogeographical changes across the century; and ii) under a high CO<sub>2</sub> concentration scenario (RCP8.5), both species will shift toward high latitudes, with marked changes for tropical **WRs** and slight changes for temperate **WRs**, specifically at the end of the century.

## **Materials and Methods**

### **Datasets: Species occurrences and environmental predictors**

For the dataset of species occurrences, an extensive online search was performed using the keyword '*Phragmatopoma*' in various reference databases (i.e. Web of Science, SCOPUS, SciElo, Google Scholar), the catalogue of the Smithsonian National Museum of Natural History, and the NONATOBBase (Pagliosa *et al.*, 2014). Additionally, original data on 57 new records was added to the dataset. Each occurrence data was georeferenced (WGS84) and record sites with low accuracy were discarded to reduce noise in the analysis. Overall, 97 literature sources were included in the analysis, resulting in 284 and 94 occurrence records for *P. caudata* and *P. virgini*, respectively.

The primary datasets of environmental drivers used are from the Coupled Model Intercomparison Project Phase 5 (IPCC, 2013; <http://cmip-pcmdi.llnl.gov/cmip5/>). The model selected was the HadGEM2-ES, from Met Office Hadley Centre, UK (Jones *et al.*, 2011; Martin *et al.*, 2011). Global climate model provided by HadGEM2-ES includes all components of the earth system (i.e. physical atmosphere and ocean components with the addition of schemes to characterize aspects of the Earth system) (Collins *et al.*, 2011; Martin *et al.*, 2011; Zelinka *et al.*, 2013), and have been used to forecast shifts in distribution of marine and terrestrial species (Good *et al.*, 2013; Saupe *et al.*, 2014; García Molinos *et al.*, 2015; McQuillan & Rice, 2015; Xavier *et al.*, 2016). The monthly *output* data of the concentration of carbon, chlorophyll, dissolved nitrate, ammonium and silicate, hydrogen ion, alkalinity, air and sea surface temperature, precipitation, salinity

and water runoff was acquired from HadGEM2-ES (Table 1). The dataset was divided into a ‘current’ period, which included the recent past (1986–2005), whereas future projections for the Representative Concentration Pathways (RCPs) 2.6 and 8.5 were subdivided into the ‘middle of the century’ (i.e. mid-century 2040–2059) and the ‘end of the century’ (i.e. late-century 2080–2099). These future projections represent contrasting scenarios: the RCP2.6 characterizes the optimistic and environmentally friendly future with low CO<sub>2</sub> concentrations, and the RCP8.5 represents the worst-case scenario with the highest CO<sub>2</sub> concentrations. Each environmental predictor was rescaled to a resolution of 0.08° × 0.08°, using bi-linear interpolation. Additionally, for each predictor, the interannual monthly mean was calculated from the primary data. The annual values (average, minimum and maximum) were then calculated totalling 36 environmental drivers layers (see supplementary material).

### **Selection of predictors**

The predictors, here classified according to the use of the source by the worms (i.e. biogenic, osmotic, thermal, and trophic; see Table 1), were selected based on environmental variables representative of the key dimensions of the niche for the studied species (Austin, 2007). This multi-dimensional niche approach was used as a step selection of variables that can influence the distribution of *Phragmatopoma* species. Following a hierarchical framework to reduce multi-collinearity, an array of a peer-to-peer correlation matrices using the set of layers from the ‘current’ time period was created that excluded highly correlated predictors (Pearson,  $r > 0.60$ ). After this step, only nine out of initially 36 predictors remained, two for each niche dimension, except the trophic, which had three predictors per species. Subsequently, to select for each species the most representative predictor for each pre-established niche dimension, a set of generalized linear models (GLMs) were built, exploring the possible combinations of variables and considering one predictor per niche. The final sets of niche predictors per species were assessed by the most influential predictive capacity across models. The predictive capacity was ranked based on a number of times a given predictor was significant across GLM models (see supplementary material). Final layers of predictors selected are as follow: pHmin (biogenic) and tosmin (thermal) for both the species, and frivermax (osmotic), simax (trophic) selected for *P. caudata*, and prmax (osmotic) and detocmax (trophic), for *P. virgini*. Predictors’ names and

units are described in Table 1. Statistical analysis of these layers can be found in the supplementary material.

## Modelling

Maximum entropy modelling (MaxEnt) was used to model the current distributions of *P. caudata* and *P. virgini* and then project their future habitat suitability according to the future IPCC-CMIP 5 projections. MaxEnt is a correlative algorithm that uses the occurrence data of species coupled to environmental data for modelling species distributions (Phillips *et al.*, 2006; Phillips & Dudik, 2008; Elith *et al.*, 2011) and can be used to predict the future impacts of CECs on marine organisms (Couce *et al.*, 2013; Verbruggen *et al.*, 2013; Saupe *et al.*, 2014). Generally, the models produced by MaxEnt are influenced by the extent of the study area and species occurrence, which are data input premises. Thus, the MaxEnt algorithm performs better when the study area for the calibration model does not include areas outside the species range occurrence (Anderson & Raza, 2010; Elith *et al.*, 2011). For this reason, the model is calibrated with the immediately surrounding region for each species known occurrence. Subsequently, the background area of each species was referred strictly to the occurring latitudinal span and longitudinally delimited by the closest cell grid representing the continental shoreline, as the two species inhabit the intertidal or shallow subtidal zones. Additionally, the OccurrenceThinner (Verbruggen *et al.*, 2013) was used to filter the data and reduce the geographical sampling bias since MaxEnt better estimates the contribution of the niche environmental variables for each species, when not overestimating the model performance (Elith *et al.*, 2011; Veloz *et al.*, 2013). OccurrenceThinner uses the occurrence records and a raster of a kernel density function of the study area to reduce occurrence records, omitting more records from densely sampled regions. This filtering resulted in 42 and 21 occurrence records for *P. caudata* and *P. virgini*, respectively.

For the species-specific model tuning, various potential sources of complexity from the MaxEnt features were investigated, considering methods proposed by Elith *et al.*, (2010; 2011), Shcheglovitova & Anderson, (2013) and Radosavljevic & Anderson, (2014) (see supplementary material). Then, the fitted model was assessed based on the performance of explanatory predictors and MaxEnt features. The maps and results reported herein are based on the MaxEnt average (5 runs), cross-validated, logistic output, and with the clamping setting as true. The model predictions were tested by partial receiver operating

characteristic analyses (*p*-ROC AUC) with  $E = 0.5$  of the maximum error rate, 50% random points and 500 iterations for the bootstrap (Peterson *et al.*, 2008; Peterson, 2012).

## Post modelling

To quantify the shifts in the distribution of tropical and temperate **WRs**, a metric based on total grid cell values (i.e. each pixel suitability) was applied. The total numbers of grid cells were 4,515 for *P. caudata* and 3,322 for *P. virgini*. For each projection, grid-cell values were extracted and frequency distribution and the delta value were computed. The delta value is the relative difference in total grid-cell frequencies between each future projection and the present day. Although the threshold of minimum training presence values was 0.11 for *P. caudata* and 0.09 for *P. virgini*, the threshold value of 0.2 was set to define unsuitable areas, pixel values  $\leq 0.2$  are included in the non-suitability category (see supplementary material). Consequently, changes in delta values correspond to a gain or a loss of suitable area. The remaining grid cells (i.e. pixel values: comprised between 0.21 and 1) correspond to the suitable area, and for which changes in the delta value were categorized as follows:  $0.21 \leq \text{low} \leq 0.4$ ;  $0.41 \leq \text{medium} \leq 0.6$ ;  $0.61 \leq \text{high} \leq 0.8$ ;  $0.81 \leq \text{very high} \leq 1$ . This analysis attempted solely to characterize and quantify ‘potential’ shifts in the distribution of each species based on their areas of environmental suitability.

## Processing all modelling

All software used in this study is listed in supplementary material.

## Abbreviations

**CECs:** Climate and environmental changes.

**WRs:** Worm reefs built by Sabellariidae.

**RCPs:** Representative concentration pathways; radiative forcing values for scenario set, containing emission, concentration and land-use trajectories (van Vuuren *et al.*, 2011)

**RCP2.6:** Mitigation scenario leading to a very low forcing level.

**RCP8.5:** Very high baseline emission scenario.



## Results

### Modelling analysis and contribution of multiple drivers

MaxEnt models showed good predictive performances for the models (Table 2). For the present-day period, the predicted areas of suitable habitat were in agreement with the current distribution of both species. The current areas of suitability cover 44.7% and 60.8% of the total extent of *Phragmatopoma caudata* and *P. virgini*, respectively. For both species, the predictors regarding the trophic and osmotic niches showed an intermediary influence in the model, although they had an inverse influential order (Table 3). The most influential predictor for both species was sea surface temperature (tos), related to the thermal niche. In contrast, pH (related to the biogenic niche) showed the lowest contribution to the model for both species (Table 3).

### Future trends of habitat suitability for worm reefs

All models predicted future differences in the distribution of habitat suitability for tropical and temperate **WRs** (Figure 1). For the 'optimistic scenario' (RCP2.6), in contrast with the current distributions of both **WRs**, a gain of suitable areas was predicted for the end of the century. However, idiosyncratic responses were forecasted; in the mid-century, tropical **WRs** would lose area, while temperate **WRs** would gain area. At the end of the century, tropical **WRs** would markedly increase their distribution, while temperate **WRs** would slightly lose area compared to mid-century situation (Figure 1). Under the 'business as usual' scenario (RCP8.5), which predicts the highest temperature increase, models also showed idiosyncratic responses of tropical and temperate **WRs** (Figure 1). Tropical **WRs** tend to lose suitable areas across the century, and a majority of changes would occur up to the mid-century. In the 50s, it is expected that non-suitable areas increase by 13.84% for a total of 16.48% in 90s (Table 4). The temperate **WRs** tend to gain suitable areas throughout the century and by the end of the century, all biogeographic areas would be suitable (Table 4). However, the major gain would occur up to the mid-century.

## Biogeographic shifts

### *Tropical worm reefs*

In contrast to the current distribution, the RCP2.6 model shows opposite shifts during the century for *P. caudata* (Figures 1, 2A–C). In the middle of the century, the model projected a reduction of the suitable area (~8%) in the Caribbean region, Venezuela and the northern Gulf of Mexico due to the loss of grid cells with low and medium classes of suitability. On the other hand, increments in high (~8%) and very high (~3%) classes of habitat suitability were found along the east coast of Brazil and the western part of the Gulf of Mexico (Figure 2B). Interestingly, for the end of the century, the model predicted more advantageous conditions with increasing areas and potential suitability, demonstrating the potential of species range expansion. With respect to the total area predicted as suitable, the models showed an increase from ~45% to ~69%. It is noteworthy that in the late century, 24% out of these 69% suitable areas are expected to reach the classes of high and very high suitability (Table 4). In general, areas largely in the Caribbean region, the West Indies, the western coast of the Gulf of Mexico and the coast of Brazil are herein projected as suitable (Figure 2C), with only small gaps of non-suitable areas in northern South America and the northern part of the Gulf of Mexico.

Under the RCP8.5 model, a considerable contraction was observed of the total area of potential distribution from the current (~45%) to the middle (~31%) and the end of the century (~28%; Figure 2A, D–E; Table 4). In general, an increase of non-suitable areas is projected for the entire northern part of South America, the Caribbean region, the West Indies, and the southwestern and northern parts of the Gulf of Mexico. Furthermore, of the total remaining suitable area, a significant amount is classified into the low and medium classes of suitability (mid-century: ~21%, late-century: ~14%; Table 4), demonstrating vulnerability due to a massive loss of suitability. Finally, the remaining suitable areas with high and very high classes of suitability (mid-century: ~10%, late-century: ~14%) are projected for the northwestern region of the Gulf of Mexico and the southeastern part of Brazil (Figure 2D–E).

### *Temperate worm reefs*

Under the RCP2.6 modelling outputs, *Phragmatopoma virgini* showed a gradual trend of a spreading distribution with increasing values of the potential suitability of habitat over the century (Figure 3A–C; Table 4). It is noteworthy that in contrast to present-day conditions, the suitability increases by 17.25% by the mid-century, reaching 78% of potential habitat suitability over the biogeographic province. Overall, projected areas that gain suitability are found towards the north of Peru and South Patagonia (Argentina and Chile), demonstrating multidirectional distribution shifts. In contrast to the mid-century, a slight increment (~2%) of the area of suitability for the end of the century was found. Furthermore, increasing values in the potential suitability for the low (~13%–10%) and high (~5%) classes was observed throughout the century, regardless of a slight loss (1.6%–0.75%) of the medium, indicating that *P. virgini* might retain its distributional range under this optimistic scenario. The biogeographic areas with increases in potential suitability were Ecuador, along the Peru coastline, and in Chile, mainly for the central part at the Regions III–VII (i.e. Atacama, Coquimbo, Valparaíso, O'Higgins and Maule).

Under the RCP8.5 model, a gain of suitable areas during the century was also predicted (Figure 3A, D–E; Table 4). The projections show that by mid-century, 83.2% of the biogeographic province will be suitable for *P. virgini*. In this period, increases in the classes of low (~16%) and high (~10%) suitability were projected, notably demonstrating species gain in suitable distribution. The potential suitability is expected to increase along the coast of Ecuador, Peru and Chile (i.e. north and central coast) in the Pacific Ocean and in Uruguay and Argentina (i.e. Buenos Aires towards south of Chubut) in the Atlantic Ocean. In general, only small gaps of remaining non-suitable area in Southern Chile (i.e. Regions XI Aisén and XII Magallanes and Antartica Chilena) and Argentina (i.e. Tierra del Fuego and Santa Cruz) were observed. Finally, regarding the projection for the end of century, no grid cell is projected to be a non-suitable area, indicating that all of the *P. virgini* biogeographic provinces will be potentially suitable. Coupled to this evident gain of suitable area, the increments were projected into the medium (~10%) and high (~20%) classes of suitability.

## Discussion

Biogeographic shifts of temperate and tropical worm reefs (**WRs**) are idiosyncratic to the climate and environmental change (**CECs**) scenarios considered. Overall, models showed an increase in suitable habitats for temperate **WRs**, with a varying magnitude depending on scenarios and time periods. For the tropical **WRs**, responses were generally more antagonistic, also depending on the scenario and period considered. This study was the first attempt at modelling the future distribution of polychaetes using multiple drivers under IPCC-CMIP 5 scenarios. Even though the values from different modelling approaches should not be comparable (Guillera-Arroita *et al.*, 2015), projections from a previous study using multiple drivers under IPCC-CMIP 5 scenarios have also shown that among marine invertebrates, idiosyncratic responses to **CECs** are expected to occur (Saupe *et al.*, 2014).

The assumptions for temperate and tropical **WRs** under RCP2.6 and RCP8.5 scenarios did apply only in part. To clarify, under RCP2.6, multi-directional changes in habitat suitability would occur, but projections showed that at the end of the century, the magnitude of changes is either slight or marked for the temperate and tropical **WRs**, respectively. Additionally, in the case of scenario RCP8.5, marked changes in the distribution pattern were observed across the century for both species, but a consistent southward shift with suitable retraction at low latitudes was found for tropical **WRs** only, whereas temperate **WRs** exhibited continuous multi-directional shifts. Therefore, the present results suggest that the common assumptions of higher latitude range shifts cannot be globalized, as the level of **CEC** conditions (i.e. the different scenarios and regional impacts) and species tipping points (i.e. tropical, temperate or, pandemic) also need to be considered.

## Environmental variables and insights into scales

In the present models, drivers' contribution rates differed between congeners, corroborating previous studies, which showed that **CECs** would not equally impact distinct biogeographic regions (Brierley & Kingsford, 2009), and that temperate and tropical species would have different responses. Tropical species are expected to be more vulnerable than temperate ones (Rosa *et al.*, 2014). Although demonstrating different patterns for either reef builder, sea surface temperature was the most important predictor, whereas pH played a

minor role in explaining the distribution of suitable areas. This result is congruent with previous modelling studies conducted for bio-engineering corals (Couce *et al.*, 2013). However, it is possible that the model could have underestimated the role of pH for **WRs** habitat suitability. In the absence of actions to reduce CO<sub>2</sub> emissions, within the next few decades, seawater pH values represent a negative impact for marine invertebrates (Orr *et al.*, 2005; Shirayama & Thornton, 2005). Furthermore, the underwater solidification of cement used by sabellariids to build their tubes, and, consequently, the reefs, appears to be initially dependent on pH differences between the worms' secretory glands and seawater (Stevens *et al.*, 2007; Wang & Stewart, 2012). Further experiments are required to better assess the vulnerability of **WRs** to pH under future ocean acidification scenarios and shed light on the accuracy of models to predict the impact of low pH on shifts of species distribution. The projected increase of CO<sub>2</sub> into the atmosphere and subsequent environmental changes throughout this century will enhance either risks: the vulnerability of tropical **WRs** at low latitudes and the spread of temperate **WRs** at high latitudes, both of which will have cascading effects on ecosystem functioning. Although warming seawater by itself would not be the unique driver to constraining biodiversity (Gattuso *et al.*, 2015), the thermal predictor had the highest contribution to models.

Species distribution models and the method herein used consider that occupied grid cells estimate suitable environmental conditions, and the set of abiotic traits in these occupied cells is more favourable than adjacencies as unoccupied cells and unlike abiotic traits. The geographic scale dealt in this study encompasses large a part of the American continents. Both worm species modeled have wide-range distribution at the continental scale, indicating that differences in local and micro-habitat variables plays relative lower importance in understanding and predicting species distribution at larger spatial scales. Spatially, the predictor layers used in this study provide sensible results at continental scales that are not necessarily accurate to local scale. Care should be applied to considerations about suitable pixel and grid cell size due to some peculiarities at fine scale, which might not be favourable for these species considering biotic (e.g. tipping points and intrinsic settlement ability) and abiotic factors (e.g. substratum availability). For example, in a grid cell a river runoff can drop coastal marine salinity to unfavourable values. In fact several **WRs** occur in costal areas adjacent to estuaries (see in Faroni-Perez, 2014; Aviz *et al.*, 2017, Eo *et al.*, 2017). During low tides **WRs** can cope with rain.

Therefore, **WRs** often undergo salinity fluctuation (i.e. eurihaline to mesohaline), but no empirical data indicate that continually low salinity values (i.e. mesohaline to oligohaline) are favourable. The species modeled have wide-range distributions, however, at local spatial scales **WRs** do not have a homogeneous distribution. For example, low recruitment ratios in *P. caudata* were associated to cold fronts passage that dispersed larvae along coastline (Faroni-Perez, 2014). Although larvae can drift to different locations, they have preferences to settle gregariously onto specific substrata, a behavior associated to sensory organs (Faroni-Perez *et al.*, 2016). Larvae settle preferentially on existing reef or hard substrata, and substratum trait (type, density, over area, heterogeneity) might exert significant influence on the models. However, marine species distribution modeling lacks high resolution intertidal geological layers encompassing the American continents and hence this predictor was not considered in the present study. In some places around the world sabellariids reefs can be found directly on soft bottoms (Faroni-Perez *et al.*, 2016), but that is not common among species of the genus *Phragmatopoma*.

Present results indicated that distribution shifts in **WRs** would occur. Studies have demonstrated that cost-effective methodological approaches, such as scaling up (Ferrari *et al.*, 2016; González-Rivero *et al.*, 2016), can be applied to target regional areas (e.g. 10–10,000 km) toward acquiring empirical data on distribution shifts. Further studies are encouraged to use the scaling up approaches for monitoring **WRs** and its associated biodiversity by a well-established temporal assessment as a key measure to detect distribution shifts as response to short-term **CECs** events, such as heat waves or cold waves. Global impacts of **CECs** on marine biodiversity are inevitable (Harley *et al.*, 2006; Poloczanska *et al.*, 2014, Gattuso *et al.*, 2015), and identifying them as a matter of urgency would promote better strategies for management actions attempting to reduce the adverse effects for biodiversity conservation.

### **Tropical and temperate worm reefs under the RCP2.6**

Under the optimistic scenario, projections of suitable areas will persist for congeners at end of the century, indicating the benefits for **WRs** to guarantee range maintenance. Similar results of suitable area persistence were found for the gastropods *Bulla occidentalis* and *Conus spurius* (see Table S2.1, MaxEnt, all variables in Saupe *et al.*, 2014;), and interestingly, the range of these mollusks co-occurs with tropical *P.*

*caudata*. Across the century, temperate reefs will continually gain suitable areas, whereas tropical reefs will face an initial reduction up to the middle of the century followed by recovery and the gain of newly suitable areas at the end of the century. A decrease in habitat suitability up to the middle of the century followed by a recovery in suitability were also found for several tropical and temperate mollusks, such as *Anomia simplex*, *Dinocardium robustum*, *Lucina pensylvanica*, *Conus spurius*, *Crepidula fornicata*, *Melongena corona*, *Oliva sayana*, *Strombus alatus*, and *Terebra dislocata* (see Table S2.1, MaxEnt, all variables, 2041–2060 and 2081–2100 in Saupe *et al.*, 2014). These projections appear very likely when taking into account that RCP2.6 scenario anticipates that increasing greenhouse gas emissions will peak in the middle of the century, with a subsequent drop to zero due to low emissions and the active removal of atmospheric greenhouse gases (IPCC, 2013). Then, under this peak-and-decline scenario, biodiversity will face alterations in the environment, which are expected to result in mild changes. Moreover, the present results are also consistent with a previous study, which showed that shifts by the middle of the century (2040–2059) will be much slower under the RCP2.6 scenario compared to the RCP8.5 scenario (Jones & Cheung, 2015). This highlights the importance of promoting effective actions on carbon emission reduction and minimizing the impacts on biodiversity.

Multi-directional shifts will be expected at the end of the century for both temperate and tropical **WRs**, and potential cascading effects are not likely to occur. Therefore, the majority of the new area will have a low class of potential habitat suitability. For instance, for tropical **WRs**, most of the projected gain in suitability will occur in the Caribbean region, but it is not evident that **WRs** will spread toward that area. Firstly, these areas are hotspots of biodiversity well known for their tropical coral reefs and fish communities (Floeter *et al.*, 2008), and sessile organisms undergo high rates of space competition (Lopez-Victoria *et al.*, 2006). Secondly, as experiments have demonstrated polyps can survive under this optimistic scenario (Fine & Tchernov, 2007), coral reefs may not face high mortality, and space competition rates would remain high, minimizing chances for the larval settlement of sabellariids. Thirdly, in the Caribbean region, many constraints prevent the establishment of **WRs**, a reason why they commonly do not occur where coral reefs exist (Goldberg, 2013). Overall, under this environmental friendly scenario, results indicate some crucial perspective: temperate and tropical **WRs** will not have their existence threatened, which benefits the associated fauna as well. There is not

much evidence of negative cascading effects for the established community.

### **Tropical and temperate worm reefs under RCP8.5**

Under the business-as-usual scenario, projections of suitable areas will markedly decrease for tropical **WRs** and increase for temperate **WRs**, either case indicating crucial issues for ecosystem functioning. The singular pattern of changes between congeners can be related to species-specific responses under future variability in the conditions of multiple drivers (Poloczanska *et al.*, 2013). Some marine species can have plastic responses, such as thermal acclimation (Somero, 2002; Helmuth *et al.*, 2006), a phenomenon particularly common in invertebrates with planktonic dispersal (Sanford & Kelly, 2011). Temperate (i.e. cold-water adapted) species are supposed to be more tolerant to global warming compared to their tropical (i.e. warm-water adapted) counterparts, mainly because the latter live close to their thermal tolerance limits (Tewksbury *et al.*, 2008; Somero, 2010; Nguyen *et al.*, 2011). This could support the habitat persistence and amplification of temperate **WRs** and the range contraction at the tropics found for tropical **WRs**. The response found for temperate **WRs**, however, is not uni-directional and may promote spatial homogenization, since habitat suitability amplifies across the whole biogeographic province. **CECs** promote a trend towards spatial homogenization of marine communities due to species distributional shifts or even decreases in survivorship rates (Garrabou *et al.*, 2009; García Molinos *et al.*, 2015). For instance, several marine organisms were affected by mass mortality events or have retracted their distribution ranges, whereas others have extended their distribution, mostly followed by recent climatic anomalies, such as heat-waves and winter storms (Garrabou *et al.*, 2009; Wernberg *et al.*, 2012; Firth *et al.*, 2015).

At the end of the century, the majority of areas at low latitudes will become unsuitable for tropical **WRs**, most likely due to **CEC**-mediated shifts of distribution towards higher latitudes. This result matches predictions that the impacts of **CECs** would be severe in the tropics (Tewksbury *et al.*, 2008; Poloczanska *et al.*, 2013). Poleward expansion and equatorial contraction in distribution were also found by modelling coral reefs (Couce *et al.*, 2013). Currently, **CECs** are already causing distribution shifts towards higher latitudes in several tropical marine species, from phytoplankton to fishes (Wernberg *et al.*, 2011;



Poloczanska *et al.*, 2014). The loss of suitability in the tropical Western Atlantic Ocean predicted for tropical **WRs** will likely mediate cascade effects on local communities. Consequent to a **WR** range contraction at low latitudes, associated species are also expected to decline due to a loss of habitat. Generally, present results corroborate several modelling forecasts for the distribution of fishes, bio-engineering corals and other invertebrates, demonstrating a marked decline in habitat suitability in tropical regions that would promote local extinction (Cheung *et al.*, 2009; Couce *et al.*, 2013). Then, since hotspots of biodiversity are mainly located in tropical and subtropical areas (Brown, 2014), model predictions indicate grave ecological issues for ecosystem functioning, and marine biodiversity at low latitudes will be threatened.

The projected range extension of temperate **WRs** would incorporate ecological issues for local communities. For example, heat-tolerant species can display plastic responses to **CECs** or even be able to shift their ranges over time for new latitudes tracking thermal niches (Somero, 2002). Within the genus *Phragmatopoma*, life-history traits indicate they are r-strategists. For instance, **WRs** can have an average of 65,000 individuals/m<sup>2</sup> (Faroni-Perez, 2014) with each female able to spawn 1,500-2,000 oocytes (McCarthy *et al.*, 2003), and the dispersal and substrate colonization rates by juveniles are high (Zamorano *et al.*, 1995; Faroni-Perez, 2014). Moreover, **WRs** can dominate the substratum and exclude less competitive species (Taylor & Littler, 1982). Therefore, it is likely that *P. virgini* will have the ability to persist and colonize new suitable sites along the South-American coasts, which would promote negative cascading effects. Since **WRs** provide ecosystem services for many organisms, it is very likely that the associated species may also extend their ranges by tracking the existence of reefs. Thus, the multi-directional persistence of temperate **WRs** might facilitate the dispersion and biological invasions of the associated fauna into new territories. Some potential biological invasions in marine ecosystems promoted by **CECs** have already been reported, for example to solitary and colonial ascidians and encrusting bryozoans (Stachowicz *et al.*, 2002), and it is suggested that they will be more intense at high latitudes (Cheung *et al.*, 2009; de Rivera *et al.*, 2011). Another plausible issue is that if dense aggregations of **WRs** can exert physical pressure resulting in space competition (Taylor & Littler, 1982), then the population dynamics of pre-established adjacent organisms such as algae, anemone and molluscs will face disturbances. Thus, the enlargement of habitat suitability found for temperate **WRs**

may drive key changes in community composition and productivity by outcompeting sensitive species.

In the Atlantic Ocean, **WRs** formed by the tropically distributed *P. caudata* are flanked in the south by *Sabellaria nanella* followed by *P. virgini*. End of century projections forecasted a southward increase in habitat suitability for *P. caudata* and a northward increase in habitat suitability for *P. virgini*, making all three taxa potentially overlap their distributions around latitudes 25° and 40°S. The future trend towards sympatry among these three western Atlantic sabellariids represents an interesting ecological scenario. There is a potential for reef forming organisms to coexist through spatial and temporal niche partitioning (Knowlton & Jackson, 1994). Sympatry can drive novel patterns of resource utilisation and habitat occupation. Some sympatric gregarious sabellariids species are known to exist in the same reef habitats, e.g. *Neosabellaria cementarium* and *Idanthysus ornamentatus* (Posey *et al.*, 1984; Pawlik & Chia, 1991), but mostly **WRs** are biogenic structures of a single species. Among **WRs**, spatial niche tuning can be mediated by pelagic-benthic processes through the larvae sensory organs and the intrinsic ability to select specific reef microhabitats to settle (Pawlik & Chia, 1991; Faroni-Perez *et al.*, 2016). Moreover, zonation preferences can lead to local niche partitioning. For example, the majority of *S. nanella* records come from subtidal areas, although recently some records have been noted in the intertidal (Bremec *et al.*, 2014), while the majority of *P. caudata* and *P. virgini* records are from the intertidal. Niche overlap between species has been described to **WRs** such as between *N. cementarium* and *I. ornamentatus* (Posey *et al.*, 1984) and *Sabellaria alveolata* and *S. spinulosa* (Holt *et al.*, 1997). Temporal niche partitioning can also occur through physiological and reproductive strategies. For example, biological rhythms of gametogenesis, spawning and recruitment can be different in phylogenetically closely related sabellariids (see in Eckelbarger, 1979; McCarthy *et al.*, 2003; Faroni-Perez, 2014; Faroni-Perez & Zara, 2014; Culloty *et al.*, 2010; Aviz *et al.*, 2017). Another possible outcome of the potential future distributional overlap is the formation of a hybrid zone. In the laboratory, some sabellariids are able to interbreed, for example *Phragmatopoma caudata*, *P. californica*, *Idanthysus ornamentatus* and *Neosabellaria cementarium* (Smith & Chia 1985; Pawlik & Chia, 1991), however developed larvae are abnormal. To date there is no evidence that *P. caudata*, *P. virgini* and *S. nanella* have similar spawning periods and would interbreed *in situ*. Synchronous spawning, interbreeding and hybrid larvae deficiency would reduce fecundity,

leading to local **WRs** decline of one or more species. My results encourage further studies to investigate whether a more finely tuned niche partitioning can support sympatric **WR** species under future **CEC** scenarios.

Overall, the present results highlight that the distribution of two important ecosystem-engineers species will shift, and depending on the future **CEC** scenarios, the species will have idiosyncratic, poleward or multi-directional responses. Although under the more optimistic scenario (RCP2.6), model predictions indicate the minimization of biodiversity loss and abrupt community changes, the predictions for the worst-case RCP scenario (RCP8.5) indicate range retraction/expansion and shifts for the distribution of worm reefs. Finally, it should be considered that in order to make more exact model predictions about the magnitude of multiple-drivers (e.g. salinity, nutrients, and pH) on future species distribution, experimental approaches are needed to resolve potential physiological thresholds and authenticate the modelling calibration.

### **Supplementary materials and methods**

The supplementary material referred to in this article can be found at <https://doi.org/10.1017/S002531541700087X>.

### **Acknowledgments**

The author would like to thank C.F.D. Gurgel, N. Schubert, P. Pagliosa, S. Floeter, for their thoughtful comments on an earlier version of the manuscript. P. Riul was very helpful with sampling bias analysis and environmental predictors. The author is grateful to the anonymous reviewers and the Editor, Dr. A. Holmes, for their constructive comments, which contributed to improving the quality of this paper. The author also acknowledges the Centre for Environmental Data Analysis (CEDA), on behalf of British Atmospheric Data Centre (BADC) and Natural Environment Research Council's (NERC) for access to CMIP5 multi-model dataset.

Financial Support: The author was supported by the National Council for Scientific and Technological Development of Brazil (CNPq – SWE 201233/2015-0) and Coordenação de Aperfeiçoamento de Pessoal de Nível Superior (CAPES). This paper is part of her PhD thesis.

## References

**Andersson, A.J., Kline, D.I., Edmunds, P.J., Archer, S.D., Bednarsek, N., Carpenter, R.C., Chadsey, M., Goldstein, P., Grottoli, A.G., Hurst, T.P., King, A.L., Kübler, J.E., Kuffner, I.B.; Mackey, K.R.M., Menge, B.A., Paytan, A.; Riebesell, U., Schnetzer, A., Warner, M.E. and Zimmerman, R.C.** (2015) Understanding ocean acidification impacts on organismal to ecological scales. *Oceanography* 28, 16–27.

**Anderson, R.P. and Raza, A.** (2010) The effect of the extent of the study region on GIS models of species geographic distributions and estimates of niche evolution: preliminary tests with montane rodents (genus *Nephelomys*) in Venezuela. *Journal of Biogeography* 37, 1378–1393.

**Ataide, M.B., Venekey, V., Rosa-Filho, J.S., and Dos Santos, P.J.P.** (2014) Sandy reefs of *Sabellaria wilsoni* (Polychaeta: Sabellariidae) as ecosystem engineers for meiofauna in the Amazon coastal region, Brazil. *Marine Biodiversity* 44, 403–413.

**Austin, M.** (2007) Species distribution models and ecological theory: A critical assessment and some possible new approaches. *Ecological Modelling* 200, 1–19.

**Aviz, D., Pinto, A.J.A., Ferreira, M.A.P., Rocha, R.M., and Rosa-Filho, J.S.** (2017) Reproductive biology of *Sabellaria wilsoni* (Sabellariidae: Polychaeta), an important ecosystem engineer on the Amazon coast. *Journal of the Marine Biological Association of the United Kingdom* (in press). doi: 10.1017/S0025315416001776.

**Bremec, C., Carcedo, C., Piccolo, M.C., Santos and Fiori, E.S.** (2014) *Sabellaria nanella* (Sabellariidae): from solitary subtidal to intertidal reef-building worm at Monte Hermoso, Argentina (39°S, south-west Atlantic) *Journal of Marine Biological Association of the United Kingdom* 93, 81–86.

**Brierley, A.S. and Kingsford, M.J.** (2009) Impacts of climate change on marine organisms and ecosystems. *Current Biology* 19, R602-R614.

**Briggs, J.C. and Bowen, B.W.** (2012) A realignment of marine biogeographic provinces with particular reference to fish distributions. *Journal of Biogeography* 39, 12–30.

**Brown, J.H.** (2014) Why are there so many species in the tropics? *Journal of Biogeography* 41, 8–22.

**Burrows, M.T., Schoeman, D.S., Buckley, L.B., Moore, P., Poloczanska, E.S., Brander, K.M., Brown, C., Bruno, J.F., Duarte,**

**C., Halpern, B.S., Holding, J., Kappel, C.V., Kiessling, W., O'Connor, M.I., Pandolfi, J.M., Parmesan, C., Schwing, F.B., Sydeman, W.J. and Richardson, A.J.** (2011) The pace of shifting climate in marine and terrestrial ecosystems. *Science* 334, 652–655.

**Capa M. and Hutchings P.** (2014) *Sabellariidae Johnston, 1865*. In Handbook of Zoology Online. Purschke, G. and Westheide, W. (eds) Berlin, Boston: De Gruyter, pp. 1–16.

**Cheung, W.W.L., Lam, V.W.Y., Sarmiento, J.L., Kearney, K., Watson, R. and Pauly, D.** (2009) Projecting global marine biodiversity impacts under climate change scenarios. *Fish and Fisheries* 10, 235–251.

**Coleman, F.C. and Williams, S.L.** (2002) Overexploiting marine ecosystem engineers: potential consequences for biodiversity. *Trends in Ecology & Evolution* 17, 40–44.

**Collins, W.J., Bellouin, N., Doutriaux-Boucher, M., Gedney, N., Halloran, P., Hinton, T., Hughes, J., Jones, C.D., Joshi, M., Liddicoat, S., Martin, G., O'Connor, F., Rae, J., Senior, C., Sitch, S., Totterdell, I., Wiltshire, A. and Woodward, S.** (2011) Development and evaluation of an Earth-System model – HadGEM2. *Geoscientific Model Development*, 4, 1051–1075.

**Couce, E., Ridgwell, A. and Hendy, E.J.** (2013) Future habitat suitability for coral reef ecosystems under global warming and ocean acidification. *Global Change Biology* 19, 3592–3606.

**Culloty S.C., Favier E., Ni Riada M., Ramsay N.F. and O’Riordan R.M.** (2010) Reproduction of the biogenic reef-forming honeycomb worm *Sabellaria alveolata* in Ireland. *Journal of the Marine Biological Association of the United Kingdom* 90, 503–507.

**de Rivera, C.E., Steves, B.P., Fofonoff, P.W., Hines, A. and H.Ruiz, G.M.** (2011) Potential for high-latitude marine invasions along western North America. *Diversity and Distributions* 17, 1198–1209.

**Dubois, S., Retière, C. and Olivier, F.** (2002) Biodiversity associated with *Sabellaria alveolata* (Polychaeta: Sabellariidae) reefs: effects of human disturbances. *Journal of Marine Biological Association of the United Kingdom* 82, 817–826.

**Eckelbarger K.J.** (1979) Ultrastructural evidence for both autotrophic and heterotrophic yolk formation in the oocytes of an annelid (*Phragmatopoma lapidosa*, Polychaeta). *Tissue and Cell* 11, 425 – 443.

**Eo, J.J., Chong, V.C. and Sasekumar, A.** (2017). Cyclical events in the life and death of an ephemeral polychaete reef on a

tropical mudflat. *Estuaries and Coasts*, (in press) doi:10.1007/s12237-017-0217-2

**Elith, J., Phillips, S.J., Hastie, T., Dudík, M., Chee, Y.E. and Yates, C.J.** (2011) A statistical explanation of MaxEnt for ecologists. *Diversity and Distributions* 17, 43–57.

**Elith, J., Kearney, M. and Phillips, S.** (2010) The art of modelling range-shifting species. *Methods in Ecology and Evolution* 1, 330–342.

**Faroni-Perez, L.** (2014) Seasonal variation in recruitment of *Phragmatopoma caudata* (Polychaeta, Sabellariidae) in the southeast coast of Brazil: validation of a methodology for categorizing age classes. *Iheringia Serie Zoologia* 104, 5–13.

**Faroni-Perez L. and Zara F.J.** (2014) Oogenesis in *Phragmatopoma* (Polychaeta: Sabellariidae): evidence for morphological distinction among geographically remote populations. *Memoirs of Museum Victoria* 71, 53–65.

**Faroni-Perez, L., Helm, C., Burghardt, I., Hutchings, P. and Capa, M.** (2016) Anterior sensory organs in Sabellariidae (Annelida). *Invertebrate Biology* 135, 423–447.

**Ferrari, R., McKinnon, D., He, H., Smith, R.N., Corke, P., González-Rivero, M., Mumby, P.J. and Upcroft B.** (2016) Quantifying multiscale habitat structural complexity: A cost-effective framework for underwater 3D modelling. *Remote Sensing*, 8, 113, doi:10.3390/rs8020113.

**Fine, M. and Tchernov, D.** (2007) Scleractinian coral species survive and recover from decalcification. *Science* 315, 1811–1811.

**Firth, L.B., Mieszkowska, N., Grant, L.M., Bush, L.E., Davies, A.J., Frost, M.T., Moschella, P.S., Burrows, M.T., Cunningham, P.N., Dye, S.R. and Hawkins, S.J.** (2015) Historical comparisons reveal multiple drivers of decadal change of an ecosystem engineer at the range edge. *Ecology and Evolution*, 5, 3210–3222.

**Floeter S.R., Rocha L.A., Robertson D.R., Joyeux J.C., Smith-Vaniz W.F., Wirtz P., Edwards A. J., Barreiros J.P., Ferreira C.E.L., Gasparini J.L., Brito A., Falcón J.M., Bowen B.W. and Bernardi G.** (2008) Atlantic reef fish biogeography and evolution. *Journal of Biogeography* 35, 22–47.

**García Molinos, J., Halpern, B.S., Schoeman, D.S., Brown, C.J., Kiessling, W., Moore, P.J., Pandolfi, J.M., Poloczanska, E.S., Richardson, A.J. and Burrows, M.T.** (2015) Climate velocity and the future global redistribution of marine biodiversity. *Nature Climate Change* 2769, 83–88.

**Garrabou, J., Coma, R., Bensoussan, N., Bally, M., Chevaldonne, P., Cigliano, M., Diaz, D., Harmelin, J.G., Gambi, M.C., Kersting, D.K., Ledoux, J.B., Lejeune, C., Linares, C., Marschal, C., Perez, T., Ribes, M., Romano, J.C., Serrano, E., Teixido, N., Torrents, O., Zabala, M., Zuberer, F. and Cerrano, C.** (2009) Mass mortality in Northwestern Mediterranean rocky benthic communities: effects of the 2003 heat wave. *Global Change Biology* 15, 1090–1103.

**Gattuso, J.P., Magnan, A., Bille, R., Cheung, W.W.L., Howes, E.L., Joos, F., Allemand, D., Bopp, L., Cooley, S.R., Eakin, C.M., Hoegh-Guldberg, O., Kelly, R.P., Poertner, H.O., Rogers, A.D., Baxter, J.M., Laffoley, D., Osborn, D., Rankovic, A., Rochette, J., Sumaila, U.R., Treyer, S. and Turley, C.** (2015) Contrasting futures for ocean and society from different anthropogenic CO<sub>2</sub> emissions scenarios. *Science* 349, aac4722-1–aac4722-10.

**Gherardi, F. and Cassidy, P.M.** (1994). Macrobenthic associates to the polychaete *Sabellaria cementarium* bioherm from northern Puget Sound, Washington. *Canadian Journal of Zoology* 72, 514–525.

**Goldberg W.M.** (2013) *The Biology of reefs and reef organisms*. Chicago University Press, ISBN: 9780226301686. 401pp.

**González-Rivero, M., Beijbom, O., Rodriguez-Ramirez, A., Holtrop, T., González-Marrero, Y., Ganase, A., Roelfsema, C., Phinn, S., and Hoegh-Guldberg, O.** (2016) Scaling up ecological measurements of coral reefs using semi-automated field image collection and analysis. *Remote Sensing*, 8, 30, doi:10.3390/rs8010030.

**Good, P., Jones, C., Lowe, J., Betts, R., and Gedney, N.** (2013). Comparing tropical forest projections from two generations of Hadley Centre Earth System Models, HadGEM2-ES and HadCM3LC. *Journal of Climate*, 26, 495–511.

**Gotelli, N.J. and Stanton-Geddes, J.** (2015) Climate change, genetic markers and species distribution modelling. *Journal of Biogeography* 42, 1577–1585.

**Guillera-Arroita, G., Lahoz-Monfort, J.J., Elith, J., Gordon, A., Kujala, H., Lentini, P. E., McCarthy, M.A., Tingley, R. and Wintle, B.A.** (2015) Is my species distribution model fit for purpose? Matching data and models to applications. *Global Ecology and Biogeography* 24, 276–292.

**Harley, C.D.G., Hughes, A.R., Hultgren, K.M., Miner, B.G., Sorte, C.J.B., Thornber, C.S., Rodriguez, L.F., Tomanek, L. and**

**Williams, S.L.** (2006) The impacts of climate change in coastal marine systems. *Ecology Letters* 9, 228–241.

**Helmuth, B., Broitman, B.R., Blanchette, C.A., Gilman, S., Halpin, P., Harley, C.D.G., O'Donnell, M.J., Hofmann, G.E., Menge, B. and Strickland, D.** (2006) Mosaic patterns of thermal stress in the rocky intertidal zone: Implications for climate change. *Ecological Monographs* 76, 461–479.

**Hoegh-Guldberg, O. and Bruno, J.F.** (2010) The impact of climate change on the world's marine ecosystems. *Science* 328, 1523–1528.

**Holt, T.J., Hartnoll, R.G. and Hawkins, S.J.** (1997) Sensitivity and vulnerability to man induced change of selected communities: Intertidal brown algal shrubs, *Zostera* beds and *Sabellaria spinulosa* reefs. *English Nature. English Nature Research Report* no. 234, 97 pp.

**IPCC** (2013) *Climate Change 2013: The Physical Science Basis. Contribution of Working Group I to the Fifth Assessment Report of the Intergovernmental Panel on Climate Change.* Cambridge, New York, NY: Cambridge University Press.

**Jones, C.D., Hughes, J.K., Bellouin, N., Hardiman, S.C., Jones, G.S., Knight, J., Liddicoat, S., O'Connor, F.M., Andres, R.J., Bell, C., Boo, K.O., Bozzo, A., Butchart, N., Cadule, P., Corbin, K.D., Doutriaux-Boucher, M., Friedlingstein, P., Gornall, J., Gray, L., Halloran, P.R., Hurtt, G., Ingram, W.J., Lamarque, J.F., Law, R.M., Meinshausen, M., Osprey, S., Palin, E.J., Chini, L.P., Raddatz, T., Sanderson, M.G., Sellar, A.A., Schurer, A., Valdes, P., Wood, N., Woodward, S., Yoshioka, M. and Zerroukat, M.** (2011) The HadGEM2-ES implementation of CMIP5 centennial simulations. *Geoscientific Model Development* 4, 543–570.

**Jones, C.G., Lawton J.H. and Shachak M.** (1997) Positive and negative effects of organisms as physical ecosystem engineers. *Ecology* 78, 1946–1957.

**Jones, M.C. and Cheung, W.W.L.** (2015) Multi-model ensemble projections of climate change effects on global marine biodiversity. *Ices Journal of Marine Science* 72, 741–752.

**Kinberg, J.G.H.** (1866) *Annulata nova.* [Continuatio]. Öfversigt af Königlich Vetenskapsakademiens förhandlingar, Stockholm. 23(9): 337–357.

**Knowlton, N. and Jackson, J.B.C.** (1994) New taxonomy and niche partitioning on coral reefs: jack of all trades or master of some? *Trends in Ecology and Evolution* 9, 7–9.



**Lenoir, J. and Svenning, J.C.** (2015) Climate-related range shifts - a global multidimensional synthesis and new research directions. *Ecography* 38, 15–28.

**Lopez-Victoria, M., Zea, S. and Wei, E.** (2006) Competition for space between encrusting excavating Caribbean sponges and other coral reef organisms. *Marine Ecology Progress Series* 312, 113–121.

**Martin, G.M., Bellouin, N., Collins, W.J., Culverwell, I.D., Halloran, P.R., Hardiman, S.C., Hinton, T.J., Jones, C.D., McDonald, R.E., McLaren, A.J., O'Connor, F.M., Roberts, M.J., Rodriguez, J.M., Woodward, S., Best, M.J., Brooks, M.E., Brown, A.R., Butchart, N., Dearden, C., Derbyshire, S.H., Dharssi, I., Doutriaux-Boucher, M., Edwards, J.M., Falloon, P.D., Gedney, N., Gray, L.J., Hewitt, H.T., Hobson, M., Huddleston, M.R., Hughes, J., Ineson, S., Ingram, W.J., James, P.M., Johns, T.C., Johnson, C.E., Jones, A., Jones, C.P., Joshi, M.M., Keen, A.B., Liddicoat, S., Lock, A.P., Maidens, A.V., Manners, J.C., Milton, S.F., Rae, J.G.L., Ridley, J.K., Sellar, A., Senior, C.A., Totterdell, I.J., Verhoef, A., Vidale, P.L., and Wiltshire, A.** (2011) The HadGEM2 family of Met Office Unified Model climate configurations. *Geoscientific Model Development*, 4, 723–757.

**McCarthy, D.A., Young, C.M. and Emson, R.H.** (2003) Influence of wave-induced disturbance on seasonal spawning patterns in the sabellariid polychaete *Phragmatonoma lapidosa*. *Marine Ecology Progress Series* 256, 123–133.

**McQuillan, M.A. and Rice, A.** (2015) Differential effects of climate and species interactions on range limits at a hybrid zone: potential direct and indirect impacts of climate change. *Ecology and Evolution*, 5, 5120–5137.

**Monaco, C.J. and Helmuth, B.** (2011) Tipping points, thresholds and the keystone role of physiology in marine climate change research. *Advances in Marine Biology* 60, 123–162.

**Mörch, O.A.L.** (1863) Revisio critica Serpulidarum. Et Bidrag til Røromenes Naturhistorie. *Naturhistorisk Tidsskrift*. København, Ser. 3 1: 347–470, pl. 11.

**Nguyen, K.D.T, Morley S.A., Lai C-H., Clark M.S., Tan K.S., Bates A.E. and Peck L.S.** (2011) Upper temperature limits of tropical marine ectotherms: global warming implications. *PLoS ONE* 6, e29340.

**Nishi, E., Matsuo, K., Capa, M., Tomioka, S., Kajihara, H., Kupriyanova, E. and Polgar, G.** (2015). *Sabellaria jeramae*, a new species (Annelida: Polychaeta: Sabellariidae) from the shallow waters

of Malaysia, with a note on the ecological traits of reefs. *Zootaxa* 4052, 555–568.

**Nunes, F.D.L., Van Wormhoudt, A., Faroni-Perez, L. and Fournier, J.** (2016) Phylogeography of the reef-building polychaetes of the genus *Phragmatopoma* in the western Atlantic Region. *Journal of Biogeography* (In press) doi: 10.1111/jbi.12938.

**Orr, J.C., Fabry, V.J., Aumont, O., Bopp, L., Doney, S.C., Feely, R.A., Gnanadesikan, A., Gruber, N., Ishida, A., Joos, F., Key, R.M., Lindsay, K., Maier-Reimer, E., Matear, R., Monfray, P., Mouchet, A., Najjar, R.G., Plattner, G.K., Rodgers, K.B., Sabine, C.L., Sarmiento, J.L., Schlitzer, R., Slater, R.D., Totterdell, I.J., Weirig, M.F., Yamanaka, Y. and Yool, A.** (2005) Anthropogenic ocean acidification over the twenty-first century and its impact on calcifying organisms. *Nature* 437, 681–686.

**Pagliosa, P.R., Doria, J.G., Misturini, D., Otegui, M.B.P., Oortman, M.S., Weis, W.A., Faroni-Perez, L., Alves, A.P., Camargo, M.G., Amaral, A.C.Z., Marques, A.C. and Lana, P.C.** (2014) NONATObase: a database for Polychaeta (Annelida) from the Southwestern Atlantic Ocean. *Database-the Journal of Biological Databases and Curation* 2014, bau002. doi: 10.1093/database/bau002.

**Pawlik, J. and Chia, R.F.S.** (1991) Larval settlement of *Sabellaria cementarium* Moore and comparisons with other species of sabellariid polychaetes. *Canadian Journal of Zoology* 69, 765–770.

**Peterson, A.T.** (2012) Niche modeling: model evaluation. *Biodiversity Informatics* 8, 41.

**Peterson, A.T., Papes, M. and Soberon, J.** (2008) Rethinking receiver operating characteristic analysis applications in ecological niche modeling. *Ecological Modelling* 213, 63–72.

**Phillips, S.J., Anderson, R.P. and Schapire, R.E.** (2006) Maximum entropy modeling of species geographic distributions. *Ecological Modelling* 190, 231–259.

**Phillips, S.J. and Dudik, M.** (2008) Modeling of species distributions with Maxent: new extensions and a comprehensive evaluation. *Ecography* 31, 161–175.

**Poloczanska, E.S., Brown, C.J., Sydeman, W.J., Kiessling, W., Schoeman, D.S., Moore, P.J., Brander, K., Bruno, J.F., Buckley, L.B., Burrows, M.T., Duarte, C.M., Halpern, B.S., Holding, J., Kappel, C.V., O'Connor, M.I., Pandolfi, J.M., Parmesan, C., Schwing, F., Thompson, S.A. and Richardson, A.J.** (2013) Global imprint of climate change on marine life. *Nature Climate Change* 3, 919–925.

**Poloczanska, E.S., Hoegh-Guldberg, O., Cheung, W., Pörtner, H.-O. and Burrows, M.** (2014) Cross-chapter box on observed global responses of marine biogeography, abundance, and phenology to climate change. *Climate Change 2014: Impacts, Adaptation, and Vulnerability. Part A: Global and Sectoral Aspects. Contribution of Working Group II to the Fifth Assessment Report of the Intergovernmental Panel on Climate Change*. C.B. Field, V.R. Barros, D.J. Dokken, K.J. Mach, M.D. Mastrandrea, T.E. Bilir, M. Chatterjee, K.L. Ebi, Y.O. Estrada, R.C. Genova, B. Girma, E.S. Kissel, A.N. Levy, S. MacCracken, P.R. Mastrandrea and L.L. White (eds.) Cambridge University Press, Cambridge, United Kingdom and New York, NY, USA, pp. 123–127.

**Poloczanska, E.S., Burrows M.T., Brown, C.J., García Molinos, J., Halpern, B.S., Hoegh-Guldberg O., Kappel, C.V., Moore P.J., Richardson A.J., Schoeman D.S. and Sydeman, W.J.** (2016) Responses of marine organisms to climate change across Oceans. *Frontiers in Marine Science*. doi: 10.3389/fmars.2016.00062

**Posey M.H., Marshall, P.A. and Graham, R.A.** (1984) A Brief description of a subtidal sabellariid (Polychaeta) reef on the Southern Oregon coast. *Pacific Science* 38, 28–33.

**Przeslawski, R., Ah Yong, S., Byrne, M., Wörheide, G. and Hutchings, P.** (2008) Beyond corals and fish: the effects of climate change on noncoral benthic invertebrates of tropical reefs. *Global Change Biology* 14, 2773–2795

**Radosavljevic, A. and Anderson, R.P.** (2014) Making better MAXENT models of species distributions: complexity, overfitting and evaluation. *Journal of Biogeography* 41, 629–643.

**Riebesell, U. and Gattuso, J.-P.** (2015) Lessons learned from ocean acidification research. *Nature Climate Change* 5, 12–14.

**Rosa, R., Lopes, A.R., Pimentel, M., Faleiro, F., Baptista, M., Trübenbach, K., Narciso, L., Dionísio, G., Pegado, M.R., Repolho, T., Calado, R. and Diniz, M.** (2014) Ocean cleaning stations under a changing climate: biological responses of tropical and temperate fish-cleaner shrimp to global warming. *Global Change Biology* 20, 3068–3079.

**Sanford, E. and Kelly, M.W.** (2011) Local adaptation in marine invertebrates. *Annual Review of Marine Science* 3, 509–535.

**Saupe, E.E., Hendricks, J.R., Peterson, A.T. and Lieberman, B.S.** (2014) Climate change and marine molluscs of the western North Atlantic: Future prospects and perils. *Journal of Biogeography* 41, 1352–1366.

**Shcheglovitova, M. and Anderson, R.P.** (2013) Estimating optimal complexity for ecological niche models: A jackknife approach for species with small sample sizes. *Ecological Modelling* 269, 9–17.

**Shirayama, Y. and Thornton, H.** (2005) Effect of increased atmospheric CO<sub>2</sub> on shallow water marine benthos. *Journal of Geophysical Research* 110, C09S08.

**Smith P.R. and Chia, F.S.** (1985) Metamorphosis of the sabellariid polychaete *Sabellaria cementarium* Moore: A histological analysis. *Canadian Journal of Zoology* 63, 2852–2866.

**Somero, G.N.** (2002) Thermal physiology and vertical zonation of intertidal animals: optima, limits, and costs of living. *Integrative and Comparative Biology* 42, 780–789.

**Somero, G.N.** (2010) The physiology of climate change: how potentials for acclimatization and genetic adaptation will determine 'winners' and 'losers'. *Journal of Experimental Biology* 213, 912–920.

**Stachowicz, J.J., Terwin, J.R., Whitlatch, R.B. and Osman, R.W.** (2002) Linking climate change and biological invasions: Ocean warming facilitates nonindigenous species invasions. *Proceedings of the National Academy of Sciences of the United States of America* 99, 15497–15500.

**Stevens, M.J., Steren, R.E., Hlady, V. and Stewart, R.J.** (2007) Multiscale structure of the underwater adhesive of *Phragmatopoma californica*: a nanostructured latex with a steep microporosity gradient. *Langmuir* 23, 5045–5049.

**Taylor, P.R. and Littler, M.M.** (1982) The roles of compensatory mortality, physical disturbance, and substrate retention in the development and organization of a sand-influenced, rocky intertidal community. *Ecology* 63, 135–146

**Tewksbury, J.J., Huey, R.B. and Deutsch, C.A.** (2008) Putting the heat on tropical animals. *Science* 320, 1296–1297.

**van Vuuren, D.P., Edmonds, J., Kainuma, M., Riahi, K., Thomson, A., Hibbard, K., Hurtt, G.C., Kram, T., Krey, V., Lamarque, J.-F., Masui, T., Meinshausen, M., Nakicenovic, N., Smith, S.J., and Rose, S.K.** (2011) The representative concentration pathways: an overview. *Climatic Change* 109, 5–31.

**VanDerWal, J., Murphy, H.T., Kutt, A.S., Perkins, G.C., Bateman, B.L., Perry, J.J. and Reside, A.E.** (2013) Focus on poleward shifts in species' distribution underestimates the fingerprint of climate change. *Nature Climate Change* 3, 239–243.

**Veloz, S.D., Nur, N., Salas, L., Jongsomjit, D., Wood, J., Stralberg, D. and Ballard, G.** (2013) Modeling climate change

impacts on tidal marsh birds: Restoration and conservation planning in the face of uncertainty. *Ecosphere* 4, 1–25.

**Verbruggen, H., Tyberghein, L., Belton, G.S., Mineur, F., Jueterbock, A., Hoarau, G., Gurgel, C.F.D. and De Clerck, O.** (2013) Improving transferability of introduced species' distribution models: New tools to forecast the spread of a highly invasive seaweed. *PLoS One* 8, e68337 1–13.

**Wang, C.S. and Stewart, R.J.** (2012) Localization of the bioadhesive precursors of the sandcastle worm, *Phragmatopoma californica* (Fewkes). *Journal of Experimental Biology* 215, 351–361.

**Wernberg, T., Smale, D.A. and Thomsen, M.S.** (2012) A decade of climate change experiments on marine organisms: procedures, patterns and problems. *Global Change Biology* 18, 1491–1498.

**Wernberg, T., Russell, B.D., Moore, P.J., Ling, S.D., Smale, D.A., Campbell, A., Coleman, M.A., Steinberg, P.D., Kendrick, G.A. and Connell, S.D.** (2011) Impacts of climate change in a global hotspot for temperate marine biodiversity and ocean warming. *Journal of Experimental Marine Biology and Ecology* 400, 7–16.

**Xavier, J.C., Peck, L.S., Fretwell, P. and Turner, J.** (2016) Climate change and polar range expansions: Could cuttlefish cross the Arctic? *Marine Biology* 163, doi:10.1007/s00227-016-2850-x

**Zamorano, J.H., Moreno, C.A. and Duarte, W.E.** (1995) Post-settlement mortality in *Phragmatopoma virgini* (Polychaeta: Sabellariidae) at the Mehuin Marine Reserve, Chile. *Marine Ecology Progress Series* 127, 149–155.

**Zelinka, M.D., Klein S.A., Taylor K.E., Andrews, T., Webb, M.J., Gregory, J.M. and Forster, P.M.** (2013) Contributions of different cloud types to feedbacks and rapid adjustments in CMIP5. *Journal of Climate* 26, 5007–5027.

## FIGURES AND TABLES

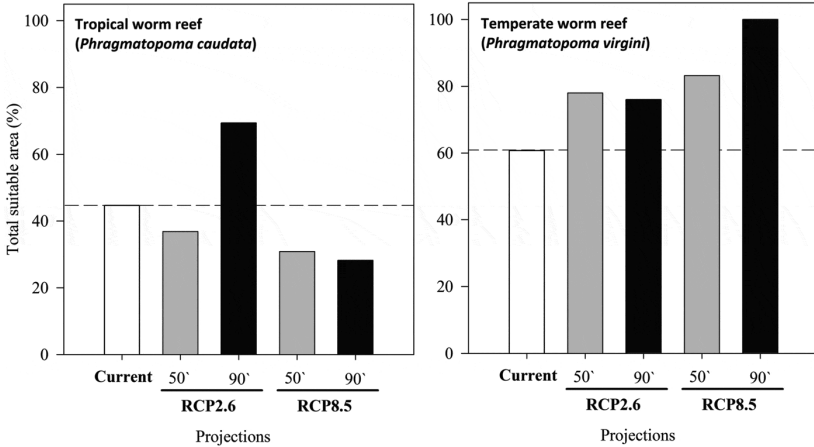


**Figure 1.** Predicted changes in total suitable areas of the tropical *Phragmatopoma caudata* and the temperate *Phragmatopoma virgini* worm reefs considering current and future predictions for RCP2.6 (low emissions) and RCP8.5 (high emissions) scenarios, and the time-scales of the 50s (mid-century: 2040–2059) and the 90s (late-century: 2080–2099).

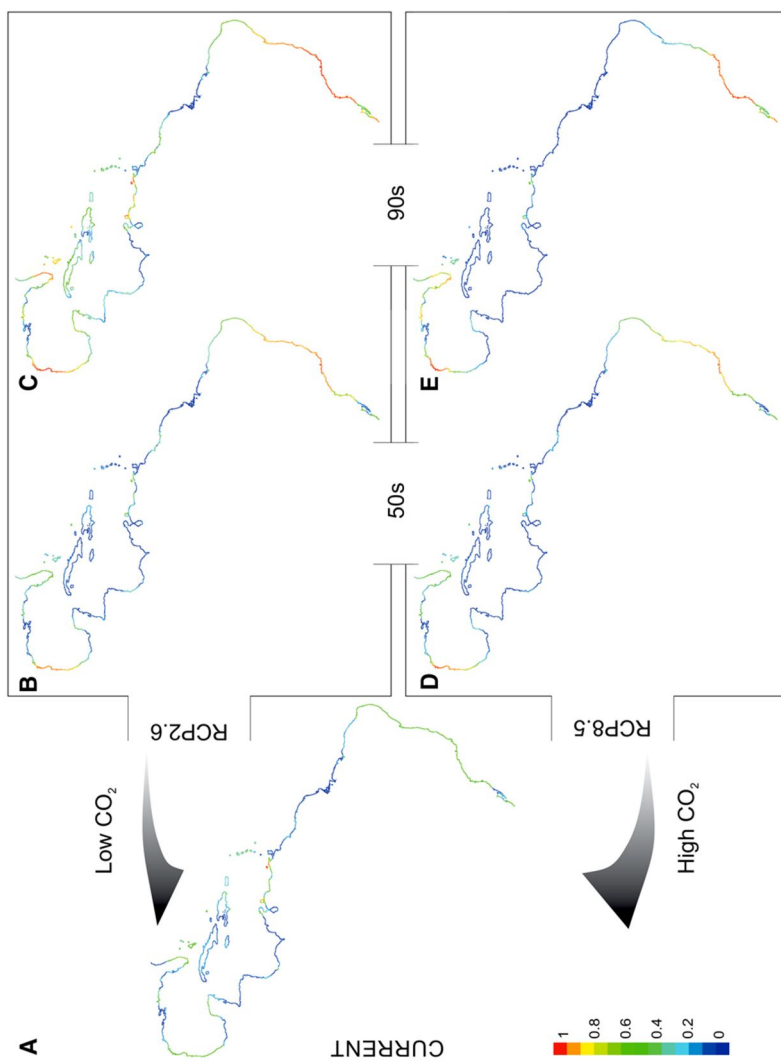


Figure 2.

### Previous Page

**Figure 2.** Maps\* show spatial variation in current (A) and future (B-E) potential suitable area distributions for tropical worm reefs (*Phragmatopoma caudata*) predicted given the RCP2.6 (low-emission) and RCP8.5 (high-emission) scenarios. Each projection (i.e. current, 50s and 90s) is based on a dataset covering two decades. Pixel colours correspond to the following: 0–0.2 = area of non-suitability (cold colours: medium to dark blue),  $0.4 \leq \text{low} \leq 0.2$  1 (colours: light blue to green);  $0.41 \leq \text{medium} \leq 0.4$  (colours: green to light green);  $0.61 \leq \text{high} \leq 0.8$  (colours: light green to yellow);  $0.81 \leq \text{very high} \leq 1$  (warm colours: orange to red). \*Continental shoreline of the tropical regions of the Western Atlantic, ranging from Florida coast (USA) to the southern coast of Brazil.

### Next page:

**Figure 3.** Maps\* show spatial variation in current (A) and future (B-E) potential suitable area distributions for temperate worm reefs (*Phragmatopoma virgini*) predicted given the RCP2.6 (low emissions) and RCP8.5 (high emissions) scenarios. Each projection (i.e. current, 50s and 90s) is based on a dataset covering two decades. Pixel colours correspond to the following: 0–0.2 = area of non-suitability (cold colours: medium to dark blue),  $0.4 \leq \text{low} \leq 0.2$  1 (colours: light blue to green);  $0.41 \leq \text{medium} \leq 0.4$  (colours: green to light green);  $0.61 \leq \text{high} \leq 0.8$  (colours: light green to yellow);  $0.81 \leq \text{very high} \leq 1$  (warm colours: orange to red). \*Continental shoreline of the temperate regions ranging from Ecuador in Southeast Pacific Ocean and Uruguay in Southwest Atlantic Ocean southward to Patagonia.



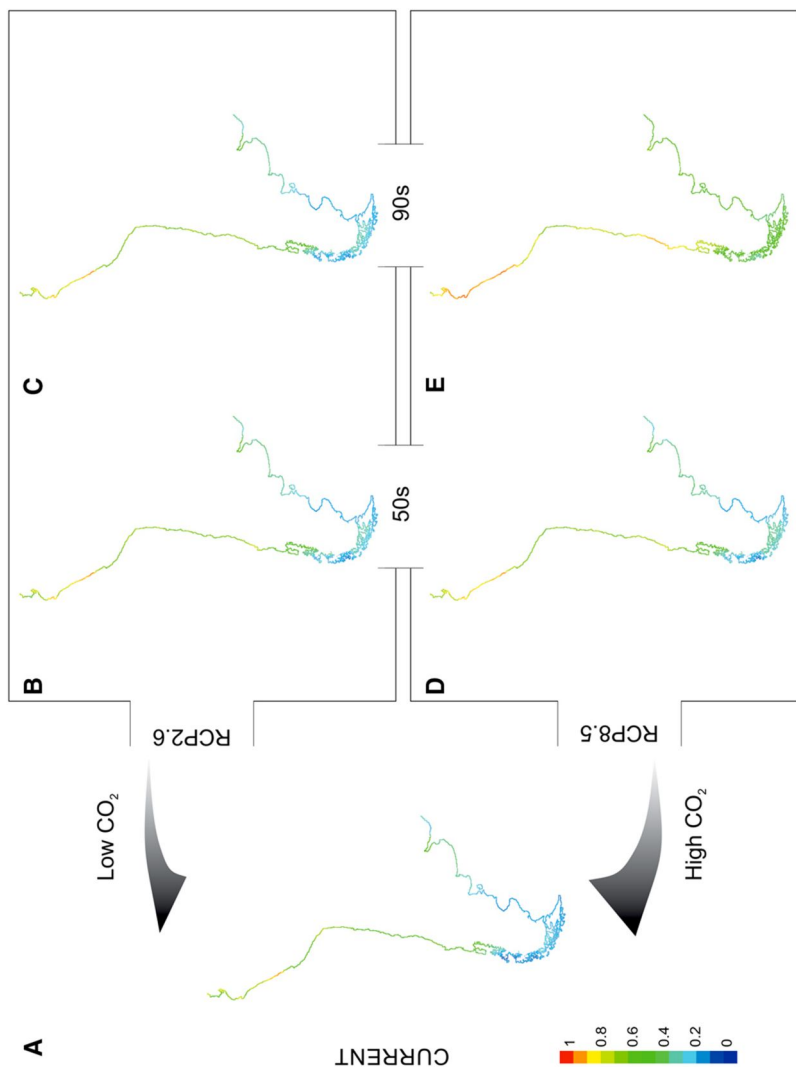


**Figure 3.**

**Table 1:** Niches and their environmental drivers with code and units used for modelling habitat suitability.

Niche	Predictor	Code	units
Trophic	Detrital Organic Carbon Concentration	detoc	mol m <sup>-3</sup>
	Dissolved Nitrate Concentration	no3	mol m <sup>-3</sup>
	Dissolved Ammonium Concentration	nh4	mol m <sup>-3</sup>
	Total Chlorophyll Mass Concentration	chl	kg m <sup>-3</sup>
	Dissolved Silicate Concentration	si	mol m <sup>-3</sup>
Biogenic	Negative log of hydrogen ion concentration	pH	mol H kg <sup>-1</sup>
	Total Alkalinity	talk	mol m <sup>-3</sup>
Thermic	Near-Surface Air Temperature	tas	K
	Sea Surface Temperature	tos	K
Osmotic	Precipitation	pr	kg m <sup>-2</sup> s <sup>-1</sup>
	Sea Surface Salinity	sos	psu
	Water Flux into Sea Water From Rivers	friver	kg m <sup>-2</sup> s <sup>-1</sup>

**Table 1:** Summary of model statistics showing the receiver operating characteristic curves for MaxEnt with  $E = 0.5$  of acceptable omission error according to  $p$ -ROC AUC values.

	P-ROC AUC	AUC Ratio	AUC null
<i>P. caudata</i>	0.83338	1.66679	0.49999
<i>P. virgini</i>	0.83583	1.67171	0.49999

**Table 2:** Influence of environmental drivers used in modelling habitat suitability. Codes used for predictors are defined in table I.

Niche (Predictor)	Percent contribution	Permutation Importance
<i>P. caudata</i>		
thermic (tos)	60.3	61.3
osmotic (friver)	16.3	25.3
trophic (si)	11.8	8
biogenic (ph)	11.6	5.4
<i>P. virgini</i>		
thermic (tos)	86.1	67.5
trophic (detoc)	10.8	23.2
osmotic (pr)	3	7.8
biogenic (ph)	0.1	1.6

**Table 4:** Projected changes in the potential suitability areas for topical (*Phragmatopoma caudata*) and temperate (*P. virgini*) worm reefs with contrast to their current habitat suitability.  $\Delta$  represents the difference in frequencies of pixel suitability between current and scenarios; RCP2.6 (low emissions) and RCP8.5 (high emissions) and between the 50s (mid-century: 2040–2059) and the 90s (late-century: 2080–2099) time period. In brackets, the total frequencies (F%) given in percentage of grid cells per projection

Species	Confidence of Suitability	Scenario and Time Period					
		Current	RCP2.6		RCP8.5		
			F(%)	$\Delta$ 50s(F%)	$\Delta$ 90s(F%)	$\Delta$ 50s(F%)	$\Delta$ 90s(F%)
<i>P. caudata</i>	area of non-suitability	55.3	7.80(63.10)	-24.70(30.61)	13.84(69.15)	16.48(71.78)	
	low	20.75	-5.09(15.66)	13.80(34.55)	-8.37(12.38)	-11.27(9.48)	
	medium	21.59	-14.11(7.49)	-10.87(10.72)	-13.24(8.35)	-16.63(4.96)	
	high	1.64	8.26(9.90)	11.23(12.87)	6.22(7.86)	5.51(7.15)	
	very high	0.71	3.15(3.85)	10.54(11.25)	1.55(2.26)	5.91(6.62)	
<i>P. virgini</i>	area of non-suitability	39.25	-17.25(22.00)	-15.23(24.02)	-22.46(16.80)	-39.25(0.00)	
	low	33.38	13.06(46.45)	10.08(43.47)	16.07(49.46)	6.56(39.95)	
	medium	17.7	-1.66(16.04)	-0.75(16.95)	-3.01(14.69)	10.05(27.75)	
	high	9.27	5.78(15.05)	5.87(15.14)	9.60(18.87)	20.44(29.71)	
	very high	0.39	0.06(0.45)	0.03(0.42)	-0.21(0.18)	2.20(2.59)	



## SUPPORTING INFORMATION

*Journal of the Marine Biological Association UK (JMBA)*

### **Climate and environmental changes driving idiosyncratic shifts in the distribution of tropical and temperate worm reefs**

**Larisse Faroni-Perez**

#### *Predictors*

Environmental layers acquired from HadGEM2-ES were divided into the time period (current, middle of the century and end of the century) and the future impacts of the simulated climate change (RCP2.6 and RCP8.5). Each predictor was rescaled, and the interannual monthly mean was calculated following the annual values: average, minimum and maximum (Table 1). The set of layers in the ‘current’ time period were subdivided into two; global spatial layers were masked and cut onto the biogeographic provinces surrounding region for each species known occurrence (i.e. strictly to the occurring latitudinal span and longitudinally delimited by the closest cell grid representing the continental shoreline). Correlation matrices were analysed to exclude highly correlated predictors (Pearson,  $r > \pm 0.60$ ), therefore remained predictors are shown in Table 1. Afterward, remained predictors were analysed by generalized linear models (GLMs) using a total number of four predictors in each model, considering all possible combinations of single predictor per niche (Table 2). A predictor was scored whilst significant in the model. Then, for each niche, based on scored rank across models the most influential predictive capacity of predictor was selected to final model (Table 2). For both the species, the final set of predictors selected by ranking were also significant by the GLM (Table 2). Statistical analysis of environmental predictors used in the final model is shown in Table 3.

**Table 1:** Environmental predictors layers acquired from IPCC, AR5 model HadGEM2-ES. Time period represent: present days (1986–2005), 50's (middle of century: 2040–2059), and the 90's (late of century: 2080–2099). Future scenarios represent: RCP2.6 (low emissions) and RCP8.5 (high emissions). Codes: ... = layers used for correlation matrices, ... = layers remained and used in GLM models, and ... = final layers selected.

Niche	Predictor	*	Current	RCP2.6		RCP8.5		
			$\Delta 00$ 's (1986-2005)	$\Delta 50$ 's (2040-2059)	$\Delta 90$ 's (2080-2099)	$\Delta 50$ 's (2040-2059)	$\Delta 90$ 's (2080-2099)	
<b>Trophic</b>	Detrital Organic Carbon Concentration	min	...					
		mean	...					
		max	...					
	Dissolved Nitrate Concentration	min	...					
		mean	...					
		max	...					
	Dissolved Ammonium Concentration	min	...					
		mean	...					
		max	...					
	Total Chlorophyll Mass Concentration	min	...					
		mean	...					
		max	...					
	Dissolved Silicate Concentration	min	...					
		mean	...					
		max	...					
<b>Biogenic</b>	Negative log of hydrogen ion concentration	min	...					
		mean	...					
		max	...					
	Total Alkalinity	min	...					
		mean	...					
		max	...					
	<b>Thermal</b>	Near-Surface Air Temperature	min	...				
			mean	...				
			max	...				
		Sea Surface Temperature	min	...				
			mean	...				
			max	...				
	<b>Osmotic</b>	Precipitation	min	...				
			mean	...				
			max	...				
Sea Surface Salinity		min	...					
		mean	...					
		max	...					
Water Flux into Sea Water From Rivers	min	...						
	mean	...						
	max	...						



**Table 2:** Results of GLM models considering all possible combinations of single predictor per niche. Predictor used in the model was scored as 1 if significant ( $p < 0.05$ ). Rank = sum of predictors' score. \*:final model selected.

	Niche	Predictors	Models																								Rank	
			1	2	3	4	5	6	7	8	9	10	11	12	13	14	15	16	17	18	19	20	21	*22	23	24		
<i>Phragmatopoma caudata</i>	Biogenic	pH	1	1			1					1	1			1			1				1	1			9	
		talk			1	1			1	1			1				1				1				1	1		8
	Osmotic	pr	1							1									1					1				4
		friver		1		1		1		1		1		1			1		1		1		1		1	1	1	12
	Thermal	tas	1	1	1	1					1		1	1					1	1	1	1						11
		tos					1	1	1	1					1	1	1	1						1	1	1	1	12
	Trophic	detoc							1																			1
		no3								1	1																	2
		si																						1	1	1	1	5
		Total	3	3	2	3	2	2	2	4	4	3	2	2	2	2	2	2	2	3	2	2	3	4	4	3	3	
<i>Phragmatopoma virginii</i>	Biogenic	pH	1	1			1	1			1	1			1	1			1	1				1	1		12	
		talk			1				1																	1		3
	Osmotic	pr			1		1																			1		3
		friver																										0
	Thermal	tas	1							1		1	1								1	1						6
		tos					1	1	1	1					1	1	1	1					1	1	1	1	1	12
	Trophic	detoc	1	1	1	1	1	1	1	1																		8
		no3																										0
		si											1	1				1	1									4
		Total	3	2	3	1	4	3	2	3	2	1	2	2	2	2	2	2	2	1	1	1	1	1	2	2	3	1

**Table 3:** Analyses of environmental predictor used in the model encompassing biogeographic provinces where occur the tropical (*Phragmatopoma caudata*) and temperate (*P. virgini*) worm reefs. Future scenarios represent RCP2.6 (low emissions) and RCP8.5 (high emissions). Time period (T.P.) represent: present days (1986–2005), 50's (middle of century: 2040–2059), and the 90's (late of century: 2080–2099). Future projections are based on IPCC, AR5 from model HadGEM2-ES.

Species and Scenarios - T.P.		* Predictors(unit)					
		friver (kg m-2 s-1)	ph (mol H kg-1)	si (mol m-3)	tos (°C)		
<i>P. caudata</i>	Present	Mean	0,0000713	8,037	0,0466852	24,22	
		Min	0,0000000	7,993	0,0425404	16,38	
		Max	0,0021711	8,081	0,0499265	30,11	
	RCP2.6	50's	Mean	0,0000746	7,968	0,0488350	25,33
			Min	0,0000000	7,923	0,0449909	17,45
			Max	0,0020941	8,008	0,0511089	31,28
		90's	Mean	0,0000701	7,979	0,0502465	25,28
			Min	0,0000000	7,936	0,0464482	17,56
			Max	0,0020551	8,017	0,0520919	31,20
	RCP8.5	50's	Mean	0,0000751	7,905	0,0489636	25,78
			Min	0,0000000	7,859	0,0452242	17,68
			Max	0,0022657	7,941	0,0509628	31,91
90's		Mean	0,0000750	7,750	0,0504605	27,44	
		Min	0,0000000	7,705	0,0470524	19,24	
		Max	0,0021309	7,779	0,0519342	33,56	
<i>P. virgini</i>	Present	Mean	0,0000750	8,037	0,0029853	11,20	
		Min	0,0000039	7,749	0,0004062	5,13	
		Max	0,0002092	8,129	0,0080088	28,60	
	RCP2.6	50's	Mean	0,0000751	7,958	0,0031143	12,10
			Min	0,0000049	7,636	0,0004409	5,86
			Max	0,0001777	8,043	0,0085590	29,76
		90's	Mean	0,0000762	7,970	0,0031871	11,99
			Min	0,0000062	7,632	0,0005030	5,72
			Max	0,0001962	8,061	0,0088986	29,77
	RCP8.5	50's	Mean	0,0000756	7,890	0,0031094	12,46
			Min	0,0000051	7,582	0,0003582	6,19
			Max	0,0001840	7,961	0,0089863	30,95
		90's	Mean	0,0000751	7,718	0,0030816	14,13
			Min	0,0000041	7,442	0,0003670	7,72
			Max	0,0001881	7,784	0,0091215	33,10

\*Predictors code: detoc=Detrital Organic Carbon Concentration (max); si=Dissolved Silicate Concentration (max); pH=Negative log of hydrogen ion concentration (min); tos=Sea Surface Temperature (min); pr = Precipitation (max); friver=Water Flux into Sea Water From Rivers (max). In brackets, the specific layer for predictor selected after peer-to-peer correlation and GLM selection processes.

### *Modelling (procedure)*

Previous studies assessed the sensitivity of MaxEnt using several options and described several modelling complexities (Anderson & Raza, 2010; Elith *et al.*, 2010; Anderson & Gonzalez, 2011; Shcheglovitova & Anderson, 2013). However, the spatial scales of these previous studies were mainly regional, unlike the continental scale in this present study. Although evaluating the sensitivity of MaxEnt was not the main objective of this study, I carefully checked for the different approaches for modelling based on the present data. Assessing species-specific model tuning instead of using default features is highly recommended (Merow *et al.*, 2013). Following Elith *et al.*, (2010), Anderson & Gonzalez, (2011), Elith *et al.*, (2011) and Shcheglovitova & Anderson, (2013), the complexity of models was checked for testing the regularization multiplier (RM) values of 1 (default) and 2.5, and the following feature classes Hinge (H) or Linear+Quadratic (LQ). The fitted model has regularization value of 1 (currently default value) and Hinge feature class, due to low omission rate and higher AUC values respectively (Tables 4-5). This metric based on the omission rate tends to select simpler models (Radosavljevic & Anderson, 2014). The final MaxEnt settings used in fitting the model of the present study are likely in Elith *et al.*, (2010).

**Table 4:** Results for *Phragmatopoma caudata* of models for the two tested feature classes: hinge (H) and linear and quadratic (LQ), with the regularization multiplier (RM) values tested 1(default) and 2.5. Fixed cumulative value 10: Training omission rate.

<i>P. caudata</i>									
	H		H 2,5RM		LQ		LQ 2,5RM		
	OR	AUC	OR	AUC	OR	AUC	OR	AUC	
1	0.026	0.846	0	0.822	0.051	0.701	0	0.702	
<b>2</b>	<b>0</b>	<b>0.866</b>	0.048	0.83	0.071	0.706	0.048	0.706	
3	0.024	0.86	0.049	0.835	0.049	0.701	0.049	0.703	
4	0.021	0.901	0	0.856	0	0.734	0.042	0.74	
5	0.023	0.88	0.047	0.851	0.047	0.664	0.023	0.661	
6	0.023	0.865	0.023	0.838	0	0.699	0.047	0.699	
7	0.026	0.877	0.026	0.857	0.132	0.674	0.053	0.673	
8	0.059	0.866	0.059	0.849	0.02	0.709	0.02	0.714	
9	0.026	0.855	0.077	0.803	0	0.709	0.051	0.721	
10	0.021	0.855	0.021	0.823	0	0.699	0.043	0.706	
Mean	0.0249	0.8671	0.035	0.8364	0.037	0.6996	0.0376	0.7025	
DP	0.01424	0.015666	0.02521	0.017411	0.042669	0.019231	0.017411	0.022387	

**Table 5:** Results for *Phragmatopoma virgini* of models for the two tested feature classes: hinge (H) and linear and quadratic (LQ), with the regularization multiplier (RM) values tested 1(default) and 2.5. Fixed cumulative value 10: Training omission rate.

<i>P. virgini</i>									
	H		H 2,5RM		LQ		LQ 2,5RM		
	OR	AUC	OR	AUC	OR	AUC	OR	AUC	
<b>1</b>	<b>0</b>	<b>0.824</b>	0.15	0.754	0.15	0.761	0.15	0.743	
2	0.12	0.849	0.12	0.815	0.12	0.803	0.12	0.783	
3	0.095	0.822	0.095	0.783	0.095	0.78	0.095	0.77	
4	0.125	0.811	0.125	0.764	0.125	0.777	0.125	0.746	
5	0.143	0.806	0.143	0.758	0.143	0.77	0.143	0.75	
6	0.15	0.802	0.15	0.753	0.15	0.758	0.15	0.747	
7	0.136	0.804	0.136	0.755	0.136	0.776	0.136	0.744	
8	0.111	0.846	0.111	0.788	0.111	0.78	0.111	0.763	
9	0.13	0.808	0.13	0.771	0.13	0.765	0.13	0.762	
10	0.136	0.812	0.136	0.781	0.136	0.779	0.136	0.772	
Mean	0.1146	0.8184	0.1296	0.7722	0.1296	0.7749	0.1296	0.758	
SD	0.043308	0.016919	0.017481	0.019837	0.017481	0.012758	0.017481	0.013968	

### *Clamping*

Additionally to regular analysis, I run *do clamping* as false and calculated the relative difference in the frequency of potential suitability classes compared to the obtained results to setting *do clamping* as true, as this MaxEnt setting needs to be tested (Anderson & Raza, 2010). The *do clamping* set as true in MaxEnt means projection is made using data range found only within the training data set (Phillips et al., 2006; Elith et al., 2011), that is recommended when occurring non-analogous relationships of the predictors across the time (Fitzpatrick & Hargrove, 2009) (Table 6). The comparison between the two clamping settings demonstrated that suitable area projections for *P. virginia* were almost not sensitive, since minor differences in the confidence of suitability occurred (Table 6). For *P. caudata*, projections for the end of century under both scenarios showed the most differences in relative entropy, and the maximum value were 12% in suitability. Considering the continental scale and the metric for potential habitat suitability, it is very likely that in regional or local scale, the difference in clamping results will be more sensitive, and further analysis are recommended.

### **Next page:**

**Table 6:** Projected changes in the potential suitability for tropical (*Phragmatopoma caudata*) and temperate (*P. virginia*) worm reefs with contrast to their current habitat suitability.  $\Delta$  represents the difference in pixel suitability between scenarios RCP2.6 (low emissions) and RCP8.5 (high emissions) and between the 50s (mid-century: 2040–2059) and the 90s (late-century: 2080–2099) time periods. In brackets, the total frequencies (F%) given in percentage of grid cells per projection. \* $\Delta$ notClamping: values represent the difference between results obtained when running models with clamping.

Species	Suitability	Clamping						ΔnotClamping*					
		Current		RCP2.6		RCP8.5		RCP2.6		RCP8.5			
		(F%)	Δ50's	Δ90's	Δ50's	Δ90's	Δ50's	Δ90's	Δ50's	Δ90's	Δ50's	Δ90's	
<i>P. caudata</i>	area of non-suitability low	55.3	7.80	-24.70	13.84	16.48	2.24	-6.89	7.77	12.67			
	medium	20.75	-5.09	13.80	-8.37	-11.27	-0.29	-7.49	-1.22	-1.35			
	high	21.59	-14.11	-10.87	-13.24	-16.63	-0.31	8.9	-1.13	1.44			
	very high	1.64	8.26	11.23	6.22	5.51	0.69	1.53	-3.17	-6.14			
		0.71	3.15	10.54	1.55	5.91	-2.33	3.94	-2.26	-6.62			
<i>P. virgini</i>	area of non-suitability low	39.25	-17.25	-15.23	-22.46	-39.25	0	0	0	0			
	medium	33.38	13.06	10.08	16.07	6.56	0	0	0	-5.87			
	high	17.7	-1.66	-0.75	-3.01	10.05	-1.38	-1.14	-1.69	4.94			
	very high	9.27	5.78	5.87	9.60	20.44	1.38	1.14	1.69	-3.01			
		0.39	0.06	0.03	-0.21	2.20	0	0	0	3.94			

### *Post Modelling:*

The technique of using threshold values to recalibrate the maps into binary showing an unsuitable or suitable area is widely used, it has been recently criticized (Guillera-Arroita *et al.*, 2015). Applying the technique of a threshold conversion map results in omitting the continuous prediction and thus a gradient of environmental suitability, which real species face. The procedure to transform the continuous results into a binary map of assumed presence or absence of suitable areas is a coarse way to assess species occurrence probabilities, due to the loss of some information provided by continuous model output. Consequently, the application of this technique is not recommended (Guillera-Arroita *et al.*, 2015). Here, for the practical purposes of fit, the present SDM to assess quantitative changes for each species, the categorical value of 0.2, was set, and the subsequent index system was applied. Although 0.2 is not statistically justified, to set this value as clear-cut, I considered either present-day distribution of suitable habitats and known occupancy areas for both the species. Therefore, this value is fine-tuned for present models and species, very likely it will differ according to species and modelling approaches. The index system gradients refer to the areas of predicted environmental suitability based on continuous model outputs and are not the probability of species distribution *sensu stricto*. This analysis attempted solely to characterize and quantify ‘potential’ shifts in the distribution of each species based on their areas of environmental suitability.

### **Software used**

#### *Model Processing*

Primarily environmental envelopes were processed using the Climate Data Operators (CDO), version 1.4.0 available at <https://code.zmaw.de/projects/cdo/files>. For all experimental models and the final modeling, I used the software MaxEnt version 3.3.3k downloaded from <https://www.cs.princeton.edu/~schapire/maxent/>. Model accuracy were calculated using NicheToolBox (Osorio-Olvera L. 2016). Also, I executed additional analyse with R (R Core Team 2012) using the following packages:

- ‘*raster*’ (Hijmans & Van Etten, 2011)
- ‘*rgdal*’ (Bivand *et al.*, 2015)
- ‘*maptools*’ (Bivand & Lewin-Koh, 2015)
- ‘*sp*’ (Pebesma & Bivand, 2005)
- ‘*MuMIn*’ (Barton, 2015)



- ‘*dismo*’ (Hijmans *et al.*, 2012)

#### References

**Anderson, R.P. and Gonzalez Jr., I.** (2011) Species-specific tuning increases robustness to sampling bias in models of species distributions: an implementation with Maxent. *Ecological Modelling* 222, 2796–2811.

**Anderson, R.P. and Raza, A.** (2010) The effect of the extent of the study region on GIS models of species geographic distributions and estimates of niche evolution: preliminary tests with montane rodents (genus *Nephelomys*) in Venezuela. *Journal of Biogeography* 37, 1378–1393.

**Barton, K.** (2015) MuMIn: multi-model inference Available at <https://cran.r-project.org/web/packages/MuMIn/index.html>

**Bivand, R. and Lewin-Koh, N.** (2015) mapproj: Tools for Reading and Handling Spatial Objects. Available at <http://CRAN.R-project.org/package=mapproj>

**Bivand, R., Keitt, T. and Rowlingson, B.** (2015) rgdal: Bindings for the Geospatial Data Abstraction Library. Available at <https://cran.r-project.org/package=rgdal>

**Elith, J., Kearney, M. and Phillips, S.** (2010) The art of modelling range-shifting species. *Methods in Ecology and Evolution* 1, 330–342.

**Elith, J., Phillips, S.J., Hastie, T., Dudik, M., Chee, Y.E. and Yates, C.J.** (2011) A statistical explanation of MaxEnt for ecologists. *Diversity and Distributions* 17, 43–57.

**Fitzpatrick, M.C. and Hargrove, W.W.** (2009) The projection of species distribution models and the problem of non-analog climate. *Biodiversity and Conservation* 18, 2255–2261.

**Guillera-Aroita, G., Lahoz-Monfort, J.J., Elith, J., Gordon, A., Kujala, H., Lentini, P. E., McCarthy, M.A., Tingley, R. and Wintle, B.A.** (2015) Is my species distribution model fit for purpose? Matching data and models to applications. *Global Ecology and Biogeography* 24, 276–292.

**Hijmans, R.J. and Van Etten, J.** (2011) Raster: Geographic data analysis and modeling. R package version 2.0-12. Available at <http://cran.r-project.org/package=raster>

**Hijmans, R.J., Phillips, S., Leathwick, J., and Elith, J.** (2012) dismo: Species distribution modeling. R package version 0.6-3. R

Foundation for Statistical Computing, Vienna, Austria. <http://cran.r-project.org/web/packages/dismo/>

**Merow, C., Smith, M.J. and Silander, J.A., Jr.** (2013) A practical guide to MaxEnt for modeling species' distributions: what it does, and why inputs and settings matter. *Ecography* 36, 1058–1069.

**Osorio-Olvera, L.** (2016) *NicheToolbox: A Web Tool for Exploratory Data Analysis and Niche Modeling*.

**Pebesma, E.J. and Bivand, R.S.** (2005) Classes and methods for spatial data in R. *R News* 5 (2). Available at <http://cran.r-project.org/doc/Rnews/>

**Phillips, S.J., Anderson, R.P. and Schapire, R.E.** (2006) Maximum entropy modeling of species geographic distributions. *Ecological Modelling* 190, 231-259.

**Radosavljevic, A. and Anderson, R.P.** (2014) Making better MAXENT models of species distributions: complexity, overfitting and evaluation. *Journal of Biogeography* 41, 629-643.

**Shcheglovitova, M. and Anderson, R.P.** (2013) Estimating optimal complexity for ecological niche models: A jackknife approach for species with small sample sizes. *Ecological Modelling*, 269, 9-17.

“Appearance may be true or misleading. We must understand if the change is or isn’t the adaptation of the struggle for existence.”

(Larisse Faroni-Perez, 2017)



**RESPONSE OF A INTERTIDAL REEF-BUILDER WORM TO  
RISING  $p\text{CO}_2$ : BIOCONSTRUCTION PLASTICITY  
PERFORMANCE UNDER DIFFERENT OCEAN  
ACIDIFICATION CONDITIONS**

Larisse Faroni-Perez, Cédric Hubas, Christophe Goulard, Stéphanie  
Auzoux-Bordenave, Jérôme Fournier, Carlos Frederico D. Gurgel

**Running head:** Bioconstruction under ocean acidification



## Abstract

Increasing emissions of carbon dioxide ( $\text{CO}_2$ ) drives ocean acidification (OA) as oceans uptake atmospheric  $\text{CO}_2$  ( $p\text{CO}_2$ ). OA affects marine organisms in a wide range of physiological functions including biomineralization and bioconstruction. Understanding how elevated  $p\text{CO}_2$  affects reefs-forming species is crucial due to potential negative cascade effects on associated biodiversity and ecosystem functioning. To assess responses of an ecosystem engineer annelid, *Sabellaria alveolata*, to rising  $p\text{CO}_2$ , we performed a two-week experiment using control, i.e. present-day  $p\text{CO}_2$  (pH  $\sim 8.0$ ), and two future  $p\text{CO}_2$  conditions (pH  $\sim 7.6$  and  $\sim 7.4$ ). We tested the performance of worms to maintain biogenic construction by analyzing adhesive quantity and amino acids (AA) composition. Our results showed significant changes in both variables as a response to OA. Levels of change in adhesive volume and AA composition were mild at pH 7.6, and prominent at pH 7.4, compared to present-day conditions. Adhesive volume in newly constructed tubes increased 170 and 280 fold at pH 7.6 and 7.4, respectively. Further changes in AA composition were due to up-regulation of aspartic acid in both future  $p\text{CO}_2$  conditions. Our results provide the first evidence of *S. alveolata* plasticity to counteract OA by quantitatively enhancing adhesive for bioconstruction, and regulating levels of aspartic acid, which is crucial for adhesive hardening process. Present finds reveal a need to better understand how OA would alter both metabolic energy allocation to maintain high levels of adhesive synthesis, and the provision of signals to larvae settlement, as the adhesive composition play a key role inducing larvae to settle on pre-existing tubes.

**Keywords:** amino acids, environmental tolerance, foundation species, climate change, coastal, intertidal, ocean acidification, physiology, *Sabellaria*, reef





## Introduction

Between 1750 and 2010, the global cumulative anthropogenic greenhouse gas emission to the atmosphere was  $2040 \pm 310$  gigatons of carbon dioxide (GtCO<sub>2</sub>). In 2010 the total annual CO<sub>2</sub> emission represented nearly 45% over the levels in 1750 (IPCC *et al.* 2014). Although the air-sea CO<sub>2</sub> flux is a regular process on global carbon cycle, from 1800 to 1994 the oceans have absorbed about 48% of the pCO<sub>2</sub> emitted by burned fossil fuels (Sabine *et al.* 2004), and the sink ratio is likely to increase significantly during the next decades (Orr *et al.* 2005; Doney *et al.* 2009). A critical effect of the continuous increasing atmospheric CO<sub>2</sub> concentration (pCO<sub>2</sub>) ending up in the oceans is undoubtedly ocean acidification (OA). Moreover, one third of strong acids derived from combustion of fossil fuels and biomass burning (i.e. HNO<sub>3</sub> and H<sub>2</sub>SO<sub>4</sub>) is also deposited in the oceans, and half of agricultural bases (i.e. NH<sub>3</sub>) are drained to coastal oceans seas by rivers and groundwater. Both, acids and bases are driving changes in coastal seawater chemistry by reducing pH and total alkalinity (Doney *et al.* 2007; Doney *et al.* 2009). As a result, global average surface seawater pH has decreased 0.1 unit, and is expected a decline of 0.3 – 0.5 pH units up to the end of this century, representing conditions outside the bounds of preindustrial variability (Caldeira & Wickett 2005). The magnitude of predictable pH anomalies will be spatially heterogeneous (Sabine *et al.* 2004), and coastal regions would be particularly more vulnerable (Doney *et al.* 2007; Gruber *et al.* 2012). For example, nearly 30% of CO<sub>2</sub> emitted is deposited in shallow seawaters (Sabine *et al.* 2004). It is therefore likely that coastal marine biodiversity will be the first one to face ocean acidification.

Several studies on the impacts of end-of-century predicted levels for OA on a range of different marine organisms have been done, such as on algae, corals, mollusks, echinoderms, crustaceans, polychaetes, and fish (Pörtner 2008; Kroeker *et al.* 2013; Wittmann & Pörtner 2013; Li *et al.* 2014). Results vary widely from negative, to neutral to positive responses, but in general terms OA will impact negatively on most of them, more specifically crustose coralline red algae (Hofmann *et al.* 2012), ophiuroid brittlestars (Wood, Spicer & Widdicombe 2008), echinoid sea urchins (Dery, Collard & Dubois 2017), harpacticoid copepods (Sarmiento *et al.* 2017), and cod fish larvae (Frommel *et al.* 2012). Reported negative impacts of OA on marine benthic invertebrates include disturbances in chemical communication for settlement (Munday *et al.* 2009), and prey susceptibility to predators (Watson,

Fields & Munday 2017). Some studies have demonstrated alterations in polychaete tube thickness and in larvae recruitment, both showing decreasing levels in response to OA (Li *et al.* 2014; Peck *et al.* 2015). Examples of positive responses under simulated OA conditions include shells of the mollusk *Austrocochlea constricta* that at pH 7.85 was ~140 times harder than at control pH 8.1 (Leung, Russell & Connell 2017), and scleractinian corals that survive low levels of OA do not produce an endoskeleton, living as an anemone form (Fine & Tchernov 2007). Several fleshy macroalgal species, such as *Dictyota dichotoma*, *Hildenbrandia rubra*, *Sargassum vulgare*, *Cladostephus spongiosus* and *Chondracanthus acicularis* were resistant or even more dominant closer to the natural CO<sub>2</sub> vents where seawater is more acidic (Koch *et al.* 2013). In general, if a species is sensitive to small decreases in pH, it will exhibit negative response at the even lower pH or higher pCO<sub>2</sub> levels (Wittmann & Pörtner 2013). However, some species that have capacity to compensate environment hazards under low levels of elevated pCO<sub>2</sub> may negatively respond to higher pCO<sub>2</sub> (Pörtner 2008; Wittmann & Pörtner 2013). Furthermore, impacts of OA involve not only species-specific responses but also lineage, or phylogenetic-specific, responses within the same species (e.g. coccolithophorids *Emiliana huxley* O'Dea *et al.* 2014, see also, Pörtner 2008; Hoffmann & Sgrò 2011; Wittmann & Pörtner 2013). Therefore species-specific studies predicting response of key organisms toward different levels of elevated pCO<sub>2</sub> are crucial for the understanding whether a lineage, population or species are vulnerable to OA, or the overall performance is resilient and species have the ability to acclimate. Acclimation is a phenotypic response when organisms perceive environmental stimulus and modify their physiological performance through cellular and metabolic processes to cope with environment hazards (Pörtner 2008).

This study used a reef-building worm, *Sabellaria alveolata*, as a model species to test the impact of different levels of CO<sub>2</sub>-driven seawater acidification on tube housing, and hence, reef construction. Biogenic reefs of *S. alveolata* are distributed from North Africa to Scotland in Northwest Atlantic Ocean, and in Mediterranean Sea. Polychaetes of the Sabellariidae family have planktonic larvae and are strictly tubicolous after metamorphosis and settlement (Capa & Hutchings 2014). Some species play important roles as ecosystem engineers (Jones, Lawton & Shachak 1994) due to gregarious settlement behaviour (Jensen & Morse 1988; Pawlik 1988) and ability to build sand-based reefs worldwide at intertidal and shallow waters (Faroni-Perez *et al.* 2016). Several efforts have been made aiming to elucidate

the synthesis, composition, secretion, and the process of hardening the sabellariids bioadhesive (Sun *et al.* 2007; Hennebert *et al.* 2015; Stewart *et al.* 2017). For tube construction, sabellariids synthesize adhesive, also called cement, that promote permanent bond to sedimentary particles captured from the water column (Gruet, Vovelle & Grasset 1987; Main & Nelson 1988; Sun *et al.* 2009). The majority of sediments glued are calcium carbonate particles followed by quartz grains (Main & Nelson 1988). Studies using X-ray diffraction approach have also shown the presence of minerals and metal ions in the bioadhesive (Fournier, Etienne & Le Cam 2010; Stewart *et al.* 2017). Sabellariidae bioadhesive components are distinctively stored into granules that are classified as homogeneous or heterogeneous accordingly to the content, morphological characteristics, and cell type responsible for their synthesis (Wang & Stewart 2013; Hennebert *et al.* 2015). The bioadhesive composition is based on a large amount of proteins, sulfated macromolecules, minerals and metals (Gruet, Vovelle & Grasset 1987; Sun *et al.* 2009; Becker *et al.* 2012; Wang & Stewart 2013; Stewart *et al.* 2017). The homogeneous vesicles store the basic proteins whereas heterogeneous vesicles store divalent cations (e.g. Ca and Mg) and acidic proteins (Wang & Stewart 2012; Wang & Stewart 2013). Differential pH between the secretory gland (~pH 5) and seawater (~pH 8) may trigger fast bioadhesive hardening (Stewart *et al.* 2004; Stewart, Wang & Shao 2011). In fact, under natural seawater conditions Sabellariidae worms excrete a small dab of adhesive, also called cement discs, onto the grain superficies to glue to the others mineral particles. Adhesive dabs cures in the first few seconds after secretion (Stewart *et al.* 2004; Stewart, Wang & Shao 2011; Wang & Stewart 2012; Hennebert *et al.* 2015). Given rapid underwater hardening process, adhesive integrity and stiffness, we ask: does OA affect bioconstruction in *Sabellaria alveolata*? If so, do observed changes in bioadhesive correspond to a compensatory response to maintain glue performance under OA conditions?

To help answer some of these questions we test whether CO<sub>2</sub>-driven seawater acidification trigger changes in the structure and chemistry of secreted bioadhesive using *S. alveolata* as model reef-building organism. Fragments of *S. alveolata* reefs were exposed for 14 days to present-days and future ocean acidification scenarios. We tested the follows hypotheses: i) *S. alveolata* can maintain bioadhesive synthesis and secretion for biogenic construction while exposed to future OA conditions, ii) the amino acids components and structure of adhesive from tubes can exhibit plasticity and hence will change as a response to

different OA conditions, and iii) changes in adhesive quantity and AA composition will be more pronounced in specimens exposed to lower future pH compared to present-day control conditions. Organisms could acclimate and counteract ocean acidification conditions if plasticity in bioconstruction process allows a compensatory mechanism that regulate and maintain performance and fitness.

## Material and Methods

### *Biological sampling and experimental setup*

Several reef blocks of *Sabellaria alveolata* were collected on the same day (August, 19<sup>th</sup> 2017) from Mont St. Michel Bay, France (48° 43' 52.77" N, 1° 33' 8.77" W). Blocks were allowed to stabilize in an open-flow tank with natural unfiltered seawater for 15 days at  $19 \pm 1^\circ\text{C}$ ,  $\text{pH } 8.0 \pm 0.1$ , salinity  $35 \pm 1$  ppt. Then, nine blocks were selected, each of them was subdivided into three smaller fragments and individually weighted. Information on reef fragment weights is available in the supplementary material (Table S1). Reef fragments were transferred into nine glass aquaria filled with 9 L natural seawater. Three pH/ $p\text{CO}_2$  treatments were used: one control and two different higher  $p\text{CO}_2$  (details below). Each pH/ $p\text{CO}_2$  treatment was replicated three times (= 9 total aquaria). Each  $p\text{CO}_2$  treatment received one of the three smaller fragments from the same reef block ensuring that blocks from the same *S. alveolata* 'colony' were exposed to all three pH/ $p\text{CO}_2$  treatments. Treatments were gradually adjusted experimental  $p\text{CO}_2$  conditions at a  $0.1 \text{ pH}_T \text{ unit.day}^{-1}$  rate, whereas the reference (control) aquaria had natural seawater. Before  $\text{pH}_T$  levels reached nominal targets, distal parts of tubes (i.e. hood) were carefully removed in order to stimulate the worms to reconstruct their tubes. Each aquarium had a 100% exchange rate every 10 min and submerged pumps (TUNZE Turbelle nanostream 6025) to ensure seawater and mineral particles circulation, a constant arrival of plankton as natural food for animals, and to prevent accumulation of metabolic waste. The mineral particles used (i.e. sand grains used by the worms to rebuild their tubes) were previously sieved, washed, autoclaved and dried at  $60^\circ\text{C}$  for several days. An exact amount of 45 g of mineral particles was added per aquarium per day. Two levels of higher  $p\text{CO}_2$ :  $\sim 1332$  ppm and  $\sim 2173$  ppm  $\text{CO}_2$ , which correspond to  $\text{pH}_T \sim 7.6$  and  $\sim 7.4$ , respectively, were used, beside the control level (= present day) at  $\sim 474$  ppm  $\text{CO}_2$ ,  $\text{pH}_T \sim 8.0$ . The acidified seawater was obtained by bubbling pure  $\text{CO}_2$  into the

sump tanks using a gas exchanger (Aqua 1000 reactor, Aqua Medic, Germany) through electrovalves (Aqua Medic, Germany) controlled by a pH-stat system (Aquastar, IKS Computer System, Karlsbad, Germany). The  $p\text{CO}_2$  levels simulated the predicted RCP8.5 scenario values in areas within the occurrence range of species for the near future (i.e. 2050) and year 2100 (Faroni-Perez 2017) (see Supp. Mat. Table S2). The experiment ran for 14 days.

A pH electrode (Aquastar, Germany) and a temperature sensor (Aquastar, Germany) connected to an automatic computer controlled system (IKS, Aquastar, Germany) were immersed in each sump tank that filled the replicated aquaria. The pH and temperature of each sump tank were recorded by IKS every 15 minutes. Daily, the  $\text{pH}_{\text{NIST}}$  (National Institute of Standards and Technology) and electromotive force (e.m.f.) were measured using a pH meter (827 pH mobile, Metrohm, Herisau, Switzerland) equipped with a glass electrode and a temperature sensor (Metrohm electrode plus, Switzerland) calibrated with  $\text{pH}_{\text{NBS}}$  buffers 4.01 and 6.97 (SI Analytics GmbH, Germany). For the calculation of the effective  $\text{pH}_{\text{T}}$  (total scale), were used once a day the e.m.f. values and sequential measurements of the e.m.f. of the cell, standard buffers of known pH, 2-aminopyridine/HCL (AMP) and tris/HCL (TRIS) (DelValls & Dickson 1998; Dickson, Sabine & Christian 2007). Also, salinity and temperature were measured daily using a pH/Cond 340 WTW (USA) conductivity meter. Seawater chemistry was calculated following Dickson et al., (2007). The target pH values established in the IKS control system were daily calculated and adjusted fitting the difference detected between the  $\text{pH}_{\text{T}}$  and the pH measured by the pH electrode connected to the IKS system. Daily variation of seawater  $\text{pH}_{\text{T}}$ , temperature and salinity during in the experiment is available in supplementary material (see Supp. Mat. Table S3).

#### *Adhesive properties*

At the end of experiment, the reef fragments were dissected to obtain freshly constructed tubes. To examine the structure of newly synthesized adhesive, five randomly chosen fresh tubes per aquarium per  $p\text{CO}_2$  treatment were fully dried at 60 °C. Photomicrographs of each tube (n=5) were obtained via a Nikon camera attached to a SMZ1000 digital microscope and NIS-Elements Viewer software. We examined and compared the volume and shape of secreted adhesive dabs among treatments. The widths of thirty dabs per  $p\text{CO}_2$  treatment were randomly measured using ImageJ software to quantify the volume of adhesive.

The 3-D schemes were developed using the software ZBrushCore® licenced to LFP.

For amino acids profile, immediately after the end of the experiment, five fresh tubes per aquarium per  $p\text{CO}_2$  treatment were inserted into individual cryotubes, frozen at  $-20^\circ\text{C}$ , and stored at  $-80^\circ\text{C}$  until analysis. Then, each sample was weighed, transferred into a vial for homogenization, and mixed with 200  $\mu\text{l}$  of HCl (6N), and proteins were then hydrolysed (24 h at  $110^\circ\text{C}$ ) in vacuum using a sealed glass ampule. Samples were dried using a speedvac after hydrolysis. The resulting amino acids were separated by ion-exchange HPLC using a high-efficiency sodium column ( $4 \times 150$  mm; Pickering Lab, LCTech, Dorfen, Germany) with a Waters 2695 separation module (Waters). The elution buffers and gradient conditions were those recommended by the manufacturer. Amino acids were first subjected to post-column derivatization with Ninhydrin (Pickering Laboratories, Mountain View, California, USA) by using a PCX 5200 derivatizer (Pickering Laboratories, Mountain View, California, USA) and later detected on a Waters 2996 Photodiode as a UV module detector at 570 nm for all the amino acids containing a primary amine, and at 440 nm for the Proline which holds a secondary amine. Quantification was performed by repeated injections of standards over a range of dilutions to determine the relationship between peak area and standard concentrations. The relative abundance of each amino acid (%) was calculated from their respective concentrations.

#### *Statistical analysis*

To assess differences in the adhesive volume among  $p\text{CO}_2$  conditions, non-parametric Kruskal-Wallis followed by Kramer (Nemenyi) pairwise *post-hoc* comparisons tests were applied to assign  $P$  values. To test the effect of  $p\text{CO}_2$  treatment on adhesive AAs composition, a permutational multivariate analysis of variance (PERMANOVA) (999 replications) was performed using Bray–Curtis dissimilarity values. The assumption of analysis of multivariate homogeneity of group variance was examined via the test ‘betadisper’. Principal components analysis (PCA) was used to visualize differences in compositional changes in AA’s among treatments. Similarity percentages analysis (SIMPER) was performed to identify the AAs that contributed most greatly to the overall Bray–Curtis dissimilarity values. All statistical analyses were performed using the ‘vegan’(Oksanen *et al.* 2017) and ‘ade4’(Dray & Dufour 2007) packages in R(R Core Team 2017).

## Results

### *Structure of bioadhesive*

New tubes constructions were observed under all pH treatments. Statistically significant difference in the volume of secreted adhesive calculated for each pH treatment was detected ( $\chi^2 = 57.562$ ,  $df = 2$ ,  $P < 0.05$ ). Mean size of adhesive dabs in the pH  $\sim 7.6$  and  $\sim 7.4$  increased 172% and 288%, respectively, compared to pH  $\sim 8.0$  (Fig. 1). Visually, tubes from the control pH showed the regular small dab size of adhesive used in particles bonding (Fig. 2A – B), whereas dab size of adhesive used in tubes under the two lower pH conditions increased abnormally (Fig. 2C – F)

### *Amino acids from cured bioadhesive*

Amino acid composition from coalesced adhesive under lower pH conditions was significantly different from the control (PERMANOVA, pseudo- $F_{2,8} = 5.591$ ,  $R^2 = 0.650$ ,  $P = 0.019$ , permutations = 999), and equitability index tended downward with low pH values (Fig. 3A – B). Global dissimilarity in amino acid composition between control (pH $\sim 8.0$ ) and both pH  $\sim 7.6$  and  $\sim 7.4$  were 12.4 and 25.1%, respectively, whereas between pH  $\sim 7.6$  and  $\sim 7.4$  was 19.2% (Tab. 1). In each of the three SIMPER pairwise possible combinations, four out of nine amino acids accounted for the majority ( $> 70\%$ ) of cumulative contributions to dissimilarities (Tab. 1). Aspartic acid was the AA that most contributed to dissimilarities among all pairwise combinations, and glycine was also in the top four. Depending of the SIMPER pairwise comparison, the contributions of valine, alanine, serine, and glutamic acid were also in the majority ( $> 70\%$ ) of cumulative contributions to dissimilarities (Tab. 1). On the other hand, phenylalanine, leucine, and isoleucine presented the lowest scores in cumulative contribution to dissimilarities among all pairwise comparisons (Tab. 1), although molar changes also occurred in these amino acids (Fig. 4). Aspartic acid accounted for more than 40% of the pairwise dissimilarity between pH 7.4 and the other two pH (Fig. 4). The pH 7.6 showed highest ratio of glycine contrasting to control and pH 7.4 (Fig. 4). The ratio of the other seven amino acids (i.e. alanine, serine, glutamic ac., valine, leucine, isoleucine, and phenylalanine) gradually decreased with the decreasing seawater pH values (Fig. 4, Supp. Mat. Figure S4).

## Discussion

We found that CO<sub>2</sub>-driven seawater acidification can significantly alter the amount of adhesive and the adhesive amino acids composition secreted by *Sabellaria alveolata*. We reject the null hypothesis of no effect of OA on the biogenic construction of *S. alveolata*. Our results also showed that *S. alveolata* exhibit compensatory response to maintain the bioadhesive performance over short-term under OA conditions. The observed changes in the volume of adhesive secreted and amino acids composition is evidence for plasticity and acclimation capacity of *S. alveolata* to future OA conditions. Our findings regarding tube plasticity under elevated *p*CO<sub>2</sub> are consistent to the levels of acclimation observed for calcifier and non-calcifier biomineralizers organisms (Koch *et al.* 2013; Leung, Russell & Connell 2017).

Acclimation as a function of decreasing pH is likely to occur in marine organisms in the form of changes in gene expression, lipid metabolism, behaviour, and ion homeostasis (Pespeni *et al.* 2013; Li *et al.* 2016). Several marine organisms have been reported as able to acclimate to elevated *p*CO<sub>2</sub> over short-term, such as non-calcified fleshy macroalgae (Koch *et al.* 2013), sea urchin (Pespeni *et al.* 2013; Moulin *et al.* 2014), barnacle (Pansch *et al.* 2014), pearl oyster (Li *et al.* 2016), including scleractinian coral (Fine & Tchernov 2007) and gastropods (Leung, Russell & Connell 2017). There are, however, evidences that negative effects of OA over long-term exposure may exist (Wood, Spicer & Widdicombe 2008; Frommel *et al.* 2012; Kroeker *et al.*, 2013, Turner *et al.*, 2015; Sarmiento *et al.* 2017), and hence acclimation results as observed in this study should be taken with caution. The increase in adhesive amount and area lead to a decrease in interstitial pore size decreasing the exposure of worms to acidified water (Fig. 2). Other potential physiological effects should also be considered. For instance, cellular homeostasis and biomineralization have elevated metabolic costs (Pörtner 2008). For example, during five days exposure to high *p*CO<sub>2</sub> conditions the non-calcifying tubicolous polychaete *Sabella spallanzanii* was able to sustain metabolism by increasing ATP levels, however, the concomitant reduction in carbonic anhydrase indicated loss of cellular homeostatic capacity that is unlikely to be upheld long term (Turner *et al.*, 2015). In the brittlestar *Amphiura filiformis* long-term exposure to elevated *p*CO<sub>2</sub> increased biomineralization rates at the expense of muscle mass indicating potential physiologic constrain (Wood, Spicer & Widdicombe 2008). Cod larvae reared under elevated



$p\text{CO}_2$  allocated energy to growth at the cost of organ development, including increased levels of tissue damage on eyes, liver, gut, pancreas, and kidney (Frommel *et al.* 2012). Although meiofauna organisms associated to coral reefs (i.e. Polychaeta, Harpacticoida and Ostracoda) were tolerant over 15 days exposure to elevated  $p\text{CO}_2$ , their densities significantly decreased over 29 days especially in conditions of elevated  $p\text{CO}_2$  (Sarmiento *et al.* 2017). By comparing our pH 7.6 and pH 7.4 results, we observed that increased bioconstruction required allocation of extra energy to produce larger amount of adhesive, which may imply in metabolic budget depression to perform others important physiological or ecological needs (e.g. cellular homeostasis, growth and reproduction), leading to unsuccessful performance and fitness, particularly in the long term. This extra cost might be a result of animals trying to shield themselves from acidified or hypoxic seawater. Some studies demonstrated that marine organisms, such as the sea urchin *Strongylocentrotus purpuratus*, allocate more energy to adjust cellular homeostasis when animals are under elevated  $p\text{CO}_2$ , which could be interpreted as a sign of physiological stress (Pörtner 2008; Wood, Spicer & Widdicombe 2008). Food availability also drives species' sensitivity to elevated  $p\text{CO}_2$  conditions. The barnacle *Amphibalanus improvisus* in high food treatment show better acclimation to elevated  $p\text{CO}_2$  than low food treatment, regardless of populations' source condition as more stable or variable  $p\text{CO}_2$  environment (Pansch *et al.* 2014). *Strongylocentrotus purpuratus* under near-future OA scenario produced an increase of ~30% in the allocation of metabolic energy demand for protein synthesis and ion transport (Pan, Applebaum & Manahan 2015). Such shifts in energy allocation almost certainly constrain the energy budget for other biochemical processes (Pan, Applebaum & Manahan 2015). Thus, considering that increased bioadhesive volume in *S. alveolata* upon exposure to high  $p\text{CO}_2$  may be costly, potentially producing changes in cells shape and tissues structures, additional histological analyses are in course. Alternatively, if under elevated  $p\text{CO}_2$  conditions *S. alveolata* can increase feeding rate to acquire more energy, than is likely that this species has adaptive functionality to survive future OA scenarios in the long term as well.

The composition of AAs involved in marine biomineralization can change in response to different environmental factors (Ingalls, Lee & Druffel 2003). Our results revealed AAs changes in adhesive composition as evidence of inherent ability of *S. alveolata* to control bioadhesive synthesis. In both elevated  $p\text{CO}_2$  treatments, we detected a significant up-regulation of aspartic acid and we interpret this up-

regulation as evidence of plasticity in the processes of bioadhesive hardening. Aspartic acid is a negatively charged AA, therefore crucial for binding with both  $Mg^{2+}$  and  $Ca^{2+}$  ions during adhesive curing (Sun *et al.* 2007). Proteins rich in aspartic acid and glutamic acid play a major role in controlling biomineralization process, and are the main components in reef-building corals skeletons and mollusks shells (Hare 1963; Constantz & Weiner 1988; Gotliv, Addadi & Weiner 2003). In coral skeletons, shifts in mole concentration of aspartic acid have been associated to physiological disturbances (Gupta, Suzuki & Kawahata 2006). In sabellariids, proteins are the major component of the adhesive and aspartic acid and glutamic acid have been described previously as major AAs constituents (Jensen & Morse 1988; Zhao *et al.* 2005; Wang & Stewart 2013). Currently, we can not determine if observed changes in the AAs composition may imply different amounts of specific protein synthesis or type of granule (i.e. homogeneous and heterogeneous). However, our results showed that change is characterized by the down-regulation of seven amino acids mostly in favour of the up-regulation of a single acidic amino acid (i.e. aspartic acid).

Although the total numbers of studies on adhesive protein characterization and synthesis in sabellariids have been increasing (Jensen & Morse 1988; Zhao *et al.* 2005; Sun *et al.* 2009; Becker *et al.* 2012), to date only three adhesive proteins have been described for *S. alveolata*: Sa-1, Sa-2 and Sa-3. Sa-1 and Sa-2 are both basic proteins rich in glycine, alanine, tyrosine and basic residues. Sa-3, with further subdivision into Sa-3A and Sa-3B, is an acidic serine-rich class of proteins (Becker *et al.* 2012). Our results indicated that independently of  $pCO_2$  conditions glycine had the most molar expression levels. A previous study on the adhesive of *Phragmatopoma californica* has also demonstrated glycine to be of highest molar expression, and the Gly-rich proteins of sabellariid are similar in composition to those found in many bivalve mollusks (Zhao *et al.* 2005).

Amino acid substitutions in biomineralization proteins were observed in the purple sea urchin *S. purpuratus* and in the pearl oyster *Pinctada fucata* in response to elevated  $pCO_2$  over short-time periods (Pespeni *et al.* 2013; Li *et al.* 2016). Such AAs shifts may provide evidence of biomineralizers counteracting OA impacts. It is important to emphasize that proteins present in cured adhesive are important inductor for new larval settlement (Jensen & Morse 1988; Waite, Jensen & Morse 1992). Therefore, changes in AAs composition in cured adhesives in response to decreasing pH can potentially lead to unsuccessful chemical cue to conspecific larvae settlement, and so,

biogenic reef replenishment. Although the sabellariid larvae's sensory organs involved in settlement have been recently described (Faroni-Perez *et al.* 2016), nothing is yet known if shifts in adhesive AAs composition due to the OA condition could drive imbalance in larvae's neurotransmitters receptors. Disturbances in neuronal capability of larvae to select conspecific tubes as place to settle would lead to unsuccessful reef accretion and maintenance. Like gregarious sabellariids, clownfish larvae also uses chemical cues from conspecifics as stimuli to chose a place to settle, and although larvae did not present morphological injury in nasal cavity under low pH conditions, they were not able to respond to chemical cues (Munday *et al.* 2009). When exposed to elevated  $p\text{CO}_2$  the dog shark *Mustelus canis* avoided the trial plume with chemical cues of food (Dixon *et al.* 2015). Therefore, recent studies revealed the impact of OA on marine lineages that heavily evolved sensory organs for ecological processes. More studies to determine whether shifts in bioadhesive AAs composition or/and larvae neuronal activity will be impaired by OA, and consequential drive changes in settlement, recruitment, and reef maintenance, are called for.

The physiological adjustments found for *S. alveolata* to maintain bioconstruction can be explained as a phenotypically plastic response. The studied population, and all known sabellariids reefs worldwide, occur in coastal zones (Faroni-Perez *et al.* 2016). Coastal zones as suitable habitats for sabellariids are associated to a multiple drivers, such as rain and river drainage effects, that directly affect pH variability (Faroni-Perez 2017). We highlight that is crucial to evaluate whether anthropogenic OA over long-term exposures affects the species acclimation ability given the observed bioconstruction shifts as plastic compensatory response

### **Acknowledgements**

We thank the assistance of the technicians and researchers of the MNHN- Biological Marine Station of Concarneau for their help during experimental setup and fieldwork. This study was supported by the MNHN to JF (ATM MNHN 'Formes Possibles, Formes Réalisées' 2015-2016), and the Brazilian Ministry of Science and Technology through the National Council for Scientific and Technological Development Award to LFP (CNPq – "Science Without Borders" 201233/2015-0). CFDG also thanks CNPq for a PQ grant (309658/2016-0). The authors declare no competing financial interests.

## References

- Becker, P.T., Lambert, A., Lejeune, A., Lanterbecq, D. & Flammang, P. (2012) Identification, characterization, and expression levels of putative adhesive proteins from the tube-dwelling polychaete *Sabellaria alveolata*. *Biological Bulletin*, **223**, 217–225.
- Caldeira, K. & Wickett, M.E. (2005) Ocean model predictions of chemistry changes from carbon dioxide emissions to the atmosphere and ocean. *Journal of Geophysical Research-Oceans*, **110**, 1–12.
- Capa, M. & Hutchings, P. (2014) Sabellariidae Johnston, 1865.
- Constantz, B. & Weiner, S. (1988) Acidic macromolecules associated with the mineral phase of scleractinian coral skeletons. *Journal of Experimental Zoology*, **248**, 253–258.
- DelValls, T.A. & Dickson, A.G. (1998) The pH of buffers based on 2-amino-2-hydroxymethyl-1,3-propanediol ('tris') in synthetic sea water. *Deep Sea Research Part I: Oceanographic Research Papers*, **45**, 1541–1554.
- Dery, A., Collard, M. & Dubois, P. (2017) Ocean acidification reduces spine mechanical strength in euechinoid but not in cidaroid sea urchins. *Environmental Science & Technology*, **51**, 3640–3648.
- Dickson, A.G., Sabine, C.L. & Christian, J.R. (2007) *Guide to best practices for ocean CO<sub>2</sub> measurements*. North Pacific Marine Science Organization, Sidney, BC, Canada.
- Dixson, D.L., Jennings, A.R., Atema, J. & Munday, P.L. (2015) Odor tracking in sharks is reduced under future ocean acidification conditions. *Global Change Biology*, **21**, 1454–1462.
- Doney, S.C., Fabry, V.J., Feely, R.A. & Kleypas, J.A. (2009) Ocean acidification: The other CO<sub>2</sub> problem. *Annual Review of Marine Science*, **1**, 169–192.
- Doney, S.C., Mahowald, N., Lima, I., Feely, R.A., Mackenzie, F.T., Lamarque, J.F. & Rasch, P.J. (2007) Impact of anthropogenic atmospheric nitrogen and sulfur deposition on ocean acidification and the inorganic carbon system. *Proceedings of the National Academy of Sciences of the United States of America*, **104**, 14580–14585.
- Dray, S. & Dufour, A.B. (2007) The ade4 package: implementing the duality diagram for ecologists. *Journal of Statistical Software*, 1–20.
- Faroni-Perez, L. (2017) Climate and environmental changes driving idiosyncratic shifts in the distribution of tropical and temperate

- worm reefs. *Journal of the Marine Biological Association of the United Kingdom*, **97**, 1023–1035.
- Faroni-Perez, L., Helm, C., Burghardt, I., Hutchings, P. & Capa, M. (2016) Anterior sensory organs in Sabellariidae (Annelida). *Invertebrate Biology*, **135**, 423–447.
- Fine, M. & Tchernov, D. (2007) Scleractinian coral species survive and recover from decalcification. *Science*, **315**, 1811–1811.
- Fournier, J., Etienne, S. & Le Cam, J.B. (2010) Inter- and intraspecific variability in the chemical composition of the mineral phase of cements from several tube-building polychaetes. *Geobios*, **43**, 191–200.
- Frommel, A.Y., Maneja, R., Lowe, D., Malzahn, A.M., Geffen, A.J., Folkvord, A., Piatkowski, U., Reusch, T.B.H. & Clemmesen, C. (2012) Severe tissue damage in Atlantic cod larvae under increasing ocean acidification. *Nature Climate Change*, **2**, 42–46.
- Gotliv, B.A., Addadi, L. & Weiner, S. (2003) Mollusk shell acidic proteins: In search of individual functions. *ChemBiochem*, **4**, 522–529.
- Gruber, N., Hauri, C., Lachkar, Z., Loher, D., Frolicher, T.L. & Plattner, G.K. (2012) Rapid progression of ocean acidification in the California current system. *Science*, **337**, 220–223.
- Gruet, Y., Vovelle, J. & Grasset, M. (1987) Biomineral components of tube cement of *Sabellaria alveolata* (L.), (Annelida Polychaeta). *Canadian Journal of Zoology-Revue Canadienne De Zoologie*, **65**, 837–842.
- Gupta, L.P., Suzuki, A. & Kawahata, H. (2006) Aspartic acid concentrations in coral skeletons as recorders of past disturbances of metabolic rates. *Coral Reefs*, **25**, 599–606.
- Hare, P.E. (1963) Amino acids in proteins from aragonite and calcite in shells of *Mytilus californianus*. *Science*, **139**, 216–217.
- Hennebert, E., Maldonado, B., Van De Weerd, C., Demeuldre, M., Richter, K., Rischka, K. & Flammang, P. (2015) From sand tube to test tube: the adhesive secretion from sabellariid tubeworms. *Bioadhesion and Biomimetics*, pp. 109–128. Pan Stanford.
- Hoffmann, A.A. & Sgrò, C.M. (2011) Climate change and evolutionary adaptation. *Nature*, **470**, 479–485.
- Hofmann, L.C., Yildiz, G., Hanelt, D. & Bischof, K. (2012) Physiological responses of the calcifying rhodophyte, *Corallina officinalis* (L.), to future CO<sub>2</sub> levels. *Marine Biology*, **159**, 783–792.

- Ingalls, A.E., Lee, C. & Druffel, E.R.M. (2003) Preservation of organic matter in mound-forming coral skeletons. *Geochimica Et Cosmochimica Acta*, **67**, 2827–2841.
- IPCC, Core Writing Team, Pachauri, R.K. & Meyer, L.A. (2014) *Climate Change 2014: Synthesis Report. Contribution of Working Groups I, II and III to the Fifth Assessment Report of the Intergovernmental Panel on Climate Change*. Geneva, Switzerland.
- Jensen, R.A. & Morse, D.E. (1988) The bioadhesive of *Phragmatopoma californica* tubes: a silk-like cement containing L-DOPA. *Journal of Comparative Physiology B*, **158**, 317–324.
- Jones, C.G., Lawton, J.H. & Shachak, M. (1994) Organisms as ecosystem engineers. *Oikos*, **69**, 373–386.
- Koch, M., Bowes, G., Ross, C. & Zhang, X.H. (2013) Climate change and ocean acidification effects on seagrasses and marine macroalgae. *Global Change Biology*, **19**, 103–132.
- Kroeker, K.J., Kordas, R.L., Crim, R., Hendriks, I.E., Ramajo, L., Singh, G.S., Duarte, C.M. & Gattuso, J.-P. (2013) Impacts of ocean acidification on marine organisms: quantifying sensitivities and interaction with warming. *Global Change Biology*, **19**, 1884–1896.
- Leung, J.Y., Russell, B.D. & Connell, S.D. (2017) Mineralogical plasticity acts as a compensatory mechanism to the impacts of ocean acidification. *Environ Sci Technol*, **51**, 2652–2659.
- Li, C.Y., Chan, V.B.S., He, C., Meng, Y., Yao, H.M., Shih, K.M. & Thiyagarajan, V. (2014) Weakening mechanisms of the serpulid tube in a high-CO<sub>2</sub> world. *Environmental Science & Technology*, **48**, 14158–14167.
- Li, S.G., Huang, J.L., Liu, C., Liu, Y.J., Zheng, G.L., Xie, L.P. & Zhang, R.Q. (2016) Interactive effects of seawater acidification and elevated temperature on the transcriptome and biomineralization in the pearl oyster *Pinctada fucata*. *Environmental Science & Technology*, **50**, 1157–1165.
- Main, M.B. & Nelson, W.G. (1988) Sedimentary characteristics of sabellariid worm reefs (*Phragmatopoma lapidosa* Kinberg). *Estuarine, Coastal and Shelf Science*, **26**, 105–109.
- Moulin, L., Grosjean, P., Leblud, J., Batigny, A. & Dubois, P. (2014) Impact of elevated *p*CO<sub>2</sub> on acid-base regulation of the sea urchin *Echinometra mathaei* and its relation to resistance to ocean acidification: A study in mesocosms. *Journal of Experimental Marine Biology and Ecology*, **457**, 97–104.

- Munday, P.L., Dixson, D.L., Donelson, J.M., Jones, G.P., Pratchett, M.S., Devitsina, G.V. & Doving, K.B. (2009) Ocean acidification impairs olfactory discrimination and homing ability of a marine fish. *Proceedings of the National Academy of Sciences of the United States of America*, **106**, 1848–1852.
- O'Dea, S.A., Gibbs, S.J., Bown, P.R., Young, J.R., Poulton, A.J., Newsam, C. & Wilson, P.A. (2014) Coccolithophore calcification response to past ocean acidification and climate change. *Nature Communications*, **5**, 7.
- Oksanen, J., Blanchet, F.G., Friendly, M., Kindt, R., Legendre, P., McGlinn, D., Minchin, P.R., O'Hara, R.B., Simpson, G.L., Solymos, P., Stevens, M.H.H., Szoecs, E. & Wagner, H. (2017) vegan: Community Ecology Package. *R package version 2.4-2*.
- Orr, J.C., Fabry, V.J., Aumont, O., Bopp, L., Doney, S.C., Feely, R.A., Gnanadesikan, A., Gruber, N., Ishida, A., Joos, F., Key, R.M., Lindsay, K., Maier-Reimer, E., Matear, R., Monfray, P., Mouchet, A., Najjar, R.G., Plattner, G.K., Rodgers, K.B., Sabine, C.L., Sarmiento, J.L., Schlitzer, R., Slater, R.D., Totterdell, I.J., Weirig, M.F., Yamanaka, Y. & Yool, A. (2005) Anthropogenic ocean acidification over the twenty-first century and its impact on calcifying organisms. *Nature*, **437**, 681–686.
- Pan, T.C.F., Applebaum, S.L. & Manahan, D.T. (2015) Experimental ocean acidification alters the allocation of metabolic energy. *Proceedings of the National Academy of Sciences of the United States of America*, **112**, 4696–4701.
- Pansch, C., Schaub, I., Havenhand, J. & Wahl, M. (2014) Habitat traits and food availability determine the response of marine invertebrates to ocean acidification. *Global Change Biology*, **20**, 765–777.
- Pawlik, J.R. (1988) Larval settlement and metamorphosis of two gregarious sabellariid polychaetes: *Sabellaria alveolata* compared with *Phragmatopoma californica*. *Journal of the Marine Biological Association of the United Kingdom*, **68**, 101–124.
- Peck, L.S., Clark, M.S., Power, D., Reis, J., Batista, F.M. & Harper, E.M. (2015) Acidification effects on biofouling communities: winners and losers. *Global Change Biology*, **21**, 1907–1913.
- Pespeni, M.H., Sanford, E., Gaylord, B., Hill, T.M., Hosfelt, J.D., Jaris, H.K., LaVigne, M., Lenz, E.A., Russell, A.D., Young, M.K. & Palumbi, S.R. (2013) Evolutionary change during experimental ocean acidification. *Proceedings of the National Academy of Sciences of the United States of America*, **110**, 6937–6942.

- Pörtner, H.O. (2008) Ecosystem effects of ocean acidification in times of ocean warming: a physiologist's view. *Marine Ecology Progress Series*, **373**, 203–217.
- R Core Team (2017) R: A Language and Environment for Statistical Computing. R Foundation for Statistical Computing, Vienna, Austria.
- Sabine, C.L., Feely, R.A., Gruber, N., Key, R.M., Lee, K., Bullister, J.L., Wanninkhof, R., Wong, C.S., Wallace, D.W.R., Tilbrook, B., Millero, F.J., Peng, T.H., Kozyr, A., Ono, T. & Rios, A.F. (2004) The oceanic sink for anthropogenic CO<sub>2</sub>. *Science*, **305**, 367–371.
- Sarmiento, V.C., Pinheiro, B.R., Montes, M.D.F. & Santos, P.J.P. (2017) Impact of predicted climate change scenarios on a coral reef meiofauna community. *Ices Journal of Marine Science*, **74**, 1170–1179.
- Stewart, R.J., Wang, C.S. & Shao, H. (2011) Complex coacervates as a foundation for synthetic underwater adhesives. *Advances in Colloid and Interface Science*, **167**, 85–93.
- Stewart, R.J., Wang, C.S., Song, I.T. & Jones, J.P. (2017) The role of coacervation and phase transitions in the sandcastle worm adhesive system. *Advances in Colloid and Interface Science*, **239**, 88–96.
- Stewart, R.J., Weaver, J.C., Morse, D.E. & Waite, J.H. (2004) The tube cement of *Phragmatopoma californica*: a solid foam. *Journal of Experimental Biology*, **207**, 4727–4734.
- Sun, C.J., Fantner, G.E., Adams, J., Hansma, P.K. & Waite, J.H. (2007) The role of calcium and magnesium in the concrete tubes of the sandcastle worm. *Journal of Experimental Biology*, **210**, 1481–1488.
- Sun, C.J., Srivastava, A., Reifert, J.R. & Waite, J.H. (2009) Halogenated DOPA in a marine adhesive protein. *Journal of Adhesion*, **85**, 126–138.
- Waite, J.H., Jensen, R.A. & Morse, D.E. (1992) Cement precursor proteins of the reef-building polychaete *Phragmatopoma californica* (fewkes). *Biochemistry*, **31**, 5733–5738.
- Wang, C.S. & Stewart, R.J. (2012) Localization of the bioadhesive precursors of the sandcastle worm, *Phragmatopoma californica* (Fewkes). *Journal of Experimental Biology*, **215**, 351–361.
- Wang, C.S. & Stewart, R.J. (2013) Multipart copolyelectrolyte adhesive of the sandcastle worm, *Phragmatopoma californica* (Fewkes):



- catechol oxidase catalyzed curing through peptidyl-DOPA. *Biomacromolecules*, **14**, 1607–1617.
- Watson, S.A., Fields, J.B. & Munday, P.L. (2017) Ocean acidification alters predator behaviour and reduces predation rate. *Biology Letters*, **13**, 20160797.
- Wittmann, A.C. & Pörtner, H.O. (2013) Sensitivities of extant animal taxa to ocean acidification. *Nature Climate Change*, **3**, 995–1001.
- Wood, H.L., Spicer, J.I. & Widdicombe, S. (2008) Ocean acidification may increase calcification rates, but at a cost. *Proceedings of the Royal Society B-Biological Sciences*, **275**, 1767–1773.
- Zhao, H., Sun, C., Stewart, R.J. & Waite, J.H. (2005) Cement proteins of the tube-building polychaete *Phragmatopoma californica*. *Journal of Biological Chemistry*, **280**, 42938–42944.

## FIGURES AND TABLE

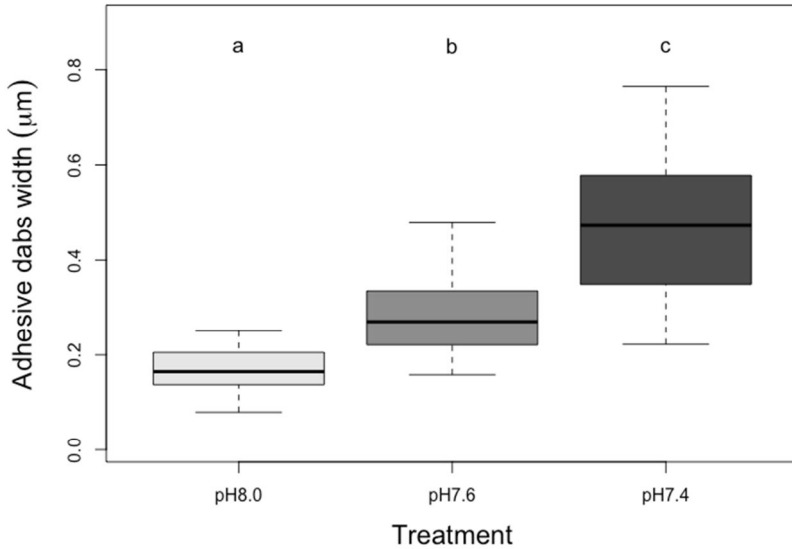


**Figure 1:** Analysis of adhesive dabs wideness (mean  $\pm$  SD) of *Sabellaria alveolata* in responses to different  $p\text{CO}_2$  treatments (Kruskal-Wallis,  $P < 0.05$ , letters indicate pairwise *post-hoc* comparisons). The box plot limits represent the interquartile range (25th to 75th percentiles), the median is the horizontal line, and the vertical lines indicate the 10th (bottom) and 90th (top) percentiles, respectively.

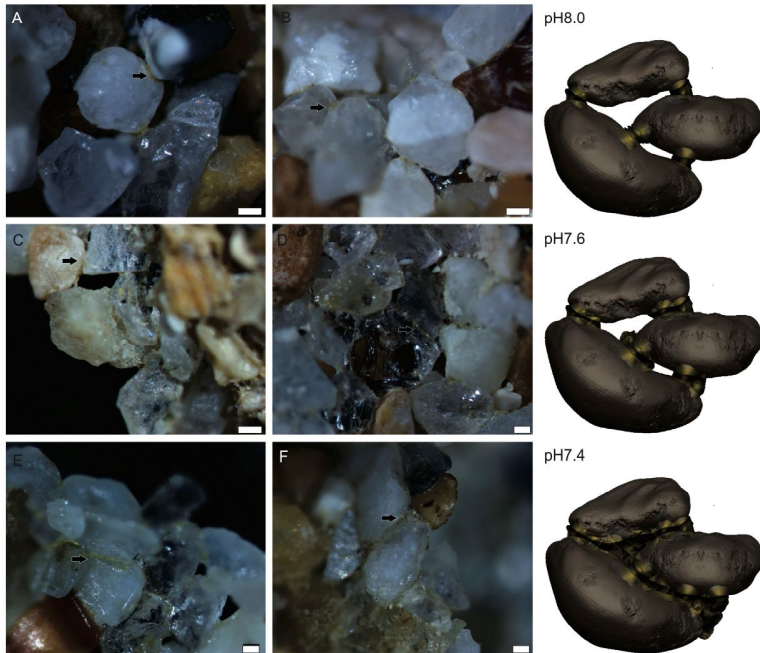


**Figure 2** Adhesive volume used by *Sabellaria alveolata* to glue sedimentary particles for tube building in different seawater pH conditions: A– B (control, pH8.0) show the regular dabs; C–D (elevated  $p\text{CO}_2$ , pH~7.6) dabs intermediary size, and E – F (elevated  $p\text{CO}_2$ , pH~7.4) dabs volume markedly increased. Scales = 200  $\mu\text{m}$ . On right side, digital reconstruction scheme of sedimentary particles and adhesive dabs.

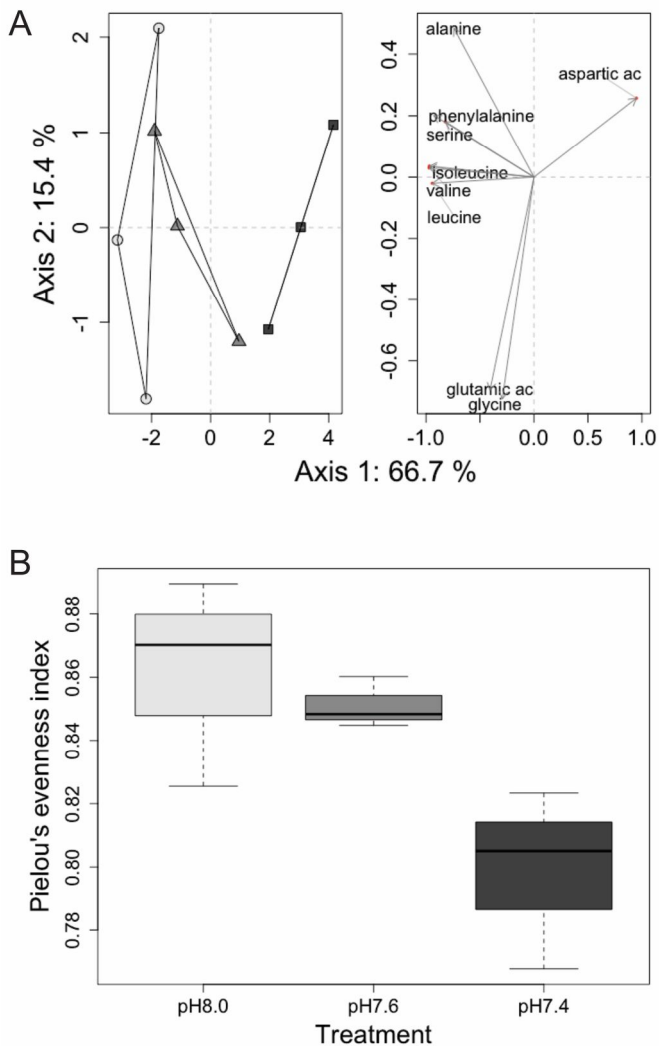


**Figure 3** : Amino acids global composition differences in the coalesced adhesive produced by *Sabellaria alveolata* in the three different  $p\text{CO}_2$  conditions. **A**: Principal component analysis of amino acids among treatments; circle = pH8.0, triangle = pH7.6, and square = pH7.4, and **B**: Equitability ( $J'$ ) of amino acids per treatment.

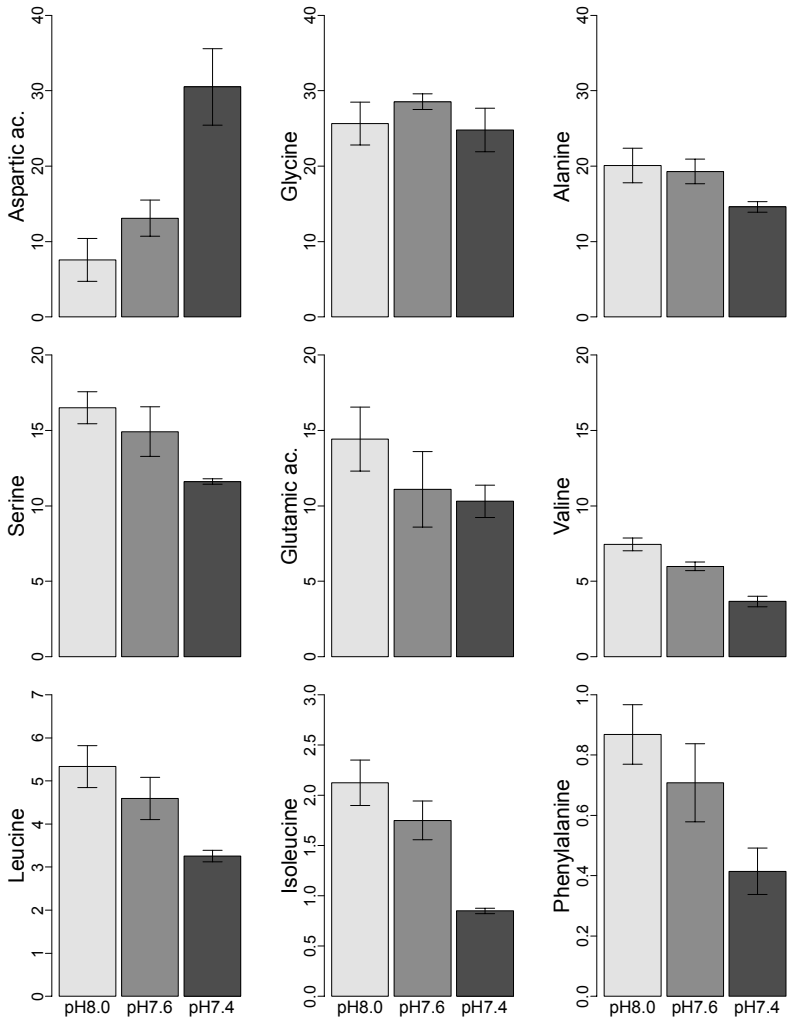


**Figure 4** :Changes in amino acids molar percentage (mean  $\pm$  SE) from cured adhesive of *Sabellaria alveolata* in responses to CO<sub>2</sub>-driven seawater acidification.

**Table 1:** SIMPER analysis of amino acids adhesives of *Sabellaria alveolata*; average and standard deviation contributions to overall dissimilarity in responses to CO<sub>2</sub>-driven seawater acidification. Rank of amino acids cumulative contributions is showed in the right column. Values in brackets represent the percentage of the pairwise overall dissimilarity.

	Amino acid	Average	sd	Cum. Cont.
pH8.0 vs pH7.6 (12.46%)	aspartic ac.	0.0329	0.0250	0.25
	glutamic ac.	0.0241	0.0165	0.43
	glycine	0.0237	0.0155	0.60
	valine	0.0165	0.0160	0.73
	alanine	0.0159	0.0109	0.85
	serine	0.0118	0.0088	0.94
	leucine	0.0048	0.0035	0.97
	isoleucine	0.0020	0.0019	0.99
	phenylalanine	0.0018	0.0015	1.00
pH8.0 vs pH7.4 (25.14%)	aspartic ac.	0.1148	0.04351	0.46
	alanine	0.0274	0.01809	0.57
	serine	0.0245	0.00806	0.66
	glycine	0.0238	0.01743	0.76
	glutamic ac.	0.0229	0.01430	0.85
	valine	0.0190	0.00415	0.92
	leucine	0.0104	0.00379	0.97
	isoleucine	0.0064	0.00170	0.99
	phenylalanine	0.0023	0.00094	1.00
pH7.6 vs pH7.4 (19.23%)	aspartic ac.	0.0870	0.0420	0.45
	alanine	0.0235	0.0133	0.57
	glycine	0.0229	0.0181	0.69
	glutamic ac.	0.0180	0.0083	0.79
	serine	0.0166	0.0125	0.87
	valine	0.0117	0.0034	0.93
	leucine	0.0067	0.0038	0.97
	isoleucine	0.0045	0.0015	0.99
	phenylalanine	0.0015	0.0011	1.00

## SUPPORTING INFORMATION

### Response of intertidal reef-builder worms to rising $p\text{CO}_2$ : bioconstruction plasticity performance under different ocean acidification conditions

**Table S1.** Reef fragments (rf) details showing the weight (kg) of each unit used in the three replicates (aquarium) per treatment. Control = pH 8.0, intermediate = pH 7.6 and low = pH7.4

Replicate	rf	Treatment		
		Control	pH intermediate	pH low
Aquarium 1	1	0.24	0.3	0.22
	2	0.2	0.25	0.27
	3	0.37	0.29	0.27
	<b>sum</b>	<b>0.81</b>	<b>0.84</b>	<b>0.76</b>
Aquarium 2	1	0.35	0.23	0.33
	2	0.27	0.21	0.2
	3	0.27	0.36	0.38
	<b>sum</b>	<b>0.89</b>	<b>0.8</b>	<b>0.91</b>
Aquarium 3	1	0.39	0.36	0.36
	2	0.24	0.26	0.17
	3	0.19	0.21	0.28
	<b>sum</b>	<b>0.82</b>	<b>0.83</b>	<b>0.81</b>
<b>Total</b>		2.52	2.47	2.48

**Table S2.** Predicted pH values for the area of *Sabellaria alveolata* occurrence were acquired from HadGEM2-ES model (Met Office Hadley Centre, UK Jones *et al.*, 2011, Martin *et al.*, 2011) at <https://badc.nerc.ac.uk> (from Centre for Environmental Data Analysis, British Atmospheric Data Centre and Natural Environment Research Council's), for climate modeling experiments from Phase 5 of the Coupled Model Intercomparison Project (CMIP5, Taylor *et al.*, 2011) for the worse case scenario, RCP8.5. Dataset were processed as in (Faroni-Perez, 2017), and we calculated inter-annual monthly minimum and maximum values. Time periods considered are: middle of century (2040–2059) and end of century (2080–2099).

	Mean $\pm$ SD	lowest	upper
2040-2059	7.783 $\pm$ 0.175	6.108	7.938
2080-2099	7.619 $\pm$ 0.225	5.958	7.775



**Table S3.** Parameters of seawater in the aquaria throughout the experimental period (mean  $\pm$  S.D.). Control = pH 8.0, intermediate = pH 7.6 and low = pH7.4.

	Control	pH intermediate	pH low
salinidade (ppt)	35.07 $\pm$ 0.067	35.09 $\pm$ 0.057	35.07 $\pm$ 0.057
temp ( $^{\circ}$ C)	19.56 $\pm$ 0.414	19.49 $\pm$ 0.417	19.5 $\pm$ 0.452
E (mV)	-67.47 $\pm$ 0.895	-48.4 $\pm$ 1.727	-36.59 $\pm$ 2.073
pH IKS	7.97 $\pm$ 0.026	7.62 $\pm$ 0.044	7.36 $\pm$ 0.055
pH T*	7.93 $\pm$ 0.03	7.6 $\pm$ 0.048	7.4 $\pm$ 0.042

\* (DelValls & Dickson, 1998)

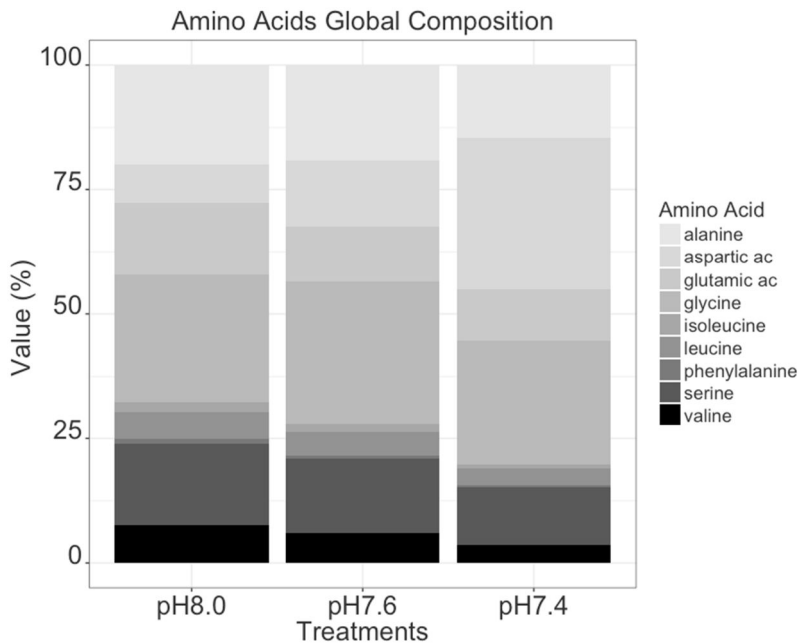


**Figure S4.** Amino acid diversity and composition from adhesive of *Sabellaria alveolata* secreted and cured for bioconstruction under each pH condition tested.

**References:**

- Delvalls TA, Dickson AG (1998) The pH of buffers based on 2-amino-2-hydroxymethyl-1,3-propanediol ('tris') in synthetic sea water. *Deep Sea Research Part I: Oceanographic Research Papers*, 45, 1541–1554.
- Faroni-Perez L (2017) Climate and environmental changes driving idiosyncratic shifts in the distribution of tropical and temperate worm reefs. *Journal of the Marine Biological Association of the United Kingdom*, 97, 1023–1035.
- Jones CD, Hughes JK, Bellouin N *et al.* (2011) The HadGEM2-ES implementation of CMIP5 centennial simulations. *Geoscientific Model Development*, 4, 543–570.
- Martin GM, Bellouin N, Collins WJ *et al.* (2011) The HadGEM2 family of Met Office Unified Model climate configurations. *Geoscientific Model Development*, 4, 723–757.
- Taylor KE, Stouffer RJ, Meehl GA (2011) An Overview of CMIP5 and the Experiment Design. *Bulletin of the American Meteorological Society*, 93, 485–498.



“Warning about Global Change:  
Would the Fittest Survive?  
A matter of fat”  
(Larisse Faroni-Perez, 2017)



**CAN MEMBRANE LIPIDS IDENTIFY ADAPTATIONS TO  
HEAT STRESS? ECOLOGY AND PHYSIOLOGY OF A  
SABELLARIID TO A WARMING OCEAN**

Larisse Faroni-Perez, Fabrice Pernet, Flavia L.D. Nunes,

Jérôme Fournier, Stanislas F. Dubois, C. Frederico D. Gurgel

**Running head:** ecophysiology and the struggle for life





## Abstract

Extreme climatic events such as heat waves are increasing in frequency and severity in marine coastal zones. Marine heat waves (HW) are imposing physiological constraints on populations driving cascade effects on marine communities and compromising ecosystems goods and services. Knowledge about species' thermal tipping points is crucial to understand and predict how marine organisms may respond to extreme events. Here, we simulated HW at three severity levels (28, 31 and 34°C) for *Sabellaria alveolata*, a reef-building annelid, to determine tipping points, sub-lethal thermal limits, and survivorship thresholds. We also tested whether changes in membrane lipid profiles can act as indexes of thermal stress. Responses of *S. alveolata* to the HW varied significantly among temperature levels. Hyperthermia at 34°C initially made animals moribund, latter leading to death within 3 days. At 31°C, lipid remodelling was not timely adjusted to maintain vital cell functions and all animals died at day 7<sup>th</sup>. In 28°C all animals survived at a cost of significant up-regulation of saturated fatty acids, selective high incorporation of monounsaturated fatty acids of families  $\omega$ -9 and  $\omega$ -11 and plasmalogens, at expense of polyunsaturated fatty acids (especially  $\omega$ -3) down-regulation. A short-period event of severe hyperthermia can impose population mortality. The membrane lipid remodelling at 28°C neutralized thermal stress within 30 days of HW simulation, but the survivorship and reproductive fitness in a longer thermal anomaly still need to be evaluated.

**Keywords:** benthic, climate change, global warming, heat wave, lipids, marine, polychaete, Sabellariidae, stress, temperature, thermal tipping point.



## Introduction

In marine coastal zones, the increasing occurrence of extreme climatic events such as heat waves, cyclones, and cold spells are imposing physiological bottlenecks to populations, causing changes in marine community structure (Firth *et al.*, 2015, Garrabou *et al.*, 2009, Hobday *et al.*, 2016, Wernberg *et al.*, 2016). Marine heat wave (HW) is defined as a discrete prolonged anomalously warm water event in ocean regions of temperature increase at least 90<sup>th</sup> percentile considering historical period of 30 years and that lasts for at least 5 days up to end of the warmer event (Hobday *et al.*, 2016). In the last few decades, HWs have increased worldwide in magnitude and frequency (Lima & Wethey, 2012). Throughout this century, several climate models expected a further increase in HW (IPCC, 2014). In 2003 a HW reached many parts of Europe with the highest values for sea surface temperatures recorded over the last 150 years affecting mainly the top 15 m of the ocean (Olita *et al.*, 2007) and least for 30 days (Hobday *et al.*, 2016). In terms of absolute values, anomalous heating reached values over 29.5°C in the Tyrrhenian Sea and east of the Sicily Coast, including a 31°C record in Tunisian Shelf (Olita *et al.*, 2007), and the overall average and maximum were 4.06°C and 5.05°C above historical baseline period respectively (Hobday *et al.*, 2016). The 2003 European HW was associated to mass mortality in several species of four phyla inhabiting infralittoral and circalittoral benthic communities: Bryozoa, Cnidaria, Mollusca and Porifera (Garrabou *et al.*, 2009). Recent investigations in the Atlantic and Pacific Oceans have also reported changes in species phenology and community structure as response to HWs (Caputi *et al.*, 2016, Mills *et al.*, 2013, Oliver *et al.*, 2017, Smale *et al.*, 2017, Wernberg *et al.*, 2016, Wernberg *et al.*, 2013). The ongoing impacts of HW in biodiversity are rapidly being recognized as critical, growing interest is observed in assessing species' thermal tipping points to understand and predict how marine organisms may respond to extreme events.

The impacts of extreme climatic events on worldwide key reef-building marine species, also considered ecosystem engineers, have drawn substantial attention among researchers. Examples of reef-building marine species include hermatypic corals, crustose coralline red algae, oysters, mussels, and tube-forming annelids. Changes in growth rate and distribution of intertidal tube-forming annelids as a result of climate change can drastically influence substrate availability, benthic diversity and community structure. For example, climate models predicted

expansion of suitable areas under future climatic scenarios for *Phragmatopoma virgini*, a temperate Southeast Pacific and Southwest Atlantic polychaete (Faroni-Perez, 2017), whereas field observations for *Sabellaria* spp. have been recording the expansion of worm-reefs intertidal structures in Malaysia (Eeo *et al.*, 2017) and Argentina (Bremec *et al.*, 2013). On the other hand, under future climatic scenarios of high CO<sub>2</sub> emissions, the suitable ranges at warm equatorial areas would severely reduce latter in this century for *Phragmatopoma caudata*, as predicted by climate models (Faroni-Perez, 2017).

*Sabellaria alveolata* is a marine reef-building polychaete in the intertidal and shallow subtidal temperate waters of Northeast Atlantic and Mediterranean Oceans (Firth *et al.*, 2015). Population decline and shifts in distribution for *S. alveolata* were associated to cold spells have been observed in the UK (Firth *et al.*, 2015). However, little is know about how *S. alveolata* populations respond to HW. In a recent study, however, Muir and co-workers demonstrated the ability of *S. alveolata* to acclimate to slight increases in temperature via membrane lipids remodelling (Muir *et al.*, 2016). Vital cell activities are structured by membrane function in which heterogeneous lipids composition play a key role by anchoring and activating proteins and by conveniently regulating trans-membrane ion transport and permeability (Hazel & Williams, 1990, van Meer *et al.*, 2008). Membrane lipids constituents are therefore fine-tuned adapted to environmental conditions, including extreme changes in climate. Most poikilotherm organisms may restructure lipids to restore membrane equilibrium and permeability to optimize their metabolism. Therefore, understanding how hyperthermia influences animal physiology through membrane lipids constituents and remodelling is crucial to comprehend how marine organisms respond to future changes in climate. Consequently, the aim of this study was to answer the following question: Under hyperthermia events, can membrane lipids remodelling profile be used as a proxy for physiological stress and population survivorship? If so, can lipid remodelling data be used to draw boundaries for species distributions?

The present study used *S. alveolata* as model organism to determine tipping points and sub-lethal thermal limits in survivor threshold as a result of a simulated HW in three levels of severity. Then, we tested whether changes in membrane lipid profiles can act as indexes of thermal physiological stress. Under the assumption that *S. alveolata* is a typical temperate species and hence is not adapted to hyperthermia, we hypothesized that i) under the most severe temperature (34°C) lethality would be rapidly reached and animals will not be able to counteract

thermal effects, and ii) in elevated temperatures (28°C and 31°C) physiological responses to counteract thermal effects would alter phospholipids composition to sustain vital functions, iii) lipids restructure would be more rapidly and expressively in animals exposed 31°C rather than 28°C, and also we expected iv) lower average levels of unsaturation index in animals exposed to thermal stress than in the reference temperature as effect of shrinkage in polyunsaturated (PUFA) fatty acids levels in favor of saturated (SFA) and monounsaturated (MUFA). Thus, we tested whether species has physiological ability to adjust metabolic stress towards survivorship in events of hyperthermia (HW). If so, animals can acclimate and likely would adapt to future climate change conditions predictable to their current range of occurrence. Alternatively, if lipid remodelling would not be successfully adjusted, vital cell functions can fail, evoking animals to death, and so, populations in their current range would likely be endangered.

## Materials and Methods

### *Sampling*

Reef fragments of *Sabellaria alveolata* were sampled on 8<sup>th</sup> April, 2016, in the vicinity of Champeaux town, Bay of Mont Saint-Michel, France, (48°43'56.27"N, 1°33'4.40"W). Reef fragments, and individuals therein, were collected using 10 x 15 cm PVC corers oriented parallel to tube openings. To avoid collecting empty tubes due to animal fast inward withdraw in response to the mechanical stress of hammering the cores into the reef, a spatula was inserted perpendicularly to the tube openings via the edge of the reef at 10 cm depth. The spatula blocked the animals from withdrawing further than 10 cm into their tubes during corer insertion. The PVC corers were hammered into the reef until they met the spatula. Additionally, several haphazardly chosen reef fragments collected without using the corers were sampled. All reef fragments were transported to LEMAR laboratory in Université de Bretagne Occidentale, France. Reef fragments, and *S. alveolata* individuals therein, were stabilized for 12 days in an open flow tank (400L), seawater at ~14°C equipped with a TUNZE Turbelle nanostream 6065 for aeration and water circulation. Reef fragments were submitted to a daily low tide simulation for 1 – 2 h, and set to diurnal light rhythm 12 – 10 h dark: 12 – 14 h light. During the low tide period, the tank and each corer were cleaned to remove feces and eventually part of decapitate animals (e.g. individuals on the edges of corer). Corers used had with holes, hand made by drilling

machine, to simulate fissures on reefs water exchange and facilitate the cleaning process. Out of 24 sampled corers, 12 with entire reefs were used for experiment.

#### *Acclimation ramp*

Prior to the onset of experiment, at 13<sup>th</sup> day after sampling, reef fragments were transferred to an acclimation tank (200L) under similar condition to the previous stage (i.e. in an open flow system, equipped with TUNZE Turbelle nanostream 6065 for aeration and water circulation and low tide simulation). Daily, reef fragments were submitted to a gradual increase ( $2 \pm 0.5$  °C) in seawater temperature, that was set after aerial exposure to room temperature  $\sim 19 - 20$ °C, simulating the low tide, and until the experimental temperatures were reached. Once each experimental temperature was reached, corers were photographed for survivorship monitoring and reef fragments were sampled for lipids analysis. The onset day of experiment (Day 0) is herein considered as the end of acclimation ramp, and therefore, prior to continuous exposure to heat stress.

#### *Experimental design*

Four treatments were used: the control ( $\sim 14$ °C), and three increased seawater temperatures: high = 28°C, very high = 31°C, and extreme high = 34°C. The projection for upper temperature value for the years 2080-2099 were obtained to the Representative Concentration Pathway (RCP) 8.5 (IPCC AR5, 2014) modified from (Faroni-Perez, 2017 see Suppl. Mat. S1), representing the worse case scenario for end-of-the-century atmospheric CO<sub>2</sub> concentration. Additionally, field data from the area of studied population were also acquired using iButton® temperature loggers (DS1922L/T) in year 2014. (Suppl. Mat. S1). These temperatures were used to assess species thresholds. A main open flow “ice break” tank (400L), with one 300W and two 600W SCHEGO with HOBBY BIOTHERM ECO 10893 controller associated and two TUNZE Turbelle nanostream 6065 for seawater circulation were used to rise temperature from 14°C to  $\sim 21$ °C, and water pump that was used to transport seawater from main tanks to head tanks. Two 300W and one 600W SCHEGO titanium heaters with HOBBY BIOTHERM ECO 10893 controller associated were used to set and control temperatures in head tank. However, one 300W heater per tank was not connected to controller in order to maintain in the open flow system a minimum of heating when target temperature achieved and controller turned off, and thus, minimizing variability. For scientific reproducibility, researchers

need to pay attention to flow rate exchange and original seawater temperature, both of which determine the number or capacity of heaters necessary to achieve target temperature. Two iButton® temperature loggers (DS1922L/T) were placed into each aquarium and head tank to record the seawater temperature. Temperatures were logged every hour with accuracy of  $\pm 0.05^{\circ}\text{C}$ . Also, each head tank had one TUNZE Turbelle nanostream 6065 for seawater circulation and one TUNZE water pump used to transport seawater from head tanks to aquariums. Each treatment header tank supplied seawater to 3 independent replicate aquaria (15 L), in an open flow system. Water flow renewed seawater in all aquaria twice every hour. One core and several small reefs fragments of approximately similar size were placed into each aquarium. Reef cores were labeled and used for survivorship monitoring whereas reef fragments were used to manipulation (i.e. dissecting tubes) to obtain animals for lipid analyses. During the experiment, low tides continued to be simulate daily, such that animals had aerial exposure to room temperature ( $\sim 19 - 20^{\circ}\text{C}$ ). During low tide periods all aquaria were cleaned by abrasion to remove faeces and avoid microorganism proliferation, and the location of reefs fragments into each aquaria, for both core and haphazardly collected fragments, were randomly changed.

### *Survival analysis*

Each corer was labeled and during the stabilization period, several photos and short videos ( $\sim 10$ min each) were taken to record the presence of living *S. alveolata* in tubes. This process was repeated at days 0, 6, 12, 18, 24, and 30 after the beginning of the experiment until either mortality exceeded 50% per tank or photo and video recording reached the end of the experimental period on the 30<sup>th</sup> day. To quantify survivorship, 30 individual tubes in each replicate corer were randomly marked, but tubes at edge of corers were disqualified (Suppl. Material – S2). Afterwards, animal activity in each respective tube was recorded throughout the experiment using the same photo and video regime describe above. A total of 90 animals per treatment were followed and recorded. Although, following the same organisms over the course of the experiment gives a repetitive measurement type, it guarantees that a given tube was not empty before the start of experiment, minimizing the chance of scoring empty tube as mortality. The approach used for survival analysis considered *S. alveolata* in ‘feeding position’ as live and hence healthy animals, whereas mortality were considered when the tubes were empty or animals were critically moribund.

### *Lipids analysis*

From each treatment considered, 15 (5 per replicate) females of *S. alveolata* were sampled from reefs fragments at days 0, 6, 12, 18, 24, and 30; exception for treatment 31°C due to mortality. Following extraction of individuals from their tubes, females were separately placed into labeled cryotubes, immersed into liquid nitrogen and stored at -80°C. Prior to lipids analysis, each female was weight. Out of five, three *S. alveolata* females with mostly similar weight among themselves were pooled and used as biological replicate for lipid profiling from each replicate aquaria. The usage of animals with similar body mass is to avoid individual bias, for example, an over contribution from a single animal in expense of the others two. Lipids were extracted as described in Folch *et al.*, (1957). Lipid extractions were placed at the top of a silica gel micro-column with 30 × 5 mm internal diameter (Kieselgel) 70–230 mesh (Merck, Lyon, France) previously heated to 450°C and deactivated with 5% water. Polar lipids were eluted with 15 mL of methanol (Marty *et al*, 1992). Tricosanoic acid (2.3 μg) was added as internal standard. Polar lipids were transesterified at 100°C for 10 min with 1 mL of boron trifluoride (12% Methanol) (Metcalf & Schmitz 1961). This transesterification produces fatty acid methyl esters (FAME) from the fatty acid esterified at the sn-1 and sn-2 position of diacylphospholipids, and the sn-2 position of plasmalogen. The transesterification also produces dimethyl acetals (DMA) from the alkenyl chains at the sn-1 position of plasmalogens (Morrison & Smith, 1964). FAME and DMA were analyzed in a HP6890 GC system (Hewlett-Packard) equipped with a DB-Wax 30 m × 0.25 mm, 0.25 μm film thickness capillary column (Agilent Technologies). Peaks were analyzed by comparison of their retention time with those of a standard (C:23) component fatty acid methyl ether (FAME) mix and other standard mixes from marine bivalves. Fatty acid contents were expressed as the mole percentage of the total fatty acid content.

### *Lipids classes calculations*

The unsaturation index (UI) was calculated as  $UI = \sum (\text{mol\% of unsaturated fatty acids} \times \text{number of double bonds of each unsaturated fatty acid})$  (Cossins, 1977). Total branched fatty acids (BrFA) were calculated as  $BrFA = \sum \text{mol\% (iso15:0 + iso16:0)}$ . Total saturated fatty acids (SFA) were calculated as  $SFA = \sum \text{mol\% (14:0 + 15:0 + 16:0 + 17:0 + 18:0 + 19:0 + 20:0)}$ . Total monounsaturated fatty acids (MUFA) were calculated as  $MUFA = \sum \text{mol\% (16:1 + 18:1 + 20:1 + 22:1)}$ . Total polyunsaturated fatty acids (PUFA) were calculated as  $PUFA = \sum \text{mol\%}$



(16:2+ 18:2 + 20:2 + 22:2 + 16:3 + 20:3 + 16:4 + 18:4 + 20:4 + 21:4 + 22:4 + 18:5 + 20:5 + 21:5 + 22:5 + 22:6). Total unsaturated fatty acids (UFA) were calculated as,  $UFA = \sum \text{mol\% (MUFA + PUFA)}$ . Monounsaturated fatty acids of families omega  $\geq 9$  were calculated as:  $\omega_{\geq 9} = \sum \text{mol\% (18:1}\omega\text{-9 + 18:1}\omega\text{-11 + 20:1}\omega\text{-11 + 20:1}\omega\text{-11)}$ . Polyunsaturated fatty acids omega-3 were calculated as the sum of eicosapentaenoic acid (EPA), docosapentaenoic acid (DPA) and docosahexaenoic acid (DHA)  $\omega\text{-3} = \sum \text{mol\% (20:5}\omega\text{-3 + 22:5}\omega\text{-3 + 22:6}\omega\text{-3)}$ . Total polyunsaturated arachidonic acid (ARA) was calculated as:  $ARA = \sum \text{mol\% (22:4}\omega\text{-6)}$ . Non-methylene-interrupted fatty acids (NMI) were calculated as  $NMI = \sum \text{mol\% (20:2i + 20:2j + 22:2i + 22:2j)}$ . Dimethylacetal fatty acids (DMA) were calculated as  $DMA = \sum \text{mol\% (16:0dma + 17:0dma + 18:0dma + 20:1dma)}$ . Ratios UFA/SFA were calculated as  $= \sum \text{mol\%UFA} \div \text{mol\%SFA}$ . The complete table of all lipids (mean  $\pm$  s.e.) is available in supplementary material (S2).

### *Statistical analyses*

To evaluate the membrane lipids as a proxy for physiological stress driving boundaries for species distributions via survivorship/acclimation ability we employed a multi-step analyses. Firstly, general linear model (GLM) analysis was performed to test the effect of increased seawater temperature on survivorship of *S. alveolata*. Data is based on 3 replicates per treatment (i.e. temperature 14, 28 and 31°C) per period (i.e. days 0, 6, 12, 18, 24, and 30). Each replicate had 30 organisms monitored. Statistical significance of GLM models was tested by chi-square P-value. Afterward, the effect of hyperthermia on mol% lipid composition profiles between control and treatments was tested in two steps by applying a distance-based permutational multivariate analysis of variance (PERMANOVA), with Euclidean distance and 999 permutations following a log (x + 1) transformation and betadisper test to verify the assumption of homogeneity of group variance. Firstly, we compared unsaturation index and overall profiles of samples to assess if the changes in membrane lipid can act as indexes of physiological stress in events of hyperthermia determining the species tipping point. Secondly, we compared the set of features in profiles adjustments to assess the physiological ability of species to adjust membrane lipids and counteract the metabolic stress towards acclimation. Data transformation was applied in order to smooth quantitative differences in data and assess the importance on compositional differences among samples. For all analysis, the period of experiment was nested within treatment. The complete summary of

GLM is available in supplementary material (S2). Graphs showing lipids data represents the mean  $\pm$  standard error based on 3 replicates per treatment per experiment period, and each replicate included 3 organisms. Due to fast mortality, data from extreme hyperthermia (34°C) were excluded from statistical analysis. All statistical analyses and graphs were performed in R (R Core Team 2017), using the packages: Community Ecology Package - ‘vegan’ (Oksanen et al., 2016) and Scientific Graphing Functions for Factorial Designs - ‘sciplot’ (Morales, 2017).

## Results

### *Survivorship response*

We detected a significant effect of temperature on *S. alveolata* survivorship (GLM,  $X^2 = 610,67$ , d.f. = 57,  $p < 0.001$ , Fig. 1). Higher temperatures produced an overall increase in mortality. A non-significant slight decrease in survivorship was observed at 28°C compared to 14°C (control) conditions. *S. alveolata* died within 3 to 7 days at 31°C and 34°C, respectively. In day six at 31°C, the average survivorship level was 40% (Fig. 1) and all animals died at day 7<sup>th</sup>. Animals showed increasing signs of physiological distress at and above 31°C. Distress signs were vigor shrank; animal bodies started to protrude far outside their housing tubes than their usual feeding position (e.g. the usually cryptic parathorax became visible); and the presence of opercula towards bottom. Moreover, at 28°C during sampling manipulation for lipids analysis in day 12<sup>th</sup> animal bodies were more delicate and rupturing than in healthy individuals (i.e. from control). However, by end of experiment bodies’ strength were more close to animals in control.

### *Lipids remodelling*

The average unsaturation index (UI) decreased in function of hyperthermia (Fig. 2), and differed among treatments (PERMANOVA, pseudo- $F_{3,12} = 8.46$ ,  $R^2 = 0.2657$ ,  $P = 0.004$ ). The global lipids profile significantly differ among the three treatments (PERMANOVA, pseudo- $F_{3,12} = 3.25$ ,  $R^2 = 0.3145$ ,  $P = 0.001$ ), the complete table of percentages of dissimilarity for each lipids is available in supplementary material (Suppl. Material S2, Tabs. S1–2). The FA classes (i.e. SFA, PUFA, MUFA) showed significant differences (PERMANOVA, pseudo- $F_{3,12} = 5.61$ ,  $R^2 = 0.2196$ ,  $P = 0.009$ ). Compared to control, 28°C and 31°C treatments presented higher levels of SFA and MUFA, and less of

PUFA (Fig. 3). In the onset day, 28°C presented higher contributions of SFA than 31°C, but in the day 6 both the average values were similar. For MUFA and PUFA in the onset day, 31°C had slight higher levels than 28°C, but in day 6 had a sharp depletion for PUFA. In day 12, animals at 28°C presented a sharp depletion of SFA and PUFA, and highest-level peak of MUFA. Afterward, in general levels of SFA and MUFA at 28°C were constantly higher than in control conditions (Fig. 3).

Regardless of temperature, PUFA  $\omega$ -3 family accounted for most of the lipid profile dissimilarity (Fig. 4, Tab.1). Animals in control condition presented the highest molar percentage of PUFA  $\omega$ -3, and in day 0 the 31°C had considerably higher levels of  $\omega$ -3 than 28°C, but levels significantly declined in day 6. Towards the end of experiment at day 30 levels of  $\omega$ -3 at 28°C also showed sharp decline. For MUFA  $\omega \geq 9$  families, the control had lowest levels with a slight increase over time. At day 0 levels of  $\omega \geq 9$  was higher in animals at 28°C than at 31°C but switched in day 6. Overall, at 28°C the  $\omega \geq 9$  levels continually increased by the end of experiment. Considering plasmalogens (i.e. DMA and NMI), levels of total DMA fluctuated in animals maintained at different temperatures over the experiment period (Fig. 5, Tab. 1 and Suppl. material – S2). Overall, DMA levels increased in animals exposed to warmer seawater, despite an observed depletion observed in the day 12 at 28°C. Overall levels on total NMI were much higher in animals exposed to 28°C compared to the control and 31°C. At the end of experiment the average NMI value was also higher than in the onset day (Fig. 5, Suppl. Material – S2). Between 28°C and 31°C the totaling of plasmalogens dissimilarity contributions were 16 and 10% for days 0 and day 6 respectively (Tab. 1).

Animals in all temperature of seawater conditions had a similar percentage of ARA at the onset day (Fig. 6). However, throughout duration of the experiment, the dynamic of ARA levels had unlikely pattern among treatments. Control had increased ARA levels up to day 12, followed by a decline. At 31°C, ARA levels had a sharp increase between days 0 to 6. At 28°C, ARA levels increased continuously up to end of experiment.

## Discussion

This study is the first to investigate how the severity of heat waves affects the survivorship and physiology of a reef-forming polychaete. *Sabellaria alveolata* cannot counteract to the tested

temperatures extremes (i.e. 34°C and 31°C) dying shortly after exposure. Under sub-lethal thermal stress (28°C) *S. alveolata* survives at a cost of timely remodelling their membrane lipids.

In acute hyperthermia (34°C), for *S. alveolata* 100% lethality occurred on the 3<sup>rd</sup> day. Thus, considering the definition of HW in which thermal anomaly lasts for at least 5 consecutive days (Hobday *et al.*, 2016), our findings indicate that short-term HW at 34°C can compromise *S. alveolata*'s entire populations. At 31°C and 28°C, *S. alveolata* could counteract thermal stress by remodelling lipids, however, the overall arrangement in lipids profile between these two temperatures were different. For example, within seven days of stress at 31°C all individuals died while at 28°C no significant differences in mortality were observed compared to control temperature (14°C). At 31°C lipid restructure was delayed in time and appeared after the onset exposure to the simulated HW. However, at day 6<sup>th</sup>, in general, lipids restructure were more expressive in animals exposed to 31°C than to 28°C.

Significant differences in membrane lipid restructuring behavior were detected among animals exposed to different temperature treatments. Based on our results, lipid profiles could be differentiated into three categories: those found among control conditions (14°C), survivors at 28°C, and deceased animals within 7 days at temperatures  $\geq$  31°C. Changes in membrane lipid profiles suggest modifications to achieve multiple purposes, being fine-tuned over time to regulate fluidity, membrane stability and metabolism in heat stressed survivors (28°C). Important observed changes towards adjusting membrane functions in survivor animals included the overall increase in the levels of SFA and plasmalogens (NMI and DMA) and the alterations in the levels of UFA (i.e. decreasing levels of polyunsaturated, mainly family  $\omega$ -3, while increasing monounsaturated  $\omega \geq 9$ ). Our results demonstrate the presence of a highly dynamic lipid adjustment capability in *S. alveolata* that could be present not only in other benthic annelids but also in other benthic invertebrates.

#### *Survivorship versus mortality under hyperthermia*

A previous study has indicated, *S. alveolata* has the ability to survive when exposed to mild thermal stress (i.e. 25°C, Muir *et al.*, 2016). However, our study demonstrated that the thermal maximum for lethality is a few °C units (i.e. 3°C) above *S. alveolata* thermal tolerance limits (around 28°C), and hence a small differences in temperature has the potential to promote mortality within a few days. Lethality results

agree with previous studies indicating a close fit between ‘safety margin for survivor’ and the species’ distribution range (Pörtner *et al.*, 2017, Sunday *et al.*, 2012). A thermal-safety margin is the zone between the realized and the hitherto lethal temperatures. Generally, marine poikilotherms organisms are more fully distributed into the extent of their tolerable thermal range compared to terrestrial poikilotherms organisms (Sunday *et al.*, 2012). Physiological approach on thermal tolerance implicates considering demands from the lower to higher levels of biological organization (i.e. from molecular to whole-body, Pörtner *et al.*, 2017). Our findings corroborate concepts of climate playing important role in species distribution, with a tight thermal-safety margin in marine organisms and thermal limitations by physiological metabolism. Previous physiological approaches also indicated the key role of oxygen for thermal tolerance (Pörtner *et al.*, 2017), however herein we examined the role of membrane lipids. Indeed, these ecophysiological approaches are complementary as biological membranes have ubiquitous influence in all metabolic levels. Therefore, the capacity to survive in thermally stressful situations via lipid remodelling is part of the varied processes associated to the struggle for existence.

Among shallow marine ecosystems, the intertidal zones and coastal waters are strongly influenced by the interplay of a range of oceanic, terrestrial and climate processes. Therefore, the impact of coastal marine HW on intertidal benthic species is a combination of multiple drivers (Hobday *et al.*, 2016). We highlight that the tidal circadian rhythm used in our experiment were not taken fully into consideration. Although we simulated low tide, during periods of reef emersion and exposure to air, reef fragments were kept in room temperature. In the field, during periods of marine HW events, animals generally face different temperatures while exposed to aerial conditions (Suppl. Mat. S1). Multiple sources of thermal stress during tide immersion and emersion may interact negatively and synergistically, possibly increasing species sensitivity to HW and mortality. For example, close to the thermal tolerance limits the oxygen supply from mitochondria to tissues is compromised (Pörtner *et al.*, 2017). Thus, is likely that limited respiration and oxygen supply during periods of ebb tides under solar heating and aerial exposure may change aerobic budget, thus waning metabolism performance to counteract thermal stress. Because marine organism distributional range closely resembles their thermal tolerance limits (Sunday *et al.*, 2012) and temperature is a major driver of marine biogeography, the impact of HW on species

distribution and community structure should not be underestimated. In fact, our experiment clearly shows that a single intense marine HW has potential to cause both, a rapid changes in lipid composition before affecting the whole organism, and changes in demography as mortality starts to occur at high rates. As all sabellariids reef-builders are ecosystem engineers and important seawater filters (Caline & Kirtley, 1992), population declines due to marine heat stress will invariably cause significant changes in community structure and benthic seascape, including changes in ecosystem function and services.

#### *Lipids remodelling under hyperthermia*

Significant decrease in the values of unsaturation index demonstrates *S. alveolata*'s ability to modify membrane phospholipids composition under mild (Muir *et al.*, 2016) and higher increases in temperatures (this study). Changes in fatty acids (FA) composition is characterized by either long-chain polyunsaturated (PUFA) down-regulation or significant up-regulation of saturated (SFA) and monounsaturated (MUFA) lipids. Previous studies showed decreased levels of PUFA in response to warmer temperatures (Munro & Blier, 2015, Pernet *et al.*, 2007, Sanina & Kostetsky, 2002), and causes for down-regulation as a result of thermal stress remains unclear. Supported by our findings, we suggest three non-exclusive plausible explanations for low levels of PUFA in thermally stressed animals: energetically high cost for organisms to maintain relative high PUFA content; to adjust membrane order through packing; and the susceptibility of long-chain  $\omega$ -3 to peroxidation (see below). To clarify, in order to rapidly cope dysfunctions from thermal stress, a pathway promoting high content of PUFA may be metabolic energy wastage, as remodelling by adding double bonds in MUFA chains do not involve considerable change for membrane phase transitions (Coolbear *et al.*, 1983, Demel *et al.*, 1972). Moreover, geometric configurations of SFA chains are straighter making membrane packing tighter than with PUFA (the many double bounds present in PUFA 'kink' the acyl chain). Therefore, remodelling by increasing levels of SFA, or even MUFA with a single double bound, is likely a metabolic pathway to adjust membrane packing and prevent ion leakage. *S. alveolata* exposed to 31°C did not timely up-regulated SFA levels, maintain a high UFA:SFA ratio, which may have infringed structural and functional requirement to rapidly cope with thermal stress. The precise regulatory pathway of membrane lipids remodelling is yet puzzling, and although the overall values of UI decreased, our detailed examination on lipid classes among animals from the different thermal

conditions clearly indicate that membrane lipids remodelling is timely dynamic and adjustable over time. Consequently, in acute thermal stress some structural and functioning requirements may not be modulated and that can result in mortality.

The general trend of PUFA down-regulation scenario, such as the observed decreasing levels of eicosapentaenoic acid (EPA), docosapentaenoic acid (DPA) and docosahexaenoic acid (DHA) as a function of higher temperatures, was quite clear in this study. These long chain omega-3 ( $\omega$ -3) fatty acids are well-known as precursors of eicosanoids and docosanoids hormone-like substances involved in anti-inflammatory processes (Farooqui *et al.*, 2007), and are also prone to lipid peroxidation due to chain size and high number of double bounds (Hulbert *et al.*, 2007, Parrish, 2013). High levels of oxidative stress can led to lipid degradation, injuring cells and tissues, resulting in aging and lethality (Hulbert *et al.*, 2007, Lesser, 2006). Therefore, depletion in the levels of long chain  $\omega$ -3 fatty acids is an anti-oxidative defense. However, the adjustment towards low levels of long chain  $\omega$ -3 fatty acids may be pondered as passive thermal tolerance of organisms, which by concept is constrained over time (Pörtner *et al.*, 2017). Copepods exposed to short-term heat stress showed depleted levels of EPA and DHA that was linked to higher mortality (Werbrouck *et al.*, 2016). Moreover, in *S. alveolata* exposed to 31°C, levels of  $\omega$ -3 fatty acids drastically decreased when animals died (i.e. dropped 13.1%, between the onset and 6<sup>th</sup> day). However, when exposed to 28°C, levels of  $\omega$ -3 fatty acids slowly decreased over time and in the end of experiment period levels were lower than values observed in animals maintained at 31°C. Altogether, our results indicate that the rapidly and intense reduction of PUFA  $\omega$ -3 fatty acids levels in response to thermal stress is likely to promote imbalance, for example, in phase transition temperature or hormone-like substances, possibly depriving cell membranes from proper function with important role involved in the excitatory response of immunity, and stress resistance (Parrish, 2013).

The observed enrichment in arachidonic acid (ARA) as response of elevated temperature conditions has also been identified in previous studies for several marine invertebrates, such as the mussel *Crenomytilus grayanus*, the starfish *Distolasterias nipon*, the ascidian *Halocynthia aurantium*, and *S. alveolata* (Muir *et al.*, 2016, Sanina & Kostetsky, 2002). Our results indicate that low levels of ARA alone are not an efficient indicator of good health as suggested by Muir *et al.*, (2016) for *S. alveolata* raised at 25°C. Indeed, when animals raised at

31°C died in response of hyperthermia, the average level of ARA was lower than in animals from control condition, however, animals raised at 28°C and survived, had initial ARA levels lower than ones in control condition up to day 12 after onset of hyperthermia, but switched levels after that. Most studies investigating ARA and its derivatives (e.g. prostaglandins and leukotrienes) in vertebrates and invertebrates animals, have demonstrated the pivotal role as pro-inflammatory effect precursors (Arts & Kohler, 2009, Funk, 2001). High levels of ARA may be of relevance as co-factor for monitoring population health in case of prolonged disturbing events. Nevertheless, caution must be taken while interpreting the raise in ARA levels since it can also be related to reproductive hormones (Funk, 2001), indicating, for example, a spawning period. Moreover, ARA has alleged other unique attributes such as to act as an inflammation signal to immune system, protection of uninjured cells, and removal of degenerating cells debris (Farooqui *et al.*, 2007). Thus, ARA has multiple metabolic pathways and its compositional level probably plays a key role in animal metabolism that may have been overlooked or confounded.

Our results indicate increased levels of plasmalogens involved in the survivorship of *S. alveolata* to hyperthermia. A previous study showed that warm-acclimation induces increased levels of non-methylene-interrupted (NMI) in different marine invertebrate phyla, and thermal adaptive role was suggested (Sanina & Kostetsky, 2002). Klingensmith (1982) described the occurrence of high levels of NMIs in plasma membranes from different tissues of *Mercenaria mercenaria* exposed to the external environment (i.e. gill, mantle, and foot), and also identified that these plasmalogens are more resistant to oxidation than EPA and DHA. Several studies proposed roles for membrane NMIs, such as: to counteract environmental abiotic stresses (i.e. pH, salinity or temperature; (Chapelle, 1987), adjusting membrane fluidity (Rabinovich & Ripatti, 1991), and as scavengers for reactive oxygen species (ROS) protecting the cell from oxidative stress (Kraffe *et al.*, 2004). In fact, oxidative stress threatens biodiversity in changing thermal conditions (Lesser, 2006, Pörtner *et al.*, 2017), and plasmalogens are scavengers of ROS then play a key role against lipid peroxidation (Hulbert *et al.*, 2014). Moreover, NMIs have lower melting point and flexibility, in comparison to their methylene-interrupted homologues, favoring adjustment of membrane molecular mobility (Rabinovich & Ripatti, 1991). The up-regulation of NMIs might be directly involved in determining survivability under heat stress conditions due to either functions; counteracting oxidative stress and regulating membrane



function. Under hyperthermia of 28°C, *S. alveolata* timely remodeled achieving up-regulation of NMI, and animals likely sustained vital functions. The absence of increased levels of NMIs in *S. alveolata* exposed to 31°C, may explain the 100% mortality within 7 days. Absence of NMI in a particular species however is not indicative of poor health, as its occurrence is peculiar to different taxa. Understanding lipid-profiling data can benefit from interaction between lipidomics with proteomics and metabolomics data, hence molecular studies are of crucial importance and should be considered in the future to improve the understanding for plausible future response of biodiversity to extreme climatic events.

Present results also indicated significant compositional changes of monounsaturated fatty acids, with selective high incorporation of  $\omega$ -9 and  $\omega$ -11, particularly in animals exposed to 28°C. Interestingly, a possible functional synergy between NMI and 20:1  $\omega$ -11 has been suggested to bivalves, these lipids can be linked or functionally equivalent (Kraffe *et al.*, 2004). Our findings suggest the existence of a tight interplay between NMI and  $\omega$ -11 (mainly 20:1  $\omega$ -11) due to their correlated increase as a function of increasing temperatures. The potential interplay of MUFA  $\omega$ -11 with cholesterol and sphingolipids was not explored by this study, however it looks very promising to be considered in future studies to determine existence of microdomains as membrane rafts. Membrane rafts (i.e. lipid domains) has been extensively endorsed as signaling platforms, a clustering of molecules involved in cascade transmission of stress signals (van Meer *et al.*, 2008). Cholesterols, a core for membrane rafts, interact with lipids accordingly to their unsaturation and the distribution of double bounds in the acyl chains (Demel *et al.*, 1972). Cholesterols have affinity for lipids with double bond position as  $\Delta \geq 9$  (Stillwell, 2016), and the majority of incorporated unsaturated fatty acids of  $\omega$ -9 and  $\omega$ -11 families fit in this category. Thus, the specific membrane remodelling in surviving animals at 28°C, increasing SFA and unsaturated fatty acids  $\omega \geq 9$ , may indicate specificity for anchoring signaling domains and membrane rafts. In light of our results, further work to explore a key interplay between membrane rafts and increased levels of SFA and UFA family  $\omega \geq 9$  towards survivorship, as a response to thermal stress, is called for.

*Insights into biogeography and macroecology of worms-reefs: a matter of lipids*

We provided empirical evidence for upper thermal niche boundaries based on physiology traits of membrane lipids. Our results from *S. alveolata* allow us to speculate on the spatial distribution of these organisms that can also be useful for worldwide reefs-building sabellariids. Firstly, expected end-of-century changes in climate are considered unprecedented due to already observed historical changes and the forecasted even faster future rates of climatic shift. As HW are predicted to increase in frequency and severity, and considering the *S. alveolata* life-span of ~5 years (Gruet, 1986, Wilson, 1971), an increased occurrence of demographic bottlenecks and the selection of the fittest in the struggle for existence (Darwin, 1859) are expected to happen within approximately 16 generations. Secondly, some plasma membrane lipids are known to be specific to anchor signaling proteins that activate cell differentiation and proliferation (Zhou *et al.*, 2015). In sabellariids, ovaries are ephemeral and the centers of germ cell proliferation are connected to blood vessels (Faroni-Perez & Zara, 2014). Remains obscure, however, whether lipids remodelling affects the signaling pathways between plasma membrane and the specific proteins that induce differentiation of stem cells for gametogenesis. Reproductive peaks generally occur in warmer months (Culloty *et al.*, 2010, Dubois *et al.*, 2007, Gruet, 1986), when the probability of severe HW incidence is higher. Therefore changes in fecundity may involve vulnerability for reefs maintenance. Thirdly, biogeographical shifts of worm-reefs are expected to occur in response to climate change (Faroni-Perez, 2017, Firth *et al.*, 2015). Indeed, the absence of ability to timely remodel membrane lipids during spike heat events likely can result in local extinction under a warming scenario. However, sabellariids lineages evolved sensory organs and larval settlement rely heavily on chemical cues from conspecific detection (Faroni-Perez *et al.*, 2016, Pawlik & Faulkner, 1988). Chemical tracking may explain larval retention during planktonic development adjacently to parental areas and the settlement feedback loop, resulting over centuries in the well-know places of worms-reefs persistence, such as *S. alveolata* reefs in UK and Europe; *Phragmatopoma caudata* reefs in Florida (US) and Brazil, and *Gunnarea gaimardi* reefs in Mozambique and South Africa. Therefore, worm-reef distributions may not have significant latitudinal shifts in response to warming, and alternatively, species would maintain their current biogeographic areas. Instead, they could shift their bathymetry towards subtidal zones over generations. Given our findings, a critical emerging issue is whether the exposure to HW, or even to heat spikes events with potential to wipe out entire populations and vanishing

genetic biodiversity, timely would favour transgenerational acclimation and catch up proper allelic frequencies to enhance species adaptation. Although accuracy for natural selection will be given by nature, experimental studies with transgenerational approaches and evolutionary adaptation to climatic changes are straightway needed and fundamental to provide important findings on species adaptive responses.

In general, sabellariids biogenic reefs occur in coastal areas and face pulsed heat stress events (Faroni-Perez *et al.*, 2016, see also Supp. Mat. S1). The timely and dynamic lipids remodelling found to maintain cell functions for survivors in hyperthermia can be interpreted as genetic and metabolic memories allowing proper thermal acclimation. The genetic and metabolic memories permit the recognition of environmental or cellular signals to mediate regulatory responses at a subsequent time using a variety of biochemical pathways (Burrill & Silver, 2010). Therefore, we call for further molecular studies with evolutionary ecology approaches to investigate and describe how biological memory would act in favour of specific pathways for physiological adjustments, enabling species to counteract oxidative stress and regulate membrane function towards adaptation under a warming future.

## Conclusions

Our results described for the first time the critical thermal maximum and the sub-lethal thermal constrains of the reef-building annelid *Sabellaria alveolata*. The species has no ability to neutralize extreme thermal stress (34 and 31°C) resulting in mortality within short period, but at sub-lethal temperature (28°C) the species survives at the cost of a complex and dynamic membrane lipids remodelling. Overall, at 31°C the species had delayed lipid remodelling with over expression of some lipids classes, and low rates of plasmalogens contrasting to 28°C. Short-period events of extreme heat waves can result in population mortality. The lipid remodelling adjustments observed at 28°C led to thermal stress reduction in 30 days duration of heat wave simulation, but the species survival and reproductive fitness in longer thermal anomaly still need to be evaluated.

## Acknowledgements

We acknowledge the assistance of staff from UBO (Université de Bretagne Occidentale) and Ifremer (Institut Français de Recherche pour l'Exploitation de la Mer) for their help with missing equipment and assistance for experimental setup. Also, we thank for the assistance during fieldwork to V. Ferreira and J.-P. Buffet. For the assistance in animals' manipulation during 'experiment time point' we thank to T. Le Verge and B. Dubief. We also thank T. Le Verge for the help in image analysis of survivorship during his internship. This study was supported by the Brazilian National Council for Scientific and Technological Development Award to LFP (CNPq–SWE 201233/2015-0). CFDG also thanks CNPq for a PQ grant (309658/2016-0). The authors declare no conflicting of interests.

## References

- Arts MT, Kohler CC (2009) Health and condition in fish: the influence of lipids on membrane competency and immune response. In: *Lipids in Aquatic Ecosystems*. (eds Kainz M, Brett MT, Arts MT). New York, NY, Springer New York.
- Bremec C, Carcedo C, Piccolo MC, Dos Santos E, Fiori S (2013) *Sabellaria nanella* (Sabellariidae): from solitary subtidal to intertidal reef-building worm at Monte Hermoso, Argentina (39 degrees S, south-west Atlantic). *Journal of the Marine Biological Association of the United Kingdom*, 93, 81–86.
- Burrill DR, Silver PA (2010) Making cellular memories. *Cell*, 140, 13–18.
- Caline B, Kirtley DW (1992) *The sabellariid reefs in the Bay of Mont Saint-Michel, France: ecology, geomorphology, sedimentology, and geologic implications*, Stuart, Florida Oceanographic Society.
- Caputi N, Kangas M, Denham A, Feng M, Pearce A, Hetzel Y, Chandrapavan A (2016) Management adaptation of invertebrate fisheries to an extreme marine heat wave event at a global warming hot spot. *Ecology and Evolution*, 6, 3583–3593.
- Chapelle S (1987) Plasmalogens and O-alkylglycerophospholipids in aquatic animals. *Comparative Biochemistry and Physiology Part B: Comparative Biochemistry*, 88, 1–6.
- Coolbear KP, Berde CB, Keough KMW (1983) Gel to liquid-crystalline phase transitions of aqueous dispersions of polyunsaturated mixed-acid phosphatidylcholines. *Biochemistry*, 22, 1466–1473.
- Cossins AR (1977) Adaptation of biological membranes to temperature. The effect of temperature acclimation of goldfish upon the

- viscosity of synaptosomal membranes. *Biochimica et Biophysica Acta (BBA) - Biomembranes*, 470, 395–411.
- Culloty SC, Favier E, Ni Riada M, Ramsay NF, O'riordan RM (2010) Reproduction of the biogenic reef-forming honeycomb worm *Sabellaria alveolata* in Ireland. *Journal of the Marine Biological Association of the United Kingdom*, 90, 503–507.
- Darwin C (1859) *The Origin of Species by means of natural selection or the preservation of favoured races in the struggle for life* Edison, New Jersey, Castle Books.
- Demel RA, Geurts Van Kessel WSM, Van Deenen LLM (1972) The properties of polyunsaturated lecithins in monolayers and liposomes and the interactions of these lecithins with cholesterol. *Biochimica et Biophysica Acta (BBA) - Biomembranes*, 266, 26–40.
- Dubois S, Comtet T, Retiere C, Thiebaut E (2007) Distribution and retention of *Sabellaria alveolata* larvae (Polychaeta : Sabellariidae) in the Bay of Mont-Saint-Michel, France. *Marine Ecology-Progress Series*, 346, 243–254.
- Eeo JJ, Chong VC, Sasekumar A (2017) Cyclical events in the life and death of an ephemeral polychaete reef on a tropical mudflat. *Estuaries and Coasts*, 40, 1418–1436.
- Faroni-Perez L (2017) Climate and environmental changes driving idiosyncratic shifts in the distribution of tropical and temperate worm reefs. *Journal of the Marine Biological Association of the United Kingdom*, 97, 1023–1035.
- Faroni-Perez L, Helm C, Burghardt I, Hutchings P, Capa M (2016) Anterior sensory organs in Sabellariidae (Annelida). *Invertebrate Biology*, 135, 423–447.
- Faroni-Perez L, Zara FJ (2014) Oogenesis in *Phragmatopoma* (Polychaeta: Sabellariidae): evidence for morphological distinction among geographically remote populations. *Memoirs of Museum Victoria*, 71, 53–65.
- Farooqui AA, Horrocks LA, Farooqui T (2007) Modulation of inflammation in brain: a matter of fat. *Journal of Neurochemistry*, 101, 577–599.
- Firth LB, Mieszkowska N, Grant LM *et al.* (2015) Historical comparisons reveal multiple drivers of decadal change of an ecosystem engineer at the range edge. *Ecology and Evolution*, 5, 3210–3222.

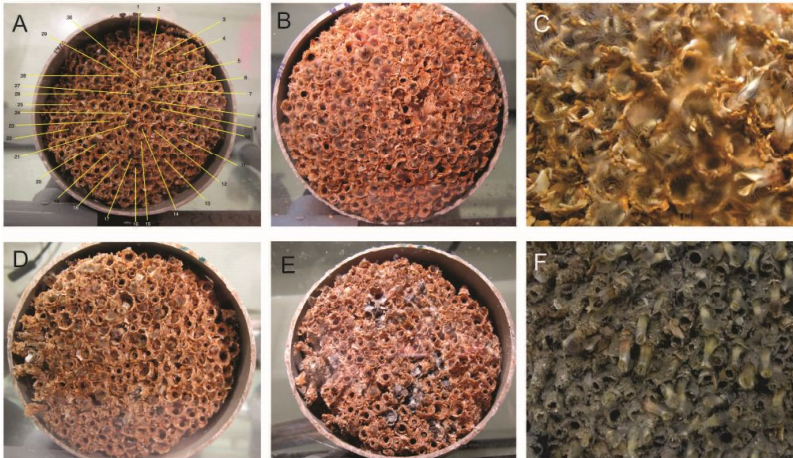
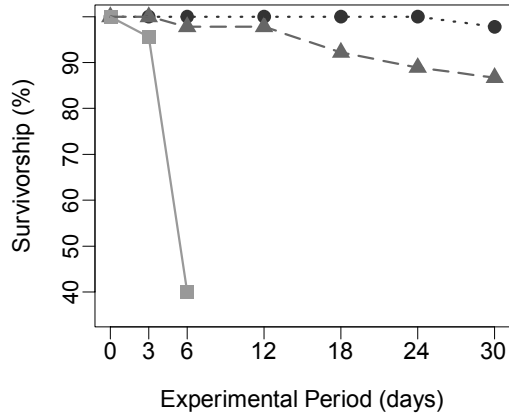
- Folch J, Lees M, Sloane Stanley GH (1957) A simple method for the isolation and purification of total lipides from animal tissues. *The Journal of Biological Chemistry*, 226, 497–509.
- Funk CD (2001) Prostaglandins and leukotrienes: Advances in eicosanoid biology. *Science*, 294, 1871–1875.
- Garrabou J, Coma R, Bensoussan N *et al.* (2009) Mass mortality in Northwestern Mediterranean rocky benthic communities: effects of the 2003 heat wave. *Global Change Biology*, 15, 1090–1103.
- Gruet Y (1986) Spatio-temporal changes of sabellarian reefs built by the sedentary polychaete *Sabellaria alveolata* (Linné). *Marine Ecology*, 7, 303–319.
- Hazel JR, Williams EE (1990) The role of alterations in membrane lipid composition in enabling physiological adaptation of organisms to their physical environment. *Progress in Lipid Research*, 29, 167–227.
- Hobday AJ, Alexander LV, Perkins SE *et al.* (2016) A hierarchical approach to defining marine heatwaves. *Progress in Oceanography*, 141, 227–238.
- Hulbert AJ, Kelly MA, Abbott SK (2014) Polyunsaturated fats, membrane lipids and animal longevity. *Journal of Comparative Physiology B*, 184, 149–166.
- Hulbert AJ, Pamplona R, Buffenstein R, Buttemer WA (2007) Life and death: metabolic rate, membrane composition, and life span of animals. *Physiological Reviews*, 87, 1175–1213.
- Klingensmith JS (1982) Distribution of methylene and nonmethylene-interrupted dienoic fatty acids in polar lipids and triacylglycerols of selected tissues of the hardshell clam (*Mercenaria mercenaria*). *Lipids*, 17, 976–981.
- Kraffe E, Soudant P, Marty Y (2004) Fatty acids of serine, ethanolamine, and choline plasmalogens in some marine bivalves. *Lipids*, 39, 59–66.
- Lesser MP (2006) Oxidative stress in marine environments: Biochemistry and Physiological Ecology. *Annual Review of Physiology*, 68, 253–278.
- Lima FP, Wetthey DS (2012) Three decades of high-resolution coastal sea surface temperatures reveal more than warming. *3:704*, 1–13.
- Mills KE, Pershing AJ, Brown CJ *et al.* (2013) Fisheries management in a changing climate lessons from the 2012 ocean heat wave in the Northwest Atlantic. *Oceanography*, 26, 191–195.

- Morrison WR, Smith LM (1964) Preparation of fatty acid methyl esters and dimethylacetals from lipids with boron fluoride–methanol. *Journal of Lipid Research*, 5, 600–608.
- Muir AP, Nunes FLD, Dubois SF, Pernet F (2016) Lipid remodelling in the reef-building honeycomb worm, *Sabellaria alveolata*, reflects acclimation and local adaptation to temperature. 6:35669, 1–10.
- Munro D, Blier PU (2015) Age, Diet, and Season Do Not Affect Longevity-Related Differences in Peroxidation Index Between *Spisula solidissima* and *Arctica islandica*. *The Journals of Gerontology: Series A*, 70, 434–443.
- Olita A, Sorgente R, Natale S, Gaberšek S, Ribotti A, Bonanno A, Patti B (2007) Effects of the 2003 European heatwave on the Central Mediterranean Sea: surface fluxes and the dynamical response. *Ocean Science Journal*, 3, 273–289.
- Oliver ECJ, Benthuyzen JA, Bindoff NL, Hobday AJ, Holbrook NJ, Mundy CN, Perkins-Kirkpatrick SE (2017) The unprecedented 2015/16 Tasman Sea marine heatwave. 8:16101, 1–12.
- Parrish CC (2013) Lipids in marine ecosystems. *ISRN Oceanography*, 2013, 1–16.
- Pawlik JR, Faulkner DJ (1988) The gregarious settlement of sabellariid polychaetes: new perspectives on chemical cues. In: *Marine biodeterioration*. (eds Thompson MF, Sarojini R, Nagabhushanam R) pp Page. New Delhi, Bombai, Calcutta, Oxford & IBH Publishing Co.
- Pernet F, Tremblay R, Comeau L, Guderley H (2007) Temperature adaptation in two bivalve species from different thermal habitats: energetics and remodelling of membrane lipids. *Journal of Experimental Biology*, 210, 2999–3014.
- Pörtner H-O, Bock C, Mark FC (2017) Oxygen- and capacity-limited thermal tolerance: bridging ecology and physiology. *The Journal of Experimental Biology*, 220, 2685–2696.
- Rabinovich AL, Ripatti PO (1991) On the conformational, physical properties and functions of polyunsaturated acyl chains. *Biochimica et Biophysica Acta (BBA) - Lipids and Lipid Metabolism*, 1085, 53–62.
- Sanina NM, Kostetsky EY (2002) Thermotropic behavior of major phospholipids from marine invertebrates: changes with warm-acclimation and seasonal acclimatization. *Comparative Biochemistry and Physiology B-Biochemistry & Molecular Biology*, 133, 143–153.

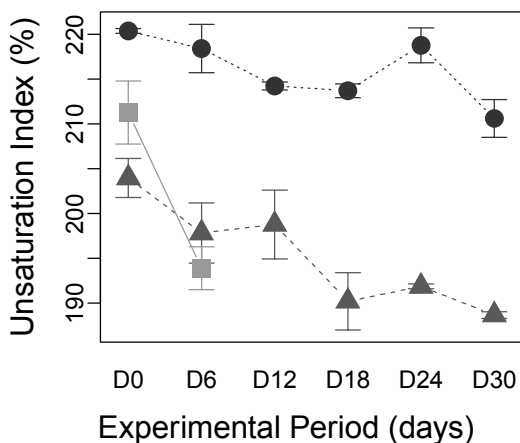
- Smale DA, Wernberg T, Vanderklift MA (2017) Regional-scale variability in the response of benthic macroinvertebrate assemblages to a marine heatwave. *Marine Ecology Progress Series*, 568, 17–30.
- Stillwell W (2016) *Introduction to Biological Membranes: Composition, Structure and Function*, Academic Press, Elsevier.
- Sunday JM, Bates AE, Dulvy NK (2012) Thermal tolerance and the global redistribution of animals. *Nature Climate Change*, 2, 686–690.
- Van Meer G, Voelker DR, Feigenson GW (2008) Membrane lipids: where they are and how they behave. *Nat Rev Mol Cell Biol*, 9, 112–124.
- Werbrouck E, Van Gansbeke D, Vanreusel A, De Troch M (2016) Temperature affects the use of storage fatty acids as energy source in a benthic copepod (*Platychelipus littoralis*, Harpacticoida). *PLoS ONE*, 11, e0151779.
- Wernberg T, De Bettignies T, Joy BA, Finnegan PM (2016) Physiological responses of habitat-forming seaweeds to increasing temperatures. *Limnology and Oceanography*, 61, 2180–2190.
- Wernberg T, Smale DA, Tuya F *et al.* (2013) An extreme climatic event alters marine ecosystem structure in a global biodiversity hotspot. *Nature Climate Change*, 3, 78–82.
- Wilson DP (1971) *Sabellaria* colonies at Duckpool, North Cornwall, 1961-1970. *Journal of the Marine Biological Association of the United Kingdom*, 51, 509–580.
- Zhou Y, Wong C-O, Cho K-J *et al.* (2015) Membrane potential modulates plasma membrane phospholipid dynamics and K-Ras signaling. *Science*, 349, 873–876.



## FIGURES AND TABLE



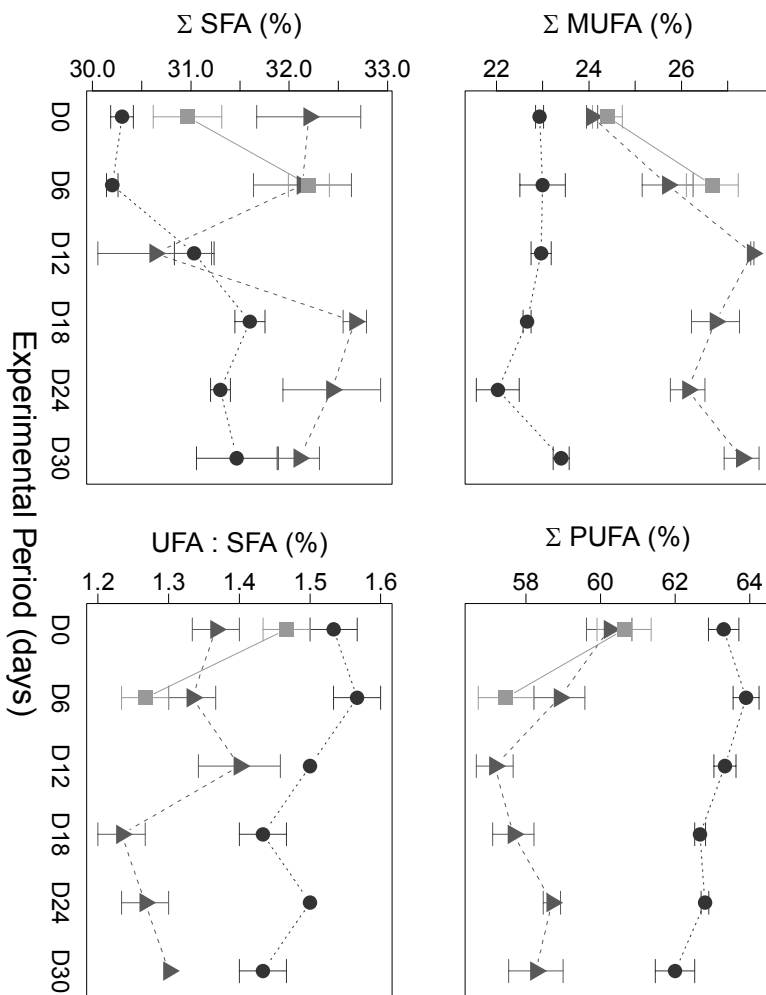
**Figure 1** Survivor of *Sabellaria alveolata* in response to temperature increase in experimental conditions (top). Symbols: Black circle with dots = control (i.e. T14°C), dark gray square with dashes = T31°C, and light gray triangle with line = T28°C. Scheme of survivor analysis of *Sabellaria alveolata* in response to temperature increase under experimental conditions, **A**: corer illustrating monitored animals. **B–C** ‘Healthy’: corer of treatment with animals in feeding position (**B**) and detail of animals in feeding position (**C**). **D–F** ‘non-Healthy’: corer of the treatment T = 31 °C with 24 hours difference (**D–E**) showing moribund, dying and dead animals. **F**: detail of moribund and dying animals.



**Figure 2** Unsaturated index average values (mean  $\pm$  s.e.) over the experimental period (days). Symbols: Black circle with dots = control (i.e. T14°C), dark gray square with dashes = T31°C, and light gray triangle with line = T28°C.

**Next page:**

**Figure 3** Average values (mean  $\pm$  s.e.) of fatty acids classes over the experimental period (days); monounsaturated (MUFA), polyunsaturated (PUFA) fatty acids in the superior line, and saturated (SFA) and ratio between total unsaturated (UFA) and total saturated (SFA) classes in the inferior line. Symbols: Black circle with dots = control (i.e. T14°C), dark gray square with dashes = T31°C, and light gray triangle with line = T28°C



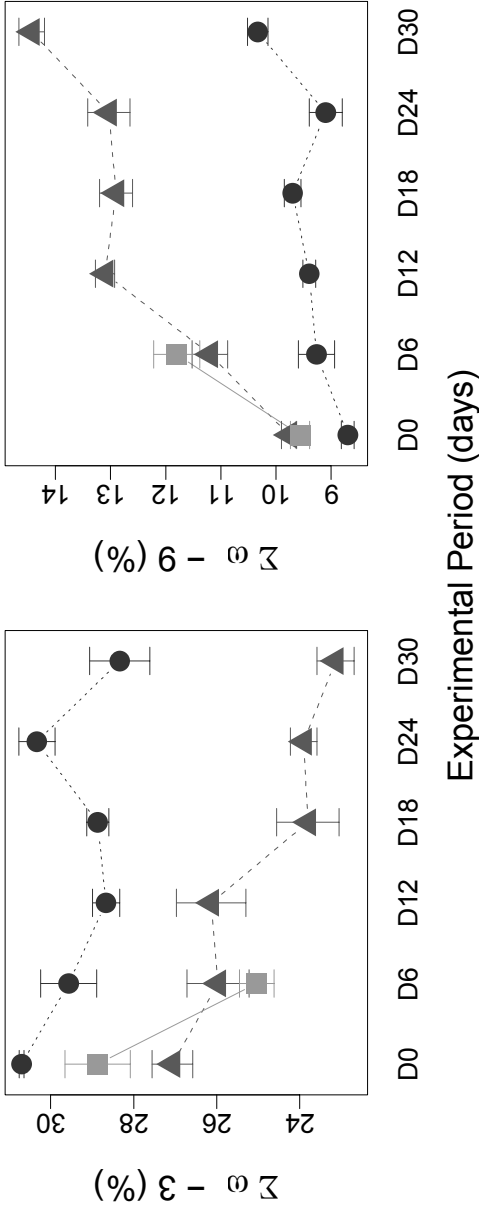


**Figure 4** Average values (mean  $\pm$  s.e.) of long-chain PUFA  $\omega$ -3 (i.e. sum of eicosapentaenoic acid (EPA), docosapentaenoic acid (DPA) and docosahexaenoic acid (DHA)), and MUFA  $\omega$  $\geq$ 9 (right).

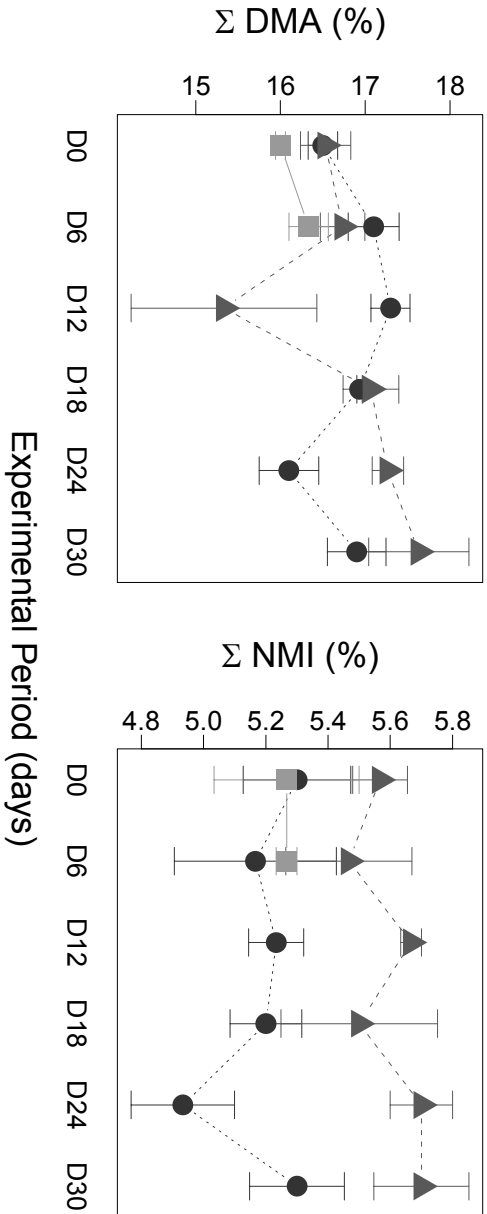


**Figure 5** Average values (mean  $\pm$  s.e.) of plasmalogens; dimethylacetal (DMA) and non-methylene-interrupted (NMI) fatty acids over the experimental period (days). Symbols: Black circle with dots = control (i.e. T14°C), dark gray square with dashes = T31°C, and light gray triangle with line = T28°C.

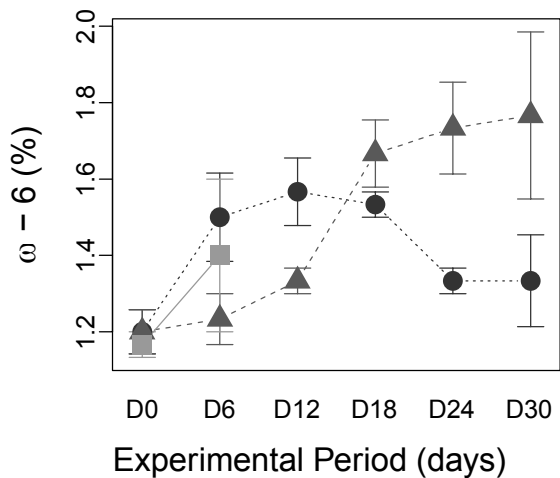


**Figure 6** Average values (mean  $\pm$  s.e.) of polyunsaturated fatty acid  $\omega-6$  (i.e. arachidonic acid, ARA) over the experimental period (days). Symbols: Black circle with dots = control (i.e. T14°C), dark gray square with dashes = T28°C, and light gray triangle with line = T31°C.

**Table 1:** Results of the cumulative contributions percentage of dissimilarity using Bray-Curtis dissimilarity index for each lipid analyzed between group pairs of tested temperatures, i.e. 14, 28 and 31°C. Day 0 = the onset day.

	Day 0				Day 6						
	14 vs 28°C	14 vs 31°C	28 vs 31°C	14 vs 28°C	14 vs 31°C	28 vs 31°C					
$\omega$ -3	43	$\omega$ -3	32	$\omega$ -3	30	$\omega$ -3	32	$\omega$ -3	34	$\omega$ -3	24
SFA	64	SFA	50	SFA	46	SFA	50	$\omega$ $\geq$ 9	52	$\omega$ $\geq$ 9	40
$\omega$ $\geq$ 9	76	$\omega$ -7	67	$\omega$ -7	61	$\omega$ $\geq$ 9	67	SFA	69	SFA	55
DMA	81	$\omega$ $\geq$ 9	78	DMA	70	$\omega$ -6	79	$\omega$ -7	82	$\omega$ -7	67
$\omega$ -6	86	DMA	85	$\omega$ -6	78	$\omega$ -7	88	$\omega$ -6	90	$\omega$ -6	79
NMI	90	NMI	90	$\omega$ $\geq$ 9	85	DMA	93	DMA	96	DMA	89
Br	93	$\omega$ -5	95	NMI	92	NMI	97	NMI	98	NMI	95
$\omega$ -5	97	$\omega$ -6	98	Br	96	Br	100	Br	100	Br	99
$\omega$ -7	100	Br	100	$\omega$ -5	100	$\omega$ -5	100	$\omega$ -5	100	$\omega$ -5	100

## SUPPORTING INFORMATION

### **Can membrane lipids identify adaptations to heat stress? Ecology and physiology of a Sabellariid to a warming ocean**

Larisse Faroni-Perez, Fabrice Pernet, Flavia L.D. Nunes,  
Jérôme Fournier, Stanislas F. Dubois, C. Frederico D. Gurgel

#### **Supplementary material S1:**

Environmental dataset of atmospheric and sea surfaces temperatures (AST and SST) were acquired from HadGEM2-ES model (Met Office Hadley Centre, UK Jones *et al.* 2011; Martin *et al.* 2011) at <https://badc.nerc.ac.uk> (from Centre for Environmental Data Analysis, British Atmospheric Data Centre and Natural Environment Research Council's), for climate modelling experiments from Phase 5 of the Coupled Model Intercomparison Project (CMIP5, Taylor *et al.* 2011). Dataset were processed as in (Faroni-Perez 2017). We calculated inter-annual monthly maximum averages and monthly maximum values (i.e. extremes). Time periods considered are: historical (1986–2005) and end of century (2080–2099) for the RCP 8.5.

Temperatures data for the area of studied population were also acquired using iButton® temperature loggers (DS1922L/T) fixed rocky boulders in adjacencies of

*S. alveolata* reefs at Mont Saint-Michel Bay (France) in year 2014. In the warmest months (late spring and all summer months), daily temperatures were recorded every 3h by the data loggers with 0.01°C of accuracy, totaling 240–248 values per month.

For the area of sampled population (Bay of Mont Saint-Michel, France), historical climatic models values indicate ~20–21°C for both AST and SST, considering both maximum averages and extremes. Under the RCP 8.5 (2080–2099), in the end of century values for AST and SST are expected to be ~5–6°C and ~4–5°C, respectively, higher than in present-days (1986–2005). For the overall biogeographic area of *Sabellaria alveolata* reefs occurrence, coastal areas of Northeast Atlantic Ocean and Mediterranean Sea, strongest warming ~6–10°C is forecasted to occur for AST and SST (Fig. 1). *In situ* data values indicate temperature ranged between 11 and 41°C and mode was ~20°C. High temperature values ( $\geq 30$  °C) were registered (Figs. 2–3).



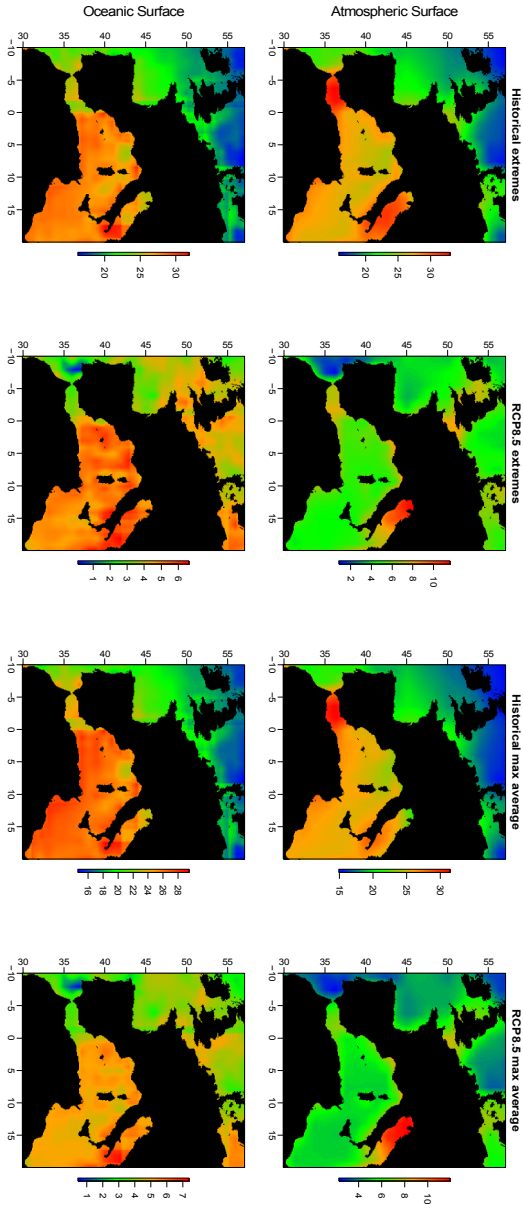


**Figure S1-1:** Temperatures ( $^{\circ}\text{C}$ ) from climatic models for historical data (1986–2005), and for end of century (2080–2099) considering the RCP8.5 (IPCC, 2014). Historical data represents the model values and in RCP8.5 data represents warming anomalies.



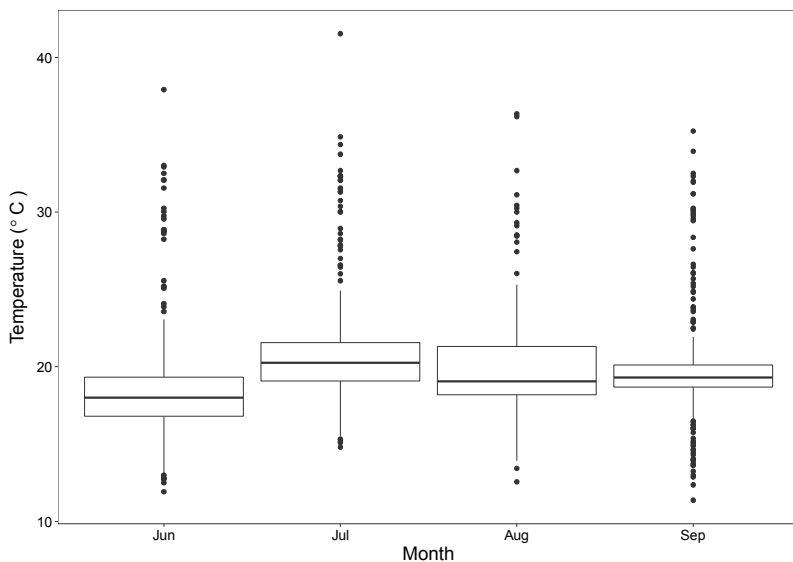


**Figure S1-2:** Monthly temperatures acquired from data loggers attached onto *Sabellaria alveolata* reefs in during warmest season in 2014.

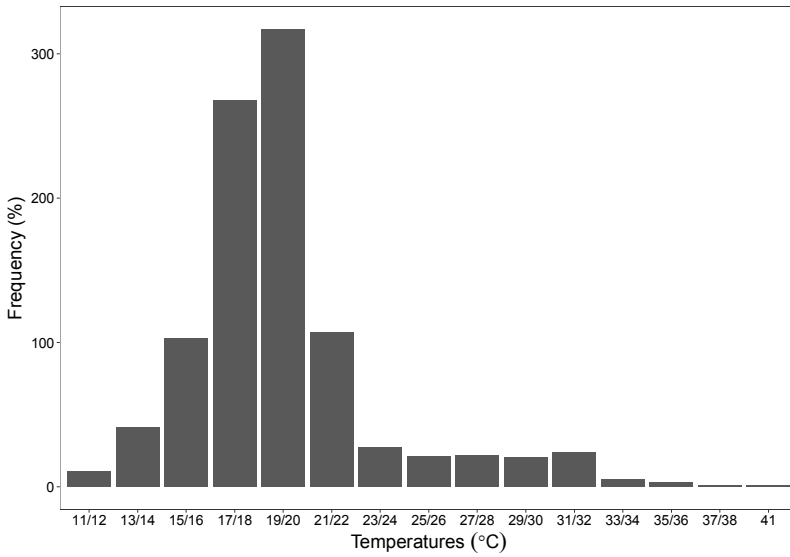


**Figure S1–3:** Frequency of temperatures classes acquired from data loggers attached onto *Sabellaria alveolata* reefs during warmest season (June – September) in 2014.

## Supplementary material S2:

**Table S2–1** Fatty acid profile and remodelling of polar lipids (mean ± s.e.) in *Sabellaria alveolata* exposed to 14°C (i.e. control), and heat wave simulation (28 and 31°C) up to 30 days weeks after the onset of the experiment (i.e. D0 = last day of acclimation ramp).

Fatty acid (mol%)	14°C						28°C						31°C	
	0	6	12	18	24	30	0	6	12	18	24	30	0	6
14:0	1.60102	1.57407	1.61408	1.63306	1.59310	1.64409	1.63812	1.73807	1.65815	1.60812	1.53814	1.46812	1.74811	1.61818
15:0	0.70405	0.76512	0.75404	0.88809	0.79403	0.83409	0.76802	0.76604	0.86604	0.93915	0.81802	0.82401	0.77406	0.81805
16:0	6.90437	6.51102	6.96413	7.01306	6.99413	6.86426	7.10440	7.43427	7.26427	7.35247	6.78405	6.88456	7.45433	7.23455
17:0	1.35907	1.42406	1.42401	1.40405	1.58417	1.39908	1.46405	1.55404	1.50403	1.50404	1.50412	1.40409	1.48404	1.61407
18:0	7.02414	7.19435	7.33434	7.43143	8.04448	7.76447	8.22444	7.91430	7.50447	7.81463	8.04448	7.68460	7.37449	8.41445
19:0	0.13402	0.28404	0.25401	0.27401	0.28403	0.26403	0.23408	0.28404	0.25403	0.29401	0.30401	0.27401	0.31407	0.34408
20:0	0.25904	0.23402	0.22401	0.23401	0.22405	0.20402	0.22402	0.24402	0.30411	0.19401	0.19401	0.21405	0.17403	0.22405
Σ SFA	17.95435	17.96433	18.52442	18.95441	19.16442	18.95438	19.66417	19.93400	19.14444	19.66458	19.19439	18.60438	19.20439	20.38489
iso15:0	0.85408	0.59410	0.57410	0.54412	0.52409	0.52410	0.90431	0.58412	0.45408	0.53419	0.65404	0.47416	0.62408	0.46407
iso16:0	0.66406	0.59406	0.62402	0.63403	0.66413	0.60407	0.70403	0.64407	0.72408	0.75413	0.72403	0.67412	0.90408	0.67407
Σ Br	1.51413	1.11416	1.19422	1.17410	1.18420	1.12407	1.60430	1.22415	1.16416	1.28432	1.37402	1.14427	1.52400	1.12413
anti15:0	0.20401	0.13403	0.16403	0.13403	0.15802	0.15402	0.15408	0.22413	0.08402	0.10403	0.12404	0.07406	0.16402	0.12402
16:0 DMA	0.41416	0.37412	0.39405	0.55404	0.40406	0.48422	0.57419	0.28411	0.35405	0.72441	0.82410	0.57440	0.11410	0.36416
17:0 DMA	1.01404	0.95404	0.99409	0.93402	0.89404	0.92404	1.11431	1.05408	1.01401	1.00408	0.95408	0.92405	0.98403	0.97405
18:0 DMA	9.31455	9.83437	9.95441	10.01413	9.49456	10.04469	9.21452	9.62475	9.89412	10.07423	10.17435	10.71421	9.16445	9.42430
20:1 DMA	5.86422	6.04421	6.09419	5.55409	5.43425	5.55419	5.70419	5.87425	5.15427	5.36427	5.44440	5.36421	5.85409	5.67429
Σ DMA	16.58433	17.19453	17.42411	17.03401	16.21462	16.99461	16.60450	16.82449	16.82449	17.16455	17.37430	17.76412	16.69412	16.43440
16:1n-5	0.46403	0.39402	0.24403	0.38403	0.36401	0.34402	0.48414	0.41405	0.50413	0.40402	0.32402	0.32401	0.46404	0.39402
16:1n-7	2.80416	2.88423	2.62418	2.67425	2.53408	2.75414	3.00408	2.95422	3.26424	2.90417	2.51406	2.79418	3.11410	3.18409
18:1n-5	0.79428	0.47409	0.42406	0.45407	0.38406	0.40404	0.65407	0.34405	0.54408	0.44407	0.43413	0.30404	0.47409	0.40405
18:1n-7	3.52430	3.12410	3.04429	3.03412	3.27412	3.04418	3.15409	3.20419	3.43412	3.17410	2.83415	2.75417	3.59418	3.56431
18:1n-9	0.96411	1.19405	1.22406	1.31407	1.13404	1.39418	1.11410	0.93418	1.38417	1.44415	1.45409	1.81417	1.84402	1.08403
18:1n-11	0.48404	0.48405	0.47407	0.49402	0.44401	0.51401	0.46416	0.54401	0.89406	0.67421	0.65410	0.64407	0.48404	0.57404
20:1n-7	1.00410	1.21417	1.13407	1.06412	1.08404	1.14404	1.50407	1.83412	1.85431	1.78414	1.69409	1.60405	1.55406	1.82411
16:2n-6	6.65415	6.72411	6.90426	7.13422	6.73446	7.62409	7.43444	8.81441	9.47114	9.96411	10.16465	11.14455	7.37428	9.25416
22:1n-11	0.16416	0.27406	0.23403	0.25401	0.29408	0.29406	0.30406	0.34402	0.38409	0.24402	0.24405	0.24403	0.30403	0.31402
Σ MUFA	16.80429	16.95465	16.48440	16.75411	16.25419	17.49420	18.08430	18.44444	21.69439	20.96412	20.30457	21.51445	18.74454	20.56466
16:2n-7	2.27414	2.43427	2.44409	2.39413	2.50416	2.44412	2.21406	2.47413	2.40422	2.56412	2.53422	2.59402	2.47408	2.56419
18:2n-6	0.37408	0.37405	0.33410	0.26404	0.29405	0.45414	0.35402	0.22404	0.19404	0.19403	0.27414	0.23407	0.25404	0.21402
18:2n-6trans	0.57404	0.35403	0.55402	0.57403	0.58403	0.61401	0.56408	0.49402	0.58405	0.64406	0.65405	0.65401	0.52404	0.52408
20:2n-6	0.68408	0.62404	0.60405	0.55403	0.57401	0.59408	0.63405	0.62406	0.55406	0.56404	0.63415	0.62403	0.58402	0.60402
22:2n-6	0.14401	0.11404	0.11402	0.11402	0.12401	0.11402	0.16403	0.11401	0.09401	0.10401	0.12403	0.13401	0.11400	0.11401
Σ dienes	4.02419	4.07404	4.03420	3.88409	4.07412	4.20420	3.91421	3.90418	3.82417	4.05403	4.20413	4.21411	3.94418	4.00421
22:2nM	1.38409	1.12412	1.18406	1.01402	1.04403	1.02409	1.22413	1.32417	1.56422	1.27412	1.32411	1.17417	1.23409	1.11422
22:2nM1	3.92423	4.06438	4.11415	4.24418	3.91433	4.28419	4.36423	4.15420	4.14421	4.25430	4.41414	4.54415	4.03432	4.19419
Σ MME	5.30433	5.17448	5.29418	5.24420	4.96432	5.30424	5.58413	5.47434	5.71401	5.52418	5.73412	5.62414	5.26414	5.39433
16:3n-3	0.66406	0.72414	0.66403	0.72403	0.70405	0.70404	0.73408	0.70402	0.61400	0.75405	0.73403	0.77407	0.66404	0.64404
16:3n-6	0.48402	0.72405	0.70413	0.67406	0.64404	0.64410	0.70423	0.73418	0.51417	0.65409	0.81408	0.63416	0.58417	0.79415
20:3n-3	0.13401	0.16402	0.06402	0.06403	0.06401	0.06401	0.13403	0.12402	0.05400	0.06401	0.06400	0.06401	0.10401	0.07401
20:3n-6	0.11402	0.08403	0.08401	0.06400	0.10404	0.07401	0.09403	0.10400	0.06400	0.04403	0.06407	0.04404	0.06401	0.07401
Σ trienes	1.88408	1.62415	1.50413	1.51410	1.50410	1.47415	1.65412	1.64415	1.24418	1.50417	1.66415	1.49416	1.21419	1.50418
18:4n-1	0.08400	0.09401	0.08403	0.09402	0.03404	0.07403	0.08401	0.05405	0.04404	0.07401	0.02403	0.07402	0.06401	0.07400
18:4n-3	0.20401	0.20404	0.21402	0.19402	0.16409	0.17403	0.23402	0.21404	0.16404	0.20401	0.26408	0.19403	0.18400	0.20401
20:4n-6	1.23413	1.51417	1.56415	1.56415	1.35409	1.34418	1.21411	1.21414	1.35413	1.66417	1.74419	1.89439	1.19404	1.44414
21:4n-6	0.06406	0.09402	0.07400	0.07400	0.09403	0.09401	0.07401	0.16407	0.08402	0.07401	0.15404	0.03404	0.06401	0.20404
22:4n-6	2.64405	3.36407	3.41435	3.22419	3.11413	3.06435	2.86428	2.68416	2.57404	2.97412	3.05422	3.28463	2.78409	2.60424
22:4n-9t	0.12403	0.10402	0.11405	0.07401	0.08401	0.08401	0.11404	0.09404	0.15407	0.09402	0.08401	0.04401	0.13404	0.08401
Σ tetraenes	4.32400	5.29419	5.45457	5.39422	4.82406	4.81444	4.56435	4.42423	4.34407	5.06404	5.30440	5.45416	4.40411	4.59457
22:5n-3	22.95423	21.97415	21.25414	21.79416	23.06414	21.12414	20.30416	19.70478	20.90413	18.19461	18.10434	17.93411	21.40417	19.07448
21:5n-3	0.44402	0.35403	0.34404	0.35402	0.40403	0.36405	0.38401	0.33400	0.28402	0.28401	0.28402	0.34404	0.38403	0.30404
22:5n-3	3.62419	4.15425	4.00415	3.86407	3.91410	4.01422	3.81416	3.62418	3.29400	3.44449	3.77414	3.58433	3.88456	3.57425
22:5n-6	0.72407	0.81408	0.80406	0.79406	0.79404	0.68401	0.61405	0.54403	0.45402	0.51403	0.67401	0.45408	0.64401	0.50404
Σ pentatrienes	27.72437	27.27416	26.39441	26.79418	28.07457	26.18413	24.90465	24.20419	24.91459	22.42419	22.62432	22.20474	26.31414	23.44474
22:6n-3	4.21427	3.59424	3.57424	3.88422	3.49427	3.35422	3.27422	2.76426	2.21406	2.30424	2.15424	1.76411	3.73406	2.54413
Σ PUFA	46.96446	47.02495	46.24418	45.94429	46.90462	45.30462	43.88493	42.49413	42.24412	46.61456	41.65426	40.83429	44.86419	41.38419

**Table S2–2:** Results of the cumulative contributions percentage of dissimilarity using Bray-Curtis dissimilarity index for each lipid analyzed between group pairs of tested temperatures; i.e. 14, 28 and 31°C. Day 0 = the onset day.

	Day 0			Day 6							
	14 vs 28°C	14 vs 31°C	28 vs 31°C	14 vs 28°C	14 vs 31°C	28 vs 31°C					
20:5ω-3	24	20:5ω-3	16	20:5ω-3	14	20:5ω-3	17	20:5ω-3	19	20:5ω-3	9.8
18:0 SFA	34	20:1ω-11	24	18:0 SFA	23	20:1ω-11	32	20:1ω-11	35	20:1ω-11	18.0
22:6ω-3	42	16:0 SFA	30	16:0 SFA	28	16:0 SFA	39	18:0 SFA	43	18:0 DMA	25.9
20:1ω-11	48	20:1ω-7	35	18:1ω-7	33	22:6ω-3	45	22:6ω-3	49	18:0 SFA	33.0
18:0 DMA	52	22:6ω-3	40	22:6ω-3	38	18:0 SFA	51	22:4ω-6	54	16:0 SFA	39.6
20:1ω-7	57	22:5ω-3	45	16:0 DMA	42	18:0 DMA	55	16:0 SFA	58	18:1ω-7	44.4
16:0 SFA	60	18:0 DMA	49	22:5ω-3	47	22:4ω-6	60	20:1ω-7	62	20:4ω-6	48.7
22:2i NMI	63	18:0 SFA	53	18:0 DMA	51	20:1ω-7	64	22:5ω-3	66	22:5ω-3	52.9
18:1ω-7	66	16:1ω-7	57	22:2i NMI	55	22:5ω-3	68	16:1ω-7	69	22:6ω-3	56.7
22:4ω-6	69	18:1ω-5	60	20:1ω-11	59	16:1ω-7	71	18:0 DMA	73	20:1 DMA	60.2
18:1ω-5	71	16:0 DMA	63	iso15:0	62	22:5ω-6	73	18:1ω-7	76	16:1ω-7	62.9
16:1ω-7	73	18:1ω-7	66	16:3ω-3	65	20:4ω-6	75	20:1 DMA	78	22:2i NMI	65.5
16:0 DMA	75	22:2i NMI	68	22:4ω-6	68	18:1ω-9	77	22:5ω-6	80	14:0 SFA	68.0
22:5ω-3	76	iso16:0	71	18:1ω-9	70	20:1 DMA	79	20:4ω-6	82	22:4ω-6	70.5
17:0 DMA	78	iso15:0	73	16:2ω-7	73	16:2ω-7	80	16:2ω-7	84	16:2ω-7	72.7
iso15:0	80	16:2ω-7	75	17:0 DMA	75	18:1ω-7	81	14:0 SFA	85	20:2j NMI	74.9
20:1 DMA	81	16:3ω-3	77	16:3ω-6	77	14:0 SFA	83	22:2i NMI	87	18:1ω-9	76.9
20:2j NMI	83	18:1ω-9	79	iso16:0	80	20:2j NMI	84	17:0 SFA	88	16:3ω-6	78.9
16:3ω-6	84	16:3ω-6	81	18:1ω-5	81	22:2i NMI	85	18:2ω-6	89	20:1ω-7	81.0
19:0 SFA	85	22:1ω-11	82	20:1 DMA	83	16:3ω-6	86	22:2i NMI	90	ant15:0	82.7
17:0 SFA	86	22:4ω-6	83	19:0 SFA	85	22:2j NMI	87	16:0 DMA	91	16:0 DMA	84.4
22:1ω-11	87	17:0 SFA	85	14:0 SFA	86	18:2ω-6	88	16:3ω-3	92	18:1ω-5	85.7
16:2ω-7	88	20:2j NMI	86	16:1ω-7	87	16:0 DMA	89	15:0 SFA	92	iso15:0	87.0
18:1ω-9	89	19:0 SFA	87	18:2ω-6	88	ant15:0	90	iso16:0	93	17:0 SFA	88.2
ant15:0	90	20:2ω-6	88	ant15:0	89	17:0 SFA	91	18:1ω-11	94	22:2j NMI	89.2
14:0 SFA	91	14:0 SFA	89	20:2j NMI	90	17:0 DMA	92	18:1ω-9	94	20:2i NMI	90.2
15:0 SFA	92	18:2ω-6	90	16:1ω-5	91	16:3ω-3	93	18:1ω-5	95	20:2ω-6	91.1
22:5ω-6	93	15:0 SFA	91	20:4ω-6	92	iso16:0	93	21:4ω-6	96	15:0 SFA	92.8
20:2ω-6	93	20:4ω-6	92	20:1ω-7	93	22:1ω-11	94	20:2j NMI	96	17:0 DMA	92.0
20:4ω-6	94	22:5ω-6	93	22:2ω-6	93	15:0 SFA	95	16:3ω-6	97	19:0 SFA	93.7
16:1ω-5	95	20:1 DMA	94	22:5ω-6	94	18:1ω-5	95	20:2i NMI	97	16:3ω-3	94.6
22:2ω-6	95	21:5ω-3	94	20:2i NMI	95	iso15:0	96	19:0 SFA	98	18:1ω-11	95.3
20:0 SFA	96	20:2i NMI	95	18:2ω-6t	95	20:2ω-6	97	22:1ω-11	98	iso16:0	95.9
16:3ω-3	97	22:2j NMI	96	15:0 SFA	96	18:1ω-11	97	iso15:0	98	20:0 SFA	96.5
22:2j NMI	97	20:0 SFA	96	22:2j NMI	96	21:4ω-6	98	17:0 DMA	99	18:4ω-1	96.9
18:1ω-11	97	16:1ω-5	97	22:4ω-9t	97	20:2i NMI	98	18:2ω-6t	99	18:4ω-3	97.4
18:2ω-6t	98	18:2ω-6t	97	17:0 SFA	97	19:0 SFA	98	22:2ω-6	99	21:4ω-6	98.2
22:4ω-9t	98	22:4ω-9t	98	20:3ω-6	98	18:4ω-1	98	20:0 SFA	100	16:1ω-5	98.2
18:2ω-6	99	21:4ω-6	98	20:2ω-6	98	18:4ω-3	99	21:5ω-3	100	18:2ω-6t	98.7
21:4ω-6	99	18:1ω-11	99	22:1ω-11	99	22:2ω-6	99	ant15:0	100	22:1ω-11	99.1
iso16:0	99	ant15:0	99	20:0 SFA	99	18:2ω-6t	99	16:1ω-5	100	18:2ω-6	99.6
21:5ω-3	99	17:0 DMA	99	18:1ω-11	99	16:1ω-5	99	18:4ω-3	100	22:5ω-6	100.0
20:3ω-6	100	18:4ω-1	100	21:5ω-3	100	21:5ω-3	100	18:4ω-1	100	20:3ω-6	100.0
20:2i NMI	100	20:3ω-6	100	18:4ω-1	100	20:0 SFA	100	20:2ω-6	100	22:2ω-6	100.0
18:4ω-3	100	18:4ω-3	100	18:4ω-3	1.00	20:3ω-6	100	20:3ω-6	100	21:5ω-3	100.0
18:4ω-1	100	22:2ω-6	100	21:4ω-6	1.00	22:4ω-9t	100	22:4ω-9t	100	22:4ω-9t	100.0

**Table S2-3:** Results of the cumulative contributions percentage of dissimilarity using Bray-Curtis dissimilarity index for each lipid analyzed between control 14°C and treatment 28°C over the experimental period (days). Day 0 = the onset day.

		14 vs 28°C									
D0		D6		D12		D18		D24		D30	
20:5ω-3	24	20:5ω-3	17	20:1ω-11	17	20:5ω-3	26	20:5ω-3	27	20:1ω-11	21
18:0 SFA	34	20:1ω-11	32	22:6ω-3	26	20:1ω-11	47	20:1ω-11	46	20:5ω-3	40
22:6ω-3	42	16:0 SFA	39	20:5ω-3	34	22:6ω-3	55	22:6ω-3	54	22:6ω-3	49
20:1ω-11	48	22:6ω-3	45	18:0 DMA	42	20:1ω-7	60	18:0 DMA	58	18:0 DMA	55
18:0 DMA	52	18:0 SFA	51	20:1 DMA	48	22:5ω-3	63	22:2i NMI	62	22:2i NMI	59
20:1ω-7	57	18:0 DMA	55	22:4ω-6	54	18:0 SFA	67	20:1ω-7	65	22:4ω-6	65
16:0 SFA	60	22:4ω-6	60	22:5ω-3	59	16:0 SFA	69	18:0 SFA	68	18:0 SFA	62
22:2i NMI	63	20:1ω-7	64	20:1ω-7	63	22:2i NMI	71	16:0 SFA	71	20:1ω-7	67
18:1ω-7	66	22:5ω-3	68	16:1ω-7	67	16:0 DMA	73	16:0 DMA	73	20:4ω-6	70
22:4ω-6	69	16:1ω-7	71	18:1ω-11	70	20:1 DMA	75	18:1ω-7	75	22:5ω-3	72
18:1ω-5	71	22:5ω-6	73	18:1ω-7	72	16:1ω-7	77	20:4ω-6	78	18:1ω-9	75
16:1ω-7	73	20:4ω-6	75	22:5ω-6	75	22:5ω-6	79	18:1ω-9	79	18:1ω-7	77
16:0 DMA	75	18:1ω-9	77	18:0 SFA	77	22:4ω-6	80	22:4ω-6	81	16:0 SFA	79
22:5ω-3	76	20:1 DMA	79	16:0 SFA	78	20:2j NMI	82	22:2j NMI	82	16:0 DMA	81
17:0 DMA	78	16:2ω-7	80	20:2j NMI	80	18:0 DMA	83	18:1ω-11	83	22:2j NMI	83
iso15:0	80	18:1ω-7	81	20:4ω-6	82	16:2ω-7	85	20:2j NMI	85	20:1 DMA	85
20:1 DMA	81	14:0 SFA	83	16:3ω-6	83	18:1ω-11	86	20:1 DMA	86	22:5ω-6	86
20:2j NMI	83	20:2j NMI	84	22:2i NMI	85	18:1ω-7	88	22:5ω-6	87	18:2ω-6	87
16:3ω-6	84	22:2i NMI	85	22:1ω-11	86	18:1ω-9	89	16:3ω-6	88	14:0 SFA	88
19:0 SFA	85	16:3ω-6	86	18:1ω-9	87	iso16:0	90	22:5ω-3	89	16:2ω-7	89
17:0 SFA	86	22:2j NMI	87	iso15:0	88	20:4ω-6	91	16:2ω-7	90	20:2j NMI	90
22:1ω-11	87	18:2ω-6	88	20:2i NMI	89	22:2j NMI	92	17:0 SFA	91	16:1ω-7	91
16:2ω-7	88	16:0 DMA	89	18:1ω-5	90	17:0 SFA	93	iso15:0	91	iso15:0	92
18:1ω-9	89	ant15:0	90	15:0 SFA	91	iso15:0	94	18:4ω-3	92	18:1ω-11	93
ant15:0	90	17:0 SFA	91	14:0 SFA	91	15:0 SFA	95	20:2ω-6	92	16:3ω-6	94
14:0 SFA	91	17:0 DMA	92	20:0 SFA	92	17:0 DMA	95	14:0 SFA	93	iso16:0	94
15:0 SFA	92	16:3ω-3	93	17:0 SFA	93	14:0 SFA	96	21:5ω-3	94	ant15:0	95
22:5ω-6	93	iso16:0	93	18:2ω-6	93	16:3ω-3	96	iso16:0	94	17:0 SFA	95
20:2ω-6	93	22:1ω-11	94	iso16:0	94	18:2ω-6t	97	18:2ω-6t	95	18:1ω-5	96
20:4ω-6	94	15:0 SFA	95	16:1ω-5	95	20:2ω-6	97	18:2ω-6	95	21:5ω-3	97
16:1ω-5	95	18:1ω-5	96	22:2j NMI	95	22:1ω-11	98	22:1ω-11	96	15:0 SFA	97
22:2ω-6	95	iso15:0	96	19:0 SFA	96	16:3ω-6	98	16:1ω-7	96	22:1ω-11	98
20:0 SFA	96	20:2ω-6	97	18:4ω-1	96	16:1ω-5	98	18:1ω-5	97	20:2ω-6	98
16:3ω-3	97	18:1ω-11	97	20:2ω-6	97	18:1ω-5	99	15:0 SFA	97	16:3ω-3	98
22:2j NMI	97	21:4ω-6	98	16:2ω-7	97	ant15:0	99	16:1ω-5	97	21:4ω-6	99
18:1ω-11	97	20:2i NMI	98	17:0 DMA	98	20:2i NMI	99	20:3ω-6	98	18:4ω-1	99
18:2ω-6t	98	19:0 SFA	98	ant15:0	98	21:5ω-3	100	21:4ω-6	98	20:3ω-6	99
22:4ω-9t	98	18:4ω-1	99	16:3ω-3	99	20:3ω-6	100	17:0 DMA	98	18:2ω-6t	99
18:2ω-6	99	18:4ω-3	99	18:2ω-6t	99	18:2ω-6	100	16:3ω-3	99	18:4ω-3	100
21:4ω-6	99	22:2ω-6	99	16:0 DMA	99	19:0 SFA	100	ant15:0	99	19:0 SFA	100
iso16:0	99	18:2ω-6t	99	22:4ω-9t	100	18:4ω-3	100	20:0 SFA	99	20:2i NMI	100
21:5ω-3	99	16:1ω-5	100	18:4ω-3	100	18:4ω-1	100	20:2i NMI	99	16:1ω-5	100
20:3ω-6	100	21:5ω-3	100	21:5ω-3	100	20:0 SFA	100	19:0 SFA	100	17:0 DMA	100
20:2i NMI	100	20:0 SFA	100	20:3ω-6	100	21:4ω-6	100	18:4ω-1	100	20:0 SFA	100
18:4ω-3	100	20:3ω-6	100	21:4ω-6	100	22:2ω-6	100	22:2ω-6	100	22:2ω-6	100
18:4ω-1	100	22:4ω-9t	100	22:2ω-6	100	22:4ω-9t	100	22:4ω-9t	100	22:4ω-9t	100

**References:**

- Faroni-Perez, L. (2017). Climate and environmental changes driving idiosyncratic shifts in the distribution of tropical and temperate worm reefs. *Journal of the Marine Biological Association of the United Kingdom*, 97, 1023–1035.
- Jones, C.D., Hughes, J.K., Bellouin, N., Hardiman, S.C., Jones, G.S., Knight, J. *et al.* (2011). The HadGEM2-ES implementation of CMIP5 centennial simulations. *Geoscientific Model Development*, 4, 543–570.
- Martin, G.M., Bellouin, N., Collins, W.J., Culverwell, I.D., Halloran, P.R., Hardiman, S.C. *et al.* (2011). The HadGEM2 family of Met Office Unified Model climate configurations. *Geoscientific Model Development*, 4, 723–757.
- Taylor, K.E., Stouffer, R.J. & Meehl, G.A. (2011). An Overview of CMIP5 and the Experiment Design. *Bulletin of the American Meteorological Society*, 93, 485–498.



**ANTERIOR SENSORY ORGANS IN SABELLARIIDAE  
(ANNELIDA)**

**Running head:** Sensory organs in Sabellariidae

Larisse Faroni-Perez, Conrad Helm, Ingo Burghardt, Pat Hutchings, and  
María Capa

*Published in*  
Invertebrate Biology

This chapter is under an agreement between Larisse Faroni-Perez and John Wiley and Sons, which consists in the *License Number 4216451136611* provided by John Wiley and Sons and Copyright Clearance Center.

How to cite:

Faroni-Perez, L., Helm, C., Burghardt, I., Hutchings, P. and Capa, M. (2016), Anterior sensory organs in Sabellariidae (Annelida). *Invertebr Biol*, 135: 423–447. doi:10.1111/ivb.12153



## Abstract

Sensory organs in Annelida are very diverse and may be useful for assessments of morphological adaptation and character evolution. We used several methods to provide new insights into processes underlying the evolutionary radiation of anterior sensory organs in Sabellariidae. The presence and morphological diversity of the median organ (MO) found in the group was reviewed in order to test its phylogenetic significance and possible relationships to the distribution and ecological traits of the lineages. To test the intraspecific phenotypic plasticity of the MO, molecular analyses were conducted that focused on mitochondrial and nuclear genes from populations of *Idanthyrsus australiensis* exhibiting variation in the morphology of the MO. We used an integrative microscopical study of the ontogeny of *Sabellaria alveolata* to describe the anterior sensory structures present in the larvae and the morphological changes occurring before, during, and after settlement. In larval stages, the palps and the dorsal hump (DH) exhibit distinct innervation. The larval DH organ, which is likely to play a major role in chemoreception for settlement, is interpreted as being the incipient form of the adult MO. These results suggest that annelid sensory organs including the MO may be useful for phylogenetic and developmental investigations.

*Additional key words:* chemoreception, gregarious settlement, marine invertebrates, polychaetes, radiation of lineages



## Introduction

Sensory organs play an important role in the evolution and adaptive radiation of animals. From the simplest receptor cell to derived complex organs, they allow individuals to perceive the environment and facilitate survivorship via subsequent responses, including feeding, defense, homing, reproduction, larval settlement, and metamorphosis. The most commonly described sensory organs are related to photo-, mechano-, and chemoreception. Chemoreception, and hence chemical communication, is involved in many aspects of annelid reproduction, including attracting a mating partner or spawning of gametes in the seawater column (Caspers 1984; Hardege et al. 1998). It is also important for metamorphosis and subsequent settlement in many species (e.g., Pawlik 1992; Qian 1999), including gregarious species of Sabellariidae JOHNSTON 1865. Chemical signals, present in the cement secreted by benthic juveniles and adults when building their tubes, are known to induce other conspecific planktonic larvae to settle. Although the chemical cues that induce gregarious larval settlement in sabellariids were described decades ago (Pawlik, 1986, 1990; Jensen & Morse 1990), the identity of the sensory organs detecting these chemical signals and their role during the pelagic–benthic transition remain unclear. The small size of larvae and their short, often unknown, planktonic period may be responsible for the limited information available (Pawlik 1992). In some sabellariid species, individuals are gregarious and build reefs (McCarthy et al. 2008; Barrios et al. 2009; Fournier et al. 2010; Desroy et al. 2011), but in other species individuals live in small clumps or are found as solitary individuals (Hutchings et al. 2012). Both gregarious and solitary species all seem to be free-spawners (Wilson 1991).

The presence of several sensory organs in sabellariids has been recognized in different ontogenetic stages of some species (Wilson 1929, 1977; Dales 1952; Eckelbarger 1976, 1978; Eckelbarger & Chia 1976; Kirtley 1994; Lechapt & Kirtley 1996; Bhaud & Fernández-Álamo 2001), but there are few detailed studies (Eckelbarger & Chia 1976; Amieva & Reed 1987; Amieva et al. 1987; Capa et al. 2015). The main sensory structures reported include ocelli, statocysts, palps, and the median organ (MO). The larval palps have been examined ultrastructurally, and are presumed to participate in substrate selection during settlement (Amieva et al. 1987), while adult palps have been associated with feeding and particle capturing (Dubois et al. 2005; Riisgård & Nielsen 2006). The MO is an anterior head appendage with

an apparent sensory function present in the adults of some species (Kirtley 1994; Lechapt & Kirtley 1996; Nishi & Núñez 1999). Recently, a detailed study of the morphology of the MO in several sabellariids stated that it is continuous with the median ridge (MR), an elongated crest running from the dorsal edge of the upper lip along the junction of the opercular lobes (Capa et al. 2015). Among sabellariids, the MO and the MR show a broad diversity of shapes and sizes and can bear other sensory structures, such as cilia and eyespots. The morphology of the MO and the MR seem to be species-specific, but some diversity within species has been recorded in *Idanthyrus australiensis* (HASWELL 1883) (Capa et al. 2015). The ontogenetic development and sensory role of the MO, as well as its taxonomic value remains to be assessed. The morphological descriptions of sabellariid larvae and their development also mention another prominent larval structure in between the dorsal palps called the dorsal hump (DH) (Wilson 1929; Eckelbarger 1976; Bhaud & Fernández-Álamo 2001). In pre-metamorphic developmental stages of *Sabellaria alveolata* LINNAEUS 1767 the presence of a conspicuous DH is associated with a distinct 'triangular nerve-net' (Brinkmann & Wanninger 2008), but no sensory function has yet been assigned to the DH.

Because little is known about the conspecific variation, morphology, and possible function of the anterior sensory organs in Sabellariidae, we:

- (i) reviewed available information about the anterior sensory organs (i.e., palps, DH, and MO) among Sabellariidae, considering ecological traits (i.e., their habitats, bathymetric distribution, and settlement behavior), and re-examined described species and provided morphological data for the palps and MO;
- (ii) re-examined the intraspecific variability in the MO of one species of *Idanthyrus* to test its value as a taxonomic character;
- (iii) described the morphology of the anterior sensory organs, DH, and palps throughout ontogenetic development in one species of sabellariid, *Sabellaria alveolata*.

These results provide new insights into the sabellariid palps, DH, and MO at different developmental stages by addressing their potential sensory role and phylogenetic significance.

## Methods

### **Sabellariidae distribution, ecological traits, and descriptions of anterior sensory organs**

Information from available literature on Sabellariidae was compiled to generate a dataset comparing the DH, the MO, and ecological traits among members of the family (Table 1; Appendix S1). Because no explicit data were provided for several species, we created a standardized approach at the generic level, in order to undertake a qualitative meta-analysis. Although the generic level gives only coarse resolution, it provides a baseline for a systematic revision. The traits considered are useful for an open-access database (Costello et al. 2015) and were: bathymetric range of distribution (i.e., maximum and minimum depth records of the benthic stages); substratum (i.e., characterization of substrata/site where specimens were sampled); and the occurrence of gregarious settlement behavior, classified as solitary (one or few units of free tubes per sample), forming small clusters (attached tubes, or 100+ specimens per sample), or forming reefs (i.e., several attached tubes with records of the biogenic substrates formation). The bathymetric ranges were: littoral (intertidal zone), continental shelf (sublittoral; 500 m), continental slope (500–3000 m), and continental rise (>3000 m). The DH and MO were considered present when mentioned specifically or when the structures were shown in species illustrations. Morphological traits of the MO, such as its presence, general morphology, shape of the distal end, presence of eyespots, and pigmentation pattern (Capa et al. 2015), have in many cases not previously been reported. To supplement this information, we examined live specimens of *Sabellaria alveolata* collected from reefs at Mont St. Michel Bay, France (48°43'52.77"N, 1°33'8.77"W) in spring of 2016, and used light microscopy to illustrate the location and structure of the anterior sensory organs. Additionally, SEM images (made in 2009) of the MO of *Sabellaria* sp. collected from Ilha da Marambaia, Brazil (23°2'46.91"S 43°58'31.48"W) in summer of 2004 were used to illustrate other morphological characters. Adult sabellariids from the deep sea collected during the cruises of the “Biology of New Caledonia” (1985–1987) housed at the National Museum of Natural History of Paris (MNHN) were also examined under light microscopy. Some images of their MO and palps were taken using a Canon EOS 60D SLR camera with macro lens. We then used the sabellariid phylogeny by Capa et al. (2012) to put our observations into a comparative context.

### ***Idanthyrus australiensis* morphology**

Over 100 adult specimens of *Idanthyrus australiensis* collected from several localities around Australia (including Western Australia, Northern Territory, Queensland, and New South Wales) and housed at

the Australian Museum (AM) were examined in detail and identification confirmed (Haswell 1883; Hutchings et al. 2012). These specimens were mainly fixed in 10% formaldehyde for 2–3 days, rinsed and transferred to 80% ethanol.

Characters considered were: the overall color pattern, the paleae morphology, the number of nuchal spines (hooks), the number and shape of lateral lobes in segment 2, and the chaetal morphology (observed under the compound microscope). Special attention was paid to the morphology of the MO and MR, and features scored included the shape and size of the MO, its pigmentation pattern, the development of the MR, and presence of eyespots along the edges of the MR. Light microscopy photographs were taken with a Leica MZ16 microscope with a Spot flex 15.2 camera attached.

### **Taxon sampling for molecular analyses**

Twenty-two of the individuals from several localities in Western Australia and New South Wales that had been fixed and preserved in ethanol were examined externally and used for molecular analyses (Table 2). In addition, another six species were included in the study: *Idanthyrus cretus* CHAMBERLIN 1919, *Phragmatopoma californica* FEWKES 1889, *P. virgini* KINBERG 1866, *P. moerchi* KINBERG 1866, *P. caudata* KRØYER in MÖRCH 1863, and *Sabellaria alveolata*.

### **DNA sequencing**

Genomic DNA was extracted from muscle tissue using standard protocols for the DNeasy Blood and Tissues Kit (QIAGEN Pty Ltd). Sequences were obtained of 517–658 bp of the mitochondrial genes cytochrome oxidase I (*cox1*) from 27 individuals, and 380–416 bp of cytochrome b (*cob*) from 15 individuals, and 586–697 bp of the nuclear gene ribosomal internal transcribed spacer 1 (ITS1), with flanking regions of 18S rDNA and 5.8S rDNA, from 24 individuals. The primers used were LCO11490 and HCO12198 for *cox1* (Folmer et al. 1994), Cytb 424F (RT-1) *cobr*825 for *cob* (Burnette et al. 2005), and ITSF and ITSRI for ITS1 (Chen et al. 2002; Capa et al. 2013). PCR mixtures contained 1× QIAGEN PCR buffer, 3 mM MgCl<sub>2</sub>, 200 μM each of deoxynucleotide (dNTP), 200 nM of each primer, 2.5 units of QIAGEN Taq DNA polymerase, and 50–100 ng of whole genomic DNA, combined with double-distilled H<sub>2</sub>O to make up 15 μL total volume. Amplifications were performed on a vapo.protect cycler (Eppendorf Inc). For *cox1* the PCR thermal cycling profile was typically 94°C for 2



min, followed by 35 cycles of 94°C for 30 s, 50°C for 45 s, 72°C for 1 min, and 3 min of final extension at 72°C. For *cob* and ITS1 a slightly different PCR thermal cycling profile was used: 94°C for 3 min, followed by 45 cycles of 94°C for 30 s, 47°C for 30 s, 72°C for 30 s, and 4 min of final extension at 72°C. Successful amplifications were purified using the ExoSAP-IT PCR purification system (USB Corporation), and then bidirectionally sequenced, using the original PCR primers, by Macrogen Inc. (Seoul, Korea). Forward and reverse strands were corrected for misreads and merged into one sequence file using Codoncode Aligner v. 3.6.1 (CodonCode Corporation, Dedham, MA, USA), and Sequencher v. 5.1 (Gene Codes Corporation). ITS1 sequence chromatograms showed no evidence of double peaks (which would suggest the presence of multiple copies), and so cloning was not pursued.

### Phylogenetic analyses

Nucleotide sequences of *cox1* and *cob* were aligned with MAFFT v. 7.0 (Kato 2013) on the mafft server (<http://mafft.cbrc.jp/alignment/server/index.html>) using the G-INS-i strategy, recommended for sequences with global homology, and ITS1 sequences were aligned using the Q-INS-i strategy, which takes into account secondary structures. Poorly aligned positions from divergent regions of ITS1 were removed using Gblocks v. 0.91b (Talavera & Castresana 2007). We used relaxed parameters to assess the impact of ambiguously aligned regions of phylogenetic signal: minimum number of sequences for a conserved position, 15; minimum number of sequences for a flanking position, 15; maximum number of contiguous non-conserved positions, 8; minimum length of a block, 5; minimum coverage to include gap positions, half. Maximum likelihood analyses were carried out with RAxML version 7.7.1 (Stamatakis et al. 2008) on the RAxML BlackBox server (<http://embnet.vital-it.ch/raxml-bb/>) using gamma-distributed rate heterogeneity and 25 rate categories. Nucleotide divergence and Kimura 2-Parameter (K2P) distances were computed with MEGA v. 6 (Tamura et al. 2013). Only perfectly homologous regions (same length, same part of locus) were considered. Statistical parsimony of haplotype networks was performed in TCS v. 1.2.1 (Clement et al. 2000) and PopART (<http://popart.otago.ac.nz>, Clement et al. 2002), analyzing *cox1*, *cob* and ITS1 aligned sequences independently and calculating 95% connection limit. In TCS, IUPAC ambiguity codes and gaps were treated as missing data. For ITS, missing

information in flanking positions was omitted and gaps considered as a fifth state.

### ***Sabellaria alveolata*, culture and fixation**

Adult specimens of *S. alveolata* were collected at Saint-Efflam (Brittany, France) during summer 2015, transferred to Bergen (Norway), and reared at 14–17°C. After artificial fertilization in filtered seawater (FSW), the developmental stages were reared at 18°C in glass bowls containing FSW. The culture was set under strict diurnal light rhythm (14 h light : 10 h dark) and fed with a mix of unicellular algae (*Isochrysis* spp., *Chaetoceros* spp.). Water was changed regularly. We defined stages of development by the number of ‘days post-fertilization’ (dpf) required for the majority of larvae to reach a specific developmental point.

For immunohistochemistry, different larval stages were anaesthetized using 7% MgCl<sub>2</sub> in FSW. Subsequently larvae were fixed in 4% paraformaldehyde (PFA) in 1x phosphate buffered saline (PBS) with Tween (1x PBS: 0.05 M PB / 0.3 M NaCl / 0.1% Tween20) for 2 h at RT (room temperature). Afterwards, specimens were rinsed in 1x PBS several times and stored in 1x PBS containing 0.05% NaN<sub>3</sub> at 4°C until usage.

For electron microscopy, larvae were fixed in 2.5% glutaraldehyde in sodium cacodylate buffer (0.1 M cacodylate, pH 7.4, 0.24 M NaCl) for 1 h at RT. After three rinses in sodium cacodylate buffer for 10 min each, the specimens were stored in sodium cacodylate buffer containing 0.05% NaN<sub>3</sub> at 4°C until usage.

### **Scanning electron microscopy (SEM)**

For SEM analyses, 20–30 specimens of each investigated stage were used. The samples were washed twice for 5 min in sodium cacodylate buffer without addition of NaN<sub>3</sub>. Afterwards, the specimens were post-fixed in osmium tetroxide (1% OsO<sub>4</sub> in sodium cacodylate buffer) for 45 min at RT and rinsed with distilled water three times for 10 min each. Subsequently, the samples were dehydrated using an increasing EtOH series (from 30% to 90% in 10% increments, followed by 95% and three changes in 100%, 5–10 min each), critical-point dried, and coated with gold/palladium. Finally, the samples were examined with a ZEISS Supra 55VP scanning electron microscope.

### **Immunohistochemistry and confocal laser scanning microscopy**

Details concerning the innervation of the DH in developmental stages of *S. alveolata* were revealed in whole animal preparations using a range of well-established antisera as neuronal markers. Although the specificities of the employed antibodies have all been established in numerous invertebrates (for references please see the Discussion), we cannot exclude the possibility that a given antiserum may bind to a related nontarget antigen in individuals of *S. alveolata*. Therefore, we refer to observed profiles of immunoreactivity against individual antigens (*n*) as antigen-like immunoreactivity (*n*-LIR). Negative controls were obtained by omitting the primary antibody in order to check for antibody specificity and yielded no fluorescence signal. For immunohistochemistry, at least 20–30 specimens of all investigated stages were rinsed twice for 5 min each in PTW (PBS with 0.1% Tween 20) at RT and subsequently transferred into 10 µg proteinase K/mL PTW for 1–1.5 min. After two short rinses in glycine (2 mg glycine/mL PTW), and three washes for 5 min each in PTW, the specimens were fixed a second time using 4% PFA in PBS containing 0.1% Tween for 20 min at RT. Subsequently, the developmental stages were rinsed 2x5 min in PTW, 2x5 min in THT (0.1 M Tris-HCl, pH 8.5, 0.1% Tween-20) and blocked for 1–2 h in 5% sheep serum in THT. The primary antibodies, polyclonal rabbit anti-5-HT (INCSTAR, Stillwater, USA, dilution 1:500), monoclonal mouse anti-acetylated  $\alpha$ -tubulin (Sigma-Aldrich, St. Louis, USA, dilution 1:500), and polyclonal rabbit anti-FMRamide (ImmunoStar Inc., Hudson, USA, dilution 1:1000) were applied for 48–72 h in THT containing 5% sheep serum at 4°C. Afterwards, specimens were rinsed in 1 M NaCl in THT, then washed five times for at least 30 min in THT, and incubated subsequently with secondary fluorochrome conjugated antibodies (goat anti-rabbit Alexa Fluor 488, Invitrogen, USA, dilution 1:500; goat anti-mouse Alexa Fluor 633, AnaSpec, Fremont, USA, dilution 1:500) in THT containing 5% sheep serum for 48 h at 4°C. Subsequently, the samples were washed six times for 30 min each in THT, stained with DAPI for 15–30 min (5 mg/mL stock solution, working solution: 2 µL in 1 mL THT, to a final concentration of 10 µg/mL) and washed 2x5 min in THT. For confocal laser-scanning microscopy (clsm), samples were mounted on glass slides in 90% glycerol/10% 10x PBS containing DABCO. Specimens were analyzed with the confocal laser-scanning microscope Leica TCS STED (Leica Microsystems, Wetzlar, Germany). Confocal image stacks were processed with Leica LAS AF v 2.3.5 (Leica Microsystems), ImageJ, and Imaris 6.3.1 (Bitplane AG, Zurich,

Switzerland). The final panels were designed using Adobe (San Jose, CA, USA) Photoshop CC and Illustrator CC.

## Results

### **Systematic review of distribution, habitat, ecological traits, and descriptions of anterior sensory organs found in Sabellariidae**

Sabellariidae includes 12 genera, with 136 nominal species distributed worldwide from littoral to continental rise environments. In benthic stages, all members can occur as solitary or living near conspecifics, but only members of five genera are known to build reefs, and so, have gregarious sociability. In general, the solitary members have their tubes attached to consolidated or soft substrata, while the formation of clumps and reefs begins with tubes attached to consolidated substrate. There are two sabellariid reefs located in France and Malaysia that are not directly attached to consolidated substrata, but are situated near others attached to hard substrata, from where the initial reef fragments could be separated. Those genera with members capable of building reefs are *Gunnarea* JOHANNSON 1927, *Idanthyrus* KINBERG 1876, *Neosabellaria* KIRTLEY 1994, *Phragmatopoma* MÖRCH 1863, and *Sabellaria* LAMARCK 1818. These biogenic structures mainly occur in the littoral zone; few large structures are in the shallow sublittoral zone, and no reefs are recorded at the continental shelf or deeper. The genus *Paraidanthyrus* KIRTLEY 1994 occurs in the intertidal and forms small clumps, but has not been reported as forming reefs. Species of the remaining six genera, *Lygdamis* KINBERG 1867, *Phalacrostemma* MARENZELLER 1895, *Bathysabellaria* LECHAPT & GRUET 1993, *Mariansabellaria* KIRTLEY 1994, *Tetreres* CAULLERY 1913, and *Gesaia* KIRTLEY 1994 are solitary; their tubes have never been reported as attached to conspecifics, even though some specimens were close to others. Only *Lygdamis* can occur from the shallowest continental slope boundary to littoral waters. The other five genera of non-gregarious sabellariids occur in deep water, from the continental slope to the continental shelf. Although we found one study mentioning that *Tetreres* occurs in shallow water, no further information was given, and this record is not considered herein. Species of *Bathysabellaria* tend to have patchy distributions; in some locations each sampling dredge collected hundreds of specimens.

In the genera *Gunnarea*, *Paraidanthyrus*, *Phragmatopoma*, *Neosabellaria*, and *Mariansabellaria* an external MO is absent in adult forms. However, eyespots can be seen on both sides of the MR. The

conspicuous MO is present in adults of at least 47 species belonging to the seven genera *Sabellaria*, *Lygdamis*, *Idanthyrus*, *Phalacrostemma*, *Bathysabellaria*, *Tetreres*, and *Gesaia*; a large plasticity of morphological traits occurs within these genera. It is important to highlight that the MO is not reported or described consistently among the species in those seven genera in which this structure has been recorded. This sensory organ was probably overlooked, and was not used in early taxonomic studies.

Following metamorphosis, the benthic stages of *Sabellaria* sp. have either a small MO or seems inconspicuous. The MO is located distally at the junction of the opercular lobes (Fig. 1A–D), and is continuous with the MR (Fig. 1E,F). The MR is an elongated crest running along the junction of opercular lobes, and marginally bears several eyespots (Fig. 1F). The external morphology of MO within the genus *Sabellaria* is variable. For example, it can be conical (Fig. 1E) or flat and trilobed (Fig. 2A). The dense ciliation along the ventral face of opercular lobes is also observed in the MO (Fig. 2A,B). At the edge of the distal margin in the MO a dense line of cilia is present that separates ventral and dorsal sides (Fig. 2B,C), which creates a local current (see Video S1). In species of the genera *Gesaia*, *Lygdamis*, and *Bathysabellaria* the MO is elongated, while in *Tetreres*, *Phalacrostemma*, and *Idanthyrus* it is small (Fig. 3A,C,D). In *Bathysabellaria* the general MO shape is conical with rounded top (Fig. 3A), and the variability observed is intraspecific, with minor differences in the size and presence of some eyespots in the MR (e.g., in *B. spinifera*, unpubl. data). Interspecific morphological diversity in the MO is observed in the genus *Lygdamis*; an enlarged MO with rounded top and absence of eyespots is observed in species occurring at the continental slope (e.g., *L. splendidus*, Fig. 3C), while species from shallow seas have several eyespots along the MO and a very pigmented distal top (e.g., *L. nasutus*). Descriptions of the MO in *Gesaia* and *Tetreres* are from available literature, and the single specimen of *Phalacrostemma* (Fig. 3D) examined is insufficient for comparative analysis.

The palps are present in all genera, but in *Bathysabellaria*, *Mariansabellaria*, *Phalacrostemma*, and *Tetreres* the palps are noticeably enlarged at the base (Fig. 3B,C,E) compared to sabellariids from intertidal zones. In three of these genera (*Mariansabellaria*, *Phalacrostemma*, and *Tetreres*), palps are also longer than in other sabellariids.

The presence of a larval DH is mentioned in the literature for all the genera in which larvae have been described: *Gesaia*, *Lygdamis*, *Idanthyrus*, *Sabellaria* and *Phragmatopoma*. In all cases, the DH is located between the larval palps in late larval stages. Morphological descriptions of these DH are insufficient for a comparative analysis.

The meta-analyses in the present study show that sabellariids can be divided into three groups. These groups integrate information from recent phylogenetic analyses, ecological traits (sociability and bathymetric distribution), and the presence or absence of anterior sensory organs (MO) in benthic stages. Figure 4 and Table 1 summarize these results.

### **Medial organ morphological diversity within *Idanthyrus australiensis* investigated with light microscopy**

Revision of specimens of *I. australiensis* (sensu Hutchings et al. 2012; Capa & Hutchings 2014; Capa et al. 2015) acknowledged phenotypic variability in the relative size, shape, and color of the MO and the MR and the number, density, and arrangement of eyespots along the sides of the MR (e.g., Fig. 5). In some cases the MO protrudes beyond the dorsal opercular edge (Fig. 5E,H,J), while in others it does not (Fig. 5B–D). At the proximal base, in the MR the general morphology of the MO is enlarged, while the distal end is variable. The top of the MO can be cylindrical rounded (Fig. 5A,B,J–L), conically elongated, and thinner (Fig. 5E–G,I), or intermediate (Fig. 5C,D,H). The MR also showed some differences among specimens examined. Some individuals have the MR as an elongated crest with parallel edges (Fig. 5B,E,F,I), while in others the MR is wider, with an ovoid shape and convex edges (Fig. 5C,D). The number, density, and arrangement of eyespots vary from a single line running along the base (Fig. 5B,E,I–L) to several densely arranged rows of eyespots along the MR edge (Fig. 5D,F–H). The palps have a longitudinal groove in the ventral face, and laterally conspicuous scattered pigmentation is present (Fig. 5A,B,H,J–L). The differences in the MO and the MR among specimens, together with the degree of pigmentation of these structures, seem not to be correlated with the size of the specimens. By contrast, other morphological differences observed seem to be related to the size of specimens and were observed only in larger sized specimens. Three pairs of nuchal spines and broad, spade-shaped lateral lobes in segment 2 are found in larger individuals, while smaller ones generally have one or two pairs of nuchal spines and longer, triangular lobes in segment 2.

### **Genetic distance, haplotype networks and phylogenetic analysis**

We found five *cox1* haplotypes along the NSW coast (Fig. 6A). The most prevalent haplotypes were shared by AM W.35309 and others (Fig. 6D, Fig. S1), and although the sample size is too small to make strong conjectures, it is most likely the original haplotype. Genetic distance among these haplotypes is 0.2–0.5%. Genetic distance between haplotypes from two specimens from WA was 13.6%; distances between each of these haplotypes and any NSW haplotype were 18.6–19.2% and 22.2–22.6%, respectively. The WA haplotypes formed two independent networks that were more different from each other than the 95% connection limit (represented by the zig-zag line in Fig. 6A).

We found a single *cob* haplotype along the NSW coastline (Fig. 6B). The genetic distance between that haplotype and the single specimen collected in WA, AM W.36968 from Ningaloo Reef, was 20.2%. Genetic variation within the ITS network included 11 haplotypes from NSW of which AM W.36969 seems to be the most prevalent; genetic distances were 0.2–2.0% (Fig. 6C). Amplification of ITS1 sequences from WA specimens failed.

Maximum likelihood analyses of the three DNA fragments separately provide congruent results (Fig. S1). Differences between topologies were associated with weakly-supported nodes, mainly at the base of the tree or within the NSW clade of *I. australiensis*. Analyses of the combined dataset provide more support to the basal nodes, although assessing deep relationships was not the goal of this study, and the markers chosen were not the most appropriate for it. However, it is interesting to notice that our results do not support monophyly in *Idanthyrus*, and both the *cox1* and ITS1 sequences of *I. cretus* obtained from GenBank were substantially different from its Australian congeners.

The specimens collected in WA (which provided *cox1* and *cob* sequences, but not ITS1) show a long internode reflecting the large genetic divergence between these two populations, as mentioned above (Fig. 6E and Fig. S1). Branches between both WA terminals are also relatively long (Fig. 6E).

### **Investigations of the larval development in *Sabellaria alveolata* using SEM**

In early stages (~25 dpf), the drop-shaped larvae bear a prominent apical tuft, a well-developed prototroch, and distinct bundles of chaetae (Fig. 7A). In this stage no DH can be observed.

Later in development, ~35 dpf, the larvae exhibit a distinguishable metatroch posterior to the prototroch, and the primordial palps are visible as minute buds situated close to the dorsal margins of the prototroch. Between these primordial palps, the prototroch is lacking, and thus a dorsal gap is formed (Fig. 7B,C). The telotroch is present as well (Fig. 7B). Within this prominent gap, a dorsal bulge (the DH) possessing distinct ciliation is visible (Fig. 7B,C). At this stage, the DH is only slightly elevated. In contrast to that, the larvae at 40 dpf possess a well-elevated and ciliated DH, and the primordial palp buds are clearly visible (Fig. 7D). At 49 dpf, the DH is still well elevated and possesses ciliation, and the primordial palps continue to grow (Fig. 7E). Notably, the developing primordial palps exhibit first sparse ciliation in this early stage.

Specimens at 75 dpf have a barrel-shaped body and still possess well-developed bundles of chaetae and a prototroch. In contrast to the previous stage, the primordial palps dramatically increase in size and amount of ciliation. Thus, the ciliation is very dense on one side and appears sparse on the other (Fig. 7F–I). At least eight chaetae-bearing parathoracic chaetigers are developed, each thorax and parathorax segment exhibits a dorsal ciliation, and a telotroch is still visible (Fig. 7F). Furthermore, the DH is present as a distinct dorsal bulge and has highly-visible ciliation (Fig. 7F,H).

Shortly prior to metamorphosis, 75–90 dpf, the larvae lose their prominent and long swimming chaetae. Instead they develop numerous paleae at the former position of the larval chaetae (Fig. 7G). The paleae-bearing appendages and the primordial palps are directed towards the posterior. Notably, the densely ciliated part of the palps is directed towards the ventral. Other morphological characteristics are as described for the previous stage. Notably, the DH increases in elevation and still possesses prominent ciliation (Fig. 7H). In this stage the larvae still have not settled, but interestingly the animals no longer swim but crawl on the surface to search for a suitable place to settle. The palps develop an anterior orientation, and the ventral-directed ciliated part appears to be used for sensing the substrate (unpubl. data).

Shortly after metamorphosis, the larvae have settled and still resemble the previous stage in many characters. The larval body now is surrounded by a transparent mucous tube (unpubl. data). In this stage, the transformation of the anterior region begins and the paleae-bearing appendages and the primordial palps are directed towards anterior, framing the anterior tip of the larvae (Fig. 7I). The paleae-bearing appendages are referred to as opercular lobes. The DH is still dorsal, but



situated between the opercular lobes at this stage. Ciliation of the latter structure is still distinguishable (Fig. 7I). The palps are relocated into a ventral position with the ciliation facing towards the substrate (Fig. 7I).

Several days after metamorphosis, the transformation of the anterior region in juvenile worms shows further progress and resembles adult-like morphology (Fig. 7J,K). The opercular lobes are situated dorsally and the palps are directed towards ventral. Thus, the number of the paleae increases, the palps elongate, and prominent opercular papillae, opercular filaments, and nuchal hooks are developed (Fig. 7J,K). The DH is still present but reduced in size and is represented by a densely ciliated dorsal field situated between the opercular papillae (Fig. 7J). The elevation of the DH is no longer recognizable.

### **Immunohistochemical analyses of different developmental stages of *Sabellaria alveolata***

The DH in larvae of *S. alveolata* is visible not earlier than 35 dpf (Fig. 8A). Earlier stages do not possess a comparable structure. The DH is represented by a dorsal bulge located within the dorsal gap of the prototroch and flanked by the developing larval palps (Fig. 8A). Notably, the entire structure of the DH exhibits prominent ciliation, whereas ciliated areas are missing on the primordial palps so far (Fig. 8A), and distinct nerves are visible running from the larval brain directly into the hump (Fig. 8B). Thus, two distinct neurite bundles run from the larval brain towards the distal end of the DH. Furthermore, FMRamide-LIR is exhibited in the entire structure of the DH (Fig. 8C). Distinct somata are not distinguishable at this stage. 5-HT-LIR is not detectable within the DH in this developmental stage.

Later in development (49 dpf) the DH increases in size and ciliation (Fig. 8D,E). The larval palps, which are sparsely ciliated structures at this stage, also show an increase in size and ciliation. Furthermore,  $\alpha$ -tubulin-LIR indicates strong innervation of the primordial palps and hump area (Fig. 8E,G). Thus, the primordial palps are each innervated by at least one prominent neurite bundle with several branching neurites in each palp (Fig. 8E), and the DH possesses a pair of neurite bundles in each structure connecting the entire structure with the larval brain (Fig. 8G). 5-HT-LIR and FMRamide-LIR reveal the presence of distinct somata sending prominent processes into the DH (Fig. 8F,H). Notably, distinct 5-HT-IR is detectable within the palps as well (Fig. 8F).

At 75 dpf, the larvae increase significantly in size. The larval palps and the DH elongate (Fig. 8I). The DH remains strongly ciliated

(Fig. 8I). In this stage two somata showing 5-HT-LIR are distinguishable at the base of the hump. One pair of neurite bundles can be seen in each palp (Fig. 8J). At least one neuronal cell exhibiting FMRamide-LIR forms a distinct process innervating the DH (Fig. 8K).

In older pre-metamorphic stages (80–90 dpf), the previously described conditions are retained unchanged (Fig. 9A,B,D). The DH is still located between the posteriorly oriented larval palps and exhibits a distinct and dense ciliation and innervation (Fig. 9C). As described above, one pair of neurite bundles showing prominent  $\alpha$ -tubulin-LIR runs from the larval brain into the hump. Additionally, at least two somata exhibiting 5-HT-LIR and one soma with strong FMRamide-LIR send processes into the distal part of the hump (Fig. 9B–D).

Shortly after metamorphosis (between 75–90 dpf) the area of the DH is significantly reduced in size (Fig. 9E) but still presents a prominent ciliation and innervation (Fig. 9H), shown by  $\alpha$ -tubulin-LIR. Whereas the hump in earlier stages was characterized as a dorso-posterior bulge, the same structure is now represented by an anterodorsal oriented, blunt-ending cone (Fig. 9F). In this stage the larval palps are oriented towards anterior, pointing into the direction of movement, and exhibit a densely ciliated and well innervated surface (Fig. 9E). Although still possessing partial ciliation, the area of the DH now exhibits a strongly diminished 5-HT-IR and FMRamide-LIR (Fig. 9F,G). The prominent neuronal cells sending processes into the hump described for earlier stages are not recognizable anymore.

Summarizing, these immunohistochemical investigations revealed the presence of a DH in larvae of *Sabellaria alveolata* around 35 dpf (Fig. 9A). In earlier larval stages, no distinct staining in the region of the DH was present when using different standard markers. From 35 dpf until metamorphosis (which takes place at the earliest ~90 dpf, depending on larval density, temperature, and food supply), the DH is prominently innervated by one pair of neurite bundles running from the larval brain into the distal hump, and the DH possesses neurons underlying the ciliation. Furthermore, the highest density of ciliation occurs in stages shortly before metamorphosis.

## Discussion

In this study, a diverse combination of approaches was used to investigate the anterior sensory organs of Sabellariidae and their possible implications for radiation of lineages. Each of these approaches

is discussed separately, with a summary of overall findings and how they advance our knowledge of annelid sensory organs.

### **Anterior sensory organs and implications for behavior and distribution in Sabellariidae**

Most solitary and deep-water sabellariids have a conspicuous MO, while those gregarious members that generally occur at shallow depths lack or have an inconspicuous MO. However, there are a few exceptions. For instance, in the benthic solitary species of *Mariansabellaria*, found in the deep sea, the MO is inconspicuous (Kirtley 1994); however, MO are present in some littoral species of *Sabellaria* (present results) and *Idanthyrsus* (Hutchings et al. 2012), which can be gregarious (although the majority of species of both genera have been reported as solitary or living in small clumps, with only a few species of *Sabellaria* and a single species of *Idanthyrsus* forming reefs). The phylogenetic relationships within Sabellariidae are not yet fully assessed (Capa et al. 2012; Hutchings et al. 2012; Capa & Hutchings 2014), so a conclusion regarding primary absence or secondary loss of the MO in current sabellariids is premature at this time. However, the present results demonstrated that the absence of MO was consistent for all other gregarious species.

The MO variability found among sabellariids with different distribution and ecological traits might be related to post-settlement functions, such as reproductive strategies (i.e., the onset of gametogenesis and gametes being released into the water column). For example, in solitary species of *Lygdamis* individuals have an enlarged and complex MO (Kirtley 1994, Capa et al. 2015) that could be linked to their reproductive strategy or fertilization behavior. The reproductive biology among sabellariids has been assumed to be conservative (Eckelbarger 1983), but variability in gametogenesis within *Phragmatopoma* has been described recently (Faroni-Perez & Zara 2014).

The DH is present in late stages of all the sabellariid larvae described (Wilson 1929, 1968; Bhaud 1975; Eckelbarger 1976, 1977, Bhaud & Fernández-Álamo 2001, Capa et al. 2015), although these represent a relatively small number compared to the total number of species in the family. The present systematic review showed that the DH has been reported across the main clades (Capa et al. 2012; Hutchings et al. 2012; Capa & Hutchings 2014), and thus it might indicate a plesiomorphic condition among sabellariids. Nevertheless, the sensory function of the DH may have evolved differently within distinct clades.

Gregarious sabellariids, such as members of *Gunnarea*, *Paraidanthysus*, *Sabellaria*, *Phragmatopoma*, and *Neosabellaria*, are known to build large clumps or even large reefs in intertidal habitats, and therefore larvae seem to be able to detect conspecific individuals (Kirtley 1994; Bailey-Brock et al. 2007; Fournier et al. 2010; Firth et al. 2015; Nishi et al. 2015). The DH could have a major role in the pelagic–benthic transition.

All sabellariids have a pair of palps, but the morphology of the palps seems to vary between the deep and shallow water species. For instance, in the genera *Phalacrostemma*, *Bathysabellaria*, *Mariansabellaria*, *Tetreres*, and *Gesaia* the palps are much wider than in *Gunnarea*, *Paraidanthysus*, *Sabellaria*, *Phragmatopoma*, and *Neosabellaria*. These two groups can also be differentiated by the presence of simple and compound feeding tentacles (see descriptions in Kirtley 1994). It is known that palps are sensory organs (Eckelbarger & Chia 1976; Amieva et al. 1987), and feeding tentacles play a role in processing sediment and food supplies (Dubois et al. 2005; Riisgård & Nielsen 2006). Although the palps have not been shown to display a strong phylogenetic signal within sabellariids (Capa et al. 2012), the morphological differences reported seem very consistent within the groups, which are supported by bathymetric distribution and other ecological traits (i.e., gregarious and littoral vs. solitary and deep-water).

### **Median organ morphology and its taxonomic value**

Our literature review of the MO in sabellariids indicates that most genera and species show a consistent presence/absence and morphological similarities in this sensory organ. However, a few exceptions should be noted. Within the species *S. alveolata* and *I. australiensis* the presence of an MO is not consistent, and in the genus *Lygdamis* interspecific morphological diversity was observed. In *I. australiensis*, intraspecific phenotypic variation was discovered recently (Capa et al. 2015). This variability may not be associated with discrete populations examined over a large sampling area of 10,000 km of linear distribution from north Western Australia to New South Wales. In fact, detailed study of a large number of specimens showed that morphological features of the MO in members of *I. australiensis* are homogenous, with only a few exceptions reported by Capa et al. (2015). In contrast to the morphological results, analyses of molecular data point to a different conclusion based on limited variation in mitochondrial and nuclear markers among New South Wales specimens, but a large genetic distance between specimens collected in New South Wales and those

collected in Western Australia. Given the lack of samples from Queensland and Northern Territory, two potential scenarios explaining these results are: (i) *I. australiensis* shows a gradient of genetic variation among different populations within its wide range of distribution, which we have not been able to assess; (ii) there is a lack of gene flow between restricted populations (i.e., New South Wales and Western Australia), which could be considered to form a species complex (represented by two lineages isolated geographically). Further morphological studies with SEM analyses to compare with molecular analysis of *I. australiensis* would be helpful in clarifying conclusions with regard to species status.

Our analyses across sabellariid genera and previous studies of the genus *Lygdamis* demonstrate the potential taxonomic value of MO and MR variation (Kirtley 1994; Capa et al. 2015). Thus, comparative analyses using a broad range of species of *Idanthyrus*, *Sabellaria* and *Lygdamis* will be useful to verify the potential taxonomic value of MO in a species resolution.

### **Development of the anterior sensory organs**

Our results reveal that the larval DH found in sabellariids represents a sensory organ incipient to the MO of adults. Although several earlier investigations deal with developmental aspects in *Sabellaria alveolata* and other sabellariids, and describe their entire development in detail (e.g., Wilson 1929, 1968, 1970; Cazaux 1964; Dales 1952; Eckelbarger 1975; Smith & Chia 1984; Amieva & Reed 1987; Amieva et al. 1987; Brinkmann & Wanninger 2008), early neuroanatomy and the presence of the DH in larval stages is only mentioned by some of them (e.g., Smith & Chia 1984; Amieva & Reed 1987; Amieva et al. 1987; Brinkmann & Wanninger 2008). Our observations, when comparing staining patterns for antibodies in pre-metamorphic larvae, are congruent with previous neuroanatomical descriptions (Brinkmann & Wanninger 2008). Thus, larvae at stages with a prominent DH and distinct ciliation of this area, possessing also well-developed primordial palps, are known to crawl on any surface to search for a suitable site for metamorphosis and settlement (Wilson 1968). These results suggest that, in this gregarious species, the DH may play an important sensory role in settlement behavior and metamorphosis. This explanation seems reasonable because after metamorphosis the MO decreases in size and the immunohistochemical signal changes. In general, sessile adult stages of different *Sabellaria* species have either a small or inconspicuous MO. In addition to the

results presented here for *S. alveolata*, we know from previous studies on the larvae of *Phragmatopoma* that they have a ciliated DH and gregarious settlement behavior as well, although adults lack an external MO (Eckelbarger 1977; Capa et al. 2015). It is known that larval transport to settlement sites can be a result not only of hydrodynamic processes, but also of the larval response to dissolved chemical cues. Together with vertical migration in the water column, these influences tend to maintain the larvae near specific settlement sites (Browne & Zimmer 2001). Thus, chemoreception in sabellariid larvae mediated by the DH could also enable their retention in sites near conspecific reefs and promote settlement success, such as observed in *S. alveolata* and *Phragmatopoma caudata* (Ayata et al. 2009; Dubois et al. 2007; Faroni-Perez 2014).

In addition to the ciliated DH, our results indicate that the ciliated palps seem to represent a sensory structure with chemosensory significance. The present findings for the palps in larvae of *S. alveolata* are consistent with the observations of Forest & Lindsay (2008) in the spionid species *Dipolydora quadrilobata* JACOBI 1883, *Polydora cornuta* BOSC 1802, and *Pygospio elegans* CLAPARÈDE 1863. In all of these taxa, serotonergic somata within the palps were described; however, only *S. alveolata* and *P. cornuta* show clusters of cell bodies regularly spaced along the palp. Moreover, the serotonergic and FMRFamide staining observed in the larval palps of *S. alveolata*, as well as in spionids (Forest & Lindsay 2008), gives further hints as to a sensory function. Ultrastructural investigations exist solely for *Phragmatopoma californica*, and behavioral investigations came to the same result (Amieva & Reed 1987; Amieva et al. 1987). Thus, the ciliation observed in the palps and the DH may function to promote and detect seawater circulation and to mediate faster chemical signal delivery to the sensory structures including the sensory cilia. Notably, in the case of *S. alveolata* these proposed functions are based only on the knowledge we have for ciliated cells found in polychaete nuchal organs (Purschke 1997). Further investigations unravelling the ultrastructure and therefore possible function of these sensory structures in sabellariids are needed.

### **New insights into sensory organs and their phylogenetic signal**

The postulated importance of sensory organs in evolutionary history and radiation of sabellariids is supported by the meta-interpretation of ecological traits and the morphological peculiarities of the DH, MO, and the palps. Notably, the morphology of the MO was

regarded as being species-specific (Capa et al. 2015). If these structures have a sensory function, the DH might be involved in settlement (recognizing specific sites to settle) and the MO in reproductive processes (mediating gametogenesis or spawning). The DH, MO, and palps are cephalic appendages exposed to water flow. Notably, those genera with benthic stages that live in highly hydrodynamic waters (i.e., littoral) and form biogenic structures tend to have a DH in larvae but small or reduced MO in adults. On the other hand, those genera that exist in areas with reduced water flow (i.e., continental shelf to abyssal zone) tend to be non-gregarious and bear a conspicuous MO and thick palps. The sensory organs described herein, DH and MO, are likely autapomorphic in Sabellariidae. To date, potential homologous characters in members of other closely related families such as Spionidae (e.g., Capa et al. 2011, 2012; Weigert et al. 2014) remain unknown, and investigations focusing on comparative analyses in terms of sensory organs are lacking so far. Other annelids also show gregarious settlement induced by conspecific interactions (e.g., Scheltema et al. 1981; Toonen & Pawlik 1996). While the chemical cues in these cases are known, the specific larval organs responsible for chemoreception are unknown. The morphological variability and the function of sensory organs within sabellariids may be associated with species radiation. Further studies should therefore test the potential value of sensory organs as sources of phylogenetic information.

### **The functional sensory role of anterior sensory organs in Sabellariidae and their relationship among annelids**

The innervation and development of the DH and palps prior to metamorphosis allows us to infer that the functional sensory role of these organs are in chemical perception, especially during settlement. Several studies have reported annelid larvae showing preferences for various substrates during settlement. However, little is known about larval chemoreceptive organs involved in such chemical perception (Pawlik 1992; Toonen & Pawlik 1996). For example, early serpulid larvae do not show preferences in substrate selection, but preferences were found in the late metatrochophore stages (Marsden 1991).

The presence of an external conspicuous MO in adults of Sabellariidae is not consistent across genera. During metamorphosis the DH can undergo hypertrophy, it can be situated more or less internally, or it can even be withdrawn making it invisible. We hypothesize that in benthic sabellariids the conspicuous MO might be involved in reproduction, such as sensing environmental factors as cues for gamete

production or chemical perception for spawning strategies. Reproductive adaptations involving endogenous and exogenous factors in annelids have been extensively demonstrated (Schroeder & Hermans 1975; Bentley & Pacey & 1992), and some anterior organs (i.e., nuchal organs) have already been described as chemoreceptors involved in reproduction (Purschke 1997). The so-called caruncle present in some families of polychaetes (e.g., Amphinomidae, Chrysopetalidae, Euphrosinidae, Poecilochaetidae, Sabellidae, Spionidae, and Trochochaetidae) represents an anterior sensory organ, which can be extended along the abdominal chaetigers (Rouse & Pleijel 2001; Purschke 2005; Tovar-Hernández & Salazar-Vallejo 2008, Capa & Murray 2009). In spionids, the caruncle may be present in late larval stages (Scheltema et al. 1997; Radashevsky & Cárdenas 2004). Spionids exhibit habitat selection during settlement (Marsden 1991, Sebesvari et al. 2006), and thus the caruncle may be related to settlement behavior. Moreover, in adult specimens the size and morphology of the caruncle varies among species (Radashevsky & Hsieh 2000). The caruncle bears ciliated nuchal organs with sensory cilia traversing an olfactory chamber located beside the caruncle (Purschke 1997; Jelsing & Eibye-Jacobsen 2010). The nuchal organs, which are also directly innervated from the brain, can generate water currents and promote a rapid exchange of sensory stimuli (Purschke 2005). The present study also shows the generation of water currents by the ciliated areas in *S. alveolata* (Video S1). The DH and MO in sabellariids, like the caruncle in spionids, exhibit great morphological diversity. Interestingly, morphological features and the presence or absence of a caruncle among different amphinomid species is also markedly variable. For instance, within the genus *Notopygos* GRUBE 1855, the characters of the caruncle are useful in distinguishing species, while in *Hermodice* KINBERG 1857 the caruncle is of minor taxonomic value (Yáñez-Rivera & Salazar-Vallejo 2011; Yáñez-Rivera & Carrera-Parra 2012). Although functionally the DH and MO in sabellariids seems comparable to other annelid sensory structures, such as the caruncle and nuchal organs, further investigations are needed to verify a possible homology of these structures. Nevertheless, the characters of the DH, MR, MO, and palps in Sabellariidae can provide helpful information for analyses of phylogenetic relationships and evolutionary radiation within the family.

## Conclusions

Our extensive data review revealed that the MO in individuals of reef-forming, gregarious sabellariid genera tends to be small,



inconspicuous, or absent, while the MO in individuals of genera that are usually found in small clumps or in solitary tubes tends to be small to enlarged in size. Based on these findings, we propose a possible role of the MO related to reproduction in solitary species. However, further investigations of the MO chemoreception functionality are needed to verify such a hypothesis. The DH, present in larvae of gregarious and non-gregarious sabellariids, appears to be an important sensory organ during late larval development that is involved in settlement behavior. Based on our results, the DH represents the larval form of the MO and can be regarded as a sabellariid autapomorphy. Although similar sensory organs are known for other annelids with analogous behavior and ecological preferences, a possible homology cannot be verified and further detailed investigations are needed. Finally, the data presented herein support the importance and necessity of further investigations dealing with annelid sensory organs and ecological traits for phylogenetic approaches that focus on relationships within sabellariids as well as on the evolution of character complexes in Annelida.

**Acknowledgments.** We would like to thank Eunice Wong, Sue Lindsay, Orlemir Carrerette, Paula Martin-Lefèvre, Noémy Mollaret, and Laura Flamme for help in taking photographs. Itziar Alvarez (Mediterranean Institute for Advanced Studies - IMEDEA) gave access to MC to the microscopy laboratory at IMEDEA. Fernando Zara (at the UNESP/RC, Brazil) and Flávia Nunes (Université de Bretagne Occidentale, France) gave access to LFP to the microscopy laboratory at UNESP/RC and UBO, respectively. We thank Harald Hausen for help with the SEM, and Suman Kumar and the whole Hausen lab (S11) for help with the *Sabellaria* culture. Furthermore, we acknowledge the staff of the Laboratory for electron microscopy (University of Bergen in Norway and UNESP/RC in Brazil) for help with sample preparation. We also acknowledge Jérôme Fournier and Tarik Meziane for access to collections at the MNHN-Paris. LFP was supported by National Council for Scientific and Technological Development, Brazil (CNPq – SWE 201233/2015-0) and CH by a personal research fellowship from the DFG (HE 7224/1-1). Authors would like to thank the anonymous reviewers and editors, Dr Robert Thacker and Dr Michael Hart, for their thoughtful comments.

**Authors' contributions:** LFP, MC, and PH designed the research hypothesis. LFP led the literature review and descriptions of the sensory organs in the benthic stages. MC, PH, and IB led the morphological and

molecular analysis of *I. australiensis*. CH led the ontogenetic analysis of *S. alveolata*. LFP wrote the manuscript. All authors commented on and approved the final version of the manuscript.

## References

- Amieva MR & Reed CG 1987. Functional morphology of the larval tentacles of *Phragmatopoma californica* (Polychaeta: Sabellariidae): composite larval and adult organs of multifunctional significance. *Mar. Biol.* **95**: 243–258.
- Amieva MR, Reed CG & Pawlik JR 1987. Ultrastructure and behavior of the larva of *Phragmatopoma californica* (Polychaeta: Sabellariidae): identification of sensory organs potentially involved in substrate selection. *Mar. Biol.* **95**: 259–266.
- Ayata SD, Ellien C, Dumas F, Dubois S & Thiebaut E 2009. Modelling larval dispersal and settlement of the reef-building polychaete *Sabellaria alveolata*: Role of hydroclimatic processes on the sustainability of biogenic reefs. *Cont. Shelf Res.* **29**: 1605–1623.
- Bailey-Brock JH, Kirtley DW, Nishi E & Pohler SMH 2007. *Neosabellaria vitiensis*, n. sp. (Annelida: Polychaeta: Sabellariidae), from Shallow Water of Suva Harbor, Fiji. *Pac. Sc.* **161**: 399–406.
- Barrios LM, Chambers S, Ismail N & Mair JM 2009. Distribution of *Idanthyrsus cretus* (Polychaeta: Sabellariidae) in the Tropical Eastern Pacific and application of PCR-RAPD for population analysis. *Zoosymposia* **2**: 487–503.
- Bentley MG & Pacey AA 1992. Physiological and environmental control of reproduction in polychaetes. *Oceanogr. Mar. Biol. Ann. Rev.* **30**: 443–481.
- Bhaud MR 1975. Nouvelles observations de Sabellariidae (annélides polychètes) dans la région malgache. *Cah. O.R.S.T.O.M., Sér. Océanogr.* **13**: 69–77.
- Bhaud MR & Fernández-Álamo MA 2001. First description of the larvae of *Idanthyrsus* (Sabellariidae, Polychaeta) from the Gulf of California and Bahía de Banderas, Mexico. *Bull. Mar. Sci.* **68**: 221–232.
- Brinkmann N & Wanninger A 2008. Larval neurogenesis in *Sabellaria alveolata* reveals plasticity in polychaete neural patterning. *Evol. Devel.* **10**: 606–618.
- Browne KA & Zimmer RK 2001. Controlled field release of a waterborne chemical signal stimulates planktonic larvae to settle. *Biol Bull* (Woods Hole) **200**: 87–91.

- Burnette B, Struck TH & Halanych KM 2005. Holopelagic *Poeobius meseres* ("Poeobiidae," Annelida) is derived from benthic flabelligerid worms. *Biol. Bull.* **208**: 213–220.
- Capa M, Faroni-Perez L & Hutchings P 2015. Sabellariidae from Lizard Island, Great Barrier Reef, including a new species of *Lygdamis* and notes on external morphology of the median organ. *Zootaxa* **4019**: 184–206.
- Capa M & Hutchings P 2014. Sabellariidae. In: *Handbook of Zoology Online*. Purschke G, Westheide eds., De Gruyter.
- Capa M, Hutchings P, Aguado MT & Bott N 2011. Phylogeny of Sabellidae (Annelida) and relationships with related taxa inferred from morphology and multiple genes. *Cladistics* **27**: 449–469.
- Capa M, Hutchings P & Peart R 2012. Systematic revision of Sabellariidae (Polychaeta) and their relationships with other polychaetes using morphological and DNA sequence data. *Zool. J. Linn. Soc.* **164**: 245–284.
- Capa M & Murray A 2009. Review of the genus *Megalomma* (Sabellidae: Polychaeta) in Australia with description of three new species, new records and notes on certain features with phylogenetic implications. *Rec. Aust. Mus.* **61**: 201–224.
- Capa M, Pons J, Hutchings P 2013. Cryptic diversity, intraspecific phenetic plasticity and recent geographical translocations in *Branchiomma* (Sabellidae, Annelida). *Zoologica Scripta* **42**: 637–655.
- Caspers H 1984. Spawning periodicity and habitat of the palolo worm *Eunice viridis* (Polychaeta: Eunicidae) in the Samoan Islands. *Mar. Biol.* **79**: 229–236.
- Caullery M 1913. Sur le genre *Pallasia* Qfg. et la region prostomiale des Sabellariens. *Bull. Soc.Zool. Fr.* **38**: 198–203.
- Cazaux C 1964. Développement larvaire de *Sabellaria alveolata* (Linné). *Bull. Inst. Oceanogr. Monaco* **62**: 1–5.
- Chamberlin RV 1919. New Polychaetous annelids from Laguna Beach, California. *J. Entomol. Zool. Pomona College* **11**: 1–23.
- Chen CA, Chen CP, Fan TY, Yu JK & Hsieh HL 2002. Nucleotide sequences of ribosomal internal transcribed spacers and their utility in distinguishing closely related *Perinereis* polychaetes (Annelida: Polychaeta: Nereididae). *Mar. Biotechnol.* **4**: 17–29.
- Clement M, Posada D & Crandall K 2000. TCS: a computer program to estimate gene genealogies. *Mol. Ecol.* **9**: 1657–1660.

- Clement M, Snell Q, Walker P, Posada D & Crandall K 2002. TCS: Estimating gene genealogies. Parallel and Distributed Processing Symposium, International Proceedings, 2, 184.
- Costello MJ, Claus S, Dekeyser S, Vandepitte L, Tuama ÉÓ, Lear D, Tyler-Walters H 2015. Biological and ecological traits of marine species. *PeerJ* **3**:e1201.
- Dales RP 1952. The development and structure of the anterior region of the body in Sabellariidae, with special reference to *Phragmatopoma californica*. *Q.J. Microsc. Sci.* **93**: 435–452.
- Desroy N, Dubois SF, Fournier J, Ricquiers L, Le Mao P, Guerin L, Gerla D, Rougerie M & Legendre A 2011. The conservation status of *Sabellaria alveolata* (L.) (Polychaeta: Sabellariidae) reefs in the Bay of Mont-Saint-Michel. *Aquat Conserv.* **21**: 462–471.
- Dubois S, Barillé L, Cognie B, Beninger PG 2005. Particle capture and processing mechanisms in *Sabellaria alveolata* (Polychaeta: Sabellariidae). *Mar Ecol Prog Ser.* **301**: 159–171.
- Dubois S, Comtet T, Retière C & Thiébaud E. 2007. Distribution and retention of *Sabellaria alveolata* larvae (Polychaeta: Sabellariidae) in the Bay of Mont-Saint-Michel, France. *Mar. Ecol. Prog. Ser.* **346**: 243–254.
- Eckelbarger KJ 1975. Developmental studies of the post-settling stages of *Sabellaria vulgaris* (Polychaeta: Sabellaridae). *Mar. Biol.* **30**: 137–149.
- Eckelbarger KJ 1976. Larval development and population aspects of the reef-building polychaete *Phragmatopoma lapidosa* from the east coast of Florida. *Bull. Mar. Sci.* **26**: 117–132.
- Eckelbarger KJ 1977. Larval development of *Sabellaria floridensis* from Florida and *Phragmatopoma californica* from southern California (Polychaeta: Sabellariidae), with a key to the sabellariid larvae of Florida and a review of development in the family. *Bull. Mar. Sci.* **27**: 241–255.
- Eckelbarger KJ 1978. Metamorphosis and settlement in the Sabellariidae. In: *Settlement and metamorphosis of marine invertebrate larvae*. Chia, FS & Rice ME, eds., pp 145–164. New York: Elsevier.
- Eckelbarger KJ 1983. Evolutionary radiation in polychaete ovaries and vitellogenic mechanisms: their possible role in life history patterns. *Can. J. Zool.* **61**: 487–504.
- Eckelbarger KJ & Chia F-S 1976. Scanning electron microscopic observations of the larval development of the reef-building

- polychaete *Phragmatopoma lapidosa*. *Can. J. Zool.* **54**: 2082–2088.
- Faroni-Perez L 2014. Seasonal variation in recruitment of *Phragmatopoma caudata* (Polychaeta, Sabellariidae) in the southeast coast of Brazil: validation of a methodology for categorizing age classes. *Iheringia*, **104**: 5–13.
- Faroni-Perez L & Zara FJ 2014. Oogenesis in *Phragmatopoma* (Polychaeta: Sabellariidae): Evidence for morphological distinction among geographically remote populations. *Mem. Mus. Vic.* **71**: 53–65.
- Firth LB, Mieszkowska N, Grant LM, Bush LE, Davies AJ, Frost MT, Moschella PS, Burrows MT, Cunningham PN, Dye SR & Hawkin SJ. 2015. Historical comparisons reveal multiple drivers of decadal change of an ecosystem engineer at the range edge. *Ecol Evol.* **15**: 3210–3222.
- Folmer O, Black M, Hoeh W, Lutz R & Vrijenhoek R 1994. DNA primers for amplification of mitochondrial cytochrome c oxidase subunit I from diverse metazoan invertebrates. *Mol. Mar. Biol. Biotech.* **3**: 294–299.
- Forest DL & Lindsay SM 2008. Observations of serotonin and FMRFamide-like immunoreactivity in palp sensory structures and the anterior nervous system of spionid polychaetes. *J. Morph.* **269**: 544–551.
- Fournier J, Etienne S & Le Cam JB 2010. Inter- and intraspecific variability in the chemical composition of the mineral phase of cements from several tube-building polychaetes. *Geobios (Villeurbanne)*, **43**: 191–200.
- Hardege JD, Mueller CT, Beckmann M, Bartels-Hardege HD & Bentley MG 1998. Timing of reproduction in marine polychaetes: The role of sex pheromones. *Écoscience* **3**: 395–404.
- Haswell WA 1883. On some new Australian tubicolous annelids. *Proc. Linn. Soc. NSW.* **7**: 633–638.
- Hutchings P, Capa M & Peart R 2012. Revision of the Australian Sabellariidae (Polychaeta) and description of eight new species. *Zootaxa*, **3306**: 1–60.
- Jelsing J & Eibye-Jacobsen D 2010. Ultrastructure of the extensively developed nuchal organs of *Laonice bahusiensis* (Annelida: Canalipalpata: Spionidae). *J. Morphol.* **271**: 376–382.
- Jensen RA & Morse DE 1990. Chemically induced metamorphosis of polychaete larvae in both the laboratory and ocean environment. *J. Chem. Ecol.* **16**: 911–930.

- Johansson KE 1927. Beitrage zur Kenntnis des Polychaeten-Familien Hermellidae, Sabelliidae und Serpulidae. *Zool. Bidr.Upps.* **11**: 1–184.
- Katoh S 2013. MAFFT multiple sequence alignment software version 7: improvements in performance and usability. (outline version 7) *Mol. Biol. Evol.* **30**: 772–780.
- Kirtley DW 1994. A review and taxonomic revision of the family Sabelliariidae Johnston, 1865 (Annelida; Polychaeta). pp. 1–223. Sabecon Press Science Series.
- Lechapt JP & Kirtley DW 1996. *Bathysabellaria spinifera* (Polychaeta: Sabelliariidae), a new species from deep water off New Caledonia, southwest Pacific Ocean. *Proc. Biol. Soc. Wash.* **109**: 560–574.
- Marsden J R 1991. Responses of planktonic larvae of the serpulid polychaete *Spirobranchus polycerus* var. *augeneri* to an alga, adult tubes and conspecific larvae. *Mar. Ecol. Prog. Ser.* **71**: 245–251.
- McCarthy DA, Kramer P, Price JR & Donato CL 2008. The ecological importance of a recently discovered intertidal sabelliariid reef in St. Croix, US Virgin Islands. *Caribb. J. Sci.* **44**: 223–227.
- Mörch OAL 1863. Revisio critica Serpulidarum. Et Bidrag til Røromenes Naturhistorie. Naturhistorisk Tidsskrift, København, Series 3, **1**: 347–470.
- Nishi E, Matsuo K, Capa M, Tomioka S, Kajihara H, Kupriyanova E & Polgar G 2015. *Sabellaria jeramae*, a new species (Annelida: Polychaeta: Sabelliariidae) from the shallow waters of Malaysia, with a note on the ecological traits of reefs. *Zootaxa.* **4052**: 555–568.
- Nishi E & Núñez J 1999. A new species of shallow water Sabelliariidae (Annelida: Polychaeta) from Madeira Island, Portugal, and Canary Islands, Spain. *Arquipélago Ciências Biológicas e Marinhas* **17A**: 37–42.
- Pawlik JR 1986. Chemical induction of larval settlement and metamorphosis in the reef building tube worm *Phragmatopoma californica* (Polychaeta: Sabelliariidae). *Mar. Biol.* **91**: 59–68.
- Pawlik JR 1990. Natural and artificial induction of metamorphosis of *Phragmatopoma lapidosa californica* (Polychaeta: Sabelliariidae), with a critical look at the effects of bioactive compounds on marine invertebrate larvae. *Bull. Mar. Sci.* **46**: 512–536.

- Pawlik JR 1992. Chemical ecology of the settlement of benthic marine invertebrates. *Oceanogr. Mar. Biol. Annu. Rev.* **30**: 273–335.
- Purschke G 1997. Ultrastructure of nuchal organs in polychaetes (Annelida)—new results and review. *Acta Zool.* **78**: 123–143.
- Purschke G 2005. Sense organs in polychaetes (Annelida). In: T Bartolomaeus & G Purschke (eds) *Morphology, Molecules, Evolution and Phylogeny in Polychaeta and related Taxa. Hydrobiologia* **535/536**: 53–78.
- Purschke G, Bleidorn C & Struck H 2014. Systematics, Evolution and Phylogeny of Annelida—a morphological Perspective. *Mem. Mus. Vict.* **71**: 247–269.
- Qian PY 1999. Larval settlement of polychaetes. *Hydrobiologia* **402**: 239–253.
- Radashevsky VI & Cárdenas CA 2004. Morphology and biology of *Polydora rickettsi* (Polychaeta: Spionidae) from Chile. *New Zeal. J. Mar. Fresh.* **38**: 243–254.
- Radashevsky VI & Hsieh HL 2000. *Pseudopolydora* (Polychaeta: Spionidae) species from Taiwan. *Zool. Stud.* **39**: 218–235.
- Riisgård HU & Nielsen C 2006. Feeding mechanism of the polychaete *Sabellaria alveolata*: comment on Dubois et al. 2005. *Mar. Ecol.-Prog. Ser.* **328**: 295–305.
- Rouse GW & Pleijel F 2001. Polychaetes. pp., 1– 354. Oxford University Press, Oxford.
- Scheltema RS, Blake JA & Williams IP 1997. Planktonic larvae of Spionid and Chaetopterid polychaetes from off the West coast of the Antarctic Peninsula *Bull. Mar. Sci.* **60**: 396–404.
- Scheltema RS, Williams IP, Shaw MA & Loudon C 1981. Gregarious settlement by the larvae of *Hydroides dianthus* (Polychaeta: Serpulidae). *Mar. Ecol.-Progr. Ser.* **5**: 69–74.
- Schroeder PC & Hermans CO 1975. Annelida: Polychaeta. in *Reproduction of marine invertebrates*, Giese AC & Pearse JS eds., pp., 1– 213. Academic Press, New York.
- Sebesvari Z, Esser F & Harder T 2006. Sediment-associated cues for larval settlement of the infaunal spionid polychaetes *Polydora cornuta* and *Streblospio benedicti*. *J. Exp. Mar. Biol. Ecol.* **337**: 109–120.
- Smith PR & Chia F-S 1984. Larval development and metamorphosis of *Sabellaria cementarium* Moore, 1906 (Polychaeta: Sabellariidae). *Can. J. Zool.* **63**: 1037–1049.

- Stamatakis A, Hoover P & Rougemont J 2008. A Rapid Bootstrap Algorithm for the RAxML Web-Servers, *Syst. Biol.* **75**: 758–771.
- Talavera G & Castresana J 2007. Improvement of phylogenies after removing divergent and ambiguously aligned blocks from protein sequence alignments. *Syst. Biol.* **56**: 564–577.
- Tamura K, Stecher G, Peterson D, Filipiński A & Kumar S 2013. MEGA6: molecular evolutionary genetics analysis version 6.0. *Mol. Biol. Evol.* **30**: 2725–2729.
- Toonen RJ & Pawlik JR 1996. Settlement of the tube worm *Hydroides dianthus* (Polychaeta: Serpulidae): cues for gregarious settlement. *Mar. Biol.* **126**: 725–733.
- Tovar-Hernández MA & Salazar-Vallejo SI 2008. Caruncle in *Megalomma* Johansson, 1925 (Polychaeta: Sabellidae) and the description of a new species from the Eastern Tropical Pacific. *J. Nat. Hist.* **42**: 1951–1973.
- Weigert A, Helm C, Meyer M, Nickel B, Arendt D, Hausdorf B, Santos SR, Halanych KM, Purschke G, Bleidorn C & Struck TH 2014. Illuminating the base of the annelid tree using transcriptomics. *Mol. Biol. Evol.* **31**: 1391–1401.
- Wilson DP 1929. The larvae of British Sabellarians. *J. Mar. Biol. Assoc. UK* **16**: 221–269.
- Wilson DP 1968. The settlement behaviour of the larvae of *Sabellaria alveolata* (L.). *J. Mar. Biol. Assoc. UK.* **48**: 387–435.
- Wilson DP 1970. Additional observations on larval growth and settlement of *Sabellaria alveolata* (L.). *J. Mar. Biol. Assoc. UK* **50**: 1–31.
- Wilson DP 1977. The distribution, development and settlement of the sabellarian polychaete *Lygdamis muratus* (Allen) near Plymouth. *J. Mar. Biol. Assoc. UK* **57**: 761–792.
- Wilson WH 1991. Sexual reproductive modes in polychaetes: Classification and Diversity *Bull. Mar. Sci.* **48**: 500–516.
- Yáñez-Rivera B & Carrera-Parra FL 2012. Reestablishment of *Notopygos megalops* McIntosh, description of *N. caribea* sp. n. from the Greater Caribbean and barcoding of “amphiamerican” *Notopygos* species (Annelida, Amphinomidae). *Zookeys* **223**: 69–84.
- Yáñez-Rivera B & Salazar-Vallejo SI 2011. Revision of *Hermodice* Kinberg, 1857 (Polychaeta: Amphinomidae). *Sci. Mar.* **75**: 251–262.



**FIGURES AND TABLES:**

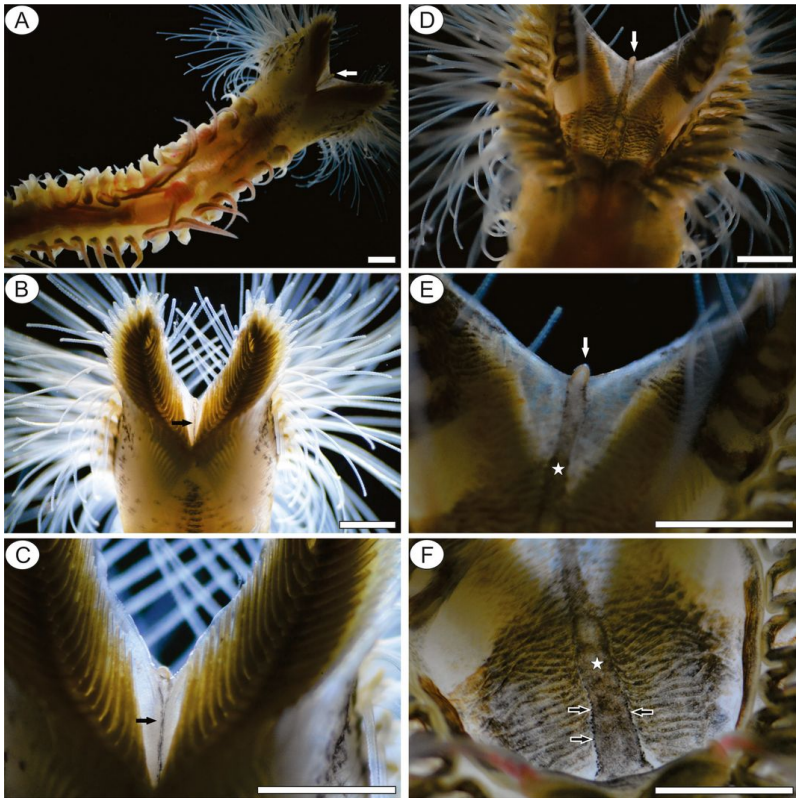


**Fig. 1.** *Sabellaria alveolata* from Mont St. Michel Bay, France. Light microscopy images from live specimen. **A.** Anterior part of the body in dorsal view indicating the median organ (MO). **B.** Opercular region in dorsal view. Black arrow indicates the junction of opercular lobes. **C.** Detail of opercular crown. Black arrow indicates the junction of opercular lobes and the distal MO. **D.** Opercular region in ventral view, white arrow indicates the MO. **E.** Detail of the MO in the junction of opercular lobes, star indicates the median ridge (MR). **F.** Detail of the MR (star), with lateral eyespots indicated (gray arrows). Scale bars: 1 mm.

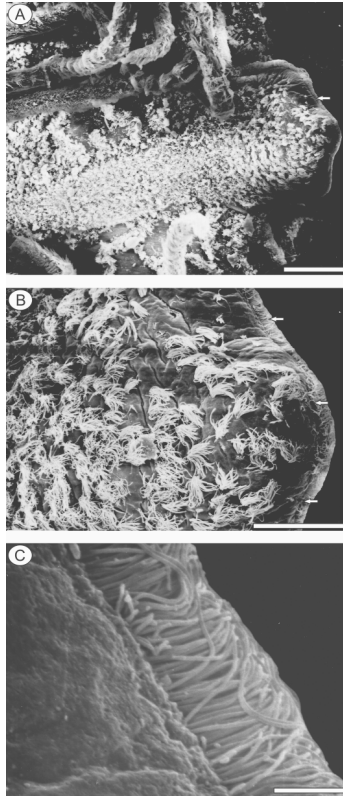


**Fig. 2.** Scanning electron microscopic image of the median organ (MO) of *Sabellaria* sp. collected in Brazil. **A.** The flat trilobed shape of MO in ventral view bearing dense ciliation. **B.** Detail of the distal tip showing the patches of cilia and the edge with cilia. **C.** Dense margin of cilia present at the distal edge. Scale bars: A, 100  $\mu\text{m}$ ; B, 50  $\mu\text{m}$ ; C, 5  $\mu\text{m}$ .

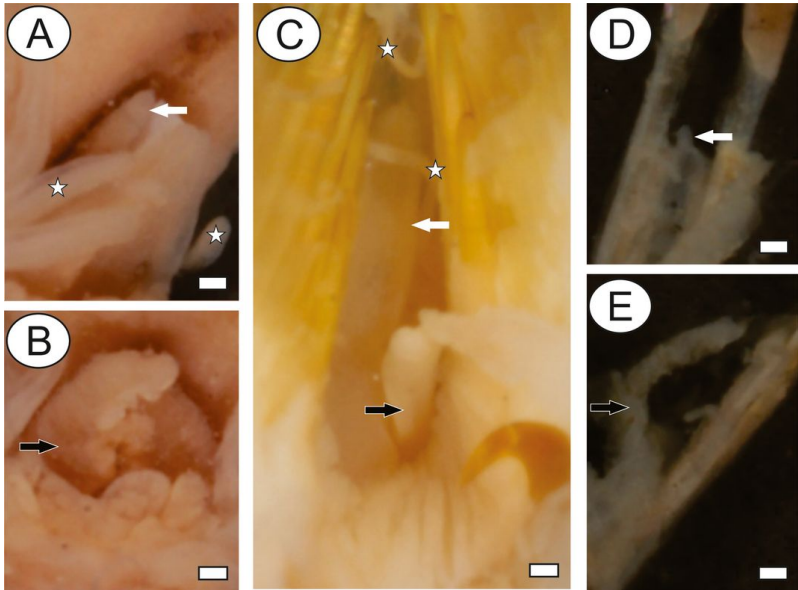


**Fig. 3.** Anterior sensory organs, median organ (MO), and palps in benthic stages of deep-sea sabellariids. **A,B.** *Bathysabellaria spinifera* (MNHN TYPE1204 IA), **C.** *Lygdamis splendidus* (MNHN TYPE1190 IA), **D,E.** *Phalacrostemma tennue* (MNHN TYPE1196 IA). White arrows point to MO, black arrows point to palps, and white stars show feeding tentacles. Scale bars: 100  $\mu$ m.

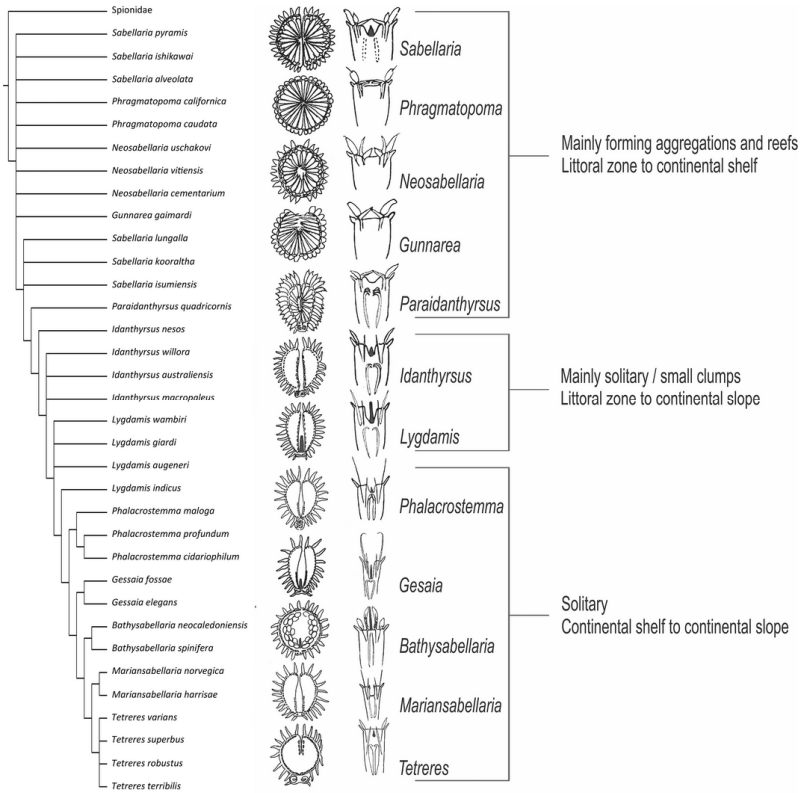


**Fig. 4.** Groups of sabellariids according to the phylogenetic hypothesis based on morphological data; drawings of top and side views of opercular structures, with their median organ shaded gray if present; and the distribution and ecological traits for each group summarized on right side. Phylogenetic hypothesis from Capa et al. 2012, and drawings modified from Kirtley 1994.

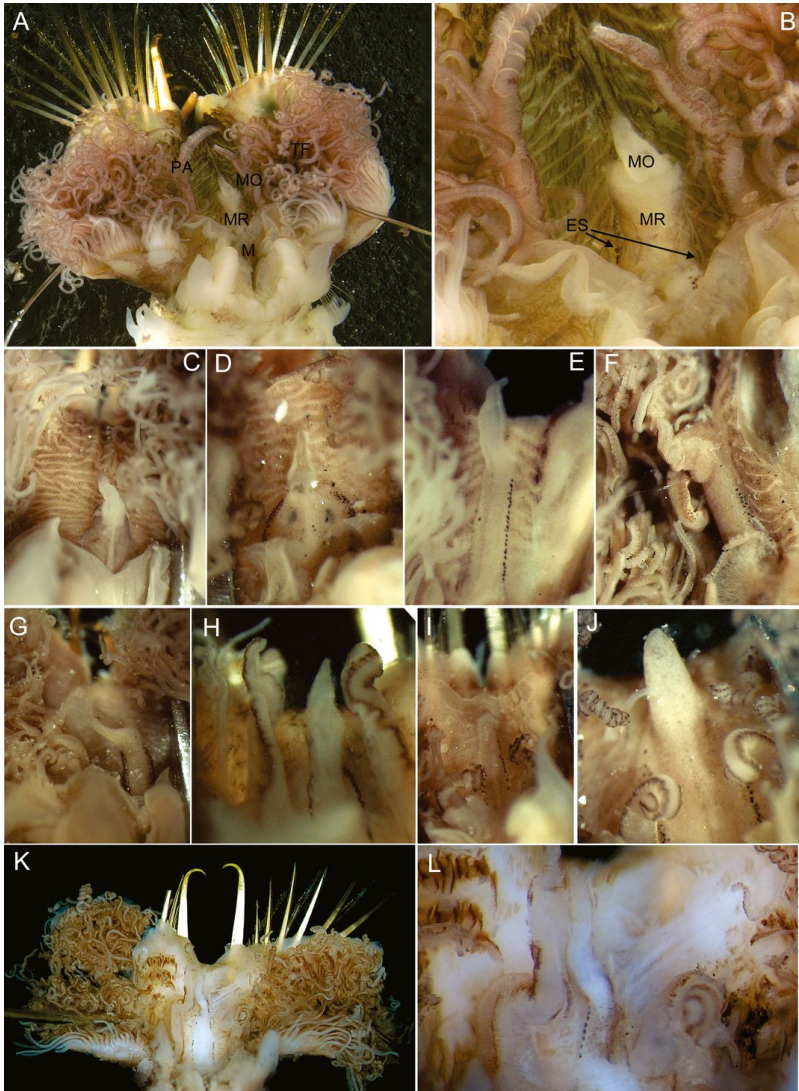
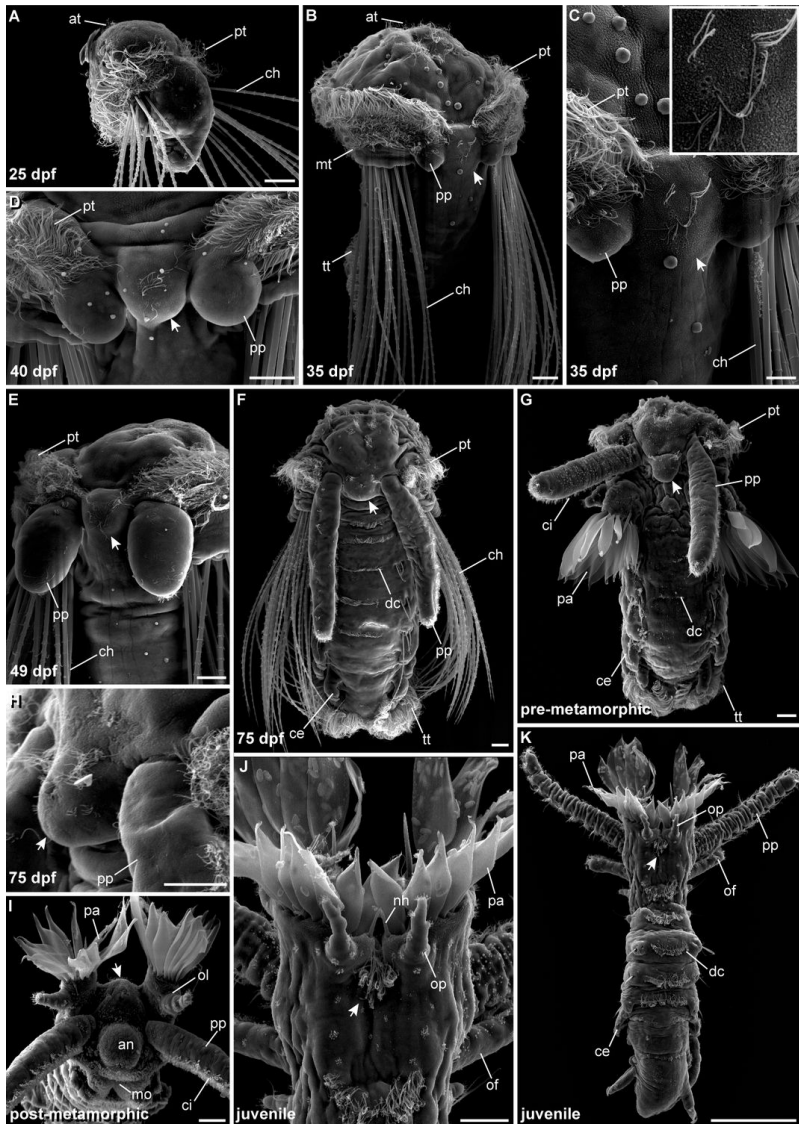


**Fig. 5.** Variation in median organ (MO) and median ridge (MR) within *Idanthysus australiensis*. **A.** Opened operculum, anterior view, showing tentacular filaments, palps, mouth, MR, and MO. **B–L.** Details of MR and MO in specimens from different localities. **A–D,** NSW; **E,F,** QLD; **G–L,** WA. **A,B,** specimen from Long Reef; **C,** AM W.26974; **D,** AM W.26971; **E,** AM W.199314; **F,** W. AM W.7087; **G,** AM W.26862; **H,** AM W.48291; **I,** AM W.26912; **J,** AM W. 36968.





**Page. Fig. 7.** The development of *Sabellaria alveolata* revealed by SEM. The position of the dorsal hump (DH) is indicated with a white arrowhead. Anterior is up, except panel I, which is an anterior view. All images are dorsal view, except panels A and H. **A.** At 25 days past fertilization (dpf) the larvae bear a prominent apical tuft (at), a prototroch (pt), and distinct bundles of chaetae (ch). No DH is

distinguishable. **B.** At 35 dpf, the larva additionally exhibits a metatroch (mt) and small buds representing the primordial palps (pp). Furthermore, the DH (arrowhead) is recognizable by a dorsal elevation and bears distinct cilia. The telotroch (tt) is visible. **C.** The DH (arrowhead) is situated in a dorsal gap of the prototroch. The inset shows the ciliation of the DH in higher magnification. **D.** Larvae at 40 dpf exhibit developing primordial palps and a well-recognizable DH (arrowhead). Note the distinct ciliation of the DH. **E.** At 49 dpf, the DH (arrowhead) is still well-recognizable and the primordial palps exhibit first signs of ciliation. **F.** Later in development (75 dpf), the larvae are barrel-shaped and possess prominent chaetigers (ce), a telotroch, and dorsal cilia (dc). The primordial palps are elongated and well ciliated. The DH (arrowhead) is represented by a dorsal elevation between the bases of the primordial palps. **G.** Shortly before metamorphosis (75–95 dpf), the larvae lack the larval chaetae. Instead, prominent posteriorly-directed paleae (pa) develop at the former position of the chaetae. All remaining characteristics are comparable with the previous stage. **H.** A higher magnification of the DH (arrowhead) of pre-metamorphic larvae reveals the presence of well-developed ciliation. **I.** Shortly after metamorphosis, an anterior view reveals the presence of the DH (arrowhead) between the opercular lobes (ol). The paleae on the opercular lobes are now directed anteriorly. The palps show towards anterior as well, with the cilia facing towards ventral. **J.** In juvenile worms the transformation of the anterior region towards adult conditions is almost finished. The animals now show an anterior crown of paleae, dorsal opercular papillae (op), and nuchal hooks (nh). The DH (arrowhead) and its distinct ciliation are visible between the opercular papillae and no longer elevated. The primordial palps are ventral. **K.** In juveniles the primordial palps are directed towards anterior, the paleae are visible, and opercular papillae and opercular filaments (of) are developed. an, anterior tip; at, apical tuft; ce, chaetiger; ch, chaetae; ci, cilia; dc, dorsal cilia; mo, mouth; mt, metatroch; nh, nuchal hooks; of, opercular filaments; ol, opercular lobes; op, opercular papillae; pa, paleae; pp, palps; pt, prototroch; tt, telotroch. Scale bars: 20  $\mu\text{m}$  (A–B, D–I), 10  $\mu\text{m}$  (C) and 100  $\mu\text{m}$  (J,K).



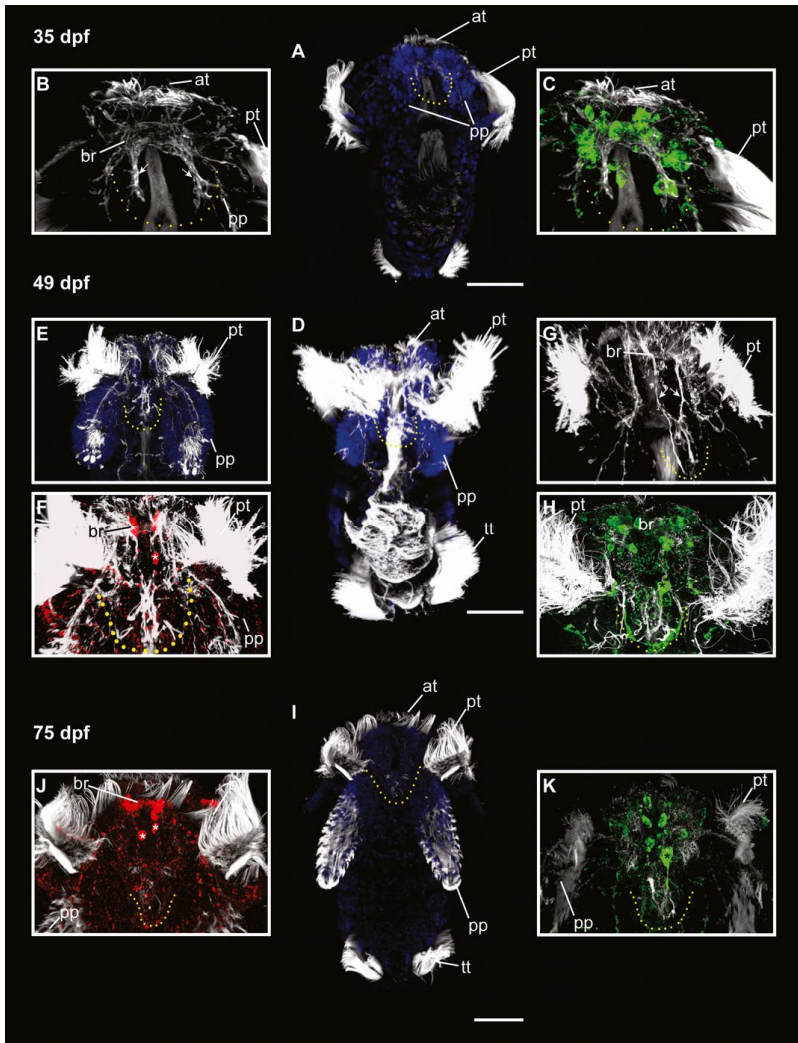


**Fig. 8.** Immunoreactivity and ciliation in late developmental stages of *Sabellaria alveolata*.  $\alpha$ -tubulin-IR (gray), serotonin (5-HT)-IR (red), FMRamide-LIR (green), and DNA staining with DAPI (blue); the position of the DH is indicated with a yellow dotted line; confocal maximum projections. Anterior is at the top of each image; all images are shown in dorsal view. **A.** Not until 35 days past fertilization (dpf) does the larva exhibit a well-developed DH, located between the developing palps (pp). The hump exhibits a distinct ciliation. The apical

tuft (at) and the prototroch (pt) are well developed in this stage. **B.** At 35 dpf, the DH represents a prominent innervation (arrowheads) shown via  $\alpha$ -tubulin staining. Two distinct neurite bundles run from the larval brain towards the distal end of the DH. **C.** FMRFamide-LIR in this stage reveals a distinct staining of the entire hump area. Unfortunately, single cells showing immunoreactivity are hardly distinguishable. **D.** At 49 dpf, the DH still represents a prominent structure located between the growing larval palps. Apical tuft, prototroch, and telotroch (tt) are present. **E.** The DH exhibits strong ciliation. **F.** 5-HT-IR is visible in distinct somata in the larval brain (br) and in close proximity to the brain (asterisk). The latter cells send processes into the hump area. **G.** Two distinct neurite bundles innervating the DH are recognizable in this stage (arrowheads). **H.** The FMRFamide-LIR increases in comparison to the previous stage. Several somata are detectable. **I.** The DH is still located between the elongated palps and increases in size at 75 dpf. It exhibits prominent ciliation. In this stage the apical tuft, the prototroch, and the telotroch are still present. **J.** 5-HT-IR exhibits distinct staining of the larval brain and marks at least two somata (white asterisks) at the base of the DH that probably innervate the hump area. **K.** FMRFamide-LIR reveals strong staining of the larval brain. Furthermore, at least one cell is stained innervating the distal part of the DH (black asterisk). at, apical tuft; br, brain; pp, palps; pt, prototroch; tt, telotroch. Scale bars=50  $\mu$ m.

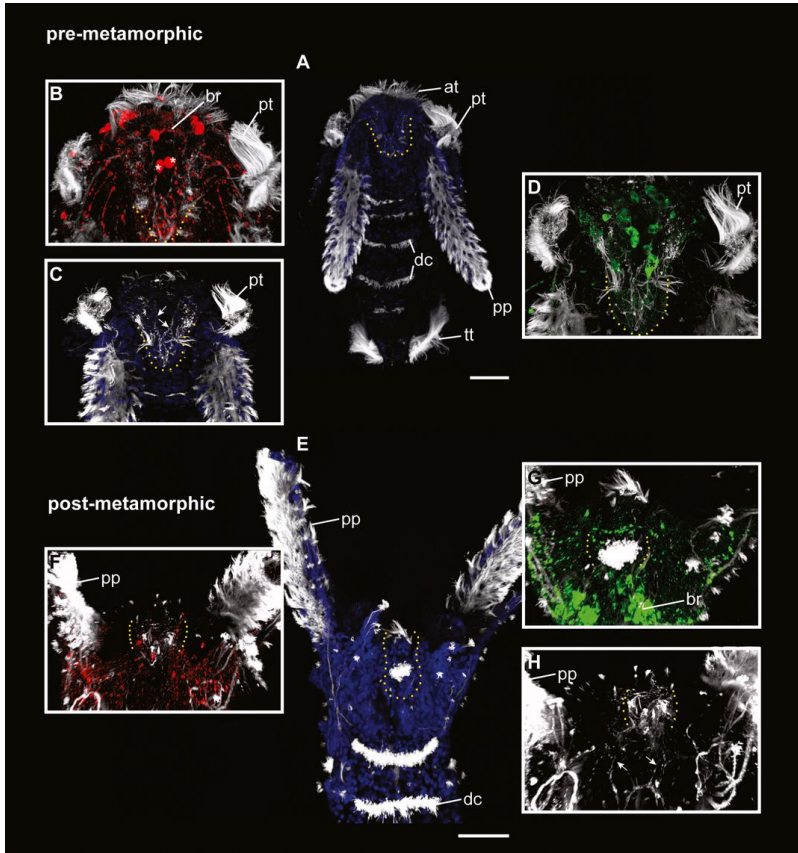


**Fig. 9.** Immunoreactivity and ciliation in pre- and post-metamorphic stages of *Sabellaria alveolata*.  $\alpha$ -tubulin-IR (gray), serotonin (5-HT) -IR (red), FMRFamide-LIR (green), and DNA staining with DAPI (blue); the position of the DH is indicated with a yellow dotted line; confocal maximum projections. Anterior is up; all images are shown in dorsal view. **A.** Prior to metamorphosis the larva has developed prominent palps (pp) and dorsal rows of cilia (dc). Apical tuft (at), prototroch (pt), and telotroch (tt) are still present. The DH is still well developed and exhibits distinct ciliation. **B.** 5-HT-IR reveals a strong staining of the brain (br) and marks two distinct somata at the base of the DH (white asterisks). **C.** Prominent ciliation and two neurite bundles running into the DH are represented via  $\alpha$ -tubulin staining. **D.** FMRFamide-LIR exhibits at least one distinct cell innervating the hump area (black asterisk). **E.** After metamorphosis, the apical tuft and the prototroch are

reduced and the palps are directed towards the anterior end. The area of the DH is diminished as well, but distinct ciliation is still present. **F.** 5-HT-IR is reduced and distinct somata are hardly recognizable. **G.** FMRF-LIR is reduced and distinct somata are hardly recognizable. **H.** The innervation with two distinct neurite bundles shown via  $\alpha$ -tubulin staining is still present within the DH area. at, apical tuft; br, brain; dc, dorsal cilia; pp, palps; pt, prototroch; tt, telotroch. Scale bars=50  $\mu$ m.

**Table 1:** Systematic revision of the dorsal hump (DH), the median organ (MO), and ecological traits across genera of Sabellariidae. MR, median ridge; –, no information available; na, not applicable; x, mentioned in literature

Groups / Genera	Total of species	Dorsal hump	Species with MO	MO, external traits	Solitary	Small clusters	Large reefs	Bathymetric range (m) of benthic stages	Substrata of benthic stages
<b>Group I</b>									
<i>Sabellaria</i>	43	present	17	small, dense ciliation; eyespots on MR	x	x	x	0–254	on rocks, shell bottom, coral, <i>Porites</i> reef, shells, on <i>Tetractita</i> , <i>Coralline</i> or hydroid zones, rubble, biofouling, on (green or red) algae, oyster beds on rocks, boulders, wood, algae (red and green), on kelp holdfast, <i>Coralline</i> or hydroid zones
<i>Phragmatopoma</i>	4	present	0	na	x	x	x	0–11 (most registers); 0–67 (1 species); 164–230 (punctual record to 1 species)	among mussels bed, brachiopod shells, mangroves, on rocks, on kelp holdfasts rocky, sandy bottom
<i>Neosabellaria</i>	7	–	0	na	x	x	x	0–87	among mussels bed, brachiopod shells, mangroves, on rocks, on kelp holdfasts rocky, sandy bottom
<i>Gunnarea</i>	1	–	0	na	x	x	x	0–47	among mussels bed, brachiopod shells, mangroves, on rocks, on kelp holdfasts rocky, sandy bottom
<i>Paraidanthysus</i>	1	–	?0	na	x	x	x	0–2	among mussels bed, brachiopod shells, mangroves, on rocks, on kelp holdfasts rocky, sandy bottom

CONT.	Total of species	Dorsal hump	Species with MO	MO, external traits	Solitary	Small clusters	Large reefs	Bathymetric range (m) of benthic stages	Substrata of benthic stages
<b>Group II</b>									
<i>Idanthysus</i>	20	present	12	small; eyespots on MR; observed in some species	x	x	x (1 species)	0-60 (most species); 14-147 (1 species); 1200-2055 (2 species)	on rocks, tide pool, muddy bottom, on corals, on bryozoan colony; with sponges, gorgonaceans or ascidians
<i>Lygdantis</i>	21	present	12	medium or long; eyespots on MO and MR observed in most species, sparse ciliation	x			2-515	coral, on algae, muddy shell gravel, sand and calcareous rubble

CONT.	Total of species	Dorsal hump	Species with MO	MO, external traits	Solitary	Small clusters	Large reefs	Bathymetric range (m) of benthic stages	Substrata of benthic stages
<b>Group III</b>									
<i>Phalacrostemma</i>	13	-	4	large;	x			203-2160	echinoids, mollusc shells
<i>Gesala</i>	8	present	2	large;	x			770-5790	-
<i>Bathysabellaria</i>	2	-	2	large; cyespots observed on MR	x			440-780	sandy bottom, foraminifera bottom
<i>Mariansabellaria</i>	4	-	?0	na	x			183-2000	sand, shells and gravel, coral dredge
<i>Tetreres</i>	12	-	2	small;	x			188-4825	fringing reef, reef flat, foraminifera bottom

**Table 2:** Collection information on the specimens used for the molecular analyses, vouchers, and GenBank accession numbers

Taxon	voucher*	cox1	cob	ITS	Country	State	Locality	Coordinates	Depth
<i>Prigmaropoma californica</i>	GB	DQ172682	NA	DQ172797	Australia	NSW	Tollgate Isl	35°44'49"S, 150°15'25"E	7.2m
<i>Prigmaropoma virginii</i>	GB	DQ172813	NA	DQ172811	Australia	NSW	Boambee Point	30°21'33"S, 153°6'25"E	intertidal
<i>Prigmaropoma murchii</i>	GB	DQ172764	NA	NA	Australia	NSW	East of Bass Island	34°28'1"S, 150°56'54"E	1.4 m
<i>Prigmaropoma caudata</i>	GB	DQ172733	NA	NA	Australia	NSW	Foster	35°16'34"S, 150°31'1"E	8.2 m
<i>Identiphyxus cratus</i>	GB	DQ172680	NA	DQ172766	Australia	NSW	Smoky Cape	30°56'58"S, 153°04'32"E	11.3 m
<i>Sebella aria alveolata</i>	GB	KR916927	NA	JN003572	UK	Essex, Harwich		51°56'46"N, 1°17'31"E	intertidal
<i>Sebella aria spinulosa</i>	W.36970	NA	NA	KX342982					
<i>Identiphyxus australiensis</i>	W.48442	KX342956	KX342971	KX342997	Australia	NSW			
<i>I. australiensis</i>	W.48441	KX342955	KX342972	KX342985	Australia	NSW			
<i>I. australiensis</i>	W.48444	KX342953	KX342969	KX342988	Australia	NSW	Boambee Point	30°21'33"S, 153°6'25"E	intertidal
<i>I. australiensis</i>	W.48443	KX342952	KX342970	KX342992	Australia	NSW	East of Bass Island	34°28'1"S, 150°56'54"E	1.4 m
<i>I. australiensis</i>	W.29041	KX342959	KX342968	KX343000	Australia	NSW	Smoky Cape	30°56'58"S, 153°04'32"E	10.3 m
<i>I. australiensis</i>	W.33227	KX342954	KX342977	NA	Australia	NSW	Smoky Cape	30°56'58"S, 153°04'32"E	10.3 m
<i>I. australiensis</i>	W.33230	KX342949	NA	KX342993	Australia	NSW	Smoky Cape	30°56'58"S, 153°04'32"E	10.3 m
<i>I. australiensis</i>	W.35233	KX342964	NA	KX342996	Australia	NSW	Smoky Cape	30°56'58"S, 153°04'32"E	10.3 m
<i>I. australiensis</i>	W.33418	KX342948	NA	KX342990	Australia	NSW	Botany Bay	33°00'60"S, 151°00'14"E	15 m
<i>I. australiensis</i>	W.35309	KX342947	KX342976	KX342986	Australia	NSW	Urnina Beach	33°32'12"S, 151°18'50"E	0 m
<i>I. australiensis</i>	W.36955	KX342963	KX342980	KX342999	Australia	NSW	Fish Rock	30°56'28"S, 153°05'58"E	25 m
<i>I. australiensis</i>	W.36957	KX342950	NA	KX342994	Australia	NSW	Back Beach	29°47'S, 153°18'E	0 m
<i>I. australiensis</i>	W.36965	KX342961	KX342973	KX342995	Australia	NSW	Katama	34°40'11"S, 150°51'38"E	12.7 m
<i>I. australiensis</i>	W.36966	KX342960	KX342973	KX342995	Australia	NSW	Vancouver, Sydney	33°50'57"S, 151°1'61"E	4 m
<i>I. australiensis</i>	W.36967	KX342951	KX342974	KX342984	Australia	NSW	Cape Banks	33°59'48"S, 151°15'14"E	22.5 m
<i>I. australiensis</i>	W.46662	NA	KX342967	KX342989	Australia	NSW	Lake Conflua	35°16'34"S, 150°31'1"E	2-5
<i>I. australiensis</i>	W.46713	KX342958	NA	KX342996	Australia	NSW	SE Green Island	35°16'34"S, 150°31'1"E	10-15
<i>I. australiensis</i>	W.47852	KX342962	KX342979	KX342991	Australia	NSW	Wallis Lake	32°11'16"S, 152°29'31"E	0.25- 0.5m
<i>I. australiensis</i>	W.47853	KX342957	KX342975	KX342987	Australia	NSW	Wallis Lake	32°11'16"S, 152°29'31"E	1.5 m
<i>I. australiensis</i>	W.36968	KX342965	KX342981	NA	Australia	WA	Ningaloo Reef	22°37'25"S, 113°38'28"E	7 m
<i>I. australiensis</i>	W.37680	KX342966	NA	NA	Australia	WA	Adelle Is, Kimberleys	15°34'53"S, 123°9'47"E	2.5 m

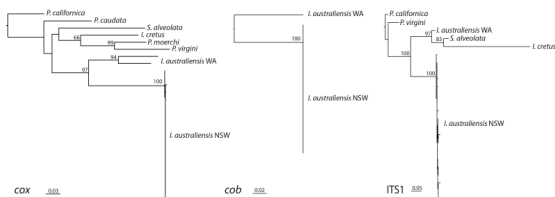
\* W numbers refer to the material lodged in the Australian Museum.



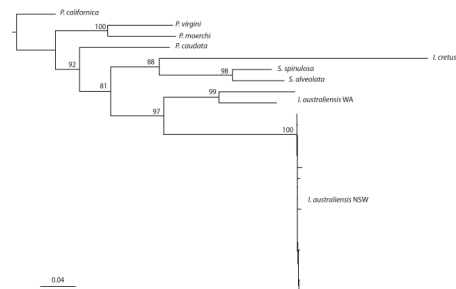
## SUPPORTING INFORMATION

*Invertebrate Biology*

## Anterior sensory organs in Sabellariidae (Annelida) Phylogeography of the reef-building polychaetes of the genus



Phylogenetic hypothesis after maximum likelihood analyses of each mitochondrial and nuclear datasets with bootstrap support of nodes.  
Scale: Average of nucleotide substitutions per site.



Phylogenetic hypothesis (RAxML) of concatenated dataset (cox1, cob, ITS1), after removing poorly aligned positions and divergent regions of the alignment with Gblocks (Castresana 2000).

### HAPLOTYPE LIST

**cox1** W.35309, W.33418, W.33230, W.36965, W.36969, W.48443, W.48444, W.33227, W.48441, W.48442, W.35309, W.47853, W.46713, W.29041  
W.36966, W.36967  
W.33233  
W.35857  
W.47852  
W.36968  
W.37680

**COB** W.66662, W.29041, W.48444, W.48443, W.48441, W.48442, W.36966, W.36969, W.47853, W.35309, W.33227, W.36967, W.47852, W.35857  
W.36968

**ITS1** W.36969, W.35309, W.33418, W.46713, W.35857, W.29041  
W.47852, W.36965  
W.47853, W.33230  
W.35309, W.48441  
W.36967  
W.46662  
W.48444  
W.48442  
W.48443  
W.36966  
W.33233

**Fig. S1.** Phylogenetic hypotheses and haplotype list

**Appendix S1.** List of named Sabellariidae species and the accessed articles.

Dr David Kirtley did the first taxonomic review of Sabellariidae and mentioned the possible importance of the median organ. Thus, his thesis was the initial point of the systematic review. All the original descriptions of species published after his thesis were accessed as well. However, in order to verify information on ecological traits of benthic stages, some original descriptions of species were also accessed. Furthermore, website search in the Sabellariidae collection at the Smithsonian National Museum of Natural History were also analyzed. Finally, literature review on larvae development descriptions was necessary to access the presence/absence of the dorsal hump.

*Bathysabellaria* LECHAPT & GRUET, 1993  
*neocaledoniensis* Lechapt & Gruet, 1993  
*spinifera* Lechapt & Kirtley, 1996

*Gesaia*  
*elegans* (Fauvel) Kirtley, 1994  
*fauchaldi* Kirtley, 1994  
*fossae* Kirtley, 1994  
*hartmanae* Kirtley, 1994  
*hessi* Kirtley, 1994  
*lanai* Kirtley, 1994  
*ryani* Kirtley, 1994  
*vityazia* Kirtley, 1994

*Gunnarea* JOHANNSSON, 1927  
*gaimardi* (Quatrefages) Kirtley, 1994

*Idanthysrus* KINBERG, 1876  
*albigenus* Ehlers, 1908  
*armatopsis* Fauchald, 1972  
*australiensis* (Haswell) Kirtley, 1994  
*bicornis* (Schmarda) Kirtley, 1994  
*bihamatus* (Caullery) Kirtley, 1994  
*boninensis* Nishi & Kirtley, 1999  
*cretus* Chamberlin, 1919  
*kornickeri* Kirtley, 1994  
*luciae* (Rochebrune) Kirtley, 1994  
*macropaleus* (Schmarda) Kirtley, 1994  
*manningi* Kirtley, 1994  
*mexicanus* Kirtley, 1994

- nesos* Hutchings, Capa & Peart, 2012  
*okinawaensis* Nishi & Kirtley, 1999  
*okudai* Kirtley, 1994  
*pennatus* (Peters) Johansson, 1927  
*saxicavus* (Baird) Kirtley, 1994  
*sexhamatus* (Grube) Kirtley, 1994  
*valentinei* Kirtley, 1994  
*willora* Hutchings, Capa & Peart, 2012
- Lygdamis* KINBERG, 1867  
*augeneri* Kirtley, 1994  
*bhaudi* Kirtley, 1994  
*curvatus* (Johansson) Kirtley, 1994  
*dayi* Kirtley, 1994  
*ehlersi* Caullery, 1913  
*giardi* McIntosh, 1885  
*gibbsi* Kirtley, 1994  
*gilchristi* (McIntosh) Kirtley, 1994  
*indicus* Kinberg, 1867  
*japonicus* Nishi & Kirtley, 1999  
*kirkegaardi* Kirtley, 1994  
*laevispinis* (Grube) Kirtley, 1994  
*malagasiensis* Kirtley, 1994  
*muratus* (Allen) Johansson, 1927  
*nasutus* Capa, Faroni-Perez & Hutchings, 2015  
*nesiotes* Chamberlin, 1919  
*rayrobertsi* Kirtley, 1994  
*robinsi* Jeldes & Lefeyre, 1959  
*splendidus* Lechapt & Kirtley 1998  
*wambiri* Hutchings, Capa & Peart, 2012  
*wirtzi* Nishi & Núñez, 1999
- Mariansabellaria* KIRTLEY, 1994  
*chilena* Kirtley, 1994  
*harrisae* Kirtley, 1994  
*norvegica* (Stromgren) Kirtley, 1994  
*tenhovei* Kirtley, 1994
- Neosabellaria* KIRTLEY, 1994  
*antipoda* (Augener), Kirtley, 1994  
*cementarium* (Moore), Kirtley, 1994  
*clandestina* (Menon & Sareen), Kirtley, 1994  
*kaiparaensis* (Augener), Kirtley, 1994  
*rupicaproides* (Augener), Kirtley, 1994

- uschakovi* Kirtley, 1994  
*vitiensis* Bailey-Brock, Kirtley, Nishi & Pohler, 2007  
*Paraidanthysrus* KIRTLEY, 1994  
   *quadricornis* (Schmarda) Kirtley, 1994  
*Phalacrostemma* MARENZELLER, 1895  
   *abyssalis* (Caullery) Kirtley, 1994  
   *cidariophilum* Marenzeller, 1895  
   *dorothyae* Kirtley, 1994  
   *gloriaae* Kirtley, 1994  
   *gwendolynae* Kirtley, 1994  
   *lechapti* Kirtley, 1994  
   *maloga* Hutchings, Capa & Peart, 2012  
   *paulineae* Kirtley, 1994  
   *perkinsi* Kirtley, 1994  
   *profundum* Lechapt & Kirtley, 1998  
   *setosa* (Treadwell) Hartman, 1966  
   *tenera* (Augener) Kirtley, 1994  
   *tenue* Lechapt & Kirtley, 1998  
*Phragmatopoma* MÖRCH, 1863  
   *attenuata* Hartman, 1944  
   *californica* (Fewkes) Hartman, 1944  
   *caudata* (Kroyer) Mörch, 1863  
   *virgini* Kinberg, 1867  
*Sabellaria* LAMARCK, 1818  
   *alcocki* Gravier, 1906  
   *alveolata* (Linnaeus) Lamarck, 1812  
   *bella* Grube, 1870  
   *bellani* Kirtley, 1994  
   *bellis* Hansen, 1882  
   *chandraae* de Silva, 1961  
   *clava* Kirtley, 1994  
   *corallinea* dos Santos Riul, Brasil & Christoffersen, 2011  
   *eupomatoides* Augener, 1918  
   *fissidens* Grube, 1870  
   *floridensis* Hartman, 1944  
   *fosterae* Kirtley, 1994  
   *fucicola* Augener, 1918  
   *gilchristi* (McIntosh) Kirtley, 1994  
   *gracilis* Hartman, 1944  
   *grueti* Kirtley, 1994  
   *guamare* dos Santos, Brasil & Christoffersen, 2014

*guinensis* Augener, 1918  
*intoshii* (Fauvel) Kirtley, 1994  
*ishikawai* Okuda, 1938  
*isumiensis* Nishi, Bailey-Brock, Santos, Tachikawa &  
 Kupriyanova, 2010  
*javanica* Augener, 1934  
*jeramae* Nishi, Matsuo, Capa, Tomioka, Kajihara,  
 Kupriyanova & Polgar, 2015  
*kooraltha* Hutchings, Capa & Peart, 2012  
*longispina* Grube, 1848  
*lotensis* Kirtley, 1994  
*lungalla* Hutchings, Capa & Peart, 2012  
*magnifica* Grube, 1848  
*marsskae* Kirtley, 1994  
*minuta* Carrasco & Bustos, 1981  
*miryaensis* Parab & Gaikwad, 1990  
*monroi* Kirtley, 1994  
*moorei* (Monro) Hartman, 1944  
*nanella* Chamberlin, 1919  
*orensanzi* Kirtley, 1994  
*pectinata* Fauvel, 1928  
*pyramis* Hutchings, Capa & Peart, 2012  
*ranjhi* (Hasan) Kirtley, 1994  
*spinulosa* Leuckart, 1849  
*taurica* (Rathke) Jakubova, 1930  
*tottoriensis* Nishi, Kato & Hayashi, 2004  
*vulgaris* Verrill, 1873  
*wilsoni* Lana & Gruet, 1989

*Tetreres* CAULLERY, 1913

*baileyae* Kirtley, 1994  
*cassidyii* Kirtley, 1994  
*jirkovi* Kirtley, 1994  
*maryriceae* Kirtley, 1994  
*perryi* Kirtley, 1994  
*philippinensis* (Treadwell) Kirtley, 1994  
*porrectus* (Ehlers) Caullery, 1913  
*robustus* Lechapt & Kirtley 1998  
*sandraae* Kirtley, 1994  
*superbus* (Caullery) Kirtley, 1994  
*terribilis* Hutchings, Capa & Peart, 2012

*varians* (Treadwell) Kirtley, 1994

## References:

- Achari GPK 1974. Polychaetes of the family Sabellariidae with special reference to their intertidal habitat. *Proc Nat Acad Sci India*, 38: 442 – 455.
- Amieva MR & Reed CG 1987. Functional morphology of the larval tentacles of *Phragmatopoma californica* (Polychaeta: Sabellariidae): composite larval and adult organs of multifunctional significance. *Mar. Biol.* **95**: 243–258.
- Amieva MR, Reed CG & Pawlik JR 1987. Ultrastructure and behavior of the larva of *Phragmatopoma californica* (Polychaeta: Sabellariidae): identification of sensory organs potentially involved in substrate selection. *Mar. Biol.* **95**: 259–266.
- Bailey-Brock, JH, Kirtley DW, Nishi E & Pohler SMH 2007. *Neosabellaria vitiensis*, n. sp. (Annelida: Polychaeta: Sabellariidae), from Shallow Water of Suva Harbor, Fiji. *Pac. Sc.* **161**: 399 – 406.
- Barrios LM, Chambers S, Ismail N & Mair JM 2009. Distribution of *Idanthyrsus cretus* (Polychaeta: Sabellariidae) in the Tropical Eastern Pacific and application of PCR-RAPD for population analysis. *Zoosymposia* **2**: 487 – 503.
- Bhaud M. 1975 Nouvelles observations de Sabellariidae (annélides polychètes) dans la région malgache. *Cah. O.R.S.T.O.M., Sér. Océanogr.* **13**: 69 – 77.
- Bhaud MR & Fernández-Álamo MA 2001. First description of the larvae of *Idanthyrsus* (Sabellariidae, Polychaeta) from the Gulf of California and Bahia de Banderas, Mexico. *Bull. Mar. Sci.* **68**: 221 – 232.
- Bremec C, Carcedo C, Piccolo MC, dos Santos E & Fiori . 2013. *Sabellaria nanella* (Sabellariidae): from solitary subtidal to intertidal reef-building worm at Monte Hermoso, Argentina (39°S, south-west Atlantic). *J. Mar. Biol. Ass. UK.* **83**: 81 – 86.
- Brinkmann N & Wanninger A 2008. Larval neurogenesis in *Sabellaria alveolata* reveals plasticity in polychaete neural patterning. *Evol. Devel.* **10**: 606 – 618.
- Capa M, Hutchings P & Peart R 2012. Systematic revision of Sabellariidae (Polychaeta) and their relationships with other polychaetes using morphological and DNA sequence data. *Zool. J. Linn. Soc.* **164**: 245 – 284.

- Capa M, Faroni-Perez L & Hutchings P. 2015. Sabellariidae from Lizard Island, Great Barrier Reef, including a new species of *Lygdamis* and notes on external morphology of the median organ. *Zootaxa* **4019**: 184 – 206.
- Dos Santos AS, Brasil AS & Christoffersen ML 2014. Sabellaria and Lygdamis (Polychaeta: Sabellariidae) from reefs off northeastern Brazil including a new species of Sabellaria. *Zootaxa*, **3881**, 125 – 144.
- Eckelbarger KJ & Chia F-S 1976. Scanning electron microscopic observations of the larval development of the reef-building polychaete *Phragmatopoma lapidosa*. *Can. J. Zool.* **54**: 2082 – 088
- Eckelbarger KJ 1975. Developmental studies of the post-settling stages of *Sabellaria vulgaris* (Polychaeta: Sabellaridae). *Mar. Biol.* **30**: 137 – 149.
- Eckelbarger KJ 1976. Larval development and population aspects of the reef-building polychaete *Phragmatopoma lapidosa* from the east coast of Florida. *Bull. Mar. Sci.* **26**: 117 – 132.
- Eckelbarger KJ 1977. Larval development of *Sabellaria floridensis* from Florida and *Phragmatopoma californica* from southern California (Polychaeta: Sabellariidae), with a key to the sabellariid larvae of Florida and a review of development in the family. *Bull. Mar. Sci.* **27**: 241 – 255.
- Eckelbarger KJ 1978. Metamorphosis and settlement in the Sabellariidae. In: Chia, FS & Rice ME eds. Settlement and metamorphosis of marine invertebrate larvae. New York: Elsevier, 145 – 164.
- Hartman O 1944. Polychaetous annelids. Part VI. Paraonidae, Magelonidae, Longosomidae, Ctenodrilidae, and Sabellariidae. Allan Hancock Pacific Expeditions, **10**: 311 – 389.
- Hutchings P, Capa M & Peart R 2012. Revision of the Australian Sabellariidae (Polychaeta) and description of eight new species. *Zootaxa*, **3306**: 1 – 60.
- Kirtley DW 1994. A review and taxonomic revision of the family Sabellariidae Johnston, 1865 (Annelida; Polychaeta). Sabecon Press Science Series, 1: 1 – 223.
- Lechapt JP & Gruet Y 1993. *Bathysabellaria neocaledoniensis*, a new genus and species of Sabellariidae (Annelida, Polychaeta) from the bathyal zones off New Caledonia (Southwest Pacific Ocean). *Zool Scripta*, **22**: 243 – 247.

- Lechapt JP & Kirtley DW 1996. *Bathysabellaria spinifera* (Polychaeta: Sabellariidae), a new species from deep water off New Caledonia, southwest Pacific Ocean. *Proc. Biol. Soc. Wash.* **109**: 560 – 574.
- Lechapt JP. & Kirtley DW 1998. New species of bathyal and abyssal Sabellariidae (Annelida: Polychaeta) from near New Caledonia (southwest Pacific Ocean). *Proc. Biol. Soc. Wash.*, **111**: 807 – 822.
- Mauro NA 1975. The premetamorphic developmental rate of *Phragmatopoma lapidosa* Kinberg, 1867, compared with that in temperate sabellariids. *Bull. Mar. Sci.* **25**: 387 – 392.
- Nishi E & Kirtley DW 1999. Three new species of Sabellariidae (Polychaeta) from Japan. *Nat Hist Res.* **5**: 93 – 105.
- Nishi E & Núñez J 1999. A new species of shallow water Sabellariidae (Annelida: Polychaeta) from Madeira Island, Portugal, and Canary Islands, Spain. *Arquipélago Ciências Biológicas e Marinhas* **17A**: 37 – 42.
- Nishi E, Kato T & Hayashi I 2004. *Sabellaria tottoriensis* n. sp. (Annelida: Polychaeta: Sabellariidae) from shallow water off Tottori, the Sea of Japan. *Zool Sci (Tokyo)*, **21**: 211 – 217.
- Nishi E, Bailey-Brock JH, Souza dos Santos A, Tachikawa H & Kupriyanova E 2010. *Sabellaria isumiensis* n. sp. (Annelida: Polychaeta: Sabellariidae) from shallow waters off Onjuku, Boso Peninsula, Japan, and re-descriptions of three Indo-West Pacific sabellariid species. *Zootaxa*, **2680**: 1 – 25.
- Nishi E, Matsuo K, Capa M, Tomioka S, Kajihara H, Kupriyanova E & Polgar G 2015. *Sabellaria jeramae*, a new species (Annelida: Polychaeta: Sabellariidae) from the shallow waters of Malaysia, with a note on the ecological traits of reefs. *Zootaxa*. **4052**: 555 – 568.
- Santos AS, Riul P, Brasil A & Christoffersen M 2010. Encrusting Sabellariidae (Annelida: Polychaeta) in rhodolith beds, with description of a new species of *Sabellaria* from Brazilian coast. *J. Mar. Biol. Assoc. U.K.* **91**: 425 – 438.
- Schmarda LK. 1861. Neue wirbellose Thiere beobachtet und gesammelt auf einer Reise un die Erdr 1853 bis 1857. Leipzig: Erster Band (zweite halfte) Turbellarian, Rotatorien un Anneliden. Wilhelm Engelmann.
- Smith PR & Chia F-S 1984. Larval development and metamorphosis of *Sabellaria cementarium* Moore, 1906 (Polychaeta: Sabellaridae). *Can. J. Zool.* **63**: 1037 – 1049.



- Wilson DP 1929. The larvae of British Sabellarians. *J. Mar. Biol. Assoc. UK* **16**: 221 – 269.
- Wilson DP 1977. The distribution, development and settlement of the sabellarian polychaete *Lygdamis muratus* (Allen) near Plymouth. *J Mar. Biol. Assoc. UK* **57**: 761 – 792.

**Video S1.** Anterior sensory organ of *Sabellaria alveolata*.

Available online at:

<http://onlinelibrary.wiley.com/store/10.1111/ivb.12153/asset/supinfo/ivb12153-sup-0003-VideoS1.mov?v=1&s=6f14eebc1498c1b989d15691fe1669f901dc9b41>

**PHYLOGEOGRAPHY OF THE REEF-BUILDING  
POLYCHAETES OF THE GENUS *PHRAGMATOPOMA* IN THE  
WESTERN ATLANTIC REGION**

**Running head:** Phylogeography of Western Atlantic *Phragmatopoma*  
*spp.*

Flavia LD Nunes, Alain Van Wormhoudt, Larisse Faroni-Perez, Jérôme  
Fournier

*Published in*  
Journal of Biogeography

This chapter is under an agreement between Larisse Faroni-Perez and John Wiley and Sons, which consists in the *License Number 4216450812511* provided by John Wiley and Sons and Copyright Clearance Center.

How to cite:

Nunes, F. L. D., Van Wormhoudt, A., Faroni-Perez, L. and Fournier, J. (2017), Phylogeography of the reef-building polychaetes of the genus *Phragmatopoma* in the western Atlantic Region. *J. Biogeogr.*, 44: 1612–1625. doi:10.1111/jbi.12938



## Abstract

**Aim:** To verify the synonymy of the reef-building polychaete *Phragmatopoma caudata* (described for the Caribbean) and *Phragmatopoma lapidosa* (described for Brazil) using molecular data. To evaluate patterns of genetic diversity and connectivity among populations from Florida to South Brazil.

**Location:** Intertidal zone in the Western Atlantic biogeographical Region: Brazil, eastern Caribbean and Florida (USA).

**Methods:** DNA sequence data from one mitochondrial (*cox-1*) and one nuclear ribosomal (*ITS-1*) loci were obtained from 11 populations of *P. caudata* spanning the coasts of Brazil, eastern Caribbean and Florida. Phylogenetic relationships among populations of *P. caudata* and other members of the genus were inferred by Bayesian methods. Population differentiation was evaluated by Bayesian analysis of population structure (BAPS), AMOVA and pairwise  $\phi_{st}$ . Demographic history was inferred by Bayesian skyline plots.

**Results:** Phylogenetic inference supported the interpretation of a single species of *Phragmatopoma* spanning the Brazilian and Caribbean Provinces of the Western Atlantic Region. Little population structure was observed across the species distribution, with the exception of the Florida population. The BAPS analysis supported a 2-population model, with population differentiation being strong and significant between Florida and all other Atlantic populations for *cox-1*, and significant between Florida and most populations for *ITS-1*. Differences in genetic diversity were not significant between Caribbean and Brazilian populations, although several populations in Brazil had low values for diversity indices. Bayesian skyline plots indicate population expansion starting at approximately 200 ka.

**Main conclusions:** *Phragmatopoma caudata* is able to maintain genetic connectivity across most of its geographical range, with population differentiation being observed only between Florida and all other localities, possibly due to ecological speciation in the transition zone between tropical and subtropical environments. Long-distance connectivity across much of the species range is likely the result of long-lived larvae that are tolerant to a wide range of environmental conditions.

## Keywords

Brazilian Province, biogeographical barrier, Caribbean Province, connectivity, larval dispersal, *Phragmatopoma caudata*, phylogenetics, phylogeography, polychaete reef, Western Atlantic Region



## Introduction

Many benthic marine invertebrates have patchy distributions as a result of the interaction among abiotic and biotic variables that limit dispersal, settlement and survival. Discontinuous distributions can affect population connectivity even in species with a long planktonic larval stage, having consequences for gene flow, genetic diversity and speciation. Thus, benthic marine invertebrates provide interesting models for addressing questions related to how species distributions reflect the interplay among dispersal dynamics, environmental conditions, biotic interactions or historical isolation (Awise, 1992; Palumbi, 1994). The tropical Atlantic fauna are affected by five major biogeographical barriers: the Mid-Atlantic Barrier, the Terminal Tethyan Event, the Amazon-Orinoco Barrier, the Isthmus of Panama and the Benguela Barrier (Floeter *et al.*, 2008). But while these barriers are effective for numerous species, exceptions exist for each one, providing opportunities for understanding the variables that contribute to species distributions, their delimitations and connectivity among their populations.

Some marine polychaetes from the family Sabellariidae Johnston, 1865 are gregarious and are important reef-building organisms in coastal environments (Goldberg, 2013). These ecosystem engineers create complex habitats supporting high levels of biodiversity and provide ecosystem services such as coastal protection (Dubois *et al.*, 2002; Noernberg *et al.*, 2010; Ataide *et al.*, 2014). While most sabellariids are solitary, the species that are reef-building typically construct biogenic structures in intertidal or shallow subtidal environments (Faroni-Perez *et al.* 2016). Reefs of *Phragmatopoma caudata* Krøyer in Mörch, 1863 are broadly distributed along the intertidal zone in the western Atlantic coastline, from Florida (USA) (34°N) to Santa Catarina (Brazil) (27°S), including many localities in the Caribbean (Kirtley, 1994). Although *P. caudata* reefs are known to exist at various locations along the Brazilian coast (Pagliosa *et al.*, 2014), records in new localities continue to be reported. For instance, new reefs formed in Fortaleza (north Brazil) following the construction of a harbour (Fournier & Panizza *pers. obs.*). Currently the northernmost known occurrence of the species in Brazil is in the state of Piauí (Santos *et al.*, 2012). Beyond the Amazon and Orinoco Rivers, the species has also been recorded in Venezuela (Liñero-Arana, 2013). Discontinuities in the range cannot at present be stated with certainty, as field observations in this geographical region are far from exhaustive, and areas with confirmed absences have yet to be described. The abundance and distribution of sabellariid reefs depend

on the availability of a hard substrate, suspended sediments, and appropriate levels of turbulence (Main & Nelson, 1988). *Phragmatopoma caudata* (as *P. lapidosa* Kinberg, 1866) reproduces by external fertilization of gametes that are produced year-round (Eckelbarger, 1976). Spawning and recruitment are highest in the summer months, from June to August in Florida, USA (McCarthy *et al.*, 2003) and February to April in São Paulo State, Brazil (Faroni-Perez, 2014). Fecundity is high, as the average female can spawn 1500-2000 oocytes (McCarthy *et al.*, 2003). During development, planktonic larvae drift in the water column from two to four weeks (Mauro, 1975; Eckelbarger, 1976). Larvae tolerate a wide temperature range (15.5°C-29.5°C), but beyond these extremes, development and survival are compromised (Eckelbarger, 1976). While tolerance to salinity has not yet been quantified for larvae, adults can tolerate brackish waters of up to 30-40% seawater (Mauro, 1977). When metatrochophore larvae are competent for metamorphosis, they settle onto hard substrate, usually a conspecific pre-existing reef, induced by chemical cues (Pawlik, 1988) and mediated by the larval sensory organs, such as the dorsal hump and palps (Faroni-Perez *et al.*, 2016). Finally, *P. caudata* has an estimated lifespan of one to two years (McCarthy *et al.*, 2003).

Systematics of the genus have been recently revised (Drake *et al.*, 2007; Capa *et al.*, 2012). Notwithstanding, the brief original descriptions for *P. caudata* and *P. lapidosa* and the disappearance of the type material led to uncertain taxonomic status. Hartman (1944) questioned whether the two species were distinct, and upon revision of Sabelliidae, Kirtley (1994) synonymized *P. lapidosa* with *P. caudata*. More recently, molecular phylogenetics supported a single Caribbean species, with distinct populations in Florida and West Indies (Drake *et al.*, 2007). However, patterns of oogenesis in individuals from Florida differed from those in Brazil, reopening the debate on plasticity or speciation (Faroni-Perez & Zara, 2014). Moreover, intraspecific variability in the composition of the cement used for reef construction was found along the Brazilian coast, suggesting potential differences among populations (Fournier *et al.*, 2010). Currently, no molecular study has taken Brazilian populations into consideration, and the question remains whether a single species is distributed from Florida to South Brazil.

The aims of this study are i) to examine if a single *Phragmatopoma* species occurs in the Western Atlantic Region, ii) to assess the genetic connectivity among populations of *P. caudata* in the



Caribbean and Brazilian biogeographical provinces and iii) to assess the effectiveness of putative biogeographical barriers on the connectivity of *P. caudata*.

## Materials and Methods

### *Study sites and sampling method*

*Phragmatopoma caudata* was collected from seven sites spanning its distribution along the coast of Brazil: Fortaleza (FOR), Tamandaré (TAM), Peracanga (PER), Ubatuba (UBA), Ilha Porchat (POR), Itanhaém (ITA) and Ilha do Mel (MEL). In addition, four sites in the Caribbean were analysed: three previously sampled sites in Florida, USA (FLO), Puerto Rico (PRI) and Virgin Islands (VIL), and one new site in Guadeloupe Island (GUA) (Figure 1, Appendix S1). Specimens were collected at low tide by breaking off small blocks of reef and removing 1-3 worms from each block. At each locality, several reef blocks were collected, separated by tens of meters, to ensure good representation of genetic diversity at each site. Individual specimens were fixed in 70% ethanol and stored at -20°C.

### *DNA extraction and sequencing*

DNA was extracted using the CTAB method (Denis *et al.*, 2009). Two loci were used in order to make comparisons with previously studied Caribbean populations (Drake *et al.*, 2007): the mitochondrial cytochrome oxidase subunit I (*cox-1*) and the first internal transcribed spacer region (*ITS-1*) of the ribosomal DNA. New primers were designed for *cox-1*: PHRALCO: 5' - TTTATATTTTGGAAATTTGGTCAGG -3'; PHRAHCO: 5' - TAAAGAACTGGGTCTCCACC-3'. Published primers were used for *ITS-1* (ITS1-fw: 5'-CACACCGCCCGTCGCTACTA-3', ITS3r: 5'-TTCGACSCACGAGCCRAGTGATC-3') (Denis *et al.*, 2009). Amplification was performed with the Ready-to-Go PCR kit (GE Healthcare, Little Chalfont, UK) using 0.1µg of DNA. Thermal cycler conditions included an initial denaturation step at 96°C for 2 min, 40 cycles at 96°C for 30s, 52°C for 30s and 72°C for 1 min, with a final extension at 72°C for 5 min. After electrophoresis, PCR products were extracted from the agarose gel and purified using the Wizard SV Gel System (Promega, Fitchburgh, WI, USA). Cloning was carried out for a subset of the *ITS-1* amplifications (23 individuals), to confirm the phase of heterozygous alleles. PCR products were ligated into the pGEMT Easy vector (Promega, Fitchburgh, WI, USA) and transformed into JM

109 competent cells (Promega, Fitchburgh, WI, USA). Five colonies were sequenced for each individual. Sequencing reactions used the BigDye v.3.1 chemistry (Applied Biosystems, Waltham, MA, USA) and was analysed on an ABI 3130 automated sequencer.

#### *Molecular data analysis*

DNA sequence chromatograms were inspected for errors and edited with SEQUENCHER 4.5 (Gene Codes Corp, Ann Arbor, MI, USA). Published sequences of *Phragmatopoma caudata* [Genbank accession numbers: DQ172733- DQ172763, DQ172801-DQ172810], *Phragmatopoma californica* (Fewkes, 1899) [DQ172682-DQ172732, DQ172768-DQ172800], *Phragmatopoma moerchi* Kinberg, 1866 [DQ172764] and *Phragmatopoma virgini* Kinberg, 1866 [DQ172813-DQ172822, DQ172811-DQ172812] were added to the dataset, and sequences of *Idanthyrus cretus* Chamberlain 1919 [DQ172680-DQ172681, DQ172765-DQ172767] were used for the outgroup (Drake *et al.*, 2007). Sequence alignment was performed using CLUSTALX in MEGA 6.0.6 using default parameters (Tamura *et al.*, 2013). For *ITS-1* sequences containing double peaks in both sequencing directions, cloned sequences and the sequences of homozygous individuals were used for haplotype reconstruction using PHASE implemented in DNASP 5 (Librado & Rozas, 2009). For phylogenetic analysis, all redundant sequences were removed, such that phylogenetic inference was made with unique sequences. A gene tree was constructed for each locus in BEAST 1.8.2 and species tree ancestral reconstruction was estimated combining both *cox-1* and *ITS-1* with the \*BEAST algorithm (Heled & Drummond, 2010). The best-fit model of nucleotide substitution was determined by hierarchical likelihood ratio test in MRMODELTEST 2.2 (<https://github.com/nylander/MrModeltest2>). The GTR+ $\gamma$ +I substitution model was used for *cox-1* and the HKY+ $\gamma$  model was used for *ITS-1*. A strict molecular clock was employed with a fixed substitution rate of 2.1% per Myr for *cox-1* and 0.25% per Myr for *ITS-1*. In the species tree, clock rates were estimated relative to *cox-1*. Substitution rates vary across species and genes, and depend on the accurate timing of vicariant events or fossil occurrences, which can incur considerable uncertainties. However, averaging the rates obtained for the same gene over several closely related taxa can improve the confidence of molecular clock estimates. The substitution rate selected for *cox-1* corresponds to the average rate across 27 transisthmian crustacean species pairs (Lessios, 2008). In addition, a rate of 2.1% per

Myr (based on crustaceans) has also been employed in previous work on *Phragmatopoma* spp. (Drake *et al.*, 2007). Fewer estimates of substitution rates are available for the invertebrate *ITS-1* locus. The rate of 0.25% per Myr used for *Phragmatopoma* was estimated for a marine gastropod (Coleman & Vacquier, 2002).

For phylogenetic analysis, the Markov chain Monte Carlo (MCMC) ran for 30 million generations with sampling at every 1000 steps. The results of three independent runs were verified for convergence using TRACER 1.5 and combined after discarding a burn-in of 20% using LOGCOMBINER 1.8.2. Target trees used the maximum clade credibility criterion in TREEANNOTATOR 1.8.2. Nodes with a posterior probability inferior to 0.90 were collapsed. Estimates of genetic distance between species pairs were calculated using the Kimura 2-parameter model in MEGA 6. For *cox-1*, positions containing missing data were eliminated, while for *ITS-1* positions containing gaps between sequence pairs were removed. Divergence time estimates based on genetic distances used the same substitution rates listed above.

Relationships among haplotypes (including redundant sequences) were inferred with a haplotype network based on maximum parsimony, constructed with TCS 1.21 (Clement *et al.*, 2000). Haplotype frequencies, the number of unique haplotypes (H), segregating sites (s), haplotype diversity (h) and nucleotide diversity ( $\pi$ ) were calculated for each sampling site using ARLEQUIN 3.1 (Excoffier *et al.*, 2005). Deviations from neutrality were assessed with Tajima's D and Fu's  $F_s$  statistics in ARLEQUIN. Population demographic history was inferred by Bayesian skyline plots implemented in BEAST (Drummond *et al.*, 2005). The population size function of the Bayesian skyline plots were fitted using a piecewise constant function, with 10 groups. In order to obtain an effective sampling size of at least 200, the MCMC chain ran for 50 million generations and was sampled every 100 for *cox-1*, and for *ITS-1*, the MCMC ran for 40 million generations sampled every 1000.

Population structure was explored for both loci using Bayesian analysis of population genetic structure (BAPS; Corander *et al.*, 2008), a clustering algorithm which uses a Bayesian predictive model to estimate the number of genetically diverged groups based on molecular data. A population mixture analysis was run using the "clustering with linked loci" option. Single-locus sequence data are expected to be genetically linked because of their close proximity along the chromosome. This option therefore takes into consideration the non-independence of linked loci. The clustering of groups with the lowest log likelihood was selected.

Population differentiation was assessed by analysis of molecular variance (AMOVA) and pairwise  $\phi_{st}$  in ARLEQUIN (Excoffier *et al.*, 2005). The significance level of pairwise tests was adjusted by a Bonferroni correction. For the three-level hierarchical AMOVAs, the results of the BAPS analysis were used to select biogeographical divisions.

## Results

### *Properties of the DNA sequences*

After sequence quality screening and trimming, a total of 146 sequences of 497 bp length were obtained for *cox-1* and 99 sequences of 403 bp length were obtained for *ITS-1* for *P. caudata*. Sequences were deposited in Genbank (accession numbers: KT182639 - KT182784 for *cox-1* and KT182785 - KT182883 for *ITS-1*). For the *cox-1* locus, population genetic analyses were calculated (1) considering all three codon positions, and (2) with the third codon position excluded. Because of high polymorphism in the third codon position, 74% of sequences were unique, leading to a haplotype network characterized by numerous loops, indicating homoplasy. Moreover, the AMOVA and population differentiation results were similar whether the third codon position was kept or excluded from the analysis. Therefore, results shown for haplotype network, allele frequencies, genetic diversity, AMOVA, pairwise  $\phi_{st}$  and BAPS consider only the first and second codon positions, while all three codon positions were kept for phylogenetic analysis and Bayesian skyline plots.

Previous work has shown that multiple alleles (>2) can be observed for *ITS-1* (Drake *et al.*, 2007). Among all sequences, multiple peaks were found in 23 nucleotide sites. More than one allele was observed for nearly all individuals (identified either by cloning or by haplotype reconstruction), but only eight individuals had more than two sites with multiple peaks. Because the present study combined published data (from Drake *et al.*, 2007) with new data, only one allele per individual was kept in the analysis as was done previously. A random number generator was used to select the haplotype kept in the analysis, to ensure that allele selection did not bias the dataset towards lower diversity by selecting the most common allele, with the caveat that this approach does not discriminate paralogous from orthologous alleles. Few mutational differences were observed among intra-individual alleles (maximally nine mutations); therefore inadvertent selection of paralogous alleles likely had only a small effect on estimates of genetic diversity or differentiation.

### *Phylogenetic analysis*

All three species of *Phragmatopoma* (*P. caudata*, *P. californica* and *P. virgini*) were monophyletic for *cox-1*, *ITS-1* and the species tree combining both loci (Figure 2). However, all phylogenetic reconstructions found the relationship between the three species to be unresolved. Low support was found for *P. caudata* being sister taxon to *P. californica* in the species trees (pp = 0.40; Figure 2a), for *P. californica* being sister to *P. virgini* in the *ITS-1* tree (pp=0.21; node collapsed; Figure 2b), and for *P. caudata* being sister to *P. virgini* in the *cox-1* tree (pp=0.86; node collapsed; Figure 2c). Sequences of individuals of *P. caudata* from Brazil belonged to the same clade as those from the Caribbean (Figure 2b,c) and identical sequences were observed among some individuals from Brazil and the Caribbean. However, *P. caudata* from Florida formed a reciprocally monophyletic clade with *P. caudata* from the rest of the Caribbean+Brazil, having high support in the analyses using *cox-1* and the combined loci (pp=1.00 for both trees; Figure 2a,c).

Pairwise genetic distances and divergence time estimates are shown in Table 1. Based on *cox-1*, *P. caudata* diverged from *P. californica* at  $8.6 \pm 1.0$  Ma and from *P. virgini* at  $9.5 \pm 1.0$  Ma. Divergence times estimated with *ITS-1* indicate an older split between *P. caudata* and *P. californica*, at  $28.2 \pm 5.4$  Ma, and of  $33.1 \pm 5.9$  Ma between *P. caudata* and *P. virgini*. *P. caudata* from Florida diverged from the remaining *P. caudata* populations at approximately  $1.5 \pm 0.3$  Ma (*cox-1*) to  $3.2 \pm 1.2$  Ma (*ITS-1*).

### *Haplotype networks and haplotype frequencies*

Haplotype frequencies for *cox-1* and *ITS-1* are shown in Figures 1b-c, and maximum parsimony haplotype networks are shown in Figure 3. Among the 17 haplotypes sequenced for *cox-1*, two were abundant among the sampled populations (C5 and C1), three were present in more than one population at low frequencies (C6, C8 and C11), with the remainder being observed in only one individual (singletons) and being restricted to one population (private haplotypes) (Figure 3a). Haplotype C5 was abundant in most populations, ranging in frequency from 69 – 100%, except in Florida, where it was absent. Haplotype C1 was abundant only in Florida (75%) and was found in three other Brazilian populations at low frequencies (Figure 1a). Overall, nearly all populations had similar haplotype frequencies for *cox-1* across the range

of *P. caudata*, including populations in Caribbean and Brazil, with the exception of the Florida population.

Among the 22 haplotypes sequenced for *ITS-1*, six were present in more than one population (in order of abundance: T7, T8, T4, T1, T3 and T13), and the remainder were private haplotypes (Figure 3c). The most common haplotype (T7) was abundant in all Brazilian populations (40-80%) and one Caribbean population (GUA, 40%). Haplotype T7 was also present in Puerto Rico and the Virgin Islands, but at lower frequencies (8-9%), and was absent in Florida (Figure 1c). Haplotypes T1 and T3 were found only in the Caribbean Province (including Florida). In sum, haplotype frequencies for *ITS-1* were similar among Brazilian populations, with greater variability being observed among the Caribbean populations. The Florida population had the most divergent pattern, with a high abundance of haplotype T1 (42%), which was absent from most other populations, except for the Virgin Islands (18%).

#### *Genetic Diversity*

Genetic diversity indices were usually greater in the Caribbean populations (FLO, PRI, VIL, GUA) relative to the Brazilian populations (FOR, TAM, PER, UBA, POR, ITA, MEL). For example, gene diversity among Caribbean populations was greater than among Brazilian populations for both *cox-1* ( $0.426 \pm 0.121$  compared to  $0.243 \pm 0.195$ ) and *ITS-1* ( $0.854 \pm 0.06$  compared to  $0.692 \pm 0.178$ ), although these differences were not statistically significant ( $p=0.125$  and  $p=0.119$  respectively). Likewise, average nucleotide diversity was greater in the Caribbean rather than Brazilian populations for both *cox-1* and *ITS-1*, but again, the difference was not significant ( $p=0.166$  and  $p=0.07$  for *cox-1* and *ITS-1* respectively) (Appendix S2). Within both regions, genetic diversity was variable across populations, but in Brazil, variability was greater, with some populations having values similar to the Caribbean, while others had much lower diversity.

Deviations from neutral expectation were also observed. Tajima's D was negative for five out of 11 populations in *cox-1* and Fu's  $F_s$  indicated significant deviation from neutrality for seven populations for *cox-1* and three populations for *ITS-1* (Appendix S2). These large negative values for Fu's  $F_s$  suggest recent population expansion in the Caribbean, and in several Brazilian populations. Bayesian skyline plots for both *cox-1* and *ITS-1* also support an interpretation of recent population expansion, dating to c. 200 ka (Figure 4a,c). The age estimate for population expansion of *P. caudata* is concordant for both loci, even though independent molecular clocks were used. Population structure

has been shown to have a confounding effect on demographic history (Heller *et al.*, 2013). Because strong differentiation was observed with respect to the Florida population, Bayesian skyline plots were also estimated after excluding sequences from Florida (Figure 4b, d). Regardless of whether individuals from Florida were excluded or kept in the analysis, a signature of population expansion was observed, all dating to c. 200 ka.

#### *Population differentiation*

BAPS found two genetically distinct groups for *cox-1*, among the sampled *P. caudata* localities (logML=-1905.8). All individuals assigned to one group were sampled from Florida, while the remaining individuals, sampled across all other populations in the Caribbean and Brazil, were assigned to the second group (Appendix S3). In order to examine whether further population structure occurred within the second group, an analysis was conducted excluding individuals from Florida. However, no further genetically distinct groups were identified, as all individuals from this reduced dataset were still all assigned to the same group (logML=-1607.3). For *ITS-1*, BAPS found four genetically distinct groups (logML=-352.4); but, only one individual was assigned to two of the four groups. The log likelihood for two groups was similar to four groups (logML=-393.5), but there was no clear geographic pattern in the assignment of individuals to either group. For example, one group contained individuals from Florida, the Caribbean (in PRI and GUA) and Brazil (TAM, PER and POR) (Appendix S3). The BAPS analysis therefore did not indicate any strong geographical trend in population differentiation for *ITS-1*.

The hierarchical population structure design in the AMOVA considered two groups (group 1: FLO; group 2: all other populations). This scenario was selected based on the results of the BAPS analysis (for *cox-1*), and patterns in haplotype frequencies and haplotype networks for both loci. Differentiation among populations (FST) was significant for both *cox-1* (FST=0.721,  $p < 0.00001$ ) and *ITS-1* (FST=0.21338,  $p < 0.00001$ ). Differentiation among groups was also significant for *ITS-1* (FCT=0.196,  $p = 0.00098$ ). Although the FCT value was high for *cox-1* (FCT=0.721), it was not significant ( $p = 0.088$ ) (Table 2). These results indicate that there is some significant population structure among *P. caudata* populations, and that much of this structure is due to the Florida population.

Values of pairwise  $\phi_{st}$  for *cox-1* clearly indicate strong differentiation of the Florida population with respect to all other

Caribbean and Brazilian populations ( $\phi_{st}$  ranges from 0.606–0.784) (Table 3). For all other pairwise comparisons,  $\phi_{st}$  was small and not significant, suggesting that connectivity is maintained among populations along the coast of Brazil and among the eastern Caribbean Islands. For *ITS-1*, nearly all pairwise  $\phi_{st}$  comparisons were non-significant after Bonferroni correction (except PER compared to FLO and PRI), indicating that for this locus, although some population structure can be detected, connectivity appears to be maintained among most populations.

## Discussion

Phylogenetic analysis based on *cox-1* and *ITS-1* confirms the monophyly of three species of *Phragmatopoma* (*P. caudata*, *P. californica* and *P. virginii*). In addition, our analyses which included one published sequence of *P. moerchi*, also indicate that this may be a separate species, as suggested by Drake *et al.* (2007). In contrast to previous work, however, the results presented here do not show conclusive phylogenetic relationships among *P. caudata*, *P. californica* and *P. virginii*, as trichotomies were observed in the *cox-1*, *ITS-1* and in the species trees. Sequencing of additional loci or sampling of additional species in the genus (such as *P. attenuata* from the Pacific, or more individuals of *P. moerchi*) may help to clarify phylogenetic relationships within the genus.

Phylogenetic analysis also indicates the existence of a single species – *Phragmatopoma caudata* – from the eastern Caribbean to southern Brazil. These are the first molecular data to support a single species spanning this broad geographical range, confirming Kirtley's (1994) synonymization of *P. lapidosa* (originally described from Brazil) and *P. caudata* (originally described from the Caribbean). However, two genetically differentiated lineages were also identified - one that spans the Brazilian coast and part of the Caribbean and another that is restricted to Florida. Genetic differentiation with respect to Florida is congruent with contrasting patterns of oogenesis observed between *P. caudata* from Brazil and Florida (Faroni-Perez & Zara, 2014). For instance, the ovaries in *P. caudata* from Brazil were composed of oogonia and oocytes attached to blood vessels during early development, whereas in Florida, oocytes were associated with blood vessels until the end of vitellogenesis. Several additional features of oogenesis differed between individuals from either locations, including the type of oogenesis (intra- versus extra-ovarian), the nature of oocyte development (auto versus heterosynthetic), and the locations of the



oocyte mitochondria cloud, Golgi complexes and ovary capsules (Faroni-Perez & Zara, 2014). These findings show various distinctive aspects of gametogenesis between Florida and Brazil. Characterization of reproductive traits in individuals from Puerto Rico and Virgin Islands (geographically close to Florida, but genetically more similar to Brazil) could help elucidate whether reproductive differences are associated with the genetic differentiation observed here, and whether species-level distinction is warranted with respect to *P. caudata* from Florida.

Recent reassessments in Atlantic biogeography find the marine fauna within the Greater Caribbean to be relatively homogeneous, with the Caribbean Province being comprised of all the northern Western Atlantic tropics, including the southern tip of Florida and the West Indian islands (Floeter *et al.*, 2008; Briggs & Bowen, 2012). *Phragmatopoma caudata*, however, differs from this general trend, and shows a split between south Florida and nearby West Indian islands. The isolation of the Florida population may have three possible explanations. Firstly, the fast flowing currents in the Florida Straits may hinder larval dispersal between Florida and the West Indies (Briggs, 1995), as has been suggested for *Symbiodinium* harboured by the octocoral *Gorgonia ventalina* (Andras *et al.*, 2011). A second possibility is long-term divergence between Caribbean and Brazilian lineages, followed by recent dispersal from Brazil into the West Indies, as suggested for the rock hind *Epinephelus adscensionis* (Carlin *et al.*, 2003). Finally, the Florida population may be a case of incipient or recent speciation. Phylogenetic analysis based on *cox-1* and the species tree based on both loci show high support for a Florida clade (Figure 2), indicating a possible cryptic species. Because phylogenetic analysis based on *ITS-1* alone does not identify a Florida clade, these results require verification from additional molecular markers and/or morphological comparisons between specimens from Florida and the rest of the range of *P. caudata*. However, differences in gonad development between *P. caudata* from Brazil and Florida support the interpretation of a cryptic species (Faroni-Perez & Zara, 2014). Florida is a transition zone between the tropics and subtropics, where ecological speciation could take place as different genotypes become adapted to contrasting environmental conditions in different habitat types. The wrasse *Halichoeres bivittatus* provides a compelling example of ecological speciation in the marine environment (Rocha *et al.*, 2005). In this species, genetic connectivity is maintained across >2400 km, from Belize to the Lesser Antilles, but strong differentiation is observed between tropical Bahamas and subtropical Florida, separated by only 300 km. In the Florida Keys, where tropical

and subtropical habitats exist in close proximity, subtropical genotypes of this species were found in cooler inshore channels while tropical genotypes were found in warmer offshore reefs (Rocha *et al.*, 2005). Ecological speciation in *P. caudata* is an intriguing hypothesis for the genetic break observed between the West Indies and Florida, and future work examining contrasting habitats along the coast of Florida and adjacent areas may help to clarify the mechanisms that have led to genetic isolation in this location.

While genetic differentiation between Florida and the eastern Caribbean has previously been documented in *P. caudata* (Drake *et al.*, 2007), our work reveals continued genetic connectivity across the Amazon-Orinoco Barrier, among populations separated by as much as 9000 km. The Amazon plume is an important barrier to dispersal for a variety of marine species such as corals (Nunes *et al.*, 2009, 2011), crustaceans (Terossi & Mantelatto, 2012), echinoderms (Lessios *et al.*, 2003), and reef fish (Mendonça *et al.*, 2013). However, it is considered a “soft barrier” or “filter” because of the large number of shared fish species on either side of the barrier (Floeter *et al.*, 2008). Indeed, connectivity between the Caribbean and Brazilian Provinces has been observed in several marine species, such as ascidians (Nóbrega *et al.*, 2004), sea urchins (Zigler & Lessios, 2004), sponges (Lazoski *et al.*, 2001) and fish (Floeter *et al.*, 2008). Similarly, the Amazon-Orinoco Barrier does not appear to be an effective barrier for dispersal for *P. caudata*, even though occurrences on either side of the Amazon and Orinoco Rivers (Parnaíba, Brazil and Puerto Viejo, Venezuela) indicate that populations may be separated by up to 2700 km. Connectivity among populations of *P. caudata* in Brazil and the West Indies may be maintained by the North Brazil and Guiana Currents, both flowing northward from the north-eastern point of Brazil towards the Amazon and onwards to the Caribbean (Figure 1a). In addition, the Amazon River discharge varies seasonally, and is weakened from January to April (Moller *et al.*, 2010), potentially allowing larval permeability from North Brazil to the eastern Caribbean Islands. Larvae of *P. caudata* develop over two to four weeks (Eckelbarger, 1976), likely contributing to the ability to disperse broadly and to maintain connectivity across great distances. Moreover, larvae of *P. caudata* can develop normally between 15.5–29.5°C, a relatively wide temperature range (Eckelbarger, 1976). Tolerance to salinity in larvae of *P. caudata* is currently unknown, but could be an additional parameter favouring long-distance dispersal. Further experiments are needed to determine tolerance to

environmental variability in larvae, but such traits could explain dispersal across the Amazon-Orinoco Barrier.

At the intra-specific level, *cox-1* was characterized by a high number of private alleles (haplotypes restricted to one population), and singletons (haplotypes observed in only one individual) in all populations of *P. caudata*. Interestingly, all singleton mutations were synonymous (i.e. did not alter the amino acid sequence of a protein). A large number of singletons could be due to a high mutation rate in the mitochondrial genome, to a large effective population size, or recent population expansion. While data to estimate a mutation rate specific to *P. caudata* are currently unavailable, large population size and/or recent population expansion may explain the large number of singletons in *cox-1*. *P. caudata* likely has large population sizes, as the density of individuals has been estimated at ~65,000 individuals/m<sup>-2</sup> (Faroni-Perez, 2014). Given that the generation time of *P. caudata* is of one year, a large fraction of individuals potentially contribute to the gene pool each year. In addition, Bayesian skyline plots (Figure 4) and significant negative values for Fu's  $F_s$  and Tajima's  $D$  are indicative of recent population expansion (dating to *c.* 200 ka). Each of these factors may explain, alone or in combination, the high polymorphism observed in the mitochondrial locus.

Within the Brazilian Province, no significant population structure was observed for *P. caudata*. Long-distance connectivity along the coast of Brazil is known for other invertebrates, including broadcasting corals (Nunes *et al.*, 2009, 2011) and fiddler crabs (Laurenzano *et al.*, 2013; Wieman *et al.*, 2014). Nevertheless, the lack of genetic differentiation along >5000 km from Fortaleza to Ilha do Mel was unexpected. For example, the “coastal/island” species of the fireworm *Eurythoe complanata* shows significant population structure along the coast of Brazil (Barroso *et al.*, 2010), despite having a similar larval duration to *P. caudata*. The data presented here suggest that *P. caudata* can overcome various barriers to dispersal that are known for other marine organisms within the Brazilian Province, such as the split between the north-flowing North Brazil Current and south-flowing Brazil Current (Santos *et al.*, 2006), the São Francisco Barrier (Floeter *et al.*, 2001; Piccioni *et al.*, 2016; Souza *et al.*, 2016) and the upwelling at Cabo Frio (for the coral *M. hispida*, L. Peluso, UFRJ, pers. comm.).

South of the Point of Natal, the Brazil Current is a powerful western-boundary current that may facilitate larval transport and gene flow (Figure 1a). Currently only a few studies have addressed genetic connectivity in annelids in the Brazilian Province (Barroso *et al.*, 2010;

Ahrens *et al.*, 2013). Future work on other annelid species may help identify traits that favour or hinder connectivity in this biogeographical region. Finally, for a better understanding of *P. caudata* population connectivity, the use of higher resolution markers such as such as microsatellites or SNPs derived from RAD-Seq could be used to examine finer-scale population structure and dispersal dynamics.

## Conclusions

Molecular data from two loci (*cox-1* and *ITS-1*) confirms the occurrence of a single species, *Phragmatopoma caudata*, from Florida to South Brazil. High levels of connectivity are implied across the species range, possibly due to high gamete density upon spawning, long pelagic larval stage, and larvae that are tolerant to a wide range of temperatures, and possibly salinity. The Amazon plume, other major rivers along the coast of Brazil or the upwelling in Cabo Frio are not effective barriers for dispersal for this species, as connectivity is maintained along the entire coast of Brazil and between Brazil and the eastern Caribbean. Population structure is observed only in comparisons with the Florida population, possibly due to ecological speciation in the transition zone between tropical and subtropical environments. Additional sampling within the Caribbean is needed to identify whether other barriers to dispersal occur within this biogeographical region.

## Acknowledgements

The authors would like to thank C. Bouchon (Université des Antilles et de la Guyane, Guadeloupe, France) for providing specimens, A.C. Panizza (CNPq and Federal University of Ceará, Fortaleza, Brazil) for assistance in the field in Brazil, C.A. Drake (Utah State University, USA) for providing sequence data information for Caribbean populations. This project was supported by the Muséum National d'Histoire Naturelle of Paris (BQR HYDROGENE 2006-2008 and ATM “Formes Possibles, Formes Réalisées” 2013-2014) to JF. FLDN was supported by the “Laboratoire d'Excellence” LabexMER (ANR-10-LABX-19) and co-funded by a grant from the French government under the program “Investissements d'Avenir”, and by a grant from the Regional Council of Brittany. L.F.P. was supported by the São Paulo Research Foundation

(FAPESP 07/56340-3) and the National Council for Scientific and Technological Development, Brazil (CNPq – SWE 201233/2015-0).

## References

- Ahrens J.B., Borda E., Barroso R., Paiva P.C., Campbell A.M., Wolf A., Nugues M.M., Rouse G.W., & Schulze A. (2013) The curious case of *Hermodice carunculata* (Annelida: Amphinomidae): evidence for genetic homogeneity throughout the Atlantic Ocean and adjacent basins. *Molecular Ecology*, **22**, 2280–2291.
- Andras J.P., Kirk N.L., & Harvell C.D. (2011) Range-wide population genetic structure of *Symbiodinium* associated with the Caribbean Sea fan coral, *Gorgonia ventalina*. *Molecular Ecology*, **20**, 2525–2542.
- Ataide M.B., Venekey V., Rosa Filho J.S., & Santos P.J.P. (2014) Sandy reefs of *Sabellaria wilsoni* (Polychaeta: Sabellariidae) as ecosystem engineers for meiofauna in the Amazon coastal region, Brazil. *Marine Biodiversity*, **44**, 403–413.
- Avise J.C. (1992) Molecular population structure and the biogeographic history of a regional fauna - a case history with lessons for conservation biology. *Oikos*, **63**, 62–76.
- Barroso R., Klautau M., Solé-Cava A.M., & Paiva P.C. (2010) *Eurythoe complanata* (Polychaeta: Amphinomidae), the “cosmopolitan” fireworm, consists of at least three cryptic species. *Marine Biology*, **157**, 69–80.
- Briggs J.C. (1995) *Global Biogeography*. Elsevier, Amsterdam.
- Briggs J.C. & Bowen B.W. (2012) A realignment of marine biogeographic provinces with particular reference to fish distributions. *Journal of Biogeography*, **39**, 12–30.
- Capa M., Hutchings P., & Peart R. (2012) Systematic revision of Sabellariidae (Polychaeta) and their relationships with other polychaetes using morphological and DNA sequence data. *Zoological Journal of the Linnean Society*, **164**, 245–284.
- Carlin J.L., Robertson D.R., & Bowen B.W. (2003) Ancient divergences and recent connections in two tropical Atlantic reef fishes *Epinephelus adscensionis* and *Rypticus saponaceus* (Percoidei: Serranidae). *Marine Biology*, **143**, 1057–1069.
- Clement M., Posada D., & Crandall K. a. (2000) TCS: A computer program to estimate gene genealogies. *Molecular Ecology*, **9**, 1657–1659.
- Coleman A.W. & Vacquier V.D. (2002) Exploring the phylogenetic utility of ITS sequences for animals: a test case for abalone (*Haliotis*). *Journal of Molecular Evolution*, **54**, 246–257.

- Corander J., Marttinen P., Tang J., Sirén J., & Tang J. (2008) Enhanced Bayesian modelling in BAPS software for learning genetic structures of populations. *BMC Bioinformatics*, **9**, 359.
- Denis F., Ravallec R., Pavillon J.-F., & Van Wormhoudt A. (2009) Genetic differentiation of Atlantic populations of the intertidal copepod *Tigriopus brevicornis*. *Scientia Marina*, **73**, 579–587.
- Drake C.A., McCarthy D.A., & Von Dohlen C.D. (2007) Molecular relationships and species divergence among *Phragmatopoma* spp. (Polychaeta: Sabellariidae) in the Americas. *Marine Biology*, **150**, 345–358.
- Drummond A.J., Rambaut A., Shapiro B., & Pybus O.G. (2005) Bayesian coalescent inference of past population dynamics from molecular sequences. *Molecular Biology and Evolution*, **22**, 1185–1192.
- Dubois, S., Retière, C. & Olivier, F. (2002) Biodiversity associated with *Sabellaria alveolata* (Polychaeta: Sabellariidae) reefs: effects of human disturbances. *Journal of the Marine Biological Association of the United Kingdom*, **82**, 817–826.
- Eckelbarger K.J. (1976) Larval development and population aspects of the reef-building polychaete *Phragmatopoma lapidosa* from the east coast of Florida. *Bulletin of Marine Science*, **26**, 117–132.
- Excoffier L., Laval G., & Schneider S. (2005) Arlequin (version 3.0): An integrated software package for population genetics data analysis. *Evolutionary Bioinformatics Online*, **1**, 47–50.
- Faroni-Perez L. (2014) Seasonal variation in recruitment of *Phragmatopoma caudata* (Polychaeta, Sabellariidae) in the southeast coast of Brazil: validation of a methodology for categorizing age classes. *Iheringia*, **104**, 5–13.
- Faroni-Perez L., Helm C., Burghardt I., Hutchings P., & Capa M. (2016) Anterior sensory organs in Sabellariidae (Annelida). *Invertebrate Biology*, **135**, 423–447.
- Faroni-Perez L. & Zara F.J. (2014) Oogenesis in *Phragmatopoma* (Polychaeta: Sabellariidae): evidence for morphological distinction among geographically remote populations. *Memoirs of Museum Victoria*, **71**, 53–65.
- Floeter S.R., Guimaraes R.Z.P., Rocha L.A., Ferreira C.E.L., Rangel C.A., & Gasparini J.L. (2001) Geographic variation in reef-fish assemblages along the Brazilian coast. *Global Ecology and Biogeography*, **10**, 423–431.
- Floeter S.R., Rocha L.A., Robertson D.R., Joyeux J.C., Smith-Vaniz W.F., Wirtz P., Edwards A.J., Barreiros J.P., Ferreira C.E.L.,

- Gasparini J.L., Brito A., Falcón J.M., Bowen B.W., & Bernardi G. (2008) Atlantic reef fish biogeography and evolution. *Journal of Biogeography*, **35**, 22–47.
- Fournier J., Etienne S., & Le Cam J.-B. (2010) Inter- and intraspecific variability in the chemical composition of the mineral phase of cements from several tube-building polychaetes. *Geobios*, **43**, 191–200.
- Godet L., Fournier J., Jaffré M., & Desroy N. (2011) Influence of stability and fragmentation of a worm-reef on benthic macrofauna. *Estuarine, Coastal and Shelf Science*, **92**, 472–479.
- Goldberg W.M. (2013) *The Biology of reefs and reef organisms*. University of Chicago Press, Chicago.
- Hartman O. (1944) Polychaetous Annelids. Part VI. Paraonidae, Magelonidae, Longosomidae, Ctenodrilidae, and Sabellariidae. *Allan Hancock Pacific Expeditions*, **10**, 311–389, plates 327–342.
- Heled J. & Drummond A.J. (2010) Bayesian inference of species trees from multilocus data. *Molecular Biology and Evolution*, **27**, 570–580.
- Heller R., Chikhi L., & Siegismund H.R. (2013) The confounding effect of population structure on Bayesian skyline plot inferences of demographic history. *PLOS ONE*, **8**, e62992.
- Kirtley D.W. (1994) *A review and taxonomic revision of the family Sabellariidae Johnston 1865 (Annelida; Polychaeta)*. Sabecon Press, Science Series, Vero Beach.
- Laurenzano C., Mantelatto F.L.M., & Schubart C.D. (2013) South American homogeneity versus Caribbean heterogeneity: population genetic structure of the western Atlantic fiddler crab *Uca rapax* (Brachyura, Ocypodidae). *Journal of Experimental Marine Biology and Ecology*, **449**, 22–27.
- Lazoski C., Solé-Cava A., Boury-Esnault N., M K., & Russo C.A.M. (2001) Cryptic speciation in a high gene flow scenario in the oviparous marine sponge *Chondrosia reniformis*. *Marine Biology*, **139**, 421–429.
- Lessios H.A. (2008) The great American schism: divergence of marine organisms after the rise of the Central American isthmus. *Annual Review of Ecology, Evolution, and Systematics*, **39**, 63–91.
- Lessios H.A., Kane J., & Robertson D.R. (2003) Phylogeography of the pantropical sea urchin *Tripneustes*: contrasting patterns of population structure between oceans. *Evolution*, **57**, 2026–2036.

- Librado P. & Rozas J. (2009) DnaSP v5: A software for comprehensive analysis of DNA polymorphism data. *Bioinformatics*, **25**, 1451–1452.
- Liñero-Arana I. (2013) New records of Sabellariidae (Annelida: Polychaeta) from the Caribbean sea. *Interciencia*, **38**, 382–386.
- Main M.B. & Nelson W.G. (1988) Sedimentary characteristics of sabellariid worm reefs (*Phragmatopoma lapidosa* Kinberg). *Estuarine, Coastal and Shelf Science*, **26**, 105–109.
- Mauro N.A. (1975) The premetamorphic developmental rate of *Phragmatopoma lapidosa* Kinberg, 1867, compared with that in temperate sabellariids (Polychaeta: Sabellariidae). *Bulletin of Marine Science*, **25**, 387–392.
- Mauro N.A. (1977) Variations in osmoregulatory capacity in two species of intertidal sabellariids (Annelida: Polychaeta) from tropical and mediterranean habitats. *Comparative Biochemistry and Physiology Part A: Physiology*, **56A**, 375–377.
- McCarthy D. a., Young C.M., & Emson R.H. (2003) Influence of wave-induced disturbance on seasonal spawning patterns in the sabellariid polychaete *Phragmatopoma lapidosa*. *Marine Ecology Progress Series*, **256**, 123–133.
- Mendonça F.F., Oliveira C., Gadig O.B.F., & Foresti F. (2013) Diversity and genetic population structure of the Brazilian sharpnose shark *Rhizoprionodon lalandii*. *Aquatic Conservation: Marine and Freshwater Ecosystems*, **23**, 850–857.
- Molleri G.S.F., Novo E.M.L. de M., & Kampel M. (2010) Space-time variability of the Amazon River plume based on satellite ocean color. *Continental Shelf Research*, **30**, 342–352.
- Nóbrega R., Solé-Cava A.M., & Russo C. a. M. (2004) High genetic homogeneity of an intertidal marine invertebrate along 8000 km of the Atlantic coast of the Americas. *Journal of Experimental Marine Biology and Ecology*, **303**, 173–181.
- Noernberg M.A., Fournier J., Dubois S., & Populus J. (2010) Using airborne laser altimetry to estimate *Sabellaria alveolata* (Polychaeta: Sabellariidae) reefs volume in tidal flat environments. *Estuarine, Coastal and Shelf Science*, **90**, 93–102.
- Nunes F., Norris R.D., & Knowlton N. (2009) Implications of isolation and low genetic diversity in peripheral populations of an amphiatlantic coral. *Molecular Ecology*, **18**, 4283–97.
- Nunes F.L.D., Norris R.D., & Knowlton N. (2011) Long distance dispersal and connectivity in amphiatlantic corals at regional and basin scales. *PLOS ONE*, **6**, e22298.



- Pagliosa P.R., Doria J.G., Misturini D., Otegui M.B.P., Oortman M.S., Weis W.A., Faroni-Perez L., Alves A.P., Camargo M.G., Amaral A.C.Z., Marques A.C., & Lana P.C. (2014) NONATObase: a database for Polychaeta (Annelida) from the Southwestern Atlantic Ocean. *Database*, **2014**, bau002.
- Palumbi S.R. (1994) Genetic divergence, reproductive isolation, and marine speciation. *Annual Review of Ecology and Systematics*, **25**, 547–572.
- Pawlik J.R. (1988) Larval settlement and metamorphosis of Sabellariid polychaetes, with special reference to *Phragmatopoma lapidosa*, a reef-building species, and *Sabellaria floridensis*, a non-gregarious species. *Bulletin of Marine Science*, **43**, 41–60.
- Picciani N., Seiblitiz I.G.L., Paiva P.C., Castro C.B., & Zilberberg C. (2016) Geographic patterns of *Symbiodinium* diversity associated with the coral *Mussismilia hispida* (Cnidaria, Scleractinia) correlate with major reef regions in the Southwestern Atlantic Ocean. *Marine Biology*, **163**, 236.
- Rocha L.A., Robertson D.R., Roman J., & Bowen B.W. (2005) Ecological speciation in tropical reef fishes. *Proceedings of the Royal Society B: Biological Sciences*, **272**, 573–579.
- Santos, M.V.Q.B., Aquino-Souza, R. & Gomes-Filho, J.G.F. (2012) Ocorrência, grau de ocupação do substrato e tamanhos das colônias de *Phragmatopoma caudata* na região entremarés da Praia da Pedra do Sal, Parnaíba-PI. *XXIX Congresso Brasileiro de Zoologia*.
- Santos S., Hrbek T., Farias I.P., Schneider H., & Sampaio I. (2006) Population genetic structuring of the king weakfish, *Macrodon ancylodon* (Sciaenidae), in Atlantic coastal waters of South America: deep genetic divergence without morphological change. *Molecular Ecology*, **15**, 4361–4373.
- Souza J.N., Nunes F.L.D., Zilberberg C., Sanchez J.A., Migotto A.E., Hoeksema B.W., Serrano X.M., Baker A.C., & Lindner A. (2016) Contrasting patterns of connectivity among endemic and widespread fire coral species (*Millepora* spp.) in the tropical Southwestern Atlantic. *Coral Reefs*, in press.
- Tamura K., Stecher G., Peterson D., Filipski A., & Kumar S. (2013) MEGA6: Molecular evolutionary genetics analysis version 6.0. *Molecular Biology and Evolution*, **30**, 2725–2729.
- Terossi M. & Mantelatto F.L.A. (2012) Morphological and genetic variability in *Hippolyte obliquimanus* Dana, 1852 (Decapoda,

- Caridae, Hippolytidae) from Brazil and the Caribbean Sea. *Crustaceana*, **85**, 685–712.
- Wieman A.C., Berendzen P.B., Hampton K.R., Jang J., Hopkins M.J., Jurgenson J., McNamara J.C., & Thurman C.L. (2014) A panmictic fiddler crab from the coast of Brazil? Impact of divergent ocean currents and larval dispersal potential on genetic and morphological variation in *Uca maracoani*. *Marine Biology*, **161**, 173–185.
- Zigler K.S. & Lessios H.A. (2004) Speciation on the coasts of the new world: phylogeography and the evolution of binding in the sea urchin genus *Lytechinus*. *Evolution*, **58**, 1225–1241.
- Ahrens J.B., Borda E., Barroso R., Paiva P.C., Campbell A.M., Wolf A., Nugues M.M., Rouse G.W., & Schulze A. (2013) The curious case of *Hermodice carunculata* (Annelida: Amphinomidae): evidence for genetic homogeneity throughout the Atlantic Ocean and adjacent basins. *Molecular Ecology*, **22**, 2280–2291.
- Andras J.P., Kirk N.L., & Harvell C.D. (2011) Range-wide population genetic structure of *Symbiodinium* associated with the Caribbean Sea fan coral, *Gorgonia ventalina*. *Molecular Ecology*, **20**, 2525–2542.
- Ataide M.B., Venekey V., Rosa Filho J.S., & Santos P.J.P. (2014) Sandy reefs of *Sabellaria wilsoni* (Polychaeta: Sabellariidae) as ecosystem engineers for meiofauna in the Amazon coastal region, Brazil. *Marine Biodiversity*, **44**, 403–413.
- Avise J.C. (1992) Molecular population structure and the biogeographic history of a regional fauna - a case history with lessons for conservation biology. *Oikos*, **63**, 62–76.
- Barroso R., Klautau M., Solé-Cava A.M., & Paiva P.C. (2010) *Eurythoe complanata* (Polychaeta: Amphinomidae), the “cosmopolitan” fireworm, consists of at least three cryptic species. *Marine Biology*, **157**, 69–80.
- Briggs J.C. (1995) *Global Biogeography*. Elsevier, Amsterdam.
- Briggs J.C. & Bowen B.W. (2012) A realignment of marine biogeographic provinces with particular reference to fish distributions. *Journal of Biogeography*, **39**, 12–30.
- Capa M., Hutchings P., & Peart R. (2012) Systematic revision of Sabellariidae (Polychaeta) and their relationships with other polychaetes using morphological and DNA sequence data. *Zoological Journal of the Linnean Society*, **164**, 245–284.
- Carlin J.L., Robertson D.R., & Bowen B.W. (2003) Ancient divergences and recent connections in two tropical Atlantic reef fishes

- Epinephelus adscensionis* and *Rypticus saponaceus* (Percoidei: Serranidae). *Marine Biology*, **143**, 1057–1069.
- Clement M., Posada D., & Crandall K. a. (2000) TCS: A computer program to estimate gene genealogies. *Molecular Ecology*, **9**, 1657–1659.
- Coleman A.W. & Vacquier V.D. (2002) Exploring the phylogenetic utility of ITS sequences for animals: a test case for abalone (*Haliotis*). *Journal of Molecular Evolution*, **54**, 246–257.
- Corander J., Marttinen P., Tang J., Sirén J., & Tang J. (2008) Enhanced Bayesian modelling in BAPS software for learning genetic structures of populations. *BMC Bioinformatics*, **9**, 359.
- Denis F., Ravallec R., Pavillon J.-F., & Van Wormhoudt A. (2009) Genetic differentiation of Atlantic populations of the intertidal copepod *Tigriopus brevicornis*. *Scientia Marina*, **73**, 579–587.
- Drake C.A., McCarthy D.A., & Von Dohlen C.D. (2007) Molecular relationships and species divergence among *Phragmatopoma* spp. (Polychaeta: Sabellariidae) in the Americas. *Marine Biology*, **150**, 345–358.
- Drummond A.J., Rambaut A., Shapiro B., & Pybus O.G. (2005) Bayesian coalescent inference of past population dynamics from molecular sequences. *Molecular Biology and Evolution*, **22**, 1185–1192.
- Dubois, S., Retière, C. & Olivier, F. (2002) Biodiversity associated with Sabellaria alveolata (Polychaeta: Sabellariidae) reefs: effects of human disturbances. *Journal of the Marine Biological Association of the United Kingdom*, **82**, 817–826.
- Eckelbarger K.J. (1976) Larval development and population aspects of the reef-building polychaete *Phragmatopoma lapidosa* from the east coast of Florida. *Bulletin of Marine Science*, **26**, 117–132.
- Excoffier L., Laval G., & Schneider S. (2005) Arlequin (version 3.0): An integrated software package for population genetics data analysis. *Evolutionary Bioinformatics Online*, **1**, 47–50.
- Faroni-Perez L. (2014) Seasonal variation in recruitment of *Phragmatopoma caudata* (Polychaeta, Sabellariidae) in the southeast coast of Brazil: validation of a methodology for categorizing age classes. *Iheringia*, **104**, 5–13.
- Faroni-Perez L., Helm C., Burghardt I., Hutchings P., & Capa M. (2016) Anterior sensory organs in Sabellariidae (Annelida). *Invertebrate Biology*, **135**, 423–447.
- Faroni-Perez L. & Zara F.J. (2014) Oogenesis in *Phragmatopoma* (Polychaeta: Sabellariidae): evidence for morphological

- distinction among geographically remote populations. *Memoirs of Museum Victoria*, **71**, 53–65.
- Floeter S.R., Guimaraes R.Z.P., Rocha L.A., Ferreira C.E.L., Rangel C.A., & Gasparini J.L. (2001) Geographic variation in reef-fish assemblages along the Brazilian coast. *Global Ecology and Biogeography*, **10**, 423–431.
- Floeter S.R., Rocha L.A., Robertson D.R., Joyeux J.C., Smith-Vaniz W.F., Wirtz P., Edwards A.J., Barreiros J.P., Ferreira C.E.L., Gasparini J.L., Brito A., Falcón J.M., Bowen B.W., & Bernardi G. (2008) Atlantic reef fish biogeography and evolution. *Journal of Biogeography*, **35**, 22–47.
- Fournier J., Etienne S., & Le Cam J.-B. (2010) Inter- and intraspecific variability in the chemical composition of the mineral phase of cements from several tube-building polychaetes. *Geobios*, **43**, 191–200.
- Godet L., Fournier J., Jaffré M., & Desroy N. (2011) Influence of stability and fragmentation of a worm-reef on benthic macrofauna. *Estuarine, Coastal and Shelf Science*, **92**, 472–479.
- Goldberg W.M. (2013) *The Biology of reefs and reef organisms*. University of Chicago Press, Chicago.
- Hartman O. (1944) Polychaetous Annelids. Part VI. Paraonidae, Magelonidae, Longosomidae, Ctenodrilidae, and Sabellariidae. *Allan Hancock Pacific Expeditions*, **10**, 311–389, plates 327–342.
- Heled J. & Drummond A.J. (2010) Bayesian inference of species trees from multilocus data. *Molecular Biology and Evolution*, **27**, 570–580.
- Heller R., Chikhi L., & Siegmund H.R. (2013) The confounding effect of population structure on Bayesian skyline plot inferences of demographic history. *PLOS ONE*, **8**, e62992.
- Kirtley D.W. (1994) *A review and taxonomic revision of the family Sabellariidae Johnston 1865 (Annelida; Polychaeta)*. Sabecon Press, Science Series, Vero Beach.
- Laurenzano C., Mantelatto F.L.M., & Schubart C.D. (2013) South American homogeneity versus Caribbean heterogeneity: population genetic structure of the western Atlantic fiddler crab *Uca rapax* (Brachyura, Ocypodidae). *Journal of Experimental Marine Biology and Ecology*, **449**, 22–27.
- Lazoski C., Solé-Cava A., Boury-Esnault N., M K., & Russo C.A.M. (2001) Cryptic speciation in a high gene flow scenario in the oviparous marine sponge *Chondrosia reniformis*. *Marine Biology*, **139**, 421–429.

- Lessios H.A. (2008) The great American schism: divergence of marine organisms after the rise of the Central American isthmus. *Annual Review of Ecology, Evolution, and Systematics*, **39**, 63–91.
- Lessios H.A., Kane J., & Robertson D.R. (2003) Phylogeography of the pantropical sea urchin *Tripneustes*: contrasting patterns of population structure between oceans. *Evolution*, **57**, 2026–2036.
- Librado P. & Rozas J. (2009) DnaSP v5: A software for comprehensive analysis of DNA polymorphism data. *Bioinformatics*, **25**, 1451–1452.
- Liñero-Arana I. (2013) New records of Sabellariidae (Annelida: Polychaeta) from the Caribbean sea. *Interciencia*, **38**, 382–386.
- Main M.B. & Nelson W.G. (1988) Sedimentary characteristics of sabellariid worm reefs (*Phragmatopoma lapidosa* Kinberg). *Estuarine, Coastal and Shelf Science*, **26**, 105–109.
- Mauro N.A. (1975) The premetamorphic developmental rate of *Phragmatopoma lapidosa* Kinberg, 1867, compared with that in temperate sabellariids (Polychaeta: Sabellariidae). *Bulletin of Marine Science*, **25**, 387–392.
- Mauro N.A. (1977) Variations in osmoregulatory capacity in two species of intertidal sabellariids (Annelida: Polychaeta) from tropical and mediterranean habitats. *Comparative Biochemistry and Physiology Part A: Physiology*, **56A**, 375–377.
- McCarthy D. a., Young C.M., & Emson R.H. (2003) Influence of wave-induced disturbance on seasonal spawning patterns in the sabellariid polychaete *Phragmatopoma lapidosa*. *Marine Ecology Progress Series*, **256**, 123–133.
- Mendonça F.F., Oliveira C., Gadig O.B.F., & Foresti F. (2013) Diversity and genetic population structure of the Brazilian sharpnose shark *Rhizoprionodon lalandii*. *Aquatic Conservation: Marine and Freshwater Ecosystems*, **23**, 850–857.
- Molleri G.S.F., Novo E.M.L. de M., & Kampel M. (2010) Space-time variability of the Amazon River plume based on satellite ocean color. *Continental Shelf Research*, **30**, 342–352.
- Nóbrega R., Solé-Cava A.M., & Russo C. a. M. (2004) High genetic homogeneity of an intertidal marine invertebrate along 8000 km of the Atlantic coast of the Americas. *Journal of Experimental Marine Biology and Ecology*, **303**, 173–181.
- Noernberg M.A., Fournier J., Dubois S., & Populus J. (2010) Using airborne laser altimetry to estimate *Sabellaria alveolata* (Polychaeta: Sabellariidae) reefs volume in tidal flat environments. *Estuarine, Coastal and Shelf Science*, **90**, 93–102.

- Nunes F., Norris R.D., & Knowlton N. (2009) Implications of isolation and low genetic diversity in peripheral populations of an amphiatlantic coral. *Molecular Ecology*, **18**, 4283–97.
- Nunes F.L.D., Norris R.D., & Knowlton N. (2011) Long distance dispersal and connectivity in amphiatlantic corals at regional and basin scales. *PLOS ONE*, **6**, e22298.
- Pagliosa P.R., Doria J.G., Misturini D., Otegui M.B.P., Oortman M.S., Weis W.A., Faroni-Perez L., Alves A.P., Camargo M.G., Amaral A.C.Z., Marques A.C., & Lana P.C. (2014) NONATObase: a database for Polychaeta (Annelida) from the Southwestern Atlantic Ocean. *Database*, **2014**, bau002.
- Palumbi S.R. (1994) Genetic divergence, reproductive isolation, and marine speciation. *Annual Review of Ecology and Systematics*, **25**, 547–572.
- Pawlik J.R. (1988) Larval settlement and metamorphosis of Sabellariid polychaetes, with special reference to *Phragmatopoma lapidosa*, a reef-building species, and *Sabellaria floridensis*, a non-gregarious species. *Bulletin of Marine Science*, **43**, 41–60.
- Picciani N., Seiblitiz I.G.L., Paiva P.C., Castro C.B., & Zilberberg C. (2016) Geographic patterns of *Symbiodinium* diversity associated with the coral *Mussismilia hispida* (Cnidaria, Scleractinia) correlate with major reef regions in the Southwestern Atlantic Ocean. *Marine Biology*, **163**, 236.
- Rocha L.A., Robertson D.R., Roman J., & Bowen B.W. (2005) Ecological speciation in tropical reef fishes. *Proceedings of the Royal Society B: Biological Sciences*, **272**, 573–579.
- Santos, M.V.Q.B., Aquino-Souza, R., Gomes-Filho, J.G.F. (2012) Ocorrência, grau de ocupação do substrato e tamanhos das colônias de *Phragmatopoma caudata* na região entremarés da Praia da Pedra do Sal, Parnaíba-PI. XXIX Congresso Brasileiro de Zoologia.
- Santos S., Hrbek T., Farias I.P., Schneider H., & Sampaio I. (2006) Population genetic structuring of the king weakfish, *Macrodon ancylodon* (Sciaenidae), in Atlantic coastal waters of South America: deep genetic divergence without morphological change. *Molecular Ecology*, **15**, 4361–4373.
- Souza J.N., Nunes F.L.D., Zilberberg C., Sanchez J.A., Migotto A.E., Hoeksema B.W., Serrano X.M., Baker A.C., & Lindner A. (2016) Contrasting patterns of connectivity among endemic and widespread fire coral species (*Millepora* spp.) in the tropical Southwestern Atlantic. *Coral Reefs*, in press.

- Tamura K., Stecher G., Peterson D., Filipinski A., & Kumar S. (2013) MEGA6: Molecular evolutionary genetics analysis version 6.0. *Molecular Biology and Evolution*, 30, 2725–2729.
- Terossi M. & Mantelatto F.L.A. (2012) Morphological and genetic variability in *Hippolyte obliquimanus* Dana, 1852 (Decapoda, Caridae, Hippolytidae) from Brazil and the Caribbean Sea. *Crustaceana*, 85, 685–712.
- Wieman A.C., Berendzen P.B., Hampton K.R., Jang J., Hopkins M.J., Jurgenson J., McNamara J.C., & Thurman C.L. (2014) A panmictic fiddler crab from the coast of Brazil? Impact of divergent ocean currents and larval dispersal potential on genetic and morphological variation in *Uca maracoani*. *Marine Biology*, 161, 173–185.
- Zigler K.S. & Lessios H.A. (2004) Speciation on the coasts of the new world: phylogeography and the evolution of binding in the sea urchin genus *Lytechinus*. *Evolution*, 58, 1225–1241.

### **Supporting Information**

Additional Supporting Information may be found in the online version of this article:

Appendix S1. Sampling coordinates and location details.

Appendix S2. Genetic diversity indices for (a) *cox-1* and (b) *ITS-1*

Appendix S3. BAPS assignments for (a) *cox-1* and (b) *ITS-1*.

### **Author contributions:**

AVW and JF conceived the project; JF and LFP collected the samples; AVW and FLDN did the molecular analyses, AVW, FLDN and JF analysed the data. FLDN, AVW, LFP and JF contributed to writing the manuscript.

Editor: Michelle Gaither

### **Data accessibility**

DNA sequences produced during this study have been deposited in Genbank (see Methods and Materials for details). Raw data can be requested by contacting the corresponding author.

## FIGURES AND TABLES:

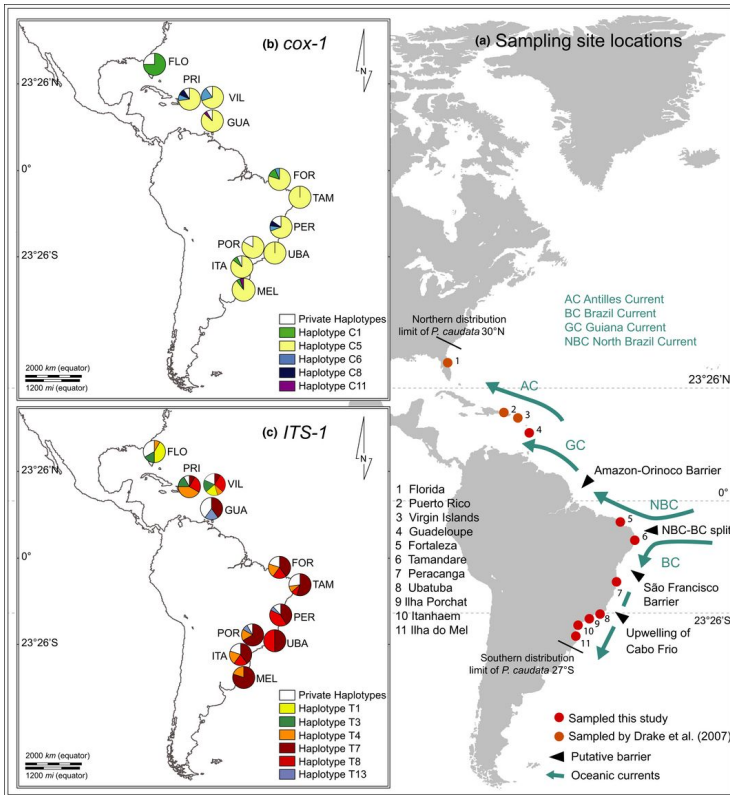


**Figure 1.** (a) Map of the sampling site locations of *P. caudata*, showing the direction of major ocean currents in January for the western Atlantic Ocean and Caribbean Sea. Haplotype frequencies are shown for each population for (b) of *cox-1* and (c) *ITS-1*. Population codes: Florida (FLO), Puerto Rico (PRI), Virgin Islands (VIL), Guadeloupe (GUA), Fortaleza (FOR), Tamandaré (TAM), Peracanga (PER), Ubatuba (UBA), Porchat (POR), Itanhaém (ITA) and Ilha do Mel (MEL).



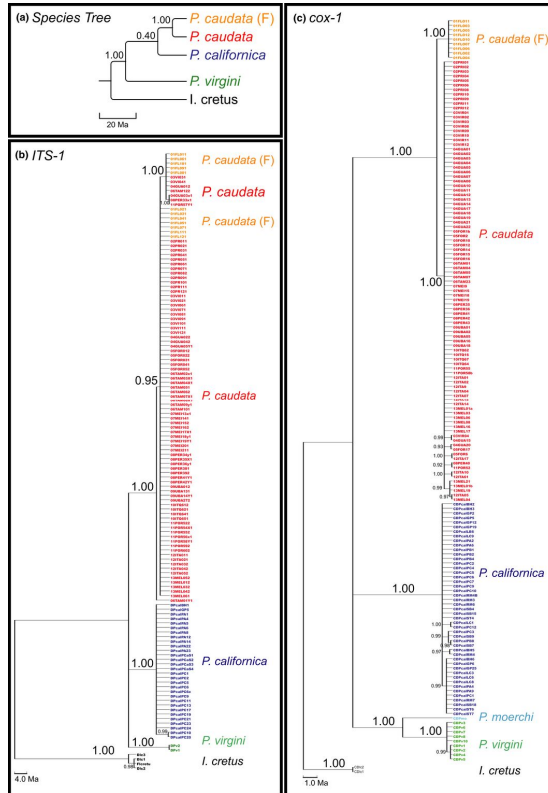


**Figure 2.** Phylogenetic reconstruction of relationships among species of *Phragmatopoma*. (a) Species tree based on combined data from *cox-1* and *ITS-1*; (b) based on sequences of *ITS-1* and (c) based on sequences of *cox-1*. Posterior probabilities are shown for nodes with support >0.90. Species are colour-coded as follows: red: *P. caudata*, orange: *P. caudata* from the Florida population, blue: *P. californica*; green: *P. virgini*; cyan: *P. moerchi*; black: *I. cretus*. (F) denotes individuals of *P. caudata* from the Florida population.

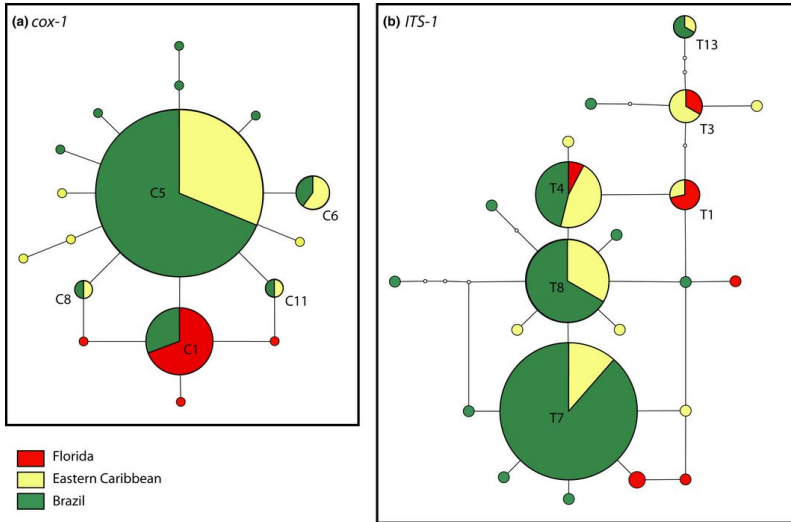


**Figure 3.** Haplotype networks based on sequences of *P. caudata* for (a) *cox-1* and (b) *ITS-1*. Each circle represents a haplotype and its size is proportional to the frequency of the haplotype across all populations. Empty circles represent mutational steps between sampled haplotypes. Haplotypes are colour-coded by geographic region: red = Florida (FLO); yellow = eastern Caribbean (PRI, VIL, GUA); green = Brazil (FOR, TAM, PER, UBA, POR, ITA, MEL). See Figure 1 for population code names.

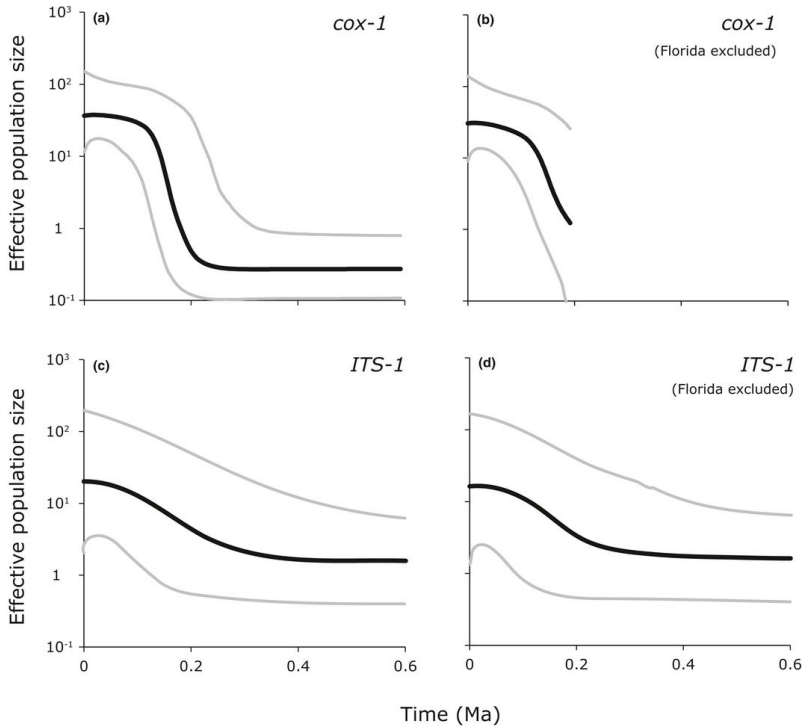


**Figure 4.** Bayesian skyline plots showing changes in effective population size of *P. caudata* over time based on sequences from: (a) *cox-1*; (b) *cox-1* excluding individuals from Florida; (c) *ITS-1* and (d) *ITS-1* excluding individuals from Florida.

**Table 1.** Estimates of evolutionary divergences between species pairs of *Phragmatopoma*, and outgroup, *I. cretus*. The number of base substitutions per site from averaging over all sequence pairs between species is shown below the diagonal, and standard error estimates are shown above the diagonal for (a) *cox-1* and (c) *ITS-1*. Divergence time estimates using locus-specific substitution rates are shown for each species pairs for (b) *cox-1* and (d) *ITS-1*. (F) denotes the Florida population of *P. caudata*.

(a) Genetic distances between species pairs based on <i>cox-1</i>						
	1	2	3	4	5	6
1 <i>I. cretus</i>		0.019	0.022	0.022	0.024	0.024
2 <i>P. californica</i>	0.180		0.021	0.022	0.021	0.020
3 <i>P. moerchi</i>	0.192	0.186		0.016	0.021	0.020
4 <i>P. virgini</i>	0.203	0.202	0.121		0.021	0.021
5 <i>P. caudata</i> (F)	0.216	0.193	0.194	0.194		0.007
6 <i>P. caudata</i>	0.218	0.181	0.183	0.200	0.032	

(b) Divergence time estimates between species pairs based on a 2.1% substitution rate for <i>cox-1</i>						
	1	2	3	4	5	6
1 <i>I. cretus</i>		0.9	1.0	1.1	1.1	1.1
2 <i>P. californica</i>	8.6		1.0	1.0	1.0	1.0
3 <i>P. moerchi</i>	9.2	8.8		0.8	1.0	1.0
4 <i>P. virgini</i>	9.7	9.6	5.8		1.0	1.0
5 <i>P. caudata</i> (F)	10.3	9.2	9.2	9.3		0.3
6 <i>P. caudata</i>	10.4	8.6	8.7	9.5	1.5	

(c) Genetic distances between species pairs based on <i>ITS-1</i>					
	1	2	3	4	5
1 <i>I. cretus</i>		0.036	0.036	0.036	0.036
2 <i>P. californica</i>	0.353		0.013	0.014	0.013
3 <i>P. virgini</i>	0.339	0.075		0.015	0.015
4 <i>P. caudata</i> (F)	0.340	0.073	0.085		0.003
5 <i>P. caudata</i>	0.339	0.070	0.083	0.008	

(d) Divergence time estimates between species pairs based on a 0.25% substitution rate for <i>ITS-1</i>					
	1	2	3	4	5
1 <i>I. cretus</i>		14.6	14.2	14.4	14.3
2 <i>P. californica</i>	141.2		5.3	5.4	5.4
3 <i>P. virgini</i>	135.5	29.9		6.0	5.9
4 <i>P. caudata</i> (F)	136.0	29.2	33.9		1.2
5 <i>P. caudata</i>	135.5	28.2	33.1	3.2	

**Table 2.** Analysis of molecular variance (AMOVA) for (a) *cox-1* and (b) *ITS-1*; based on two groups of populations of *P. caudata*: Group 1: Florida (FLO); Group 2: Puerto Rico (PRI), Virgin Islands (VIL), Guadeloupe (GUA), Fortaleza (FOR), Tamandaré (TAM), Peracanga (PER), Ubatuba (UBA), Porchat (POR), Itanhaém (ITA) and Ilha do Mel (MEL). FCT: variation among groups; FSC: variation among populations within groups; FST: variation within populations. Significant values ( $P < 0.05$ ) are highlighted in bold.

Source of variation	df	Sum of Squares	Variance Components		% of Variation
(a) Analysis of Molecular Variance for <i>cox-1</i>					
Among groups	1	10.556	0.47092	Va	72.07
Among populations within groups	9	1.649	0.00006	Vb	0.01
Within populations	135	24.623	0.18239	Vc	27.92
Total	145	36.829	0.65338		
Fixation Indices		<b>p-value</b>			
F <sub>SC</sub> (Vb)	0.00035	0.37146			
F <sub>ST</sub> (Vc)	<b>0.72085</b>	0.00000			
F <sub>CT</sub> (Va)	0.72075	0.08798			
(b) Analysis of Molecular Variance for <i>ITS-1</i>					
Among groups	1	12.894	0.24476	Va	19.57
Among populations within groups	9	10.559	0.02209	Vb	1.77
Within populations	88	86.567	0.98372	Vc	78.66
Total	98	110.02	1.25057		
Fixation Indices		<b>p-value</b>			
F <sub>SC</sub> (Vb)	0.02196	0.13881			
F <sub>ST</sub> (Vc)	<b>0.21338</b>	0.00000			
F <sub>CT</sub> (Va)	<b>0.19572</b>	0.00098			
Population Structure:					
Population 1	FLO				
Population 2	PRI, VIL, GUA, FOR, TAM, PER, UBA, POR, ITA, MEL				

**Table 3.** Pairwise  $\phi_{ST}$  among populations of *P. caudata*. Values in the upper triangle were calculated based on ITS-1, while values in the lower triangle were calculated based on cox-1. Statistically significant values ( $P < 0.05$ ) are highlighted in bold. Underlined values indicate significance after Bonferroni correction ( $P < 0.00091$ ).

	FLO	PRI	VIL	GUA	FOR	TAM	PER	UBA	POR	ITA	MEL
	1	2	3	4	5	6	7	8	9	10	11
Florida											
Puerto Rico	FLO 1	<b>0.234</b>	0.060	0.001	<b>0.284</b>	<b>0.207</b>	<b>0.339</b>	<b>0.305</b>	<b>0.305</b>	<b>0.284</b>	<b>0.329</b>
Virgin Islands	PRI 2	<b>0.615</b>	-0.005	<b>0.229</b>	0.204	<b>0.132</b>	<b>0.195</b>	0.260	<b>0.249</b>	0.204	<b>0.337</b>
Guadeloupe	VIR 3	<b>0.661</b>	-0.024	0.051	0.150	0.090	<b>0.173</b>	0.164	<b>0.205</b>	0.150	<b>0.241</b>
Fortaleza, BR	GUA 4	<b>0.746</b>	0.009	0.082	0.071	0.026	0.163	0.085	0.069	0.071	0.097
Tamandaré, BR	FOR 5	<b>0.632</b>	0.003	0.018	0.034	-0.091	-0.049	-0.166	-0.086	-0.167	-0.146
Percanganga, BR	TAM 6	<b>0.753</b>	-0.046	0.028	-0.070	0.002	-0.012	-0.123	-0.024	-0.110	-0.073
Ubaituba, BR	PER 7	<b>0.606</b>	-0.039	-0.017	0.019	-0.055	-0.022	-0.142	0.030	-0.049	0.013
Porchat, BR	UBA 8	<b>0.784</b>	-0.009	0.074	-0.043	0.000	-0.022	-0.016	-0.065	-0.166	-0.053
Ianhém, BR	POR 9	<b>0.706</b>	0.003	0.053	0.005	-0.051	-0.026	-0.016	-0.026	-0.086	-0.125
Ilhá do Mel, BR	ITA 10	<b>0.691</b>	0.009	0.062	0.001	-0.058	0.003	-0.026	0.001	-0.086	-0.146
	MEL 11	<b>0.735</b>	0.025	0.086	-0.021	-0.067	0.016	-0.038	0.008	-0.029	

## SUPPORTING INFORMATION

*Journal of Biogeography*

### Phylogeography of the reef-building polychaetes of the genus *Phragmatopomaim* the Western Atlantic Region

**Appendix S1.** Sampling details, showing the number of specimens collected per sampling site (n) and the number of DNA sequences obtained for each locus. Geographical coordinates are provided for sites sampled in this study.

Species <sup>a</sup>	n	<i>ITS1</i>	<i>cox1</i>	Location	Code	Date	Collector
<i>P. caudata</i>	12 <sup>a</sup>	12	12	USA Dade County, S. Miami Beach (Florida)	FLO	Dec 2002	D. McCarthy
<i>P. caudata</i>	12 <sup>a</sup>	12	11	USA Puerto Rico, Punta Cangrejos	PRI	Aug 2004	C. Drake
<i>P. caudata</i>	11 <sup>a</sup>	11	10	USA Virgin islands, St. Croix	VIL	Jul 2004	D. McCarthy
<i>P. caudata</i>	24	5	23	Guadeloupe, pointe Madame 16°21'0"N - 61°43'13"W	GUA	Mar 2011	C. Bouchon
<i>P. caudata</i>	17	5	15	Brazil Fortaleza (Ceará) 3°48'18"S - 38°24'46"W	FOR	May 2007	J. Fournier
<i>P. caudata</i>	22	11	7	Brazil Tamandaré (Pernambuco) 8°45'28"S - 35°05'39"W	TAM	Dec 2007	L.F. Perez
<i>P. caudata</i>	20	17	13	Brazil Peracanga (Espírito Santo) 20°43'47"S - 40°31'39"W	PER	Jan 2008	L.F. Perez
<i>P. caudata</i>	10	4	10	Brazil Ubatuba (São Paulo) 23°21'45"S - 44°53'27"W	UBA	Oct 2005	J. Fournier
<i>P. caudata</i>	17	12	12	Brazil Ilha Porchat (São Paulo) 23°58'36"S - 46°22'34"W	POR	Jan 2008	L.F. Perez
<i>P. caudata</i>	17	5	14	Brazil Itanhaém (São Paulo) 24°12'08"S - 46°48'41"W	ITA	Jan 2007	J. Fournier
<i>P. caudata</i>	19	5	19	Brazil Ilha do Mel (Paraná) 25°34'26"S - 48°18'41"W	MEL	Nov 2007	J. Fournier
Total	181	99	146				

<sup>a</sup> according to published information

**Appendix S2.** Genetic diversity indices and neutrality tests for each population of *P. caudata* based on sequence data obtained for (a) *cox-1* and (b) *ITS-1*.  $N_a$  = number of sampled alleles; H = number of unique haplotypes; s = number of segregating sites; h = gene diversity;  $\pi$  = average nucleotide diversity. Statistically significant values ( $\alpha=0.05$ ) are highlighted in bold. Population name codes are shown in Appendix S1

(a) Genetic diversity indices for *cox-1* (excluding 3rd codon position)

Population	$N_a$	H	s	h	$\pi$ (x1000)	Tajima's		Fu'sFs	$p$ -value
						D	$p$ -value		
FLO	12	4	3	0.455 ± 0.170	1.506 ± 1.547	<b>-1.629</b>	0.021	<b>-2.124</b>	0.007
PRI	11	4	4	0.491 ± 0.175	2.191 ± 1.987	<b>-1.712</b>	0.016	<b>-1.415</b>	0.032
VIL	10	3	2	0.511 ± 0.164	1.673 ± 1.684	-0.691	0.239	-0.594	0.109
GUA	23	4	3	0.249 ± 0.117	0.786 ± 1.006	<b>-1.731</b>	0.014	<b>-2.956</b>	0.001
FOR	15	3	2	0.362 ± 0.145	1.147 ± 1.287	-1.002	0.211	-0.918	0.070
TAM	7	1	0	0	0	0	1		
PER	13	5	5	0.539 ± 0.161	2.317 ± 2.032	<b>-1.863</b>	0.005	<b>-2.443</b>	0.008
UBA	10	1	0	0	0	0	1		
POR	12	3	2	0.318 ± 0.164	1.004 ± 1.209	-1.451	0.065	<b>-1.325</b>	0.030
ITA	14	3	2	0.275 ± 0.148	0.861 ± 1.091	-1.481	0.051	<b>-1.475</b>	0.017
MEL	19	3	2	0.205 ± 0.119	0.634 ± 0.899	<b>-1.511</b>	0.043	<b>-1.804</b>	0.012

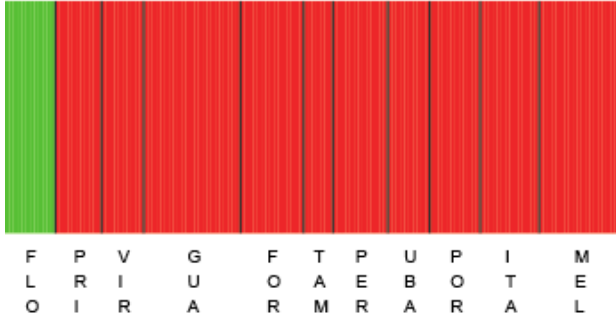
(b) Genetic diversity indices for *ITS-1*

Population	$N_a$	H	s	h	$\pi$ (x1000)	Tajima's		Fu'sFs	$p$ -value
						D	$p$ -value		
FLO	12	6	7	0.818 ± 0.096	7.312 ± 4.634	1.049	0.872	-0.346	0.395
PRI	12	5	4	0.788 ± 0.090	2.902 ± 2.258	0.022	0.628	-1.513	0.083
VIL	11	7	6	0.909 ± 0.066	5.549 ± 3.729	0.453	0.693	<b>-2.525</b>	0.029
GUA	5	4	8	0.900 ± 0.161	10.95 ± 7.586	1.028	0.819	0.286	0.489
FOR	5	4	3	0.900 ± 0.161	3.483 ± 2.963	-0.175	0.474	<b>-1.648</b>	0.046
TAM	11	6	11	0.727 ± 0.144	6.603 ± 4.297	-1.174	0.105	-0.835	0.248
PER	17	5	9	0.691 ± 0.075	3.896 ± 2.732	-1.484	0.062	-0.210	0.425
UBA	4	2	1	0.667 ± 0.204	1.658 ± 1.861	1.633	0.963	0.540	0.480
POR	12	4	8	0.561 ± 0.154	4.523 ± 3.148	-1.253	0.101	0.698	0.682
ITA	5	4	3	0.900 ± 0.161	3.483 ± 2.963	-0.175	0.497	<b>-1.648</b>	0.046
MEL	5	2	2	0.400 ± 0.237	1.990 ± 1.982	-0.973	0.198	1.040	0.607

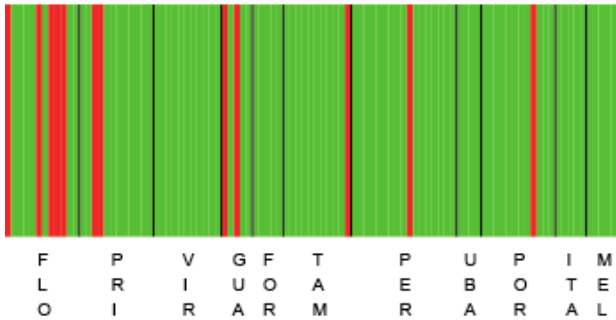


**Appendix S3.** Bayesian Analysis of Population Structure (BAPS) assignments based on a 2-population model for individuals of *Phragmatopoma caudata* sampled from 11 localities for (a) *cox-1* and (b) *ITS-1*. Population name codes are shown in Appendix S1.

(a) Bayesian Analysis of Population Structure for *cox-1*



(b) Bayesian Analysis of Population Structure for *ITS-1*





## CONCLUSÃO FINAL DA TESE

---

Os modelos de distribuição de espécies previram que as mudanças climáticas e ambiental (MCA) causarão alterações na distribuição e prevalência de recifes de sabelarídeos tropical (*Phragmatopoma caudata*) e temperado (*Phragmatopoma virgini*). Dependendo do cenário futuro considerado, as espécies terão respostas idiossincráticas, com alterações sentido pólo ou multidirecionais. No cenário mais otimista (RCP2.6), as previsões do modelo indicam a aumento de habitats adequados ao final do século para ambas as espécies, embora para a espécie tropical foi previsto uma leve perda de área em meados do século. As previsões para o cenário de continuidade da emissão em elevadas taxas de  $p\text{CO}_2$  (RCP8.5) indicam ao longo do século retração e expansão em área de habitats adequados para o sabelarídeo tropical e temperado, respectivamente.

*Sabellaria alveolata* mantida, por 14 dias, em condições de acidificação dos oceanos consegue manter a síntese e a secreção de adesivo para a construção biogênica. No entanto, para ambas as condições de pH testadas, houveram alterações no volume utilizado para colar os grãos de sedimento, e também, nos aminoácidos componentes do bioadesivo. As alterações foram mais acentuadas no adesivo dos organismos submetidos à condição mais extrema (pH 7.4) do que na condição intermediária (pH 7.6). Entretanto, observou-se haver variabilidade nas respostas dos organismos dentro do tratamento de menor pH (e.g. volume do adesivo secretado, e do amino ácido ácido aspártico). Esta variabilidade pode evidenciar diversidade genética que no transcorrer de gerações poderia potencialmente resultar em adaptação da espécie a condições de acidificação dos oceanos.

Em condições de hipertermia extrema (34 e 31°C) *Sabellaria alveolata* não apresentou habilidade para neutralizar o estresse, resultando em mortalidade. Mas, em temperatura sub-letal (28°C) a espécie sobrevive ao custo de uma complexa e dinâmica remodelagem dos lipídeos estruturais. Em 31°C, a espécie demonstrou reestruturação lipídica tardia, com sobreexpressão de algumas classes de lipídios e baixas taxas de plasmalógenos se comparada aos valores em 28°C. Eventos curtos de picos de calor extremos podem resultar em mortalidade da população em poucos dias. Os ajustes de reestruturação lipídica a 28°C permitiram redução do estresse térmico em simulação de onda de calor por 30 dias. No entanto, a sobrevivência e a capacidade reprodutiva dos organismos sob os efeitos de anomalias térmicas mais longas precisam ainda ser avaliadas.

Todos os resultados mostram que MCA causarão alterações geográficas, comportamentais, e fisiológicas significativas nas populações das espécies de Sabellariidae pesquisadas. Estas mudanças podem resultar em dois padrões, não mutuamente excludentes, que são: i) extinções locais, contrações, e deslocamento latitudinal e/ou batimétrico na distribuição de populações, e ii) conservação da atual distribuição como resultado de processo de aclimatação e adaptação transgeracional. Em conclusão, embora a biodiversidade bêntica marinha possa apresentar plasticidade fisiológica e comportamental potencial para manter populações, as respostas associadas não podem ser generalizadas e dependerão principalmente da frequência, intensidade e período de tempo em que ocorrerão as mudanças climáticas e do ambiente.

## REFERÊNCIAS

- Ataide MB, Venekey V, Rosa JS, Dos Santos PJP (2014) Sandy reefs of *Sabellaria wilsoni* (Polychaeta: Sabellariidae) as ecosystem engineers for meiofauna in the Amazon coastal region, Brazil. *Marine Biodiversity*, **44**, 403–413.
- Braby CE, Somero GN (2006) Following the heart: temperature and salinity effects on heart rate in native and invasive species of blue mussels (genus *Mytilus*). *Journal of Experimental Biology*, **209**, 2554–2566.
- Briggs JC, Bowen BW (2012) A realignment of marine biogeographic provinces with particular reference to fish distributions. *Journal of Biogeography*, **39**, 12–30.
- Burrows MT, Schoeman DS, Buckley LB *et al.* (2011) The pace of shifting climate in marine and terrestrial ecosystems. *Science*, **334**, 652–655.
- Caldeira K, Wickett ME (2005) Ocean model predictions of chemistry changes from carbon dioxide emissions to the atmosphere and ocean. *Journal of Geophysical Research-Oceans*, **110**, 12.
- Caline B, Kirtley DW (1992) *The sabellariid reefs in the Bay of Mont Saint-Michel, France : ecology, geomorphology, sedimentology, and geologic implications*, Stuart, Fla., Florida Oceanographic Society.
- Caputi N, Kangas M, Denham A, Feng M, Pearce A, Hetzel Y, Chandrapavan A (2016) Management adaptation of invertebrate fisheries to an extreme marine heat wave event at a global warming hot spot. *Ecology and Evolution*, **6**, 3583–3593.
- Doney SC, Fabry VJ, Feely RA, Kleypas JA (2009) Ocean Acidification: The Other CO<sub>2</sub> Problem. *Annual Review of Marine Science*, **1**, 169–192.
- Doney, S.C., Mahowald, N., Lima, I., Feely, R.A., Mackenzie, F.T., Lamarque, J.F. & Rasch, P.J. (2007) Impact of anthropogenic atmospheric nitrogen and sulfur deposition on ocean acidification and the inorganic carbon system. *Proceedings of the National Academy of Sciences of the United States of America*, **104**, 14580–14585.
- Dubois S, Retiere C, Olivier F (2002) Biodiversity associated with *Sabellaria alveolata* (Polychaeta : Sabellariidae) reefs: effects of human disturbances. *Journal of the Marine Biological Association of the United Kingdom*, **82**, 817–826.

- Faroni-Perez L, Helm C, Burghardt I, Hutchings P, Capa M (2016) Anterior sensory organs in Sabellariidae (Annelida). *Invertebrate Biology*, **135**, 423–447.
- Firth LB, Mieszowska N, Grant LM *et al.* (2015) Historical comparisons reveal multiple drivers of decadal change of an ecosystem engineer at the range edge. *Ecology and Evolution*, **5**, 3210–3222.
- García Molinos J, Halpern BS, Schoeman DS *et al.* (2015) Climate velocity and the future global redistribution of marine biodiversity. *Nature Clim. Change*.
- Garrabou J, Coma R, Bensoussan N *et al.* (2009) Mass mortality in Northwestern Mediterranean rocky benthic communities: effects of the 2003 heat wave. *Global Change Biology*, **15**, 1090–1103.
- Gherardi F, Cassidy PM (1994) Macrobenthic associates of bioherms of the polychaete *Sabellaria cementarium* from northern Puget Sound, Washington. *Canadian Journal of Zoology*, **72**, 514–525.
- Gilman SE, Wethey DS, Helmuth B (2006) Variation in the sensitivity of organismal body temperature to climate change over local and geographic scales. *Proceedings of the National Academy of Sciences*, **103**, 9560–9565.
- Gore RH, Scotto LE, Becker LJ (1978) Community composition, stability, and trophic partitioning in decapod crustaceans inhabiting some subtropical sabellariid worm reefs: studies on decapod crustacea from the Indian River Region of Florida, IV. *Bulletin of Marine Science*, **28**, 221–248.
- Gruet Y, Vovelle J, Grasset M (1987) Biomineral components of tube cement of *Sabellaria alveolata* (L), (Annelida Polychaeta). *Canadian Journal of Zoology-Revue Canadienne De Zoologie*, **65**, 837–842.
- Hazel JR, Landrey SR (1988) Time course of thermal adaptation in plasma membranes of trout kidney. II. Molecular species composition. *American Journal of Physiology*, **255**, 628–634.
- Hazel JR, Williams EE (1990) The role of alterations in membrane lipid composition in enabling physiological adaptation of organisms to their physical environment. *Progress in Lipid Research*, **29**, 167–227.
- Helmuth B, Broitman BR, Blanchette CA *et al.* (2006) Mosaic patterns of thermal stress in the rocky intertidal zone: Implications for climate change. *Ecological Monographs*, **76**, 461–479.

- Hobday AJ, Alexander LV, Perkins SE *et al.* (2016) A hierarchical approach to defining marine heatwaves. *Progress in Oceanography*, **141**, 227–238.
- Ippc, Core Writing Team, Pachauri RK, Meyer LA (2014) *Climate Change 2014: Synthesis Report. Contribution of Working Groups I, II and III to the Fifth Assessment Report of the Intergovernmental Panel on Climate Change*, Geneva, Switzerland.
- Jensen RA, Morse DE (1988) The bioadhesive of *Phragmatopoma californica* tubes: a silk-like cement containing L-DOPA. *Journal of Comparative Physiology B*, **158**, 317–324.
- Jones CG, Lawton JH, Shachak M (1994) Organisms as ecosystem engineers. *Oikos*, **69**, 373–386.
- Jones MC, Cheung WWL (2015) Multi-model ensemble projections of climate change effects on global marine biodiversity. *Ices Journal of Marine Science*, **72**, 741–752.
- Koch M, Bowes G, Ross C, Zhang XH (2013) Climate change and ocean acidification effects on seagrasses and marine macroalgae. *Global Change Biology*, **19**, 103–132.
- Kroeker KJ, Kordas RL, Crim R *et al.* (2013) Impacts of ocean acidification on marine organisms: quantifying sensitivities and interaction with warming. *Global Change Biology*, **19**, 1884–1896.
- Lenoir J, Svenning JC (2015) Climate-related range shifts - a global multidimensional synthesis and new research directions. *Ecography*, **38**, 15–28.
- Leung JY, Russell BD, Connell SD (2017) Mineralogical plasticity acts as a compensatory mechanism to the impacts of ocean acidification. *Environ Sci Technol*, **51**, 2652–2659.
- Li CY, Chan VBS, He C, Meng Y, Yao HM, Shih KM, Thiagarajan V (2014) Weakening Mechanisms of the Serpulid Tube in a High-CO<sub>2</sub> World. *Environmental Science & Technology*, **48**, 14158–14167.
- Lima FP, Wetthey DS (2012) Three decades of high-resolution coastal sea surface temperatures reveal more than warming. **3**, 704.
- Lindeman KC, Snyder DB (1999) Nearshore hardbottom fishes of southeast Florida and effects of habitat burial caused by dredging. *Fishery Bulletin*, **97**, 508–525.
- Main MB, Nelson WG (1988) Sedimentary characteristics of sabellariid worm reefs (*Phragmatopoma lapidosa* Kinberg). *Estuarine, Coastal and Shelf Science*, **26**, 105–109.

- Makowski C, Seminoff JA, Salmon M (2006) Home range and habitat use of juvenile Atlantic green turtles (*Chelonia mydas* L.) on shallow reef habitats in Palm Beach, Florida, USA. *Marine Biology*, **148**, 1167–1179.
- Mills KE, Pershing AJ, Brown CJ *et al.* (2013) Fisheries Management in a Changing Climate Lessons from the 2012 Ocean Heat Wave in the Northwest Atlantic. *Oceanography*, **26**, 191–195.
- Muir AP, Nunes FLD, Dubois SF, Pernet F (2016) Lipid remodelling in the reef-building honeycomb worm, *Sabellaria alveolata*, reflects acclimation and local adaptation to temperature. **6**, 35669.
- Nelson WG, Demetriades L (1992) Peracarids associated with sabellariid worm rock (*Phragmatopoma lapidosa* Kinberg) at Sebastian Inlet, Florida, U.S.A. *Journal of Crustacean Biology*, **12**, 647–654.
- Nunes FLD, Van Wormhoudt A, Faroni-Perez L, Fournier J (2017) Phylogeography of the reef-building polychaetes of the genus *Phragmatopoma* in the western Atlantic Region. *Journal of Biogeography*, **44**, 1612–1625.
- Oliver ECJ, Benthuisen JA, Bindoff NL, Hobday AJ, Holbrook NJ, Mundy CN, Perkins-Kirkpatrick SE (2017) The unprecedented 2015/16 Tasman Sea marine heatwave. **8**, 16101.
- Orr JC, Fabry VJ, Aumont O *et al.* (2005) Anthropogenic ocean acidification over the twenty-first century and its impact on calcifying organisms. *Nature*, **437**, 681–686.
- Pawlik JR, Faulkner DJ (1988) The gregarious settlement of sabellariid polychaetes: new perspectives on chemical cues In: *Marine biodeterioration*. (eds Thompson MF, Sarojini R, Nagabhushanam R) pp Page. New Delhi, Bombai, Calcutta, Oxford & IBH Publishing Co.
- Pernet F, Tremblay R, Comeau L, Guderley H (2007) Temperature adaptation in two bivalve species from different thermal habitats: energetics and remodelling of membrane lipids. *Journal of Experimental Biology*, **210**, 2999–3014.
- Pörtner H-O, Bock C, Mark FC (2017) Oxygen- and capacity-limited thermal tolerance: bridging ecology and physiology. *The Journal of Experimental Biology*, **220**, 2685.
- Pörtner HO (2008) Ecosystem effects of ocean acidification in times of ocean warming: a physiologist's view. *Marine Ecology Progress Series*, **373**, 203–217.
- Przeslawski R, Ah Yong S, Byrne M, Worheide G, Hutchings P (2008) Beyond corals and fish: the effects of climate change on noncoral



- benthic invertebrates of tropical reefs. *Global Change Biology*, **14**, 2773–2795.
- Sabine CL, Feely RA, Gruber N *et al.* (2004) The oceanic sink for anthropogenic CO<sub>2</sub>. *Science*, **305**, 367–371.
- Saupe EE, Hendricks JR, Peterson AT, Lieberman BS (2014) Climate change and marine molluscs of the western North Atlantic: future prospects and perils. *Journal of Biogeography*, **41**, 1352–1366.
- Smale DA, Wernberg T, Vanderklift MA (2017) Regional-scale variability in the response of benthic macroinvertebrate assemblages to a marine heatwave. *Marine Ecology Progress Series*, **568**, 17–30.
- Somero GN (2002) Thermal Physiology and Vertical Zonation of Intertidal Animals: Optima, Limits, and Costs of Living. *Integrative and Comparative Biology*, **42**, 780–789.
- Somero GN (2010) The physiology of climate change: how potentials for acclimatization and genetic adaptation will determine 'winners' and 'losers'. *Journal of Experimental Biology*, **213**, 912–920.
- Stevens MJ, Steren RE, Hlady V, Stewart RJ (2007) Multiscale structure of the underwater adhesive of *Phragmatopoma californica*: A nanostructured latex with a steep microporosity gradient. *Langmuir*, **23**, 5045–5049.
- Stewart RJ, Wang CS, Song IT, Jones JP (2017) The role of coacervation and phase transitions in the sandcastle worm adhesive system. *Advances in Colloid and Interface Science*, **239**, 88–96.
- Sun CJ, Srivastava A, Reifert JR, Waite JH (2009) Halogenated DOPA in a marine adhesive protein. *Journal of Adhesion*, **85**, 126–138.
- Sunday JM, Bates AE, Dulvy NK (2012) Thermal tolerance and the global redistribution of animals. *Nature Climate Change*, **2**, 686–690.
- Van Meer G, Voelker DR, Feigenson GW (2008) Membrane lipids: where they are and how they behave. *Nat Rev Mol Cell Biol*, **9**, 112–124.
- Vanderwal J, Murphy HT, Kutt AS, Perkins GC, Bateman BL, Perry JJ, Reside AE (2013) Focus on poleward shifts in species' distribution underestimates the fingerprint of climate change. *Nature Climate Change*, **3**, 239–243.
- Wang CS, Stewart RJ (2012) Localization of the bioadhesive precursors of the sandcastle worm, *Phragmatopoma californica* (Fewkes). *Journal of Experimental Biology*, **215**.

- Wernberg T, Bennett S, Babcock RC *et al.* (2016) Climate-driven regime shift of a temperate marine ecosystem. *Science*, **353**, 169–172.
- Wernberg T, Smale DA, Tuya F *et al.* (2013) An extreme climatic event alters marine ecosystem structure in a global biodiversity hotspot. *Nature Climate Change*, **3**, 78–82.
- Wittmann AC, Portner HO (2013) Sensitivities of extant animal taxa to ocean acidification. *Nature Climate Change*, **3**, 995–1001.